Allyl and carbonyl complexes of the groups VI and VII transition metals.

White, James W.

Award date:
1979

Awarding institution:
University of Bath

ALLYL AND CARBONYL COMPLEXES OF THE GROUPS VI AND VII TRANSITION METALS

submitted by

James W White

for the Degree of Doctor of Philosophy

of the University of Bath

1979

James W. White

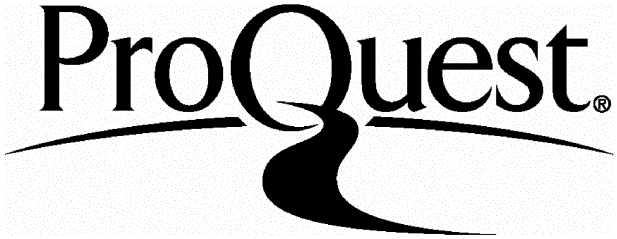

ACKNOWLEDGEMENTS

I gratefully acknowledge the encouragement and guidance I have received from my Supervisors, Dr. D.A. Edwards and Dr. B.J. Brisdon, during this study.

I wish to thank my wife, Sue, for her patience and understanding throughout and for painstakingly typing this work.

Thanks are also due to my colleague, Kathy Hill, for proof-reading the thesis.

I am indebted to the Science Research Council for financial support.

SUMMARY

The contents of this thesis fall naturally into four sections which form the subjects of Chapter 2 - 5. Chapter 1 comprises a general introduction and literature survey of the most relevant areas.

In Chapter 2 the preparation and characterisation of a series of carbonylmetallate anions fac-$[MX(CO)_3L_2]^-$ where M = Mo or W, X = Cl, Br or I and L_2 = 1, 10-phenanthroline or 2, 2'-bipyridine from the corresponding cis-$[M(CO)_4L_2]$ complexes is described. Solution infrared studies indicated that these complexes do not isomerise to the mer-isomers as suggested previously, but are solvolysed in acetonitrile with the formation of fac-$[M(CO)_3L_2(MeCN)]$. Reaction of the anions with various allyl halides resulted in high yields of the η^3-allyl complexes $[(\eta^3\text{-}RC_3H_4)MX(CO)_2L_2]$. The significance of these observations for the mechanism of the allyl oxidative-addition reaction is discussed.

Reactions between $Mn(CO)_5X$ and Et_4NX (X = Cl, Br) in boiling chloroform and between $Re(CO)_5X$ and Et_4NX (X = Cl, Br, I) in boiling decalin are described in Chapter 3. The final products are the compounds $Et_4N[M_2(CO)_6(\mu\text{-}X)_3]$. Vibrational spectroscopic results indicate that the anions possess confacial bi-octahedral geometry with three bridging halogen atoms. The anions did not react with allyl halides to give η^3-allyl derivatives.

Details of the preparation of $[(\eta^1\text{-}C_3H_5)Re(CO)_5]$ from $[Re(CO)_5]^-$ and its photo-decarbonylation to $[(\eta^3\text{-}C_3H_5)Re(CO)_4]$ are presented in Chapter 4. Both allyl complexes have been characterised using ^1H NMR, mass spectrometry and particularly liquid-phase infrared and Raman spectroscopies. Although the vibrations of the $Re(CO)_5$ unit in the η^1-allyl compound can be assigned in terms of C_{4v}

symmetry, such a local symmetry approximation has been found to be invalid for the η^3-allyl compound whose vibrational spectrum requires discussion in terms of the overall C_s symmetry. The η^1- and η^3- allyl internal modes are discussed in terms of C_s symmetry. For comparative purposes the methyl derivatives $[MeRe(CO)_5]$ (Me = $^{12}CH_3$, $^{13}CH_3$, $^{12}CD_3$) have also been synthesised and their mass and vibrational spectra studied.

In Chapter 5 some carbonyl substitution reactions of $[(\eta^3\text{-}C_3H_5)M(CO)_4]$ (M = Mn, Re) are reported. The use of thermal or photolytic methods has allowed the synthesis of the complexes $[(\eta^3\text{-}C_3H_5)M(CO)_3L]$, (M = Mn, L = PPh_3, $AsPh_3$, PCy_3, PBu^n_3, $PMePh_2$); M = Re, L = PPh_3) and $[(\eta^3\text{-}C_3H_5)M(CO)_2L_2]$, (M = Mn, L = $PMePh_2$, $P(OMe)_3$, $P(OEt)_3$, $\frac{1}{2}Ph_2PCH_2PPh_2$; M = Re, L = PPh_3). These complexes are considered to possess pseudo-octahedral structures, the carbonyl ligands being <u>facial</u> in the tricarbonyls and <u>cis</u> in the dicarbonyls. The ^1H NMR spectra are characteristic of symmetrical η^3-allyl species and show strong ^1H-^{31}P coupling. Mass spectra have been obtained and fragmentation pathways suggested mainly on the basis of observed metastable peaks. A single crystal X-ray structure determination has been carried out on the complex $[(\eta^3\text{-}C_3H_5)Mn(CO)_2\{P(OMe)_3\}_2]$. The crystals are monoclinic with <u>a</u> = 18.618(11), <u>b</u> = 9.218(7), <u>c</u> = 10.607(11) Å, <u>β</u> = 102.1(1)°, Z = 4 and space group $P2_1/a$. 1742 independent reflections above background have been collected and refined to <u>R</u> = 0.059. Considering the η^3-allyl group to occupy two coordination sites, the metal has a distorted octahedral environment being bonded to two mutually <u>trans</u>- phosphorus atoms 2.175(5), 2.219(5) Å, two <u>cis</u>-carbonyl groups 1.75(2), 1.83(2) Å and a η^3-allyl ligand with Mn-C 2.223(17), 2.114(14), 2.229(13) Å.

Appendices 1 - 5 contain details of experimental methods, starting materials, group theory, secular equations and computer programmes used in this work. Appendix 6 lists the structure factors and thermal parameters associated with the crystal structure determination.

CONTENTS

FIGURES Page

TABLES Page

ABBREVIATIONS

a	asymmetric
acac	acetylacetonate
Ar	aryl
ax	axial
bipy	2,2'-bipyridine
Bu	butyl
cht	cycloheptatriene
Cy	cyclohexyl
dpae	1,2-bis(diphenylarsino)ethane
dppe	1,2-bis(diphenylphosphino)ethane
dppm	1,2-bis(diphenylphosphino)methane
e	electron
eq	equatorial
eq.	equation
Et	ethyl
hfacac	hexafluoroacetylacetonate
hv	ultra violet radiation
K	CO stretching force constant
K_i	CO interaction force constant
Me	methyl
m*	metastable ion
Ph	phenyl
phen	1,10-phenanthroline
Pr	propyl
py	pyridine
R	alkyl
r.t.	ambient temperature
TMS	tetramethylsilane
ψ	molecular orbital
ϕ	atomic orbital
Δ	heat
Λ	conductivity
Γ	group theoretical representation

Nuclear Magnetic Resonance (NMR):

d	doublet
J	coupling constant
m	multiplet
ppm	parts per million
q	quartet
s	singlet
t	triplet
δ	chemical shift

Infrared (IR) and Raman (R) Spectra:

dp	depolarised	ν	stretching vibration
m	medium	ρ_r	rocking mode
pol	polarised	ρ_s	scissors deformation
s	strong	ρ_t	twisting mode
sh	shoulder	ρ_w	wagging mode
v	very	τ	torsion
w	weak		
δ	deformation		
π	out-of-plane deformation		

CHAPTER ONE

INTRODUCTION

INTRODUCTION

The chemistry of allyl transition metal compounds has been the subject of much recent research arising in part from their importance as intermediates in both catalytic cycles and many organic reactions. Thus, they are extremely effective catalysts for stereospecific polymerisation and oligomerisation of alkenes and dienes[1-5] and participate in the isomerisation[6,7], oxidation[8], hydrogenation[9-11] and carbonylation[12,13] reactions of unsaturated organic compounds. There are several review articles concerning the use of allyl-metal systems in organic chemistry[1,2,5,14,15] and, together with many subsequent publications[10,11,16-20] concerning the reactions of more recently reported compounds, they illustrate the usefulness of such systems to the synthetic chemist.

Interest in allyl-metal compounds has also been stimulated by some of their unusual intrinsic properties[21-25] and the challenge presented by, for example, the theory of allyl-metal bonding[26-32] and the interpretation of often complicated spectroscopic features[33-42].

To date most of the considerable chemical effort has been applied to allyl complexes of the later transition metals. In particular those of the nickel triad have received much attention although recently there has been a shift of emphasis to the iron group[43]. In contrast the chemistry of allyl derivatives of the early transition metals has been comparatively neglected.

The work described in this thesis is concerned with the synthesis and characterisation of new groups VI and VII transition metal-allylcarbonyl compounds and their derivatives. The major synthetic

route adopted involves the use of highly reactive carbonylmetallate anions as precursors and accordingly the chemistry of some of these compounds is discussed.

BONDING AND STRUCTURE OF ALLYL-METAL COMPOUNDS

Nomenclature

The naming of compounds in this work will follow the rules laid down by the 1970 IUPAC Commission on the Nomenclature of Inorganic Compounds[44], with due regard given to more recent trends generally adopted by authors. In particular, the nomenclature for metal complexes involving unsaturated organic ligands has changed several times over the past fifteen years and various notations for allyl-metal systems may be encountered in the literature. Probably the earliest was the σ- and π-representation, the former denoting a single localised carbon-metal bond and the latter a multicentred delocalised system. Due to its simplicity this method is still widely used today.

In order to designate structure, Cotton[45] introduced the 'hapto' (from the Greek haptien, to fasten) notation, which specified the number of atoms bound to the central metal atom by the prefix h^n- (where n = number of atoms bound to the metal). The IUPAC system is basically similar but with h replaced by the Greek letter eta, η. In cases where some, but not all, ligand atoms are involved in bonding, locant designators may be inserted preceeding η. A simple example will serve to clarify the situation.

Notation for the butenylcarbonylcobalt complexes

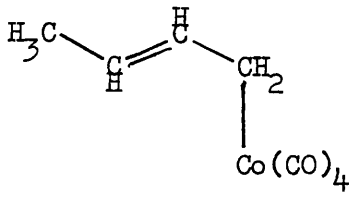

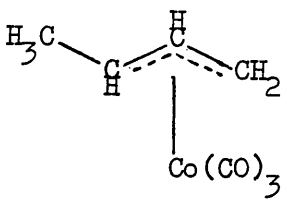

Early:	tetracarbonyl- σ-crotylcobalt	tricarbonyl- π-crotylcobalt
Cotton:	h^1-2-butenyl tetracarbonylcobalt	h^3-2-butenyl tricarbonylcobalt
IUPAC:	(1-η-2-butenyl) tetracarbonylcobalt(I)	(1-3-η-2butenyl) tricarbonylcobalt(I)
Acceptable alternatives:	η^1-2-butenyl tetracarbonylcobalt	η^3-2-butenyl tricarbonylcobalt
	σ-2-butenyl tetracarbonylcobalt	

Note: A recent comment in the literature[46] has shown that the nomenclature for complexes involving unsaturated organic ligands is the subject of continuing discussion.

Structural Types

The allyl group may adopt one of several modes of bonding in metal complexes including the following:

(i) η^3-allyl; a multicentred delocalised bond system is formed between the three carbon atoms of the allyl ligand and the metal.

(ii) η^1-allyl; a formal σ-bond between the metal and terminal carbon atom of the allyl group is formed, leaving a localised double bond on the adjacent carbon atoms.

(iii) bridging or μ-allyl; the allyl group is simultaneously bonded to two metal centres, thereby acting as a bridging ligand. e.g. $[Pt(\mu\text{-}C_3H_5)acac]_2$[47] and $[(\eta^3\text{-}C_3H_5)(\mu\text{-}C_3H_5)Cr]_2$[48]

(iv) ionic allyl; e.g. C_3H_5Na[49]. Compounds of this type are undoubtedly ionic. However they do not produce ions in solution but exist as strongly bound ion pairs.

(v) unsymmetrically bonded allyl; this category covers those systems not easily classified. Compounds falling into this class are sometimes erroneously designated σ-π-allyls. This is to indicate that both types of interaction may be present, however they are best thought of as unsymmetrical η^3-systems. e.g. $[PtCl(\eta^3\text{-}2\text{-}MeC_3H_4)PPh_3]$[50] (Figure 1.1)

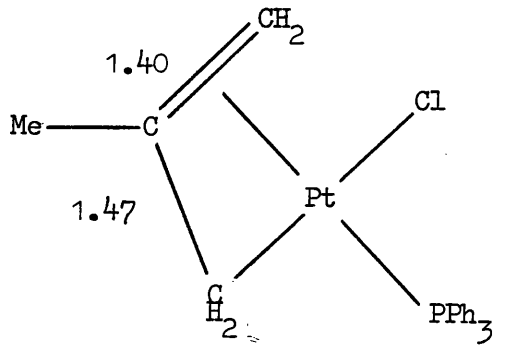

Figure 1.1: The structure of $[PtCl(\eta^3\text{-}2\text{-}MeC_3H_4)PPh_3]$

Very recently some η^3-allyl complexes of nickel sulphide clusters, e.g. $[(\eta^3\text{-}C_3H_5)_6Ni_6S_3]$[24] and $[(\eta^3\text{-}C_3H_5)_2Ni_2(C_7H_8S_3)]$[51], have been reported which may represent a new structural type but as yet no confirmation of structure is available.

The majority of simple allyl-metal compounds are either η^3- or η^1-bonded and accordingly these are treated in more detail subsequently. In addition there are a great many more complicated systems in which an η^3-bonded entity is present. Some examples of these are given at the end of this section.

Symmetrical η^3-allyl-metal bonding

In η^3-allyl-metal systems the allyl group is frequently symmetrically bonded to the metal atom (within experimental error). The terminal M-C(allyl) distances are approximately equal whilst the central M-C(allyl) distance is usually slightly shorter. Some typical examples where X-ray crystal structure analyses have confirmed this feature are given in Table 1.1. The plane of the allyl carbon atoms is not, however, perpendicular to (dihedral angle $\chi = 90^\circ$) the metal xz plane, as might be expected by analogy with simple olefin complexes but for most complexes χ is greater than 90° (Table 1.1) This variation may be rationalised in terms of maximising the bonding orbital overlap which occurs at differing values of χ.

Table 1.1 appears overleaf.

Table 1.1: Selected Structural Data for some η^3-Allyl Transition Metal Compounds

Compound	Ref.	Bond Lengths(Å)			Dihedral Angle
		MC(1)	MC(2)	MC(3)	χ (deg)
$[(\eta^3\text{-}C_3H_5)Mo(CO)_2\{(CH_3O)_3P\}_2Cl]$	52	2.40	2.36	2.40	112.2
$[(\eta^3\text{-}C_3H_5)Mo(CO)_2(bipy)py][BF_4]$	53	2.31	2.28	2.29	107.9
$[(\eta^3\text{-}C_3H_5)Fe(CO)_3]_2$	54	2.21	2.10	2.20	98.8
$[(\eta^3\text{-}C_3H_5)_2Ru(PPh_3)_2]$[a]	55	2.23	2.13	2.25	
$[(\eta^3\text{-}C_3H_5)Co(CO)_3]$[a]	56	2.10	1.98	2.10	
$[(\eta^3\text{-}C_3H_5)IrCl(CO)(PMe_2Ph)_2][PF_6]$	57	2.28	2.24	2.25	126
$[(\eta^3\text{-}2\text{-}C_2H_5CO_2C_3H_4)NiBr]_2$	58	2.05	1.90	2.06	106.2
$[(\eta^3\text{-}C_3H_5)Pd(CH_3CO_2)]_2$	59	2.15	2.01	2.15	125 ; 110
$[(\eta^3\text{-}C_3H_5)PdCl]_2$	60[b]	2.12	2.10	2.12	111.5
	61	2.14	2.02	2.17	108

[a] dihedral angles for these compounds are not easily defined

[b] determined at -140°C

A diagrammatic view of the $[(\eta^3\text{-}C_3H_5)PdCl]_2$ dimer using the angles and bond lengths of Reference 60 is given in Figure 1.2.

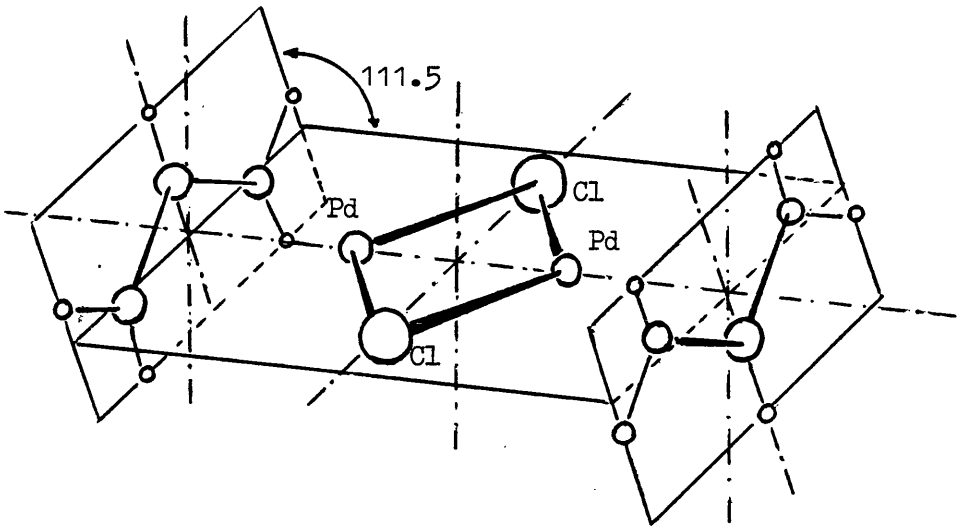

Figure 1.2: Schematic drawing of the $[(\eta^3\text{-}C_3H_5)PdCl]_2$ dimer

The allyl anion has three delocalised π-molecular orbitals, ψ_1, ψ_2, ψ_3,[28,62] resulting from a linear combination of the carbon p_z-orbitals remaining after the σ- framework has been constructed[63] (Figure1.3, overleaf). Convention dictates that the η^3-allyl group contributes one unit to the oxidation number of the metal*. Thus the allyl anion is formally a four electron donor. In this case ψ_1 and ψ_2 are both doubly filled molecular orbitals, each capable of donating two electrons to vacant metal orbitals of suitable symmetry and energy. Theoretically the vacant ψ_3 orbital is available for back bonding from the metal, providing the same requirements are fulfilled.

*although this does not preclude the idea that the allyl ligand may be a three electron donor and contribute zero to the oxidation number.

Atomic Orbitals Molecular Orbitals

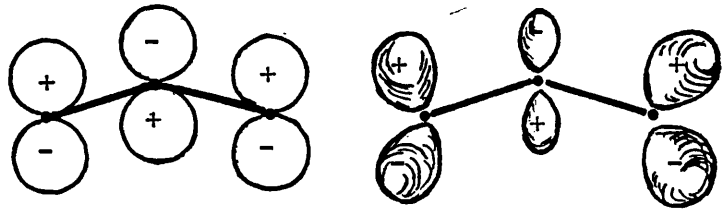

Antibonding

$$\psi_3 = \tfrac{1}{2}(\phi_1 + \phi_3 - \sqrt{2}\phi_2)$$

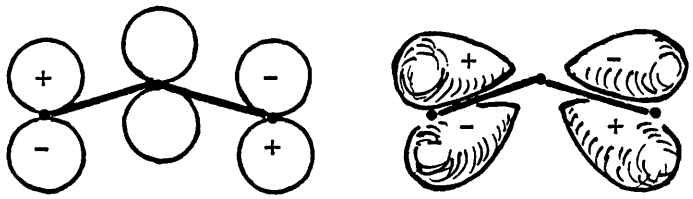

Non-bonding

$$\psi_2 = \sqrt{\tfrac{1}{2}}(\phi_1 - \phi_3)$$

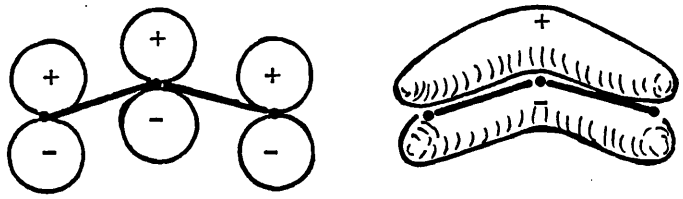

Bonding

$$\psi_1 = \tfrac{1}{2}(\phi_1 + \phi_3 + \sqrt{2}\phi_2)$$

Figure 1.3: The π-molecular orbitals of the allyl anion

Consideration of the symmetry of both allyl-anion and metal orbitals reveals that there are two distinct mechanisms by which bonding can occur, (I and II in Figure 1.4). Moreover the resulting orientations of the allyl group with respect to the metal xz plane differs by 90° as shown in Figure 1.4.

From experimental observations, particularly on the allylpalladium system[59-61,64], it is evidently a poor approximation to regard

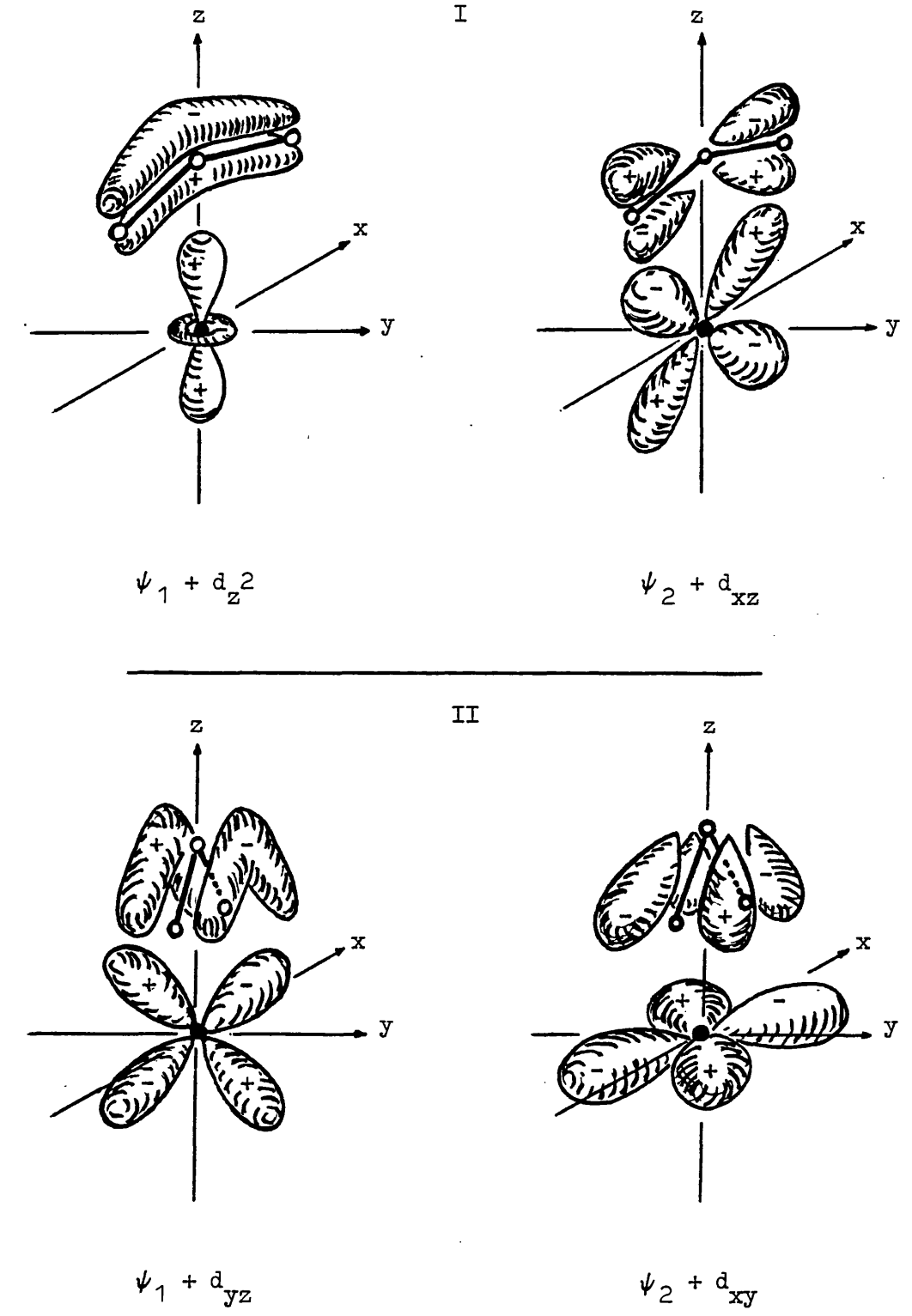

Figure 1.4: Possible orientations for allyl-transition metal bonding interactions

(I: $\chi = 90^\circ$ II: $\chi = 180^\circ$)

either of these two extremes as solely responsible for allyl-metal bonding. Consequently a purely qualitative description suggests that to maximise bonding interactions the dihedral angle, χ, must lie between the extreme values $\chi = 180^{\circ}$ and $\chi = 90^{\circ}$. This accounts for the observed 'allyl tilt' which is common to most allyl-metal systems.

Semi-quantitative calculations of overlap integrals for several allyl-metal systems have been carried out[26,29,30,65] and where these include maximisation of overlap as a function of χ, fair agreement between experiment and theory is found. In some cases the agreement between observed and calculated values is very good indeed e.g. for $[(\eta^3\text{-}C_3H_5)PdCl]_2$, χ(obs.) = 108°, 111.5° and χ(calc.) = 102°-114°[26].

The discussion so far has paid little attention to possible d-ψ_3 interactions and indeed most workers consider these to be of small significance. This is in accordance with the view previously noted that the allyl ligand is an electron donor. However some authors[27] conclude that metal-ψ_3 electron transfer is of some importance in rationalising the observed 'allyl tilt', whilst others compare its importance with back bonding in ferrocene[66]. It is clear that the bonding in η^3-allyl-metal compounds is the subject of continuing controversy and that no completely satisfactory solution has yet been found (see for example the discussion in Reference 57).

η^1-Allyl-metal bonding

Using valence-bond terminology, one terminal carbon atom of an isolated allyl group is sp^3 hybridised, whilst the remaining two atoms are sp^2 hybrids linked by a localised double bond. For

bonding considerations the η^1-allyl ligand may be treated as a simple alkyl substituent. Consequently bonding involves overlap of a carbon sp^3 orbital with suitable metal orbitals resulting in the creation of a formal σ-bond which allows free rotation of the allyl group about the carbon-metal axis. π-Interactions are also symmetry allowed and have been invoked to describe the bonding in some fluoroalkyl compounds[67]. However such interactions are not important for simple alkyl ligands[68]. Thus the η^1-allyl ligand contributes one electron to the valence shell of the metal and zero to the oxidation number.

Since the metal-carbon σ-interaction does not fundamentally perturb the ligand (c.f. η^3-allyl analogues) it should retain the major features of an uncoordinated allyl group, such as the sp^2 and sp^3 bond angles and the variation in carbon-carbon bond lengths. Two examples where solid state structures containing η^1-allyl ligands have been determined are: $[(\eta^1\text{-}C_3H_5)Pt(PPh_3)_2Cl]$[69] (Figure 1.5) and $[(\eta^5\text{-}C_5H_5)(\eta^1\text{-}C_3H_5)Nb(CS_2)]$[70]. These confirm that the carbon-carbon bond lengths are appreciably different and, even in the solid state, the allyl (CC=C) angle is close to the ideal value.

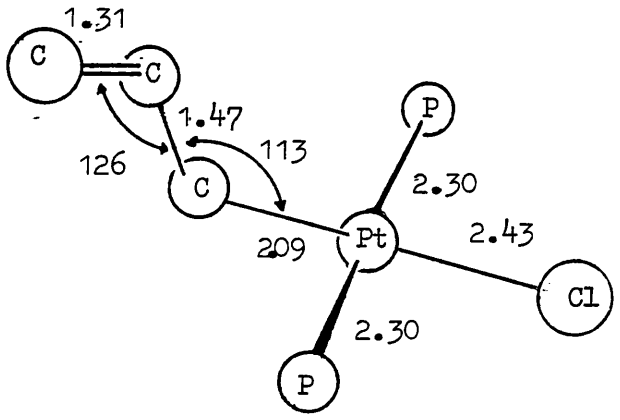

Figure 1.5: The skeletal structure of $[(\eta^1\text{-}C_3H_5)Pt(PPh_3)_2Cl]$

η^1-Allyl-metal derivatives are not as common as their η^3-counterparts although the few studies undertaken indicate that transition metal-carbon σ-bonds are thermodynamically stable. For example the Pt-CH_3 bond dissociation energy in $[(\eta^5\text{-}C_5H_5)Pt(CH_3)_3]$ is 164 $KJmol^{-1}$ [71] and for Ti-CH_3 in $[(\eta^5\text{-}C_5H_5)Ti(CH_3)_2]$ *ca.* 250 $KJmol^{-1}$ [72]. The inherent instability of most η^1-allyl-metal systems is attributed to the many pathways available for kinetic decomposition, such as homolytic metal-carbon fission and β-hydrogen transfer.

Other allyl-metal systems

In order to simplify the rationale the discussion of bonding in previous sections has been mainly confined to the basic allyl moiety, C_3H_5. Clearly the C_3H_5 unit can be multiply substituted, part of a cyclic system or even contain hetero-atoms and so the bonding in such systems may be considerably modified. However an extension of the arguments put forward above may reasonably be employed as the basis for describing some of the more complicated systems. There are numerous examples to be found in the literature, of which a selected few are given below:

Multiply substituted η^3-allyl systems:

(i) Complexes of the type $[(\eta^5\text{-}C_5H_5)Mo(CO)_2(\eta^3\text{-}CH_2C(CO_2R')CHR)]$, (R = Me, Ph),(R' = H, Me, Et) were the products of a novel reaction between the σ-bonded acetylene compounds $[(\eta^5\text{-}C_5H_5)Mo(CO)_3(\eta^1\text{-}CH_2C{\equiv}CR)]$ and alcohols, R'OH or water at ambient temperatures[73].

(ii)

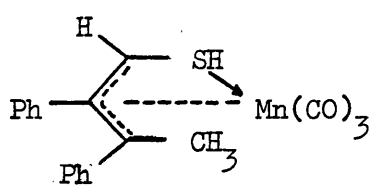

This unusual sulphur-substituted η^3-allylmanganese complex

was formed by the alkylation, reduction and ring opening of diphenylcylcopropenethione on treatment with $[Mn(CO)_5]^-$ and CH_3I in aqueous methanol[22].

(iii)

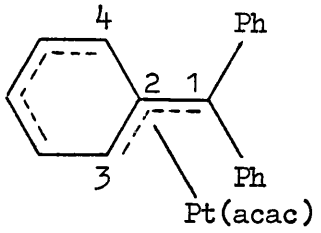

The platinum complex above has a complicated, temperature dependant, NMR spectrum indicating fluxional behaviour which results in the equivalence of carbon atoms 1 - 4 on the NMR time scale[74]. The corresponding palladium complexes show three independent types of fluxional behaviour over the temperature range $-40^{\circ}C$ to $+60^{\circ}C$.

(iv) Complex NMR spectra are a common feature of multiply substituted allyl systems as in the example below where a crystal structure determination was needed to confirm the spectral results[75].

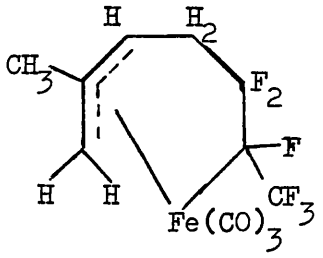

Cyclic allyl systems:

Examples of complexes, in which part of a cyclic ligand is bound to a transition metal in the trihapto- manner may be found for a variety of ring sizes. These range from the special case of the three membered cyclopropenyl ring to much larger eight or nine membered cyclic systems. In some of the large ring systems the trihapto- form of the ligand prevails over other possible alternatives which would involve bonding through more atoms. This is usually a direct consequence of the preference the metal has

for attaining the eighteen electron configuration and often results in fluxional behaviour of the complex. The many examples of this type illustrate that the 'eighteen electron rule' is normally obeyed and is therefore of use in the discussion of the allyl transition metal complexes in general. The following examples are given in order of increasing ring size:

(i) Three membered ring systems such as

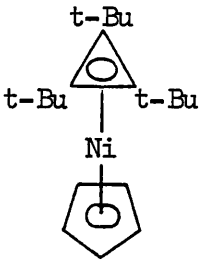

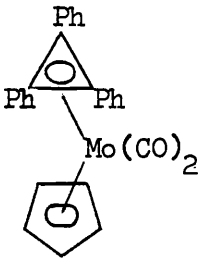

are readily synthesised from trisubstituted cyclopropenyl halides[76-78].

(ii) Two examples of four membered rings containing an η^3-bonded moiety are[79,80]:

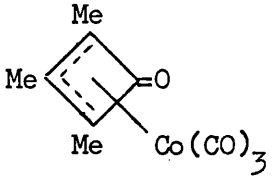

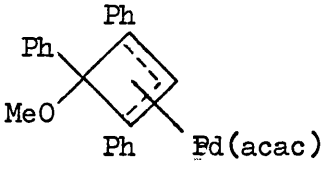

The latter example exists in equilibrium with another isomeric form involving a ring opened butadienyl structure.

(iii) Five membered rings[81,82] e.g.

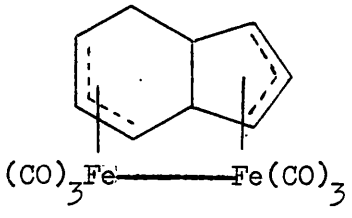

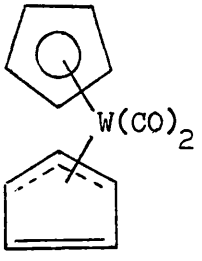

A crystal structure analysis of the tungsten complex confirms that it contains a trihapto-cyclopentadienyl ligand with an

uncoordinated C=C bond, thus avoiding a twenty electron valence configuration of the metal atom.

(iv) Examples of six membered ring systems such as,

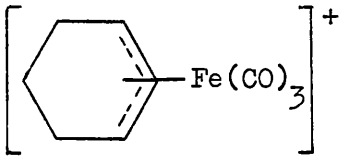

which is formed by protonation of the corresponding cyclohexadiene complex in strongly acid medium[83] and

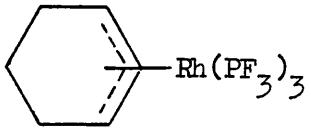

which is prepared by the insertion of 1,3-cyclohexadiene into the metal hydrogen bond in $HRh(PF_3)_4$ [84], are very common.

(v) Seven, eight and nine membered ring systems are less common and are usually very reactive. For example the η^3-bonded complex (a) is formed by nucleophilic attack by CN^- on the cycloheptadienyl-rutheniumtricarbonyl cation, a reaction which is easily reversed on treatment with Ph_3C^+ [85]. The iridium complex (b)[86] is a further example which demonstrates well the preference of the metal for an eighteen electron configuration and the very reactive niobium complex (c) was assigned an η^3-allyl type structure on the basis of infrared and variable temperature NMR results[87].

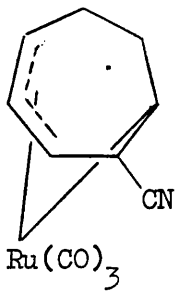

(a)

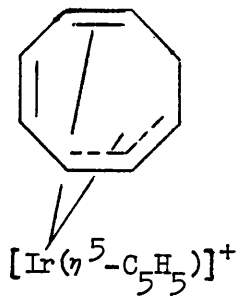

(b)

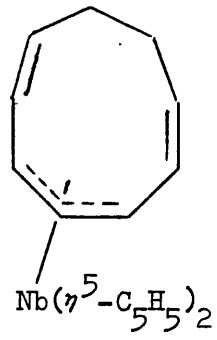

(c)

Hetero-allyl systems:

(i) Novel diaza-η^3-allyl complexes such as,

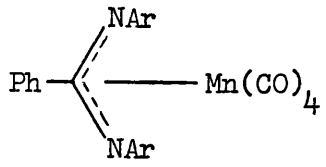

(Ar = Ph, p-tolyl)

were obtained in a photodecarbonylation reaction of the cyclic carbamoyl complexes $[(CO)_4\overline{MnCO.N(Ar)C(Ph)N}(Ar)]$[88].

(ii)

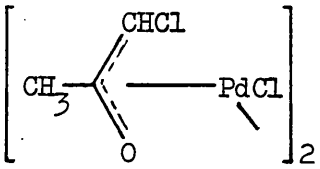

The above complex is an example of an oxo-η^3-allyl complex which was prepared in 93% yield from the reaction between diazoacetone and $[(PhCN)_2PdCl_2]$[89].

(iii) Silicon analogues of η^3-allyl complexes represent the first examples of stable 'doubly bonded silicon' compounds[90] e.g.

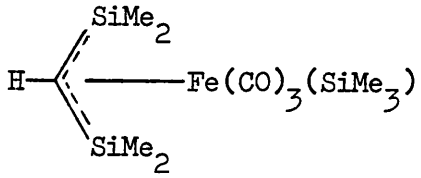

(iv) The complex $[(B_3H_7)Pt(PPh_3)_2]$ contains the $B_3H_7^{2-}$ ion which is isoelectronic with $C_3H_5^-$ and the authors claim that it is a π-borallyl analogue of $[(C_3H_5)Pt(PPh_3)Cl]$ on the basis that they undergo similar reactions[91].

SPECTROSCOPIC CHARACTERISATION OF ALLYL-METAL COMPOUNDS

Proton NMR Spectroscopy

η^1-Allyl-metal complexes:

An η^1-allyl group bonded to a metal atom contains four types of magnetically inequivalent hydrogen atoms (assuming free rotation about the carbon-metal and carbon-carbon σ-bonds). These are designated a, b, c and x in Figure 1.6.

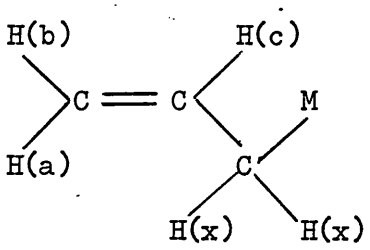

Figure 1.6: The η^1-allyl group

Chemical shift ranges for the different protons are typically H(a), H(b), δ = 3.5-5.0; H(c), δ = 5.5-6.5 and H(x), δ = 1.5-3.0 ppm. Providing simple first order splitting rules apply and the molecule is not fluxional, an $ABCX_2$ pattern, similar to that found for the allyl halides[92], is expected for such compounds. This type of spectrum for example is observed for $[(\eta^1\text{-}C_3H_5)Mn(CO)_5]$[93]: H(a) = 4.92 (d, 17 Hz), H(b) = 4.68 (d, 10 Hz), H(c) = 6.15 (m), 2H(x) = 1.85 (d, 9 Hz) and $[(\eta^5\text{-}C_5H_5)(\eta^1\text{-}C_3H_5)Nb(CS_2)]$[94]: H(a), H(b) $\simeq$ 4.5 (m), H(c) = 5.90 (m), 2H(x) = 2.73 (d, 8 Hz), (ppm relative to TMS).

There are however examples of η^1-allyl compounds where the ^{1}H NMR spectrum is considerably simplified and corresponds to an AX_4 spin system. For example the room temperature spectrum of $[(\eta^1\text{-}C_3H_5)Ti(Et_2N)_3]$[95], H(a) = H(b) = 2H(x) = 6.45 (d, 11 Hz),

H(c) = 3.1 (quintet, 11 Hz). It is likely that the equivalence of the terminal protons is the result of a rapid $\eta^1 \rightarrow \eta^3 \rightarrow \eta^1$ exchange process. Indeed this seems certain for the $[(\eta^1\text{-}C_3H_5)Pd(PPhMe_2)L_2]$, systems[96] ($L_2 = O_2CC_5H_4N$; S_2CNMe_2), where NMR measurements over a range of temperature clearly show the presence of both η^1- and η^3- species.

η^3-Allyl-metal complexes:

Whereas the η^1-allyl group has four inequivalent hydrogen atoms, a static, symmetrical η^3-bonded allyl group has only three magnetically distinct hydrogens. These are shown as H(a), H(m) and H(x) in Figure 1.7.

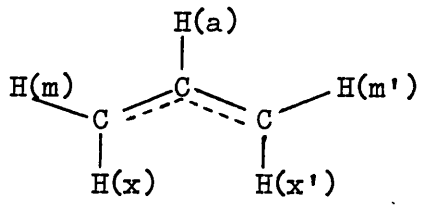

Figure 1.7: The symmetrical η^3-allyl group

Again the first order rules are applicable and an AMM'XX' pattern is expected. However the coupling constants J(MX) and J(MX'), being small, are only detected in high resolution studies and so the majority of symmetrical η^3-allyl spectra can be assigned to an AM_2X_2 spin system. Indeed it was the observation of such a spectrum that first demonstrated the symmetrical nature of the η^3-allyl-metal bond in $[(\eta^3\text{-}C_3H_5)Co(CO)_3]$[97] and $[(\eta^3\text{-}C_3H_5)Mn(CO)_4]$[98].

Comparison of η^3-allyl spectra with those of known organic alkene systems (Figure 1.8) enables the assignment of the cis- and trans- or syn- and anti- protons to be made.

Coupling constants for η^3-allyl complexes are typically in the

ranges 9-14 Hz (anti), 5-10 Hz (syn), 0-2 Hz (gem) and although lower than those of alkenes, the sequence of relative values J (trans) > J (cis) > J (gem) is maintained.

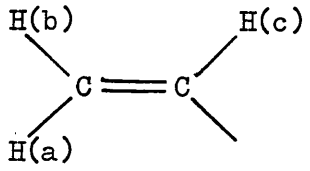

J(ac) trans = 11-20 Hz

J(bc) cis = 6-14 Hz

J(ab) gem = 0-3.5 Hz

Figure 1.8: Typical ^{1}H-coupling constants in alkenes[99]

Added confidence to the assignments is gained if the experimentally measured syn-, anti-, geminal and long distance coupling constants are compared with values obtained from theoretical calculations[100,101]. The observed and calculated results are usually in close agreement. A diagram of an AM_2X_2 spectrum with typical chemical shift values is given in Figure 1.9.

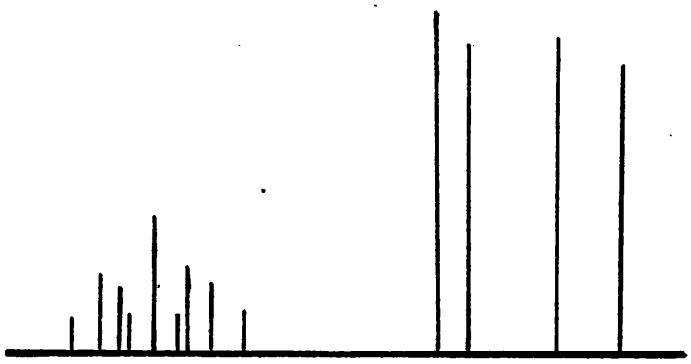

Assignment	H(a)		H(m)	H(x)
Intensity ratio	1	:	2	: 2
Typical δ values (ppm vs. TMS)	(6.5-4)		(5-2)	(4-1)

Figure 1.9: Diagram of an AM_2X_2 η^3-allyl NMR spectrum

As with η^1-allyl complexes the ^{1}HNMR spectra of some η^3-allyl complexes (e.g. $[Zr(\eta^3\text{-}C_3H_5)_4]$[104] and $[Th(\eta^3\text{-}C_3H_5)_4]$[1]) are sometimes misleadingly simple and an AX_4 spin system may be observed. This is often due to a rapid interchange of syn- and anti- protons causing their equivalence on the time scale of the NMR experiment. Such dynamic processes are detected by variable temperature studies in which the AX_4 spectrum may be 'frozen out' to give the expected AM_2X_2 pattern. For example the coalescence temperature for $[Zr(\eta^3\text{-}C_3H_5)_4]$ is about -40°C[105] and for $[Th(\eta^3\text{-}C_3H_5)_4]$ about 50°C[1]. The hafnium complex $[Hf(\eta^3\text{-}C_3H_5)_4]$ displays an AX_4 spectrum even at -72°C indicating that the activation energy for the dynamic process in this compound is very low[105,106].

As a result of substitution e.g. $[(\eta^3\text{-}1\text{-}MeC_3H_4)Co(CO)_3]$[107], stereoisomerism e.g. $[(\eta^5\text{-}C_5H_5)(\eta^3\text{-}C_3H_5)Mo(CO)_2]$[108], or fluxional processes involving intramolecular rearrangements e.g. $[(PPh_3)_2Cl_2Rh(\eta^3\text{-}2\text{-}MeC_3H_4)]$[109] and intermolecular rearrangements e.g. $[(\eta^3\text{-}C_4H_7)PdCl]_2$[110], the NMR spectra of η^3-allyl compounds may be considerably more complex than expected. Fluxional behaviour amongst η^3-allyl complexes is extremely commonplace and may be due to one of three types of rearrangement, namely (i) syn-anti exchange, (ii) syn-syn, anti-anti exchange, (iii) conformational changes. These movements can be a result of rearrangement of the η^3-allyl group relative to the rest of the molecule or to the fluxional nature of the molecule as a whole. In most cases it is not easy to distinguish the precise mechanism and various authors have differing opinions. However for syn- anti- exchange the most widely accepted mechanism is the η^3- η^1-η^3 movement, which is depicted in Figure 1.10 for the $[(\eta^3\text{-}2\text{-}MeC_3H_4)RhCl_2(PPh_3)_2]$ system[109].

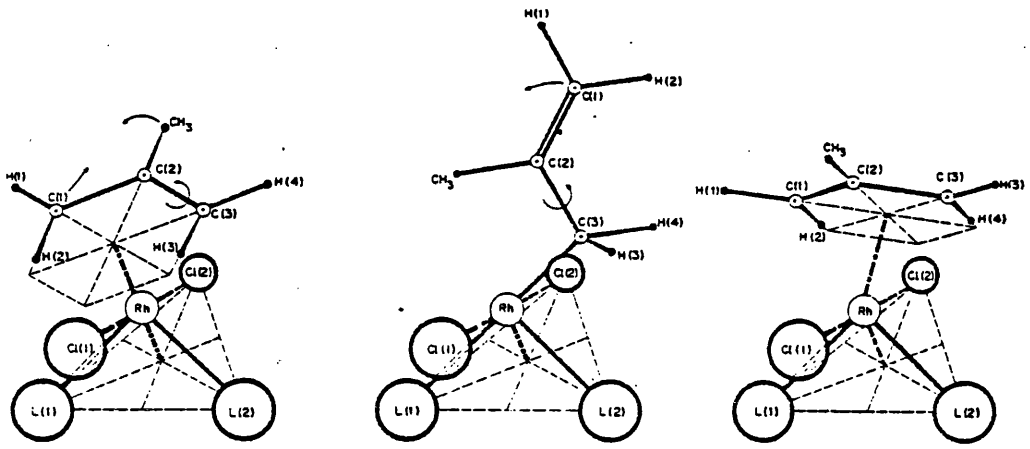

Figure 1.10: Syn-anti conversion via a η^1-allyl form

From the preceding discussion it is clear that ^{1}H NMR spectroscopy is a very powerful technique for the study of allyl-metal complexes of all types. The information gained, particularly by variable temperature measurements on fluxional systems, is extremely useful in structure elucidation, a fact which is reflected in the great volume of NMR data accumulated in the literature. Thus ^{1}H NMR probably provides the most important physicochemical method for the investigation of allyl-metal systems. However the solution to most problems is usually provided by considering the combined results of several different methods.

13-Carbon NMR Spectroscopy

During the past ten years the use of ^{13}C NMR spectroscopy for the study of organometallic compounds has greatly increased, with the

advent of more sensitive and widely available spectrometers[103]. However, with the exception of perhaps palladium complexes[36,104,110], relatively little data has been obtained for η^3-allyl-transition metal systems. Nevertheless ^{13}C chemical shifts of η^3-allyl ligands[11,36,39,104,111-113] can be quite characteristic. The terminal carbons C(1) and C(3) have shifts in the range 35-80 ppm (relative to TMS) and the central carbon C(2) resonance falls in the range 90-140 ppm (Table 1.2), reflecting the electron distribution within the allyl group. Thus C(1) and C(3) possess more electron density than C(2), which is deshielded and found at lower field. This is consistent with the donation of π-electron density into the allyl-ψ_2 orbital which has a nodal plane containing C(2)[39,112].

Table 1.2: Selected ^{13}C NMR Data

Compound	Ref	^{13}C Chemical Shift (ppm; TMS = 0) C(1)	C(2)	C(3)
$[(\eta^3\text{-}2\text{-}MeC_3H_4)Pd(PEt_2Ph)_2][BF_4]$	36	71.0	136.3	71.0
$[(\eta^3\text{-}C_3H_5)PdCl]_2$	104	63.2	111.9	63.2
$[(\eta^3\text{-}C_3H_5)PdBr]_2$	104	65.2	111.3	65.2
$[(\eta^3\text{-}C_3H_5)PdI]_2$	104	68.0	110.2	68.0
$[(\eta^3\text{-}C_3H_5)Pd(PPh_3)Cl]$	104	62.0	118.7	79.4
$[(\eta^3\text{-}1\text{-}MeC_3H_4)NiBr]_2$	112	71.2	105.6	49.6
$[(\eta^3\text{-}C_3H_5)Mn(CO)_2\{(Oi\text{-}Pr)_3P\}_2]$	11	43.0	93.3	43.0
$[(\eta^3\text{-}1\text{-}EtC_3H_4)Mn(CO)_4]$	39	37.0	92.7	71.0
$[(\eta^3\text{-}C_3H_5)Mo(CO)_2\{P(OMe)_3\}_2Cl]$	113	76.0	114.4	76.0
$[(\eta^3\text{-}2\text{-}MeC_3H_4)Mo(CO)_2\{P(OMe)_3\}_2Cl]$	113	75.4	130.0	75.4

^{13}C Chemical shifts appear to be sensitive to substitution in the trans-position at the metal[104,112] since the chemical shift of the

terminal carbons move to a higher field in the order, I<Br<Cl<acac<C_5H_5. The few ^1H - ^{13}C coupling constants measured fall in the range 155-165 Hz[39,112] which is typical of sp^2 hybridised carbon atoms.

Vibrational Spectroscopy

Partial data for allyl vibrations, particularly between 1650-1300 cm^{-1} has been reported for many allyl transition metal complexes[114]. It is in this region that vibrational spectroscopy is of greatest value in determining whether the allyl group is η^1- or η^3- bonded. Some typical results giving ν(C=C) for η^1-allyl complexes and the highest band in the 1510-1370 cm^{-1} region for η^3-complexes appear in Table 1.3.

Table 1.3: Characteristic Frequencies (cm^{-1}) for η^1 and η^3-allyl Groups in Some Transition Metal Complexes

Compound	η^1-allyl	η^3-allyl	Ref
$[(\eta^1\text{-}C_3H_5)Ti\{N(Et)_2\}_3]$	1602		95
$[(\eta^5\text{-}C_5H_5)_4(\eta^3\text{-}C_3H_5)_2(\eta^1\text{-}C_3H_5)Zr_2Cl]$	1599,1588	1533	115
$[(\eta^3\text{-}C_3H_5)_3V]$		1520	115
$[(\eta^5\text{-}C_5H_5)_2(\eta^1\text{-}C_3H_5)Nb(CS_2)]$	1605		94
$[(\eta^5\text{-}C_5H_5)_2(\eta^3\text{-}C_3H_5)Nb]$		1480	116
$[(\eta^5\text{-}C_5H_5)(\eta^1\text{-}C_3H_5)W(CO)_3]$	1609		117
$[(\eta^5\text{-}C_5H_5)(\eta^3\text{-}C_3H_5)W(CO)_2]$		1476	117
$[(\eta^1\text{-}C_3H_5)Mn(CO)_5]$	1617		118
$[(\eta^3\text{-}C_3H_5)Ru(CO)_3Cl]$		1462	119

The η^1-bonded complexes have a characteristically strong infrared and Raman active band attributed to ν(C=C) (A'), whereas the spectra of η^3- derivatives contain no such band. Their vibrational spectra do however show three moderate intensity bands between 1510-1370 cm^{-1} which may be assigned, although not unambiguously, to the ν(CCC) (A''), $\delta_a(CH_2)$ (A'') and $\delta_s(CH_2)$ (A') modes.

The vibrational spectra of several η^3-allyl complexes have been studied in detail[40,120-126], and with only minor differences in specific assignments, overall agreement is good. For an η^3-allyl group of C_s symmetry group theory predicts eighteen normal modes of vibration (10A' + 8A'') (Table 1.4).

Table 1.4: Numbers and Symmetries of Normal Modes for an η^3-Allyl Group

Vibrational mode[a]	C_s Symmetry species
ν(CH)	A'
$\nu(CH_2)$	2A' + 2A''
$\delta(CH_2)$	A' + A''
π(CH)	A'
δ(CH)	A''
ν(CCC)	A' + A''
$\rho_t(CH_2)$	A' + A''
$\rho_w(CH_2)$	A' + A''
$\rho_r(CH_2)$	A' + A''
δ(CCC)	A'

[a]symbols used are conventional[127]

In addition to these there are four modes associated with allyl-metal skeletal vibrations (Figure 1.11), which may be regarded as

one stretching (A'), two tilting (A' + A") and one torsional mode (A"). Such modes are often difficult to assign, however assignments have been made for $[(\eta^3\text{-}C_3H_5)PdCl]_2$ based upon frequency shifts observed in ^{104}Pd and ^{110}Pd isotopically labelled species[124].

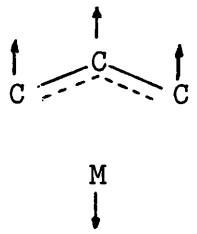

A' symmetry stretch

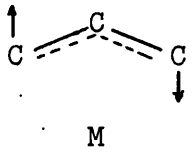

A" symmetry tilt

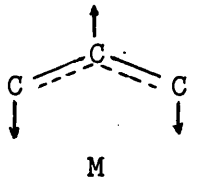

A' symmetry tilt

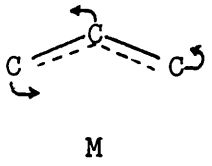

A" symmetry torsion

Figure 1.11: η^3-Allyl-metal skeletal vibrations

Of the η^1-allyl transition metal complexes reasonably complete vibrational data have been reported only for $[(\eta^1\text{-}C_3H_5)Mn(CO)_5]$[128] (Table 1.5). The assignments are similar to those of η^1-allyl derivatives of main group elements[129]. For comparison the vibrational spectra, together with proposed assignments arising from allyl modes, for $[(\eta^1\text{-}C_3H_5)Mn(CO)_5]$[129] and $[(\eta^3\text{-}C_3H_5)Mn(CO)_4]$[40] are presented in Table 1.5 overleaf.

Table 1.5: Vibrational Frequencies (cm^{-1}) and Assignments Proposed for Allyl Modes in $[(\eta^1\text{-}C_3H_5)Mn(CO)_5]$ and $[(\eta^3\text{-}C_3H_5)Mn(CO)_4]$

$[(\eta^1\text{-}C_3H_5)Mn(CO)_5]$[128]		$[(\eta^3\text{-}C_3H_5)Mn(CO)_4]$[40]	
Frequency[a]	Assignment	Frequency[a]	Assignment
3085	A' $\nu(CH)$	3078	A'' $\nu(CH_2)$
3000	A' $\nu(CH_2)$	3025	A' $\nu(CH)$
2975	A' $\nu(CH_2)$	2973	A' $\nu(CH_2)$
2934	A'' $\nu(CH_2)$	2964	A'' $\nu(CH_2)$
2865	A' $\nu(CH_2)$	2948	A' $\nu(CH_2)$
1617	A' $\nu(C=C)$	1503	A'' $\delta_a(CH_2)$[c]
1465		1462	A' $\delta_s(CH_2)$
1448	4A' + A'' In plane bending modes[b]	1397	A'' $\nu_a(CCC)$[c]
1405		1214	A' $\pi(CH)$
1382		1143	A'' $\delta(CH)$
1297		1017	A' $\nu_s(CCC)$
1204		1007	A' $\rho_t(CH_2)$
1080		980	A'' $\rho_t(CH_2)$
1032	A' + 4A'' Out of plane bending modes[b]	920	A' $\rho_w(CH_2)$
1017		883	A'' $\rho_w(CH_2)$
989		788	A'' $\rho_r(CH_2)$
920		774	A' $\rho_r(CH_2)$
752		520	A' $\delta(CCC)$
882	A' $\nu(CC)$	412	A'' allyl-Mn modes
-	A' $\delta(CCC)$[b]	387	A'
-	A' $\nu(MC)$[b]	327	A'

[a] recorded in CCl_4 solutions; [b] specific assignments not given

[c] the assignment of these bands in related complexes is often reversed

Mass Spectrometry

Despite the fact that mass spectral data for allyl-transition metal systems is at present very limited, mass spectrometry can be used to provide useful information concerning the molecular ion, a common feature amongst allyl-metal complexes which is often present in high abundance, and prefered decomposition pathways. The mass spectra of several isoleptic η^3-allyl complexes have been reported [106,130] and these compounds seem to follow straightforward fragmentation patterns. However when the η^3-allyl unit is present in a mixed ligand system[130-135] it does not appear possible to assign a general fragmentation scheme. Instead there are probably several concurrent fragmentation paths involving loss of C_3H_5 and other ligands (e.g. CO, halogen[136]). Decomposition of the C_3H_5 unit by loss of CH_3 or H_2 whilst still attached to the metal atom is also found. The latter process results in the formation of cyclopropenium ions and has been observed for several η^3-allyl-metal complexes[131,132,134,136]. For example the most abundant ion in the mass spectrum of $[(\eta^5\text{-}C_5H_5)(\eta^3\text{-}C_3H_5)Ru(CO)]$ was $[(C_5H_5)Ru(C_3H_3)]^+$ [136].

PREPARATION OF ALLYL-TRANSITION METAL COMPOUNDS

η^1-Allyl Complexes

The main routes to η^1-allyl-transition metal compounds are similar to those used for the synthesis of many other carbon-metal σ-bonded compounds although careful control of reaction conditions is often required because η^1-derivatives may be subject to easy decomposition to η^3-allyl compounds.

(i) Grignard reactions:

This method represents one of the most used routes for σ-alkyl complexes which has been adapted for the synthesis of η^1-allyls e.g.

$[(R_2N)_3TiBr] + allylMgCl \longrightarrow [(\eta^1\text{-allyl})Ti(R_2N)_3] + MgBrCl$ [95]

(ii) Synthesis using anionic metal species:

Treatment of suitable anionic transition metal complexes with allyl halides under controlled conditions often leads to the formation of an η^1-allyl complex e.g.

$[Mn(CO)_5]^- + allylX \longrightarrow [(\eta^1\text{-allyl})Mn(CO)_5] + X^-$ [93,118]

$[Ru(CO)_2Cp]^- + allylX \longrightarrow [(\eta^1\text{-allyl})Ru(CO)_2Cp] + X^-$ [132]

$2[Co(CN)_5]^{3-} + allylX \longrightarrow [(\eta^1\text{-allyl})Co(CN)_5]^{3-} + [Co(CN)_5X]^{3-}$ [137]

The above reactions are general methods which have been adapted from normal alkyl-transition metal synthesis but the following illustrate reactions which are specific to the allyl group.

(iii) Addition of 1,3-dienes to metal hydrides:

Certain metal hydrides are reactive towards conjugated dienes, the products being substituted η^1-allyl complexes e.g.

$[(\eta^5\text{-}C_5H_5)Fe(CO)_2H] + CH_2CHCHCH_2 \longrightarrow [(\eta^5\text{-}C_5H_5)(\eta^1\text{-}C_4H_7)Fe(CO)_2]$ [138]

(iv) η^3- to η^1- conversions:

Such conversions are usually accompanied by the coordination of a simple molecule such as SO_2 or CS_2 to the metal e.g.

$[(\eta^5\text{-}C_5H_5)(\eta^3\text{-}C_3H_5)Nb] + CS_2 \longrightarrow [(\eta^5\text{-}C_5H_5)(\eta^1\text{-}C_3H_5)Nb(CS_2)]$ [94]

$[(\eta^3\text{-}C_3H_5)Rh(PPh_3)_2Cl_2] + SO_2 \longrightarrow [(\eta^1\text{-}C_3H_5)Rh(PPh_3)_2(SO_2)Cl_2]$ [139]

η^3-Allyl Complexes

The number of η^3-allyl-transition metal complexes is very large and

consequently their methods of preparation are many and diverse. However several generally applicable syntheses can be distinguished, some of which involve η^1- complexes already described as intermediates which may or may not be isolable. In addition there are specific reactions which lead, sometimes unexpectedly, to the isolation of η^3-allyl complexes, some examples of which are given at the end of this section.

(i) Use of anionic metal species:

The use of anionic transition metal complexes for the synthesis of novel organometallic species is widely exploited and several reviews[140-143] demonstrate the versatility of such compounds. Allyl compounds are no exception and the route has been successfully employed to produce many such derivatives under mild conditions[93, 118, 132, 144-149] e.g.

$$[Cr(CO)_3(bipy)Cl]^- + allylCl \longrightarrow [(\eta^3\text{-allyl})Cr(CO)_2(bipy)Cl] + Cl^- + CO \quad [145]$$

$$[W(CO)_4(acac)]^- + allylX \longrightarrow [(\eta^3\text{-allyl})W(CO)_2(acac)X]^- + 2CO \quad [147]$$

$$[Co(CO)_4]^- + C_3F_5I \longrightarrow [(\eta^3\text{-}C_3F_5)Co(CO)_3] + I^- + CO \quad [148]$$

$$[V(CO)_4(diars)]^- + allylCl \longrightarrow [(\eta^3\text{-allyl})V(CO)_3(diars)] + Cl^- + CO \quad [149]$$

(ii) Oxidative addition reactions:

Oxidative addition reactions occur when the addition of allylX to a transition metal complex increases the metal oxidation state by two units. Various mechanisms have been proposed for this type of reaction including nucleophilic attack of the metal at the carbon atom bearing halogen[150], a concerted insertion reaction[151], a radical chain process[152] and initial coordination of the C=C to the metal as the rate determining step[153]. The above anionic reactions are particular examples of oxidative additions but this type of reaction is frequently employed to produce neutral η^3-allyl

complexes e.g.

$[Mo(CO)_4(phen)] + allylX \longrightarrow [(\eta^3\text{-allyl})Mo(CO)_2(phen)X] + 2CO$ [154]

$[W(CO)_3(MeCN)_3] + allylX \longrightarrow [(\eta^3\text{-allyl})W(CO)_2(MeCN)_2X] + MeCN + CO$ [78]

$[Ir(CO)(PPhMe_2)_2Cl] + allylX \longrightarrow [(\eta^3\text{-allyl})Ir(CO)(PPhMe_2)_2Cl] + X^-$ [57]

(iii) Grignard reactions:

Allyl magnesium halides often react with transition metal halides to give η^3-allyl complexes directly. Indeed this has been the major route to the so called 'pure allyl' or isoleptic compounds (i.e. those containing no other ligands) e.g.

$NiBr_2 + 2allylMgCl \longrightarrow [(\eta^3\text{-allyl})_2Ni] + 2MgBrCl$ [155]

$\frac{1}{2}[(\eta^6\text{-}C_6H_6)Mo(\eta^3\text{-allyl})Cl]_2 + allylMgCl \longrightarrow [(\eta^6\text{-}C_6H_6)Mo(\eta^3\text{-allyl})_2] + MgCl_2$ [156,157]

$CrCl_3 + 3allylMgBr \longrightarrow [(\eta^3\text{-allyl})_3Cr] + MgClBr + MgBr_2 + MgCl_2$ [1]

These reactions may be regarded as a transfer of the allyl moiety from a main group metal to a transition metal with halide expulsion. A similar type of reaction has been reported using allyl-tin reagents[158,159] e.g.

$Re(CO)_5Br + allylSnMe_3 \longrightarrow [(\eta^3\text{-allyl})Re(CO)_4] + BrSnMe_3 + CO.$

A mechanism involving the coordination of the C=C bond has been proposed and is illustrated in Figure 1.12 overleaf.

(iv) Reactions of conjugated dienes:

η^3-Allyl species may be generated either by hydride addition to diene-metal complexes or by addition of dienes to transition metal hydrides or alkyls e.g.

$[(\eta^6\text{-}C_6H_6)(\eta^4\text{-}C_4H_6)(\eta^3\text{-}C_3H_5)Mo]^+ + H^- \longrightarrow [(\eta^6\text{-}C_6H_6)(\eta^3\text{-1-}MeC_3H_4)(\eta^3\text{-}C_3H_5)Mo]$ [157]

$[(\eta^1\text{-}C_6H_5)Mn(CO)_5] + C_4H_6 \longrightarrow [(\eta^3\text{-}1\text{-}C_6H_5CO\text{-}3\text{-}MeC_3H_3)Mn(CO)_4]$ [160,161]

$[HNi\{P(OMe)_3\}_4]^+ + C_4H_6 \longrightarrow [(\eta^3\text{-}1\text{-}MeC_3H_4)Ni\{P(OMe)_3\}_3]^+ + P(OMe)_3$ [162]

In the second example studies using 1,1,4,4-tetradeuterobutadiene reveal that a 1-4 hydrogen shift occurs to give rise to the observed product $[(\eta^3\text{-}1\text{-}C_6H_5CO\text{-}3\text{-}CD_3.CDCHCH)Mn(CO)_4]$

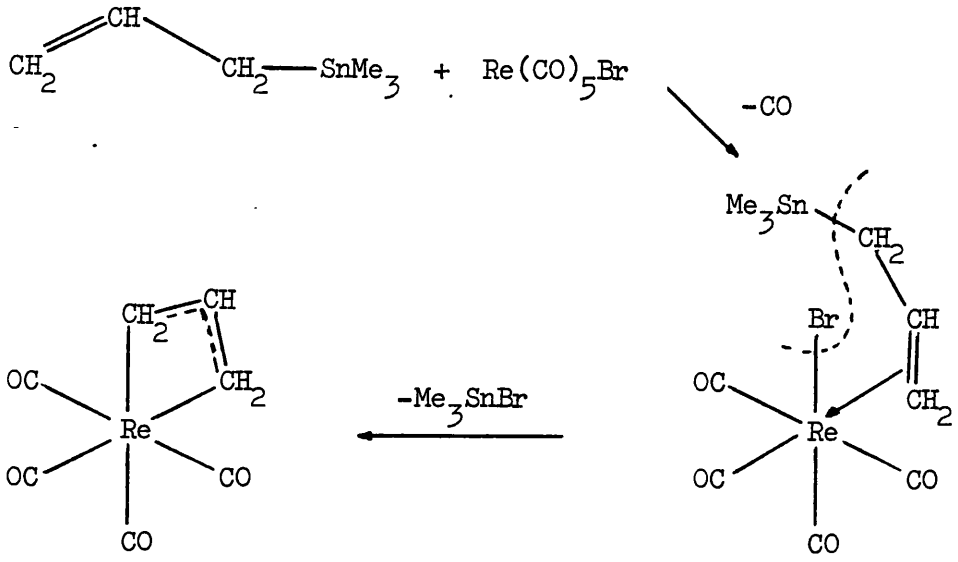

Figure 1.12: Proposed mechanism for the reaction between $Re(CO)_5Br$ and $allylSnMe_3$

(v) Loss of HX from simple alkene complexes:

$[(\eta^2\text{-}C_3H_6)PdCl_2]_2 \longrightarrow [(\eta^3\text{-}C_3H_5)PdCl]_2 + 2HCl$ [163]

(vi) Ligand exchange:

There are many examples where ligand exchange in previously prepared η^3-allyl complexes affords new compounds [146,154,164,165] e.g.

$[(\eta^3\text{-}C_3H_5)Mo(CO)_2(bipy)Cl] + TlSC_6F_5 \longrightarrow$

$[(\eta^3\text{-}C_3H_5)Mo(CO)_2(bipy)(SC_6F_5)] + TlCl$ [154]

$[(\eta^3\text{-}C_3H_5)_2Mo_2(CO)_4(\mu\text{-}Cl)_3]^- + 2C_5H_5N \longrightarrow$

$2[(\eta^3\text{-}C_3H_5)Mo(CO)_2(C_5H_5N)_2Cl] + Cl^-$ [165]

Direct reaction with metals:

Allyl halides react directly with highly reactive transition metals prepared either by alkali-metal reduction of metal salts in hydrocarbon solvents[166,167] or by vaporisation and cocondensation[168] e.g.

$$Pd(powder) + 2allylBr \longrightarrow [(\eta^3\text{-allyl})PdBr]_2$$ [166]

$$Ni(atoms) + allylBr \longrightarrow [(\eta^3\text{-allyl})NiBr]_2$$ [168]

(viii) η^1 to η^3 conversions:

There are many examples reported in the literature in which, by various methods, an η^1-allyl group may be converted to an η^3-allyl group, with expulsion of another ligand e.g.

$$[(\eta^1\text{-}C_3H_5)Mn(CO)_5] \xrightarrow[\text{or heat}]{h\nu} [(\eta^3\text{-}C_3H_5)Mn(CO)_4] + CO$$ [93,118]

$$[(\eta^5\text{-}C_5H_5)_2(\eta^1\text{-}C_3H_5)_2W] + HPF_6 \longrightarrow [(\eta^5\text{-}C_5H_5)_2(\eta^3\text{-}C_3H_5)W]PF_6 + C_3H_6$$ [169]

$$[(\eta^5\text{-}C_5H_5)(\eta^1\text{-}C_3H_5)Ru(CO)_2] \xrightarrow{h\nu} [(\eta^5\text{-}C_5H_5)(\eta^3\text{-}C_3H_5)Ru(CO)] + CO$$ [132]

(ix) Specific reactions:

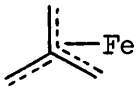

$$\text{-}Fe(CO)_3 + HCl \longrightarrow [(\eta^3\text{-}2\text{-}MeC_3H_4)Fe(CO)_3Cl]$$ [170]

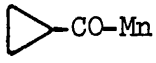

$$\text{-}CO\text{-}Mn(CO)_5 + PPh_3 \longrightarrow [(\eta^3\text{-}C_3H_5)Mn(CO)_3(PPh_3)] + 3CO$$ [171]

$$[(\eta^3\text{-}C_3H_5)_2Ni] + Fe_2(CO)_9 + 2I_2 \longrightarrow 2[(\eta^3\text{-}C_3H_5)Fe(CO)_3I] + NiI_2 + 3CO$$ [172]

$$2[(\eta^7\text{-}C_7H_7)Mo(CO)_2Br] \xrightarrow{NaOCH_3} [(\eta^7\text{-}C_7H_7)(\eta^3\text{-}C_7H_7)Mo_2(CO)_2(\mu\text{-}OCH_3)_3] + 2CO$$ [173]

$$NiCl_2 + C_4H_6 + 2PPh_3 + Zn \xrightarrow{C_6H_6/EtOH} [(\eta^3\text{-}C_4H_7)Ni(PPh_3)_2][ZnCl_3]$$ [174]

$$[(\eta^5\text{-}C_5H_5)Mo(CO)_3(\eta^1\text{-}CH_2C{\equiv}CH)] + CH_3OH \longrightarrow [(\eta^5\text{-}C_5H_5)Mo(CO)_2(\eta^3\text{-}2\text{-}CH_3CO_2C_3H_4)]$$ [73]

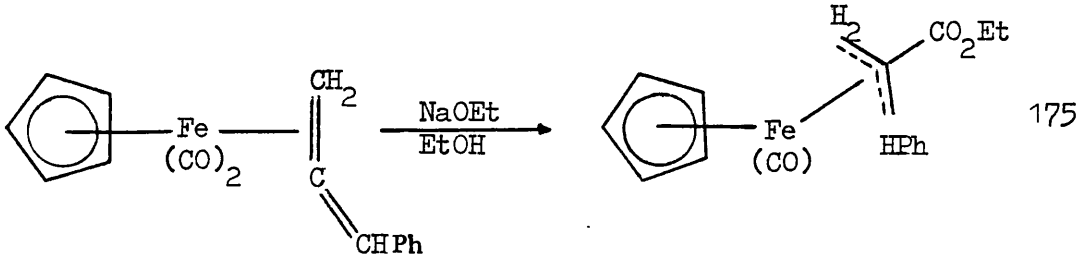

175

$$[HPt(PPh_3)_2(CO)][ClO_4] + CH_2{=}CHCH_2NH_2 \longrightarrow [(\eta^3\text{-}C_3H_5)Pt(PPh_3)_2][ClO_4] + CO + NH_3 \quad ^{176}$$

$$[HRh(PF_3)_4] + CH_2{=}C{=}CH_2 \longrightarrow [(\eta^3\text{-}C_3H_5)Rh(PF_3)_3] + PF_3 \quad ^{177}$$

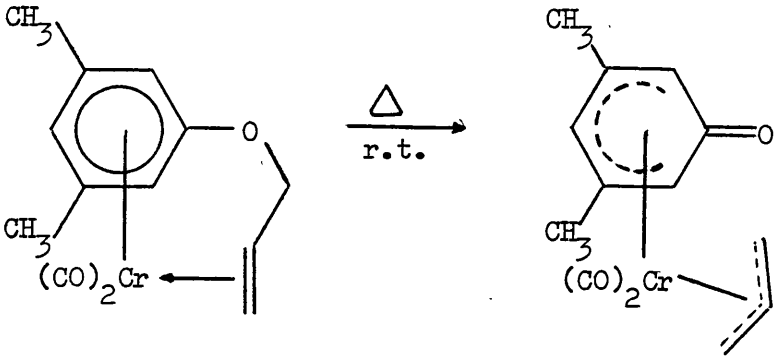

178

ALLYL COMPLEXES OF GROUP VI TRANSITION METALS

From the preceding discussion it is evident that numerous allyl complexes of the Group VI transition metals have been prepared and characterised. These range from the 'pure allyl' or so called isoleptic complexes e.g. $[Cr(C_3H_5)_3]$ to those containing a wide variety of mixed ligands. The majority of such complexes obey the eighteen electron rule and often form stable crystalline solids. In cases where this is not so, the compounds formed are exceedingly reactive, for example, a solution of trisallylchromium (formally 15e) absorbs carbon monoxide at one atmosphere pressure even at $-60^{\circ}C$, leading eventually to the complete expulsion of allyl ligands, thus:

$$[(C_3H_5)_3Cr] + 6CO \longrightarrow Cr(CO)_6 + \tfrac{3}{2}C_6H_{10} \quad ^{1}$$

Allyl complexes of the Group VI metals frequently exhibit interesting structural and spectral features in addition to novel and synthetically useful reactions. The following selected examples most of which merely involve an unsubstituted C_3H_5 unit, provide an

indication of the range of such compounds. There are of course numerous examples of substituted and cyclic allyl derivatives of these metals, many of which are described alongside the unsubstituted allyls in the references cited below.

Isoleptic Allyl Compounds

As well as $[Cr(C_3H_5)_3]$ complexes of the type $[(\eta^3\text{-}C_3H_5)_4M]$ (M = Mo,W)[1] and $[(\eta^3\text{-}C_3H_5)(\mu\text{-}C_3H_5)M]_2$ (M =Cr,Mo,W)[1,48,198] fall into this category. Crystal structure determinations on the latter[48,198] indicate that the allyl groups, including the two bridging ligands, are all symmetrical and that the complexes contain extremely short M-M quadruple bonds (Figure 1.13).

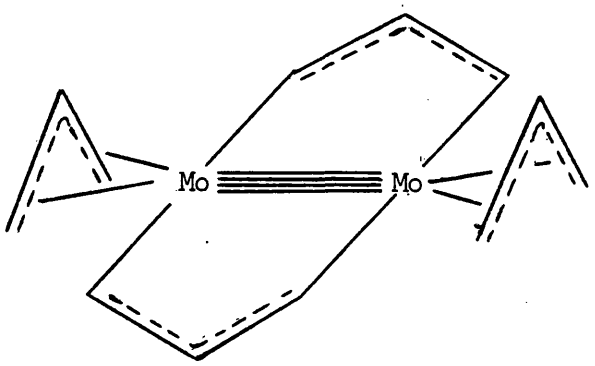

Figure 1.13: A diagrammatic representation of the structure of $[(C_3H_5)_2Mo]_2$[198]

Allyl Carbonyl Complexes

Many of the known allyl complexes of Group VI transition metals also contain carbonmonoxide ligands. Of these, by far the most common type is that containing an allyldicarbonyl unit in which the terminal carbon atoms of a symmetrically bonded allyl group usually lie above two mutually cis-carbonyl groups (Figure 1.14). Cationic, neutral and anionic complexes of this type have been isolated and

may contain a variety of bidentate nitrogen donors[53,145-147,154,164,165,170,181-187], phosphorus or arsenic donors[34,35,42,113,188-192], and oxygen donors[25,146,147,173,192,193], in conjunction with halides, pseudo halides, monodentate Lewis bases, carboxylates etc.

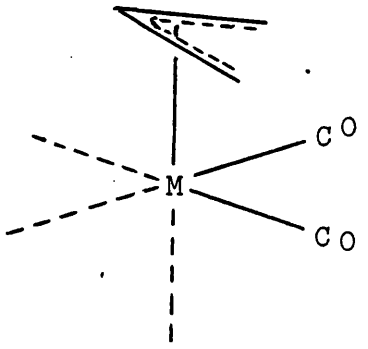

Figure 1.14: The allyldicarbonyl unit in a pseudo octahedral environment

Typical examples are $[(\eta^3\text{-}C_3H_5)W(SC_6F_5)(CO)_2(phen)]$[154], $[(\eta^3\text{-}C_3H_5)Mo(AsPh_3)(CO)_2(bipy)][BF_4]$[164] and $[(\eta^3\text{-}C_3H_5)Mo(NCS)(CO)_2(bipy)]$[182]. In the latter example a single crystal X-ray structure determination has confirmed the above stereochemistry for the $C_3H_5M(CO)_2$ unit. This fac-arrangement of the allyl group and two carbonyl ligands has been found for at least ten other complexes, for example $[(\eta^3\text{-}C_3H_5)Mo(CO)_2(salal)py]$[218] and $[(\eta^3\text{-}C_3H_5)MoCl(CO)_2(dppe)]$[190] and has been proposed for many others, such as $[(\eta^3\text{-}C_3H_5)MoX(CO)_2(dpae)]$[189] (X = Cl, Br, I),on the basis of spectroscopic data. Many complexes of this type are prepared from $[(\eta^3\text{-}C_3H_5)MoX(CO)_2(MeCN)_2]$ by a simple ligand displacement reaction. However the complex $[(\eta^3\text{-}C_3H_5)MoCl(CO)_2\{P(OMe)_3\}_2]$, which was readily prepared by this route, adopts an unusual pentagonal bipyramidal structure[52] (Figure 1.15, overleaf).

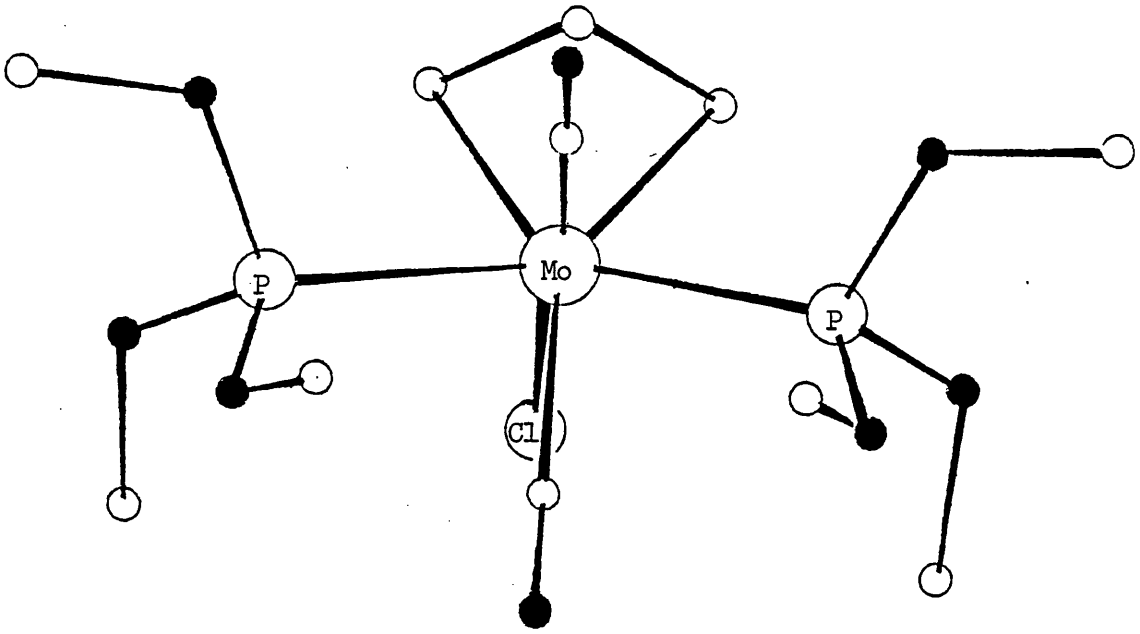

Figure 1.15: The structure of $[(\eta^3\text{-}C_3H_5)MoCl(CO)_2\{P(OMe)_3\}_2]$

Some of the first examples of anionic complexes containing the $C_3H_5Mo(CO)_2$ unit were prepared by the reaction of allyl halides with the parent β-diketonate tetracarbonyl anions $[M(CO)_4(diket)]^-$ [147] (M = Mo, W) to give complexes of the type $AsPh_4[(\eta^3\text{-}C_3H_5)WCl(CO)_2(hfacac)]$ and $Et_4N[(\eta^3\text{-}C_4H_7)MoCl(CO)_2(acac)]$. Recent X-ray studies have again confirmed the presence of the usual allyldicarbonyl stereochemistry (Figure 1.14) in the related compounds $[(\eta^3\text{-}C_3H_5)Mo(py)(CO)_2(acac)]$ [25] and

$$[(\eta^3\text{-}C_3H_5)W(O_2CCF_3)(CO)_2(CH_3OCH_2CH_2OCH_3)]$$ [193].

Although less common, there are several examples of allylcarbonyl complexes containing other than two carbonyl groups. An interesting example is provided by the compound $[(\eta^5\text{-}C_5H_5)(\eta^3\text{-}C_3H_5)Mo(CO)(NO)][PF_6]$ [194] for which variable temperature NMR studies show that, in solution, an equilibrium

exists between the endo- and exo- isomers, thus:

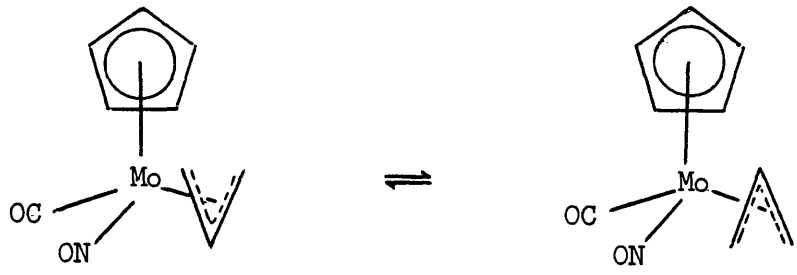

Three carbonyl groups and a monodentate carboxylate ligand are present in $[(\eta^3\text{-}C_3H_5)MoCl(CO)_3(O_2CC_4H_9)]^-$ and related complexes[147], whilst tricarbonyl complexes containing a 'monohapto' allyl group are also known e.g. $[(\eta^5\text{-}C_5H_5)(\eta^1\text{-}C_3H_5)M(CO)_3]$, (M = Mo,W)[28,195]. Irradiation of cyclohexane solutions of hexacarbonyltungsten and allyl halides with ultra violet light yields unstable complexes of the formulae $[(\eta^3\text{-}C_3H_5)W_2(CO)_6Cl_3]$ and $[(\eta^3\text{-}C_3H_5)WX(CO)_4]$ (X = Br,I)[196]. Infrared spectral results suggest that the latter must contain a cis-$M(CO)_4$ moiety although variable temperature NMR spectra indicate the presence of isomers resulting from conformational changes about the allyl group. Several compounds containing the ions $[(\eta^3\text{-}C_3H_5)_2Mo_2(CO)_4X_3]^-$ (X = Cl,Br) have been isolated[117,165,197] and the presence of triply bridging halogens postulated. This feature has been confirmed for $[(\eta^3\text{-}C_3H_5)Mo(CO)_2(MeCN)_3][(\eta^3\text{-}C_3H_5)_2Mo_2(CO)_4(\mu\text{-}Cl)_3]$ by an X-ray crystal structure determination[21].

Allyl Complexes with Carbocyclic Ligands

Examples of Group VI transition metal-allyl complexes which also contain a carbocyclic ligand (such as cyclopentadiene) are numerous and many of these have been mentioned previously. Four particularly interesting examples are outlined in the reaction scheme below,

which represents a system in which the allyl moiety may be η^1-,η^2-, or η^3- bonded[199].

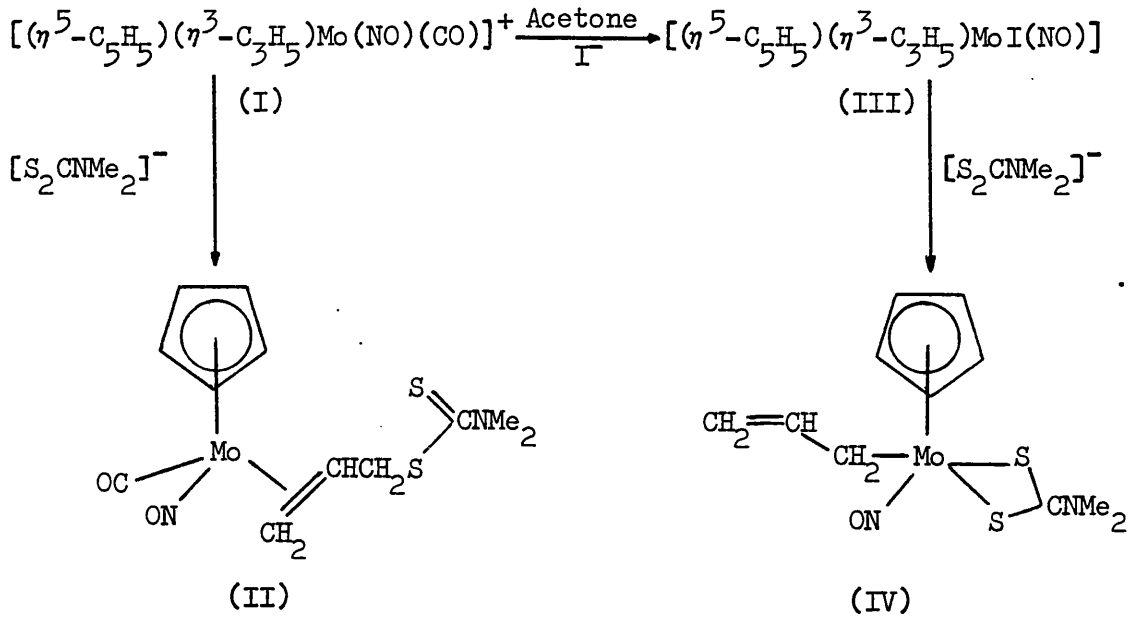

(II) (IV)

The complex (I) reacts with $[S_2CNMe_2]^-$ giving (II), which contains a substituted η^2-allyl group, probably derived from (I) by direct nucleophilic attack of the dithiocarbamate at a terminal allylic carbon atom. If, however, the reactant is the iodide ion, CO is expelled and the η^3-bonded group is retained in the resulting complex (III). This complex may subsequently be treated with $[S_2CNMe_2]^-$ to afford (IV) in which the allyl group is forced to adopt the monohapto configuration by the polyhapto dithiocarbamate group. Structures (II) and (IV) have been confirmed by X-ray analysis[199].

Other typical examples which contain the allyl ligand in conjunction with carbocyclic ligands are $[(\eta^6\text{-}C_6H_6)(\eta^3\text{-}C_3H_5)_2Mo]$ and derivatives thereof[156,157] and $[(\eta^5\text{-}C_5H_5)_2M(\eta^1\text{-}C_3H_5)_2]$, (M = Mo,W)[169]. The latter may easily be protonated by dilute aqueous HPF_6 to give the corresponding η^3-allyl complexes $[(\eta^5\text{-}C_5H_5)_2M(\eta^3\text{-}C_3H_5)][PF_6]$ with liberation of propane.

ALLYL COMPLEXES OF THE GROUP VII TRANSITION METALS

In contrast to those from Group VI, allyl derivatives of the Group VII transition metals are very few in number and the majority of these are manganese compounds. The first η^1-allyl manganese complexes were prepared in 1958[200] by the reaction of the pentacarbonylmanganate(I) anion with allyl halides. Their subsequent decarbonylation, achieved either by heating at 80°C or by u.v. irradiation, afforded the corresponding η^3-allyl complexes [93,118] according to the equation:

$$Na[Mn(CO)_5] + C_3H_5Cl \longrightarrow [(\eta^1\text{-}C_3H_5)Mn(CO)_5] + NaCl$$

$$[(\eta^1\text{-}C_3H_5)Mn(CO)_5] \xrightarrow{80^\circ C \text{ or } h\nu} [(\eta^3\text{-}C_3H_5)Mn(CO)_4] + CO$$

Since that time reports[39,40,102,128,212,215] of similar carbonylmanganese compounds such as $[(\eta^1\text{-}RC_3H_4)Mn(CO)_5]$, (R = 1-Me, 2-Me, 1,1-$Me_2$, 1-Ph, 1-Cl)[215] and $[(\eta^3\text{-}RC_3H_4)Mn(CO)_4]$, (R = Et, i-Pr)[39], (R = 1-FC_6H_4, 2-FC_6H_4)[212] have appeared sporadically, including some mentioned in patents[201a-d].

Until very recently the only reported ligand substituted η^3-allylmanganese complex was $[(\eta^3\text{-}C_3H_5)Mn(CO)_3(PPh_3)]$[171] which was produced by a concomitant decarbonylation and ring opening process in the reaction between PPh_3 and the cyclopropyl derivative, as follows:

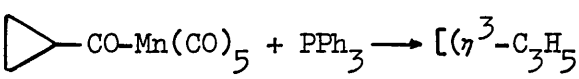

A rather similar ring opening reaction[22] yielded the first η^3-allyl manganese complex containing a sulphur donor ligand thus:

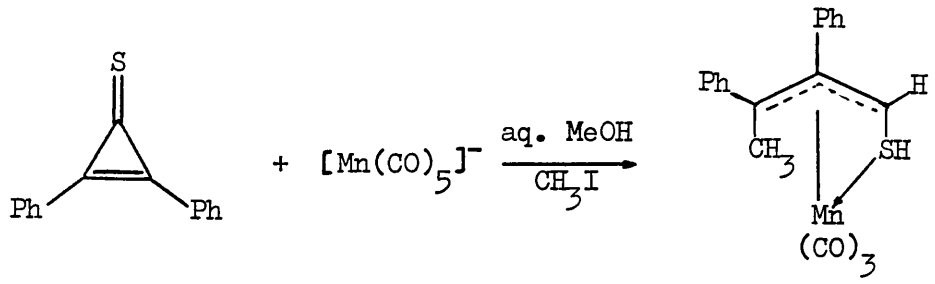

Whilst this work was in progress a report appeared in which the preparation of the derivatives $[(\eta^3\text{-}C_3H_5)Mn(CO)_{4-n}(PR_3)_n]$, (R = OMe, n = 2,3; R = Et, Oi-Pr, n = 2), by partial substitution of CO, was described[11]. All of the complexes catalysed the hydrogenation of alkenes with rates that increased as the steric bulk of the phosphorus ligand increased. The trisubstituted derivative was very active but suffered from competing loss of allyl ligand to give propene and concomitant catalyst death. A novel Mn(I) - Mn(III) couple, involving the intervention of an η^1-allylmanganese(III) complex and ligand dissociation, was proposed to account for the catalytic activity but rapid η^3- $\rightleftharpoons$ η^1- interconversion could not be observed spectroscopically.

Allylrhenium compounds are restricted to the isoleptic derivative $[(\eta^3\text{-}C_3H_5)_4Re_2]$[23] and a few allylrheniumcarbonyl complexes*. The former complex was first synthesised in 1977 by the reaction of rhenium pentachloride with excess allylmagnesiumchloride. Its structure was subsequently determined by a single crystal X-ray

*with the exception of an early, unsubstantiated report[217] of the complex:

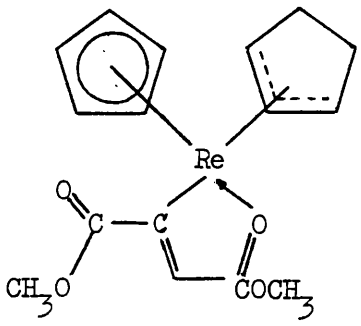

study[216] (Figure 1.16).

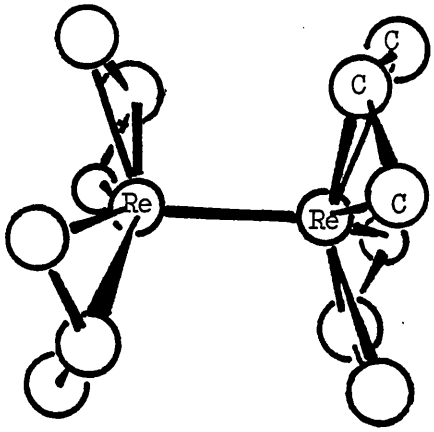

Figure 1.16: The structure of tetra-η^3-allyldirhenium

In contrast to the Cr and W compounds of the same stoichiometry[48, 198], $[(\eta^3\text{-}C_3H_5)_4Re_2]$ has a highly symmetrical structure (D_{2h}) and no bridging allyl groups. There are ten essentially metal-based electrons, two beyond the eight required to form a quadruple Re-Re bond. A molecular orbital calculation reveals that the highest filled orbital is of Re-Re δ*-antibonding character which effectively cancels out the corresponding Re-Re δ-bonding component. Thus, with two strong π- and one σ- bonding orbitals, the Re-Re interaction can be considered to be essentially a triple bond.

Two reports mention the isolation of the η^1-allylpentacarbonylrhenium complexes $[(\eta^1\text{-}C_3H_5)Re(CO)_5]$[132] and $[(\eta^1\text{-}1,1\text{-}Me_2C_3H_3)Re(CO)_5]$[215] from the reactions of $Na[Re(CO)_5]$ with the appropriate allyl halide. However these compounds were at best only impure and poorly characterised.

Compounds such as $[(\eta^3\text{-}2\text{-}MeC_3H_4)Re(CO)_4]$ and $[(\eta^3\text{-}1\text{-}PhC_3H_4)Re(CO)_4]$ as well as the unsubstituted η^3-allyltetracarbonyl and corresponding manganese complexes, were also obtained[158,159] from the reactions of $Re(CO)_5X$ (X = Cl, Br) with the appropriate η^1-allyltrimethyltin

reagents, $[(RC_3H_4)Sn(CH_3)_3]$, (Figure 1.12). However, full infrared and NMR spectral data were not given. In addition $[(\eta^3\text{-}C_3H_5)Re(CO)_4]$ was produced, although less effectively, from $Re_2(CO)_{10}$ and $[(\eta^1\text{-}C_3H_5)Sn(CH_3)_3]$ in refluxing diglyme (a reaction time of 100 h was required).

Addendum

In June 1979 whilst this script was in preparation a preliminary communication[219] appeared which reported the preparation of η^3-allyltetracarbonylmanganese from the reaction of dimanganese decacarbonyl with allylchloride by phase transfer catalysis. The same technique was also employed to obtain the triphenylphosphine substituted derivative $[(\eta^3\text{-}C_3H_5)Mn(CO)_3(PPh_3)]$[171] which the authors erroneously claimed to be a new compound.

CHAPTER TWO

ANIONIC TRICARBONYL DERIVATIVES OF MOLYBDENUM AND TUNGSTEN AND THEIR REACTIONS WITH ALLYL HALIDES

INTRODUCTION

Highly nucleophilic carbonylmetallate anions are known to react with allyl halides under very mild conditions. As a result many new η^3-allyl halides[146,147,221-223], including some previously unobtainable chromium compounds[145], have been prepared by this method.

The anionic tricarbonyl derivatives $[MX(CO)_3L_2]^-$ (M = Mo, W; X = halide; L_2 = bipy; phen), first prepared from $[M(CO)_3cht]$[224] (eq 2.1), are the precursors for the facile synthesis of a series of η^3-allyl complexes, $[(\eta^3\text{-}C_3H_5)MX(CO)_2L_2]$

$$[M(CO)_3cht] + L_2 + X^- \longrightarrow [MX(CO)_3L_2]^- + cht \qquad 2.1$$

A more convenient route to these anions was subsequently found[146] (eq 2.2), but full experimental details were not given.

$$[M(CO)_4bipy] + X^- \longrightarrow [MX(CO)_3bipy]^- + CO \qquad 2.2$$

In this chapter the preparation and characterisation of a series of molybdenum and tungsten anions are described and their use in the synthesis of several η^3-allyl derivatives is illustrated.

EXPERIMENTAL

Details of physical techniques, solvents and starting materials appear in appendices 1 and 2.

Preparation of $[MX(CO)_3L_2]^-$ salts

These complexes were prepared by the direct reaction of *cis*-$[M(CO)_4L_2]$ (M = Mo, W; L_2 = bipy, phen) with Ph_4PX or Et_4NX (X = Cl, Br or I) in CH_3CN/toluene or CH_3CN/xylene mixtures.

Typical procedures for one molybdenum and one tungsten complex are given below and individual details of reaction conditions, yields and elemental analyses for each complex prepared by this route are presented in Table 2.1.

$Ph_4P[MoCl(CO)_3phen]$: $[Mo(CO)_4phen]$ (0.388 g/1 mmol) was reacted with Ph_4PCl (0.562 g/1.5 mmol) in refluxing 4:1 toluene/acetonitrile (40 cm^3) for 1 h. On cooling, the product was filtered off, washed rapidly with a little cold methanol and dried *in vacuo*. Yield 97%.

$Et_4N[WI(CO)_3bipy]$: $[W(CO)_4bipy]$ (0.452 g/1 mmol) was heated with finely divided Et_4NI (1.29 g/5 mmol) in refluxing 8:1 xylene/acetonitrile (40 cm^3) for 8 h. The product was filtered off, washed rapidly with ice-cold water (as were all iodo products), then methanol and dried *in vacuo*. Yield 93%.

Preparation of $[(\eta^3\text{-}RC_3H_4)MX(CO)_2L_2]$ complexes :

The complex $R_4Z[MX(CO)_3L_2]$ (1 mmol) was added to a stirred solution of allyl halide (10 mmol) in methanol (10 cm^3) at ambient temperatures. When the reaction was complete (0.2 h for Mo and 1.0 h for W compounds) the solid product was filtered off, washed with methanol and dried *in vacuo*. The complex $[(\eta^3\text{-}2\text{-}MeC_3H_4)WCl(CO)_2bipy]$ crystallised only slowly and the reaction mixture was allowed to stand at 0°C for 72 h prior to filtration. Yields, analytical and selected infrared data appear in Table 2.4.

Preparation of $[(\eta^3\text{-cyclohexenyl})MoBr(CO)_2bipy]$:

$Ph_4P[MoBr(CO)_3bipy]$ (0.38 g/0.5 mmol) was added to a deoxygenated solution of 3-bromocyclohexene (0.81 g/5 mmol) in chloroform (5 cm^3) at -15°C. The product was filtered off, washed with dichloromethane and dried *in vacuo*. Yield 42%. The corresponding 1,10-phenanthroline

Table 2.1: Experimental and Analytical Data for the Anionic Tricarbonyl Complexes

Complex (No.)	Solvent[a]	Mole Ratio $M(CO)_4L_2$: R_4ZX	Reaction Time (h)	Yield (%)	Elemental Analysis found (calc) (%) C	H	N
$Ph_4P[MoCl(CO)_3phen]$ (I)	T	1:1.5	1	97	61.5 (63.7)	4.00 (3.84)	4.04 (3.81)
$Ph_4P[MoBr(CO)_3phen]$ (II)	T	1:1.5	1	86	58.3 (60.1)	3.51 (3.62)	3.81 (3.62)
$Ph_4P[MoI(CO)_3phen]$ (III)	Xy	1:3	16	~70	b		
$Ph_4P[MoCl(CO)_3bipy]$ (IV)	T	1:1.5	1	97	61.1 (62.5)	4.12 (3.97)	3.93 (3.94)
$Ph_4P[MoBr(CO)_3bipy]$ (V)	T	1:1.5	1	96	56.6 (58.8)	4.11 (3.73)	3.94 (3.71)
$Ph_4P[MoI(CO)_3bipy]$ (VI)	Xy	1:3	16	~90	b		
$Ph_4P[WCl(CO)_3phen]$ (VII)	Xy	1:1.5	16	95	56.1 (56.9)	3.70 (3.43)	3.47 (3.40)
$Ph_4P[WBr(CO)_3phen]$ (VIII)	Xy	1:1.5	16	94	52.6 (54.0)	3.39 (3.25)	3.17 (3.23)
$Ph_4P[WI(CO)_3phen]$ (IX)	Xy	1:3	16	~60	b		
$Ph_4P[WCl(CO)_3bipy]$ (X)	Xy	1:1.5	16	98	54.2 (55.6)	3.58 (3.53)	3.35 (3.51)

Table 2.1: Cont'd

Complex (No.)	Solvent[a]	Mole Ratio $M(CO)_4L_2$: R_4ZX	Reaction Time (h)	Yield (%)	Elemental Analysis found (calc) (%) C	H	N
$Ph_4P[WBr(CO)_3bipy]$(XI)	Xy	1:1.5	16	83	52.8 (52.7)	3.37 (3.35)	3.23 (3.32)
$Et_4N[MoCl(CO)_3phen]$(XII)	T	1:1.5	4	86	52.0 (52.5)	5.20 (5.37)	7.89 (7.99)
$Et_4N[MoCl(CO)_3bipy]$(XIII)[c]	T	1:1.5	4	66	49.7 (50.3)	5.67 (5.62)	8.19 (8.37)
$Et_4N[MoI(CO)_3phen]$(XIV)	Xy	1:5	8	53	44.5 (44.8)	4.66 (4.57)	7.03 (6.81)
$Et_4N[MoI(CO)_3bipy]$(XV)	Xy	1:5	8	58	41.3 (42.5)	4.30 (4.76)	6.82 (7.00)
$Et_4N[WI(CO)_3phen]$(XVI)	Xy	1:5	8	90	38.2 (39.2)	3.83 (4.00)	5.76 (5.96)
$Et_4N[WI(CO)_3bipy]$(XVII)	Xy	1:5	8	93	37.4 (37.0)	4.12 (4.14)	5.90 (6.17)

[a] T = 4:1 Toluene/CH_3CN; Xy = 8:1 Xylene/CH_3CN. [b] Unstable and always contaminated with decomposition products. [c] Readily forms a hydrate which is easily desiccated over silicagel.

anion reacted in a similar manner, but the η^3-cyclohexenyl derivative so formed was easily oxidised and could not be prepared in an analytically pure state.

RESULTS AND DISCUSSION

$[MX(CO)_3L_2]^-$ tricarbonyl anions

The anionic complexes listed in Table 2.1 were all obtained in high yields as deep purple/black crystalline solids, which slowly decomposed on standing in air to reform cis-$[M(CO)_4L_2]$ as one of the decomposition products. With the exception of all but the very unstable iodo-molybdenum complexes, the compounds could be stored indefinitely in sealed, nitrogen filled ampoules. For example, a two-year-old sample of $Ph_4P[WBr(CO)_3bipy]$ reacted smoothly with allyl bromide to give $[(\eta^3\text{-}C_3H_5)WBr(CO)_2bipy]$ in 90% yield. The complexes were at most sparingly soluble in non-coordinating solvents, such as $CHCl_3$ and CH_2Cl_2, and were immediately solvolysed by coordinating solvents, as demonstrated by infrared measurements and by the NMR spectrum of $Et_4N[MoCl(CO)_3bipy]$ in CH_3CN. After only three minutes the NMR pattern of this complex in the aromatic region clearly indicated the presence of at least two species and as time progressed the entire spectrum lost intensity, whilst becoming even more complex. Consequently most of the spectroscopic data were confined to solid state measurements (Table 2.2).

Complexes of stoichiometry $[MX(CO)_3L_2]$, where L_2 is a bidentate ligand, may exist in either of two isomeric forms (Figure 2.1). The facial arrangement allows π-bonding to occur between each of the three carbonyl groups and three separate metal d_π-orbitals,

whereas for the mer-isomer, two of the carbonyl ligands are in direct competition for the same d_π-orbital. Thus by neglecting other factors and considering only simple π-bonding effects, the fac-isomer is favoured and is indeed by far the most common stereochemistry found for metal tricarbonyl complexes. However the meridional arrangement is possible and sometimes occurs in complexes which also contain other good π-acceptors, (e.g. phosphines and phosphites[225]), where other factors such as steric hindrance become important.

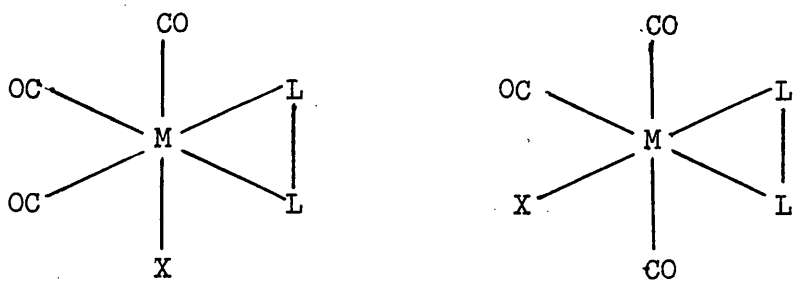

fac-isomer mer-isomer

Figure 2.1: Facial and meridional tricarbonyl isomers

Complexes of this type belong to the point group C_s and group theory (Appendix 3) predicts that both isomers should give rise to three infrared active ν(CO) vibrations (2A' + A"). In general the fac-isomer may be distinguished from the mer-isomer by band intensity measurements. In the former case three strong absorptions are predicted whereas one weak and two strong bands are expected for the latter[229]. For example the compound $[MnBr(CO)_3\{P(OMe)_2Ph\}_2]$ is a rare example where both the fac- and mer- isomers have been isolated. The fac-isomer has three strong ν(CO) bands at 2045, 1975, 1927 cm^{-1} whereas the mer-isomer has a weak band at 2052 and strong bands at 1972, 1929 cm^{-1}. These structural assignments were originally based upon infrared data[230] but subsequently confirmed

by single crystal X-ray diffraction studies[231].

All the anions reported in this chapter show three strong carbonyl absorptions in the solid state and in solution in non-coordinating solvents (Table 2.2), and are consequently assigned a *fac*-configuration. In coordinating solvents at room temperature the anions are rapidly solvolysed (eq 2.3) and the infrared spectra of acetonitrile solutions of any of the complexes showed features characteristic of $[M(CH_3CN)(CO)_3L_2]$, (M = Mo, W and L_2 = bipy, phen). Thus when complexes I, II, III, XII, and XIV, for example, were dissolved in acetonitrile the infrared spectra were identical, within experimental error, to that reported for $[Mo(CH_3CN)(CO)_3phen]$ which has bands at 1910 and 1787 cm^{-1} in the $\nu(CO)$ region [225].

$$PPh_4[MoCl(CO)_3phen] + CH_3CN \longrightarrow [Mo(CH_3CN)(CO)_3phen] + Ph_4PCl \qquad 2.3$$

If the spectra were recorded within seconds of dissolution, or in acetonitrile saturated with halide ions which retarded the solvolytic reaction, the carbonyl stretching frequencies of both the solvolysed and the anionic species were discernable. On the basis of very similar spectroscopic results, it had previously been reported that for the closely related complexes $Me_4N[MoI(CO)_3bipy]$ and $[Ni(phen)_3][Mo(SH)(CO)_3bipy]$[224] *fac*- to *mer*- isomerisation occurred on dissolution in acetonitrile. Since there was no evidence of *fac*- to *mer*- isomerisation in any of the complexes reported here and in view of the above results such a process seems unlikely. Indeed the infrared band positions quoted for the proposed *mer*-isomers coincide extremely well with those of the expected solvated species.

Force constant data for the carbonyl anions (Table 2.2) were calculated by the Cotton-Kraihanzel method as modified by Dalton et al.[220].

Table 2.2: Selected Infrared and Force Constant Data for the Carbonyl Anions $[MX(CO)_3L_2]^-$

Complex	ν(MX) (cm^{-1})	ν(CO)[a] (cm^{-1})			Carbonyl force constants (mdyne/Angstrom)[b]			
		A'_1	A'_2	A''	K_c	$K_{c'}$	K_1	K_2
I	227	1880	1765	1742	0.59	0.60	12.9	13.4
II	146	1886	1751br		0.50	0.70	12.9	13.4
III		1884	1764	1742	0.60	0.63	12.9	13.5
IV	227	1887	1769	1748	0.59	0.62	12.9	13.5
V	153	1886	1772	1751	0.57	0.60	13.0	13.5
VI		1884	1763	1740	0.61	0.63	12.8	13.5
VII	234	1874	1764	1743	0.55	0.57	12.8	13.4
		1880	1760	1743[c]	0.56	0.62	12.8	13.4
VIII	147	1874	1743br		0.48	0.68	12.8	13.2
		1880	1766	1745[c]	0.57	0.59	12.9	13.4
IX		1875	1746br		0.47	0.67	12.8	13.3
X	230	1877	1763	1743	0.56	0.59	12.8	13.4
XI	158	1867	1753	1736	0.54	0.60	12.7	13.3
		1879	1758	1742[c]	0.56	0.63	12.8	13.4
XII	229	1879	1763	1719	0.74	0.60	12.7	13.4
XIII	222	1884	1766	1737	0.45	0.64	13.2	13.7
XIV	129	1900	1778br		0.60	0.64	12.6	13.2
		1892	1771	1751[c]	0.59	0.63	13.0	13.6
XV	129	1899	1756br		0.51	0.72	12.7	13.2
XVI	127	1870	1747	1726	0.64	0.62	12.8	13.5
		1881	1762	1752[c]	0.51	0.62	12.9	13.4
XVII	125	1877	1737br		0.53	0.75	13.0	13.5

[a] Recorded on Nujol mulls unless otherwise stated

[b] Calculated by the procedure given in reference 220

[c] Solution data in CH_2Cl_2

Details of group theory, secular equations and computer programs used in these calculations appear in appendices 3, 4 and 5 respectively. In previous studies of cis-$[L_2YM(CO)_3]$ derivatives, where L_2 = bipy or phen and Y = monodentate Lewis base and M = Mo or W[220,225], the assignment $A'_1 > A'_2 > A''$ has been used in such calculations, resulting in axial $\nu(CO)$ force constants K_2 greater than equatorial $\nu(CO)$ force constants K_1, as expected from simple π-bonding considerations. However for some manganese complexes cis-$[MnX(CO)_3L_2]$ containing an electronegative halide ligand X, K_1 becomes larger than K_2 and the A'' mode has been assigned to the band at intermediate frequency[220,234,236]. Since the anionic Group VI complexes under consideration are isoelectronic with neutral Group VII derivatives of the same stoichiometry, both assignments were thought worthy of consideration and consequently force constants were also calculated based on the alternative band order $A'_1 > A'' > A'_2$ (Table 2.3).

Table 2.3: Force Constant Data for Alternative Assignments for $Et_4N[MoCl(CO)_3phen]$ (XII) and $Et_4N[MoI(CO)_3phen]$ (XIV)

Complex	Assignments			Force Constants				Delta
	A'_1	A'_2	A''	K_c	K_c'	K_1	K_2	K_c/K_c'
XII	1879	1763	1719	0.74	0.60	12.7	13.4	1.22
	1879	1719	1763	0.27	0.82	12.8	13.1	0.33
XIV	1892	1771	1751	0.59	0.63	13.0	13.6	0.93
	1892	1751	1771	0.38	0.73	13.0	13.4	0.51

These calculations yielded $\nu(CO)$ force constants of a similar magnitude to those given in Table 2.2 with $K_2 > K_1$, but with widely divergent interaction constants (delta = K_c/K_c', as low as 0.33),

and hence this second possible assignment seems less likely than that used in Table 2.2. Neither K_1 or K_2 varies significantly throughout the molybdenum or tungsten series. This contrasts with some manganese pentacarbonyl halide complexes where the nature of the halogen has a marked effect on the cis-CO stretching constant[234]. This was attributed to 'direct ligand-ligand donation' via a mechanism illustrated in Figure 2.2.

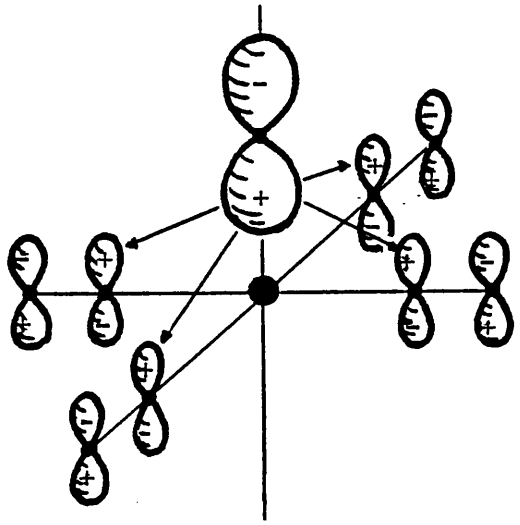

Figure 2.2: Orbitals involved in halide to carbonyl electron transfer

Thus as the halide orbitals become more diffuse, the interaction becomes greater and K(cis) smaller. This effect does not extend to the anionic complexes under discussion probably as a direct result of the increased covalent radii of these Group VI elements.

The effect of back-donation of the increased charge on the central atom of the anions into carbon-2π-orbitals results in a significant decrease of the ν(CO) force constants compared with many neutral fac-$[MY(CO)_3L_2]$ species[220,225,238]. For example the values of K_1 and K_2 for the anions are in the ranges 12.6 - 13.0 and 13.2 - 13.7 respectively, whereas for $[Mo\{(PhO)_3P\}(CO)_3bipy]$ K_1 = 13.9, K_2 = 14.6 and for $[W(Ph_3P)(CO)_3phen]$ K_1 = 13.4, K_2 = 14.2 [220].

Two solid state infrared spectra (Nujol), typical of the anionic complexes in this series are illustrated in Figure 2.3. Apart from

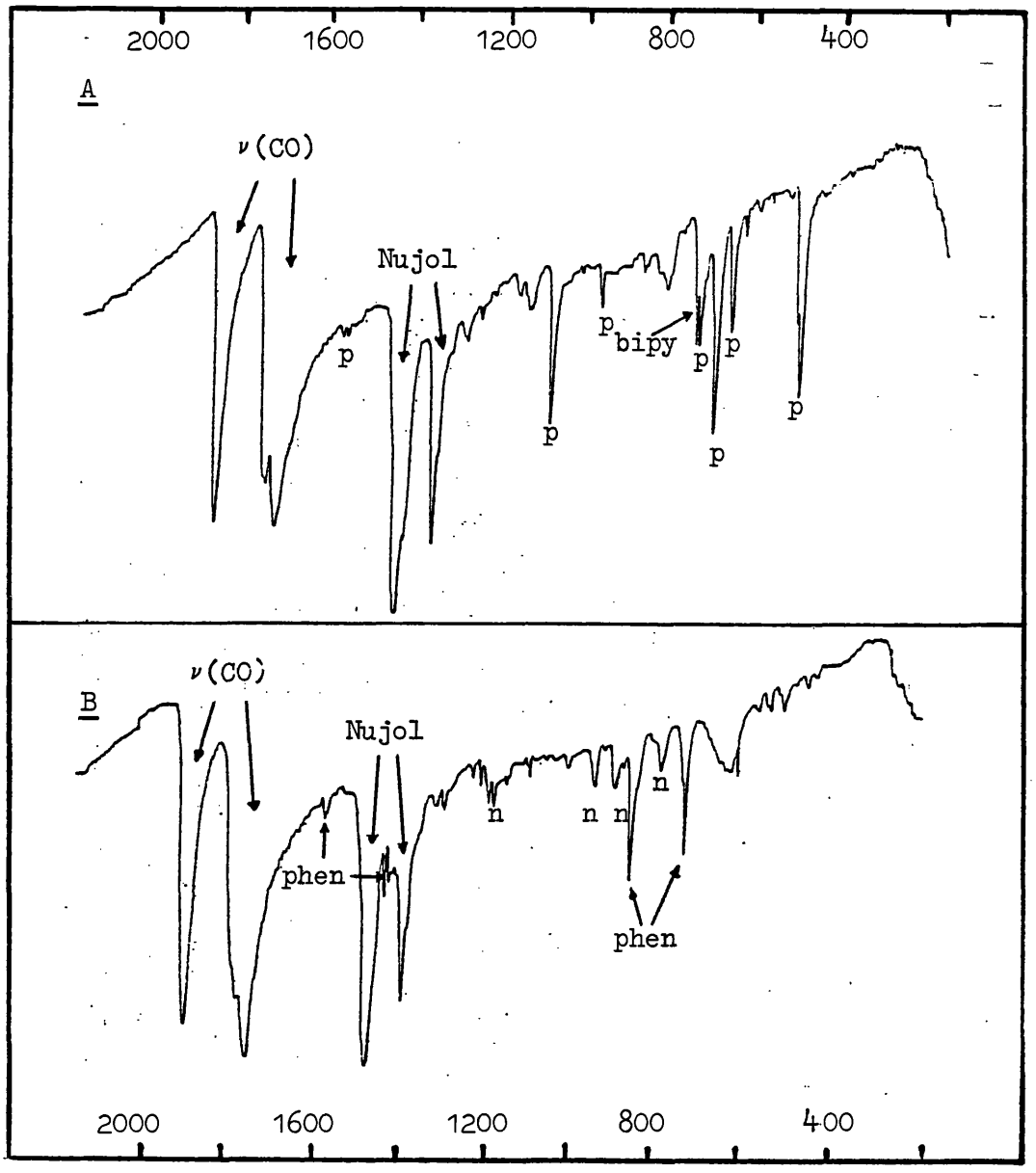

Figure 2.3: Solid state infrared spectra (Nujol) 2000-200 cm^{-1}

A. $Ph_4P[MoCl(CO)_3bipy]$ B. $Et_4N[WI(CO)_3phen]$

(p = bands due to Ph_4P^+; n = bands due to Et_4N^+.)

the three very strong ν(CO) absorptions, the only other medium-strong features may be assigned to vibrations arising from the bidentate ligands bipy or phen and the respective cations Ph_4P^+ and Et_4N^+. No bands due to ν(MC) or δ(MCO) could be assigned with confidence.

In the far-infrared region only a single strong halogen-sensitive band was found for each of the anions (Table 2.2). These could be

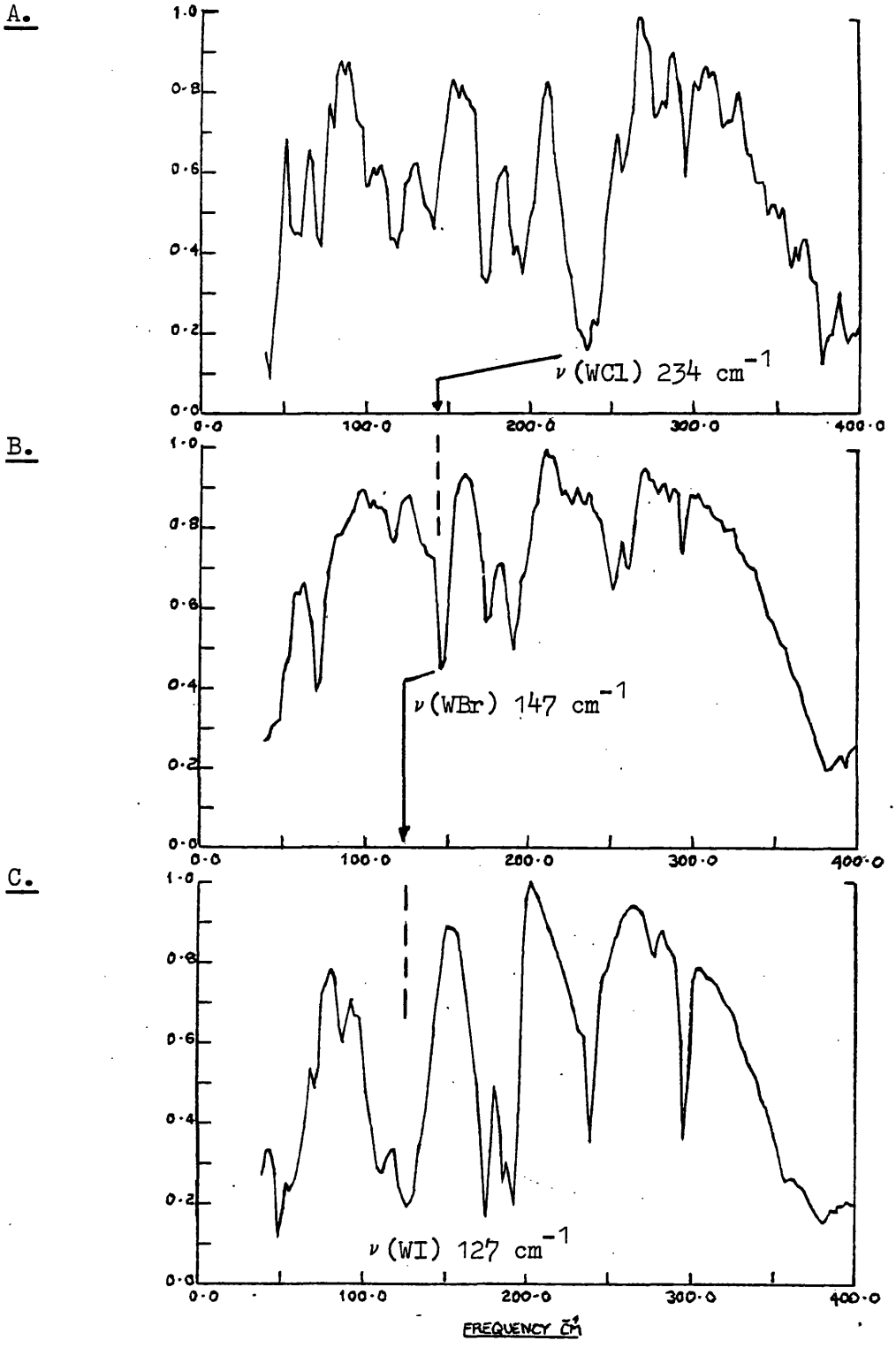

Figure 2.4: Far-infrared spectra of the complexes:

A. $Ph_4P[WCl(CO)_3phen]$ B. $Ph_4P[WBr(CO)_3phen]$

C. $Et_4N[WI(CO)_3phen]$

Ratios: $\nu(WCl)/\nu(WBr) = 0.63$; $\nu(WCl)/\nu(WI) = 0.54$

confidently assigned to ν(MX) because the ν(MBr)/ν(MCl) and ν(MI)/ν(MCl) frequency ratios found were extremely close to the expected values of 0.67 and 0.53 respectively. (Using the simple harmonic oscillator approximation, the MX frequencies are inversely proportional to the square root of the reduced mass of MX. Thus when only X changes the ν(MX) ratio is, theoretically, equal to the square root of the inverse ratio of atomic masses of X). This mass effect is clearly illustrated in Figure 2.4. The ν(MX) bands of the substituted anions occurred at even lower wavenumbers than those of the corresponding halopentacarbonyl anions $[MX(CO)_5]^-$ [239]. For example in $[MoX(CO)_5]^-$ ν(MoCl) = 248 cm^{-1} and ν(MoBr) = 165 cm^{-1} whereas for the anions $[MoX(CO)_3phen]^-$ prepared in this work ν(MoCl) = 229 cm^{-1} and ν(MoBr) = 146 cm^{-1}. This probably reflects the increased back-donation of negative charge onto fewer carbonyl ligands causing an increased trans-effect of CO on halogen.

Allyl derivatives $[(\eta^3\text{-allyl})MX(CO)_2L_2]$

With the exception of 3-bromocyclohexene, allyl halides reacted readily with the carbonyl anions under discussion in methanol at room temperature or below to give high yields of η^3-allyl-metal(II) derivatives (Table 2.4). This route is particularly useful for the tungsten analogues which are difficult to prepare by the direct reaction of the hexacarbonyl with allyl halides in the presence of a bidentate ligand, the procedure normally adopted for the molybdenum complexes[154,197], due to the slow kinetics and competing reactions of the tungsten intermediates. Under the same conditions η^3-cyclohexenyl derivatives, and particularly those of 1,10-phenanthroline, were always contaminated with other products. Using

Table 2.4: Selected Analytical and Infrared Data for the Complexes $[(\eta^3\text{-allyl})MX(CO)_2L_2]$

Complex	Yield (%)	Elemental Analysis[a] found (calc) (%)			Infrared Data (cm^{-1}) $\nu(CO)$[b]		$\nu(MX)$
		C	H	N	A_1	B_1	
$[(\eta^3\text{-}2\text{-}MeC_3H_4)MoCl(CO)_2phen]$ (XVIII)	86				1923	1847	266
$[(\eta^3\text{-}2\text{-}MeC_3H_4)MoCl(CO)_2bipy]$ (XIX)	90	46.7 (48.2)	3.74 (3.79)	6.95 (7.03)	1925	1836	267
$[(\eta^3\text{-}1\text{-}MeC_3H_4)MoBr(CO)_2phen]$ (XX)	83				1925	1838	168
$[(\eta^3\text{-}1\text{-}MeC_3H_4)MoBr(CO)_2bipy]$ (XXI)	82	42.2 (43.4)	3.40 (3.41)	5.73 (6.32)	1920	1831	164
$[(\eta^3\text{-}C_6H_9)MoBr(CO)_2phen]$ (XXII)	ca.20				1918	1835	
$[(\eta^3\text{-}C_6H_9)MoBr(CO)_2bipy]$ (XXIII)	42	47.1 (46.1)	3.61 (3.65)	5.73 (5.97)	1920	1838	166
$[(\eta^3\text{-}2\text{-}MeC_3H_4)MoBr(CO)_2bipy]$ (XXIV)	89	44.8 (43.4)	3.84 (3.41)	6.52 (6.32)	1928	1840	164
$[(\eta^3\text{-}C_3H_5)MoCl(CO)_2bipy]$ (XXV)	91				1930	1839	278
$[(\eta^3\text{-}C_6H_9)MoCl(CO)_2phen]$ (XXVI)	ca.25				1921	1839	
$[(\eta^3\text{-}C_3H_5)MoI(CO)_2phen]$ (XXVII)	64				1945	1873	

Table 2.4: Cont'd

Complex	Yield (%)	Elemental Analysis[a] found (calc) (%)			Infrared Data (cm^{-1}) ν(CO)[b]		ν(MX)
		C	H	N	A_1	B_1	
[(η^3-2-MeC_3H_4)WCl(CO)$_2$bipy] (XXVII)	78	38.0 (39.5)	3.10 (3.11)	5.76 (5.76)	1918	1841	268
[(η^3-C_3H_5)WBr(CO)$_2$phen] (XXIX)	85				1919	1852, 1821	
[(η^3-C_3H_5)WI(CO)$_2$phen] (XXX)	88				1940, 1918	1852, 1826	139
[(η^3-C_3H_5)WI(CO)$_2$bipy] (XXXI)	92				1918	1839	137

[a] Only determined for pure, new complexes

[b] Recorded on Nujol mulls, all bands are strong

the available infrared evidence these impurities were tentatively identified as an oxo-species, probably [$MoOBr_3$phen] which has ν(MoO) at 968 cm^{-1} [240], and a dihalotricarbonyl product, probably [$MoBr_2(CO)_3$bipy], having ν(CO) bands at 2060, 1985, 1930 cm^{-1} [241]. The occurence of such products was probably due to small amounts of free bromine produced in the starting material by the fission of the very labile carbon-bromine bond during the reaction.
In order to prepare an analytically pure sample of [$(\eta^3$-$C_6H_9)MoBr(CO)_2$bipy] a change of solvent and a lower reaction temperature were necessary. The colours of the complexes ranged from brick-red [$(\eta^3$-$C_6H_9)MoBr(CO)_2$bipy] through maroon [$(\eta^3$-2-$MeC_3H_4)MoCl(CO)_2$phen] to black [$(\eta^3$-$C_3H_5)WI(CO)_2$bipy].

Only complexes XVIII and XIX were sufficiently soluble for NMR measurements and good spectra were obtained only in liquid sulphur dioxide at -57°C. The results are summarised in Table 2.5. The spectra are in accord with the presence of a symmetrically bound η^3-allyl group with equivalence of the two syn- and of the two anti- protons. The pronounced upfield shift of the allyl-methyl group is no doubt caused by the shielding effect of the aromatic rings. The shift is greatest for the 1,10-phenanthroline complex and in the closely related compound [$(\eta^3$-2-$MeC_3H_4)Mo(NCS)(CO)_2$phen] the allyl-methyl group has been shown to lay over the plane of the aromatic ligand[181]. The NMR spectra in the aromatic region are also indicative of a highly symmetrical structure. Thus the complexes display an NMR pattern, in this region, which is very similar to the uncoordinated ligands (phen: 8.70 (d), 8.20 (d), 7.80 (q), 7.25 (s); bipy: 8.65 (d), 8.40 (d), 7.75 (t), 7.20 (m); δppm, relative to TMS in $CDCl_3$) although a general downfield shift of approximately 0.4 ppm is noteworthy.

Table 2.5: NMR Spectra in Liquid SO_2 for the Complexes $[(\eta^3\text{-allyl})MoCl(CO)_2L_2]$

Complex: $[(\eta^3\text{-2-Me}C_3H_4)MoCl(CO)_2L_2]$	Chemical Shift (δ) (multiplicity)	Assignment (rel. intensity)	Coupling Constants (Hz)
(XVIII)	9.12 (d)	H_4 (2)	J_{23} 8.0
	8.58 (d)	H_2 (2)	J_{34} 5.0
	8.02 (s)	H_1 (2)	
L_2 = 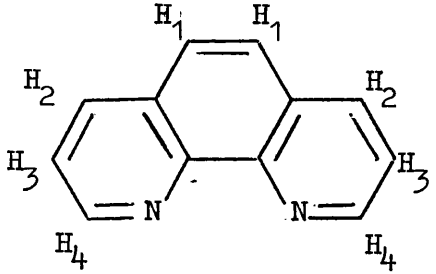	7.90 (q)	H_3 (2)	
	3.13 (s)	H_{syn} (2)	
	1.46 (s)	H_{anti} (2)	
	0.70 (s)	CH_3 (3)	
(XIX)	8.79 (d)	H_4 (2)	J_{12} 8.0
	8.25 (d)	H_1 (2)	J_{23} 7.0
	8.06 (t)	H_2 (2)	J_{34} 5.5
L_2 = 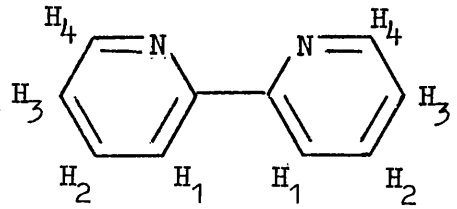	7.61 (t)	H_3 (2)	
	2.98 (s)	H_{syn} (2)	
	1.40 (s)	H_{anti} (2)	
	1.01 (s)	CH_3 (3)	

The low solubilities of the remaining complexes in Table 2.4 in suitable NMR solvents precluded their full characterisation. However the absence of an uncoordinated C=C stretch in their solid state infrared spectra and their general spectroscopic similarity to complexes XVIII and XIX and to other complexes of this stoichiometry with known structures[181,182] indicated they were also members of the η^3-allyl series.

As expected for cis-dicarbonyls the most prominent feature of the infrared spectra of these compounds were two very strong bands, of approximately equal intensity, in the ν(CO) region separated by about 80 cm^{-1}. Some of the tungsten compounds had more complex infrared spectra in this region (Table 2.4) and as suggested previously[154], this may be accounted for by the existence of isomers although no further details were given. It was also noticeable that if solutions of some of the molybdenum complexes in liquid SO_2 were allowed to evaporate and the solid state spectra subsequently reexamined they had also developed split bands although there was no evidence for retention of SO_2 in the complex. Two possible structures for the isomers may be the symmetrical (A) and unsymmetrical (B) arrangements shown in Figure 2.5. This has been confirmed for the complex $[(\eta^3\text{-}C_3H_5)Mo(py)(CO)_2(acac)]$ which exists in both forms A and B in solution but is exclusively of structure B in the solid state[25].

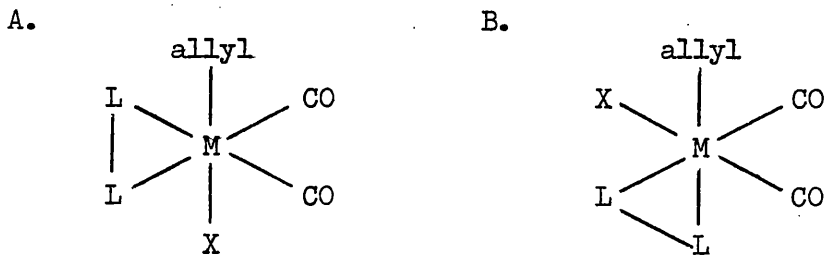

Figure 2.5: Geometrical isomers for $[(\eta^3\text{-}C_3H_5)MX(CO)_2L_2]$ complexes

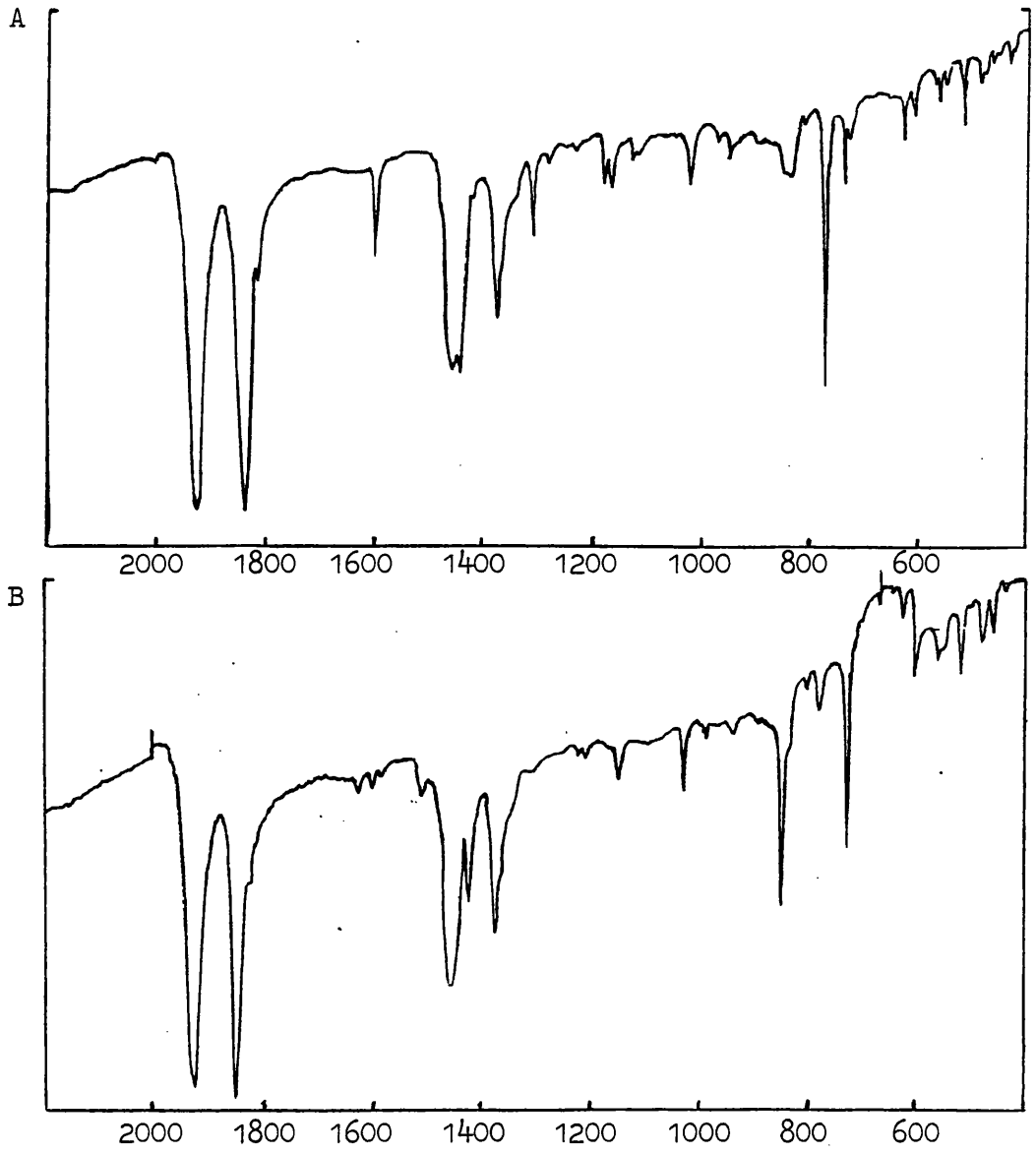

Figure 2.6: The solid state infrared spectra (Nujol 2400-400 cm^{-1})

A. $[(\eta^3\text{-}2\text{-}MeC_3H_4)MoCl(CO)_2bipy]$

B. $[(\eta^3\text{-}2\text{-}MeC_3H_4)MoCl(CO)_2phen]$

Other bands between 2400-400 cm^{-1} in the infrared spectra (Figure 2.6) could be assigned to modes typical of the coordinated aromatic ligands. For example, all the 1,10-phenanthroline complexes had medium-strong bands at approximately 1510, 1430, 1150, 850 and 730 cm^{-1} and all the bipyridyl complexes had similar intensity bands at about 1600, 1450, 1320, 1170 (d) and 780 cm^{-1}. There were

Table 2.6: Infrared Spectra (400-40 cm^{-1}) of the Complexes $[(\eta^3\text{-allyl})MX(CO)_2phen]$ (M = Mo, X = Cl,Br; M = W, X = I)

Complex (X; reference number)			$M(CO)_4phen$		Tentative
Cl(XVIII)	Br(XX)	I(XXX)	Mo	W	Assignment
293 m	291 s	298 m	292 m	303 m	ligand
266 vs					ν(MoCl)
256 m,sh	244 m	244 m	244 m	247 m	ligand
215 m	215 sh	209 s			
208 w,sh	208 vs	205 m	204 s	206 s	ν(MN)
191 s	195 sh	188 s	183 m	188 m	
176 w	178 m	173 w			
	168 vs				ν(MoBr)
154 s	154 w	159 w			
142 m	142 w	149 m			
		139 vs			ν(WI)
127 m	127 w	127 w,sh			
103 m	105 s	107 m	102 w	102 w	ligand

Ratios: $\nu(MCl)/\nu(MBr) = 0.63$; $\nu(MCl)/\nu(MI) = 0.52$.

no bands in the infrared spectra which could be assigned with any certainty to vibrational modes of the allyl group.

The η^3-allyl-metal(II) compounds had more complex far-infrared spectra than the corresponding tricarbonyl anions and consequently the ν(MX) frequencies were more difficult to assign with confidence. The most halogen-sensitive bands in the entire infrared spectra of some of the complexes XVIII - XXXI are given in Table 2.4 and are tentatively assigned as ν(MX). These values are in good agreement with data on analogous ditertiary phosphine derivatives[189] and the ratios ν(MCl) : ν(MBr) and ν(MCl) : ν(MI) correlate closely with those of the parent anions. The major features in the far-infrared spectra of three representative 1,10-phenanthroline complexes are tabulated, together with those of $[M(CO)_4phen]$[242] for comparison, in Table 2.6. In addition to ν(MX) vibrations, bands due to ν(MN), δ(CMC), δ(CMN), δ(NMN) and ligand skeletal modes are also expected in this region of the spectrum. In Table 2.6 some of these have been tentatively assigned by comparison with the known spectra of the uncoordinated 1,10-phenanthroline and the complexes $[M(CO)_4phen]$[242] (M = Mo, W).

In an attempt to elucidate the mechanism of the allyl oxidative addition, several 'mixed halide' reactions, in which different halides were attached to the parent anion and allyl halide respectively, were carried out. Two such reactions are represented by equation 2.4 and equation 2.5.

$$Ph_4P[MoCl(CO)_3bipy] + C_3H_5Br \longrightarrow [(\eta^3\text{-}C_3H_5)MoCl(CO)_2bipy] + Ph_4PBr + CO \qquad 2.4$$

$$Et_4N[MoBr(CO)_3bipy] + C_3H_5Cl \longrightarrow [(\eta^3\text{-}C_3H_5)MoBr(CO)_2bipy] + Et_4NCl + CO \qquad 2.5$$

The retention of the original metal-halogen bond could be clearly demonstrated by infrared spectroscopy, e.g. the product in eq. 2.4 had a strong ν(MoCl) absorption at 278 cm^{-1} and no band in the 170 cm^{-1} region due to ν(MoBr). Two mechanisms A and B which allow for retention of halide are given in the following reaction scheme.

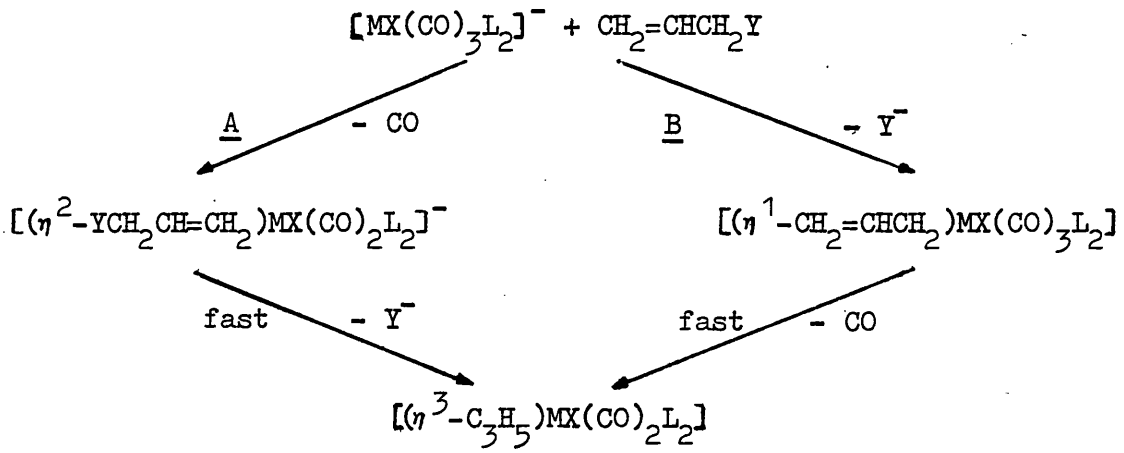

Scheme A involves loss of CO with subsequent coordination of the C=C bond to the metal, in line with evidence recently presented for the allyl halide - $[IrX(CO)(PR_3)_2]$ systems[57]. This type of mechanism is further supported by detailed kinetic studies in which the reaction of allyl bromide with $[Mo(CO)_4phen]$ afforded the product $[(\eta^3\text{-}C_3H_5)MoBr(CO)_2phen]$ in accordance with the first order rate law: $-d[Mo(CO)_4phen]/dt = K_1[Mo(CO)_4phen]$[243]. To account for the observations, slow fission of the M—CO bond trans to nitrogen as the rate determining step, followed by rapid reaction of allyl bromide via coordination of the C=C bond was proposed.

Scheme B involves the direct nucleophilic attack of the metal atom on the α-carbon atom of the allyl halide, resulting in the formation of a σ-bonded intermediate. Attempts to isolate a related σ-bonded species by reaction of the anions with methyl iodide proved unsuccessful but this does not preclude mechanism B, as any such intermediate is expected to be extremely reactive, perhaps having only a transient existence.

When 'mixed halide' reactions were carried out with iodo-anions it was noticeable that, when allowed to proceed for longer periods, the products exhibited not two but four peaks in the ν(CO) region of their infrared spectra. For example in the reaction between $[MoI(CO)_3phen]^-$ and C_3H_5Br, peaks due to both the iodo- and bromo-species were evident in the solid state spectra of the product. That this occurred by initial formation of the iodo- product and subsequent halide exchange was demonstrated when a pure sample of $[(\eta^3\text{-}C_3H_5)MoI(CO)_2phen]$ was stirred with a ten-fold excess of Br^- in acetone. The ν(CO) band positions for the bromide and iodide products (Table 2.4) were sufficiently different to enable the exchange to be monitored by infrared spectroscopy and the results are shown in Figure 2.7. Thus in order to ensure that the required halide is present after the allyl oxidation reaction it is necessary to isolate the products from the reaction mixture soon after their formation.

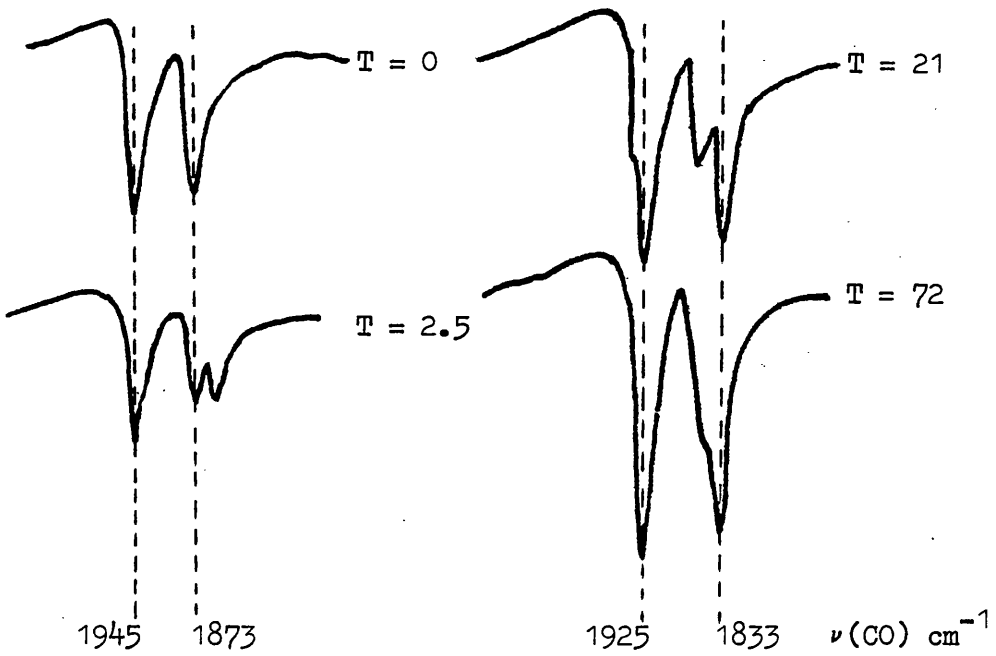

Figure 2.7: Solid state infrared spectra of $[(\eta^3\text{-}C_3H_5)MoI(CO)_2phen]/Br^-$ reaction mixtures - variation with time (T)(h)

Because of the highly nucleophilic nature of the metal carbonyl anions, their reaction with allyl halides provides an extremely useful route for the synthesis of η^3-allyl-metal complexes. For example, under the mild conditions employed by this method high yields of previously inaccessible tungsten complexes were obtained. The preparation of a range of anionic tricarbonyl derivatives $[MX(CO)_3L_2]^-$ (M = Mo, W; X = Cl, Br, I; L_2 = bipy, phen) was accomplished using only minor changes in the basic method. It therefore seems probable that this route could be extended to produce many different anions and consequently a wide variety of substituted η^3-allyl complexes of the Group VI transition metals.

CHAPTER THREE

THE PREPARATION AND CHARACTERISATION OF TRI-μ-HALOGENOHEXACARBONYLDIMETALLATE(I) ANIONS OF MANGANESE AND RHENIUM

INTRODUCTION

As the reaction between allyl halides and various anionic transition metal species provides a facile route to η^3-allyl complexes of Group VI metals, an attempt was made to extend the range of Group VII allyl-metal complexes using this procedure. Although the pentacarbonylmanganate(-I) anion is known to react with allyl chloride[93,118], it was found that the reactions of some halogeno-carbonylmanganate(I) anions, under similar conditions, failed to produce allyl containing products. Instead, these investigations led to the preparation of a series of triply halogeno-bridged binuclear anions of both manganese and rhenium.

A wide range of mono- and bi- nuclear halogenocarbonyl anions are known for the Group VII transition metals. The mononuclear anions are of two types, either cis-$[M(CO)_4XY]^-$ where M = Mn[210,211] or M = Re[208,244,245], X and Y are various combinations of Cl, Br, I atoms, or fac-$[Re(CO)_3X_3]^{2-}$ (X = Cl, Br, I)[208,244-246]. The stereochemistry about the metal in these complexes has been unequivocally established by infrared spectroscopy in the ν(CO) and ν(MX) regions. Thus the former type has four strong ν(CO) bands (3A' + A") and the latter two (A_1 + E for C_{3v} symmetry) or three (2A' + A" for lower symmetries), and two medium intensity ν(ReX) bands. These results are in agreement with group theoretical predictions for cis-tetracarbonyl and fac-tricarbonyl stereochemistries respectively. Similarly, on the basis of spectroscopic results and application of the 18-electron formalism the anions $[M_2(CO)_8X_2]^{2-}$ (M = Mn, X = Cl, Br, I; M = Re, X = I)[211,244] have been assigned metal-metal bonded structures (A in Figure 3.1). The types $[Re_2(CO)_7X_2Y]^-$ (X = Y = Cl, Br, I; X = Cl, Y = Br)[244,245] and $[Re_2(CO)_6X_4]^{2-}$ (X = Cl, Br)[246] are alternatively thought to

contain two bridging halogen atoms and no metal-metal bond (B and C in Figure 3.1), although in each case distinction between the two most likely structures was not possible.

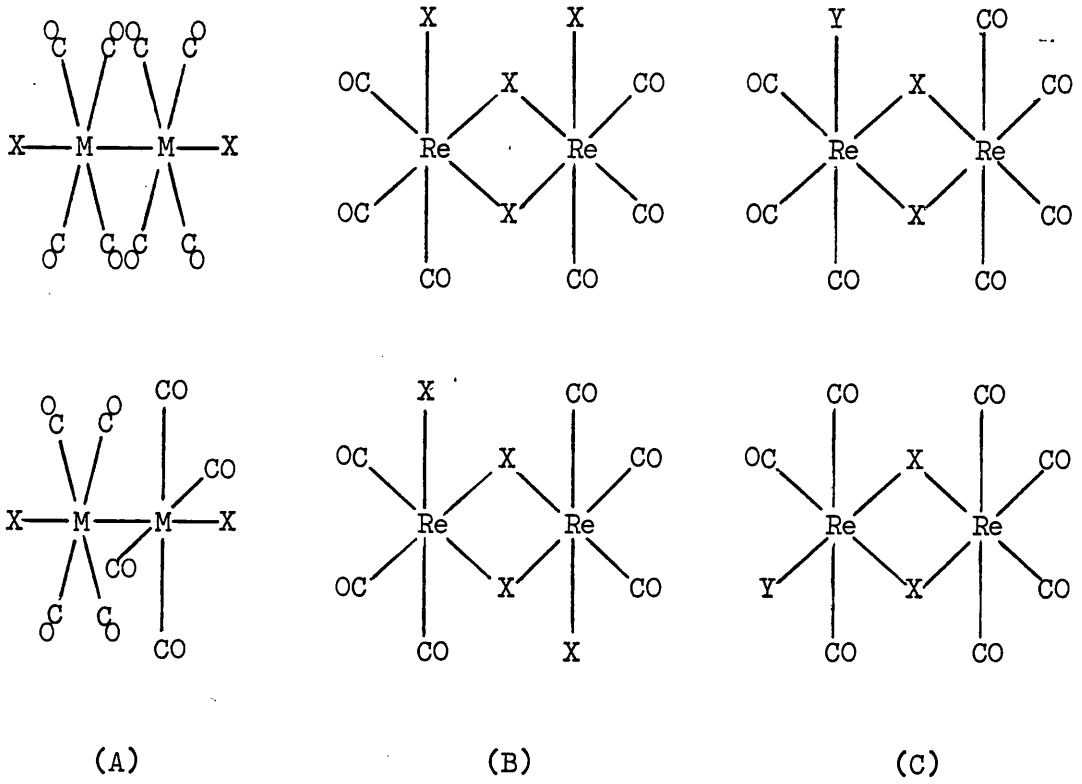

Figure 3.1: Possible structures for binuclear halogenocarbonyl anions of manganese or rhenium

Recent reports have indicated that the tri-μ-halogeno anions $[M_2(CO)_6(\mu\text{-}X)_3]^-$ may also be prepared. Thus $Et_4N[Mn_2(CO)_6(\mu\text{-}Cl)_3]$ [247] was isolated as the product of a photochemical reaction between $Mn_2(CO)_{10}$ and Et_4NCl in chloroform. The bromo-analogue was formed in a similar manner but could not be separated from other products produced simultaneously. X-ray diffraction studies on species of the formulae $[(\eta^6\text{-arene})Re_3(CO)_9X_3]$, (arene = C_6H_5Me, X = Br; arene = C_6Me_6, X = Cl)[248] and [HPOR][$Re_2(CO)_6X_3$] (POR = octaethylporphine, X = Cl; POR = mesoporphine IX dimethylester, X = Br)[249, 250], have shown that they also contain triply-bridged anions (Figure 3.2). The former type therefore also contain

$[(\eta^6\text{-arene})Re(CO)_3]^+$ cations.

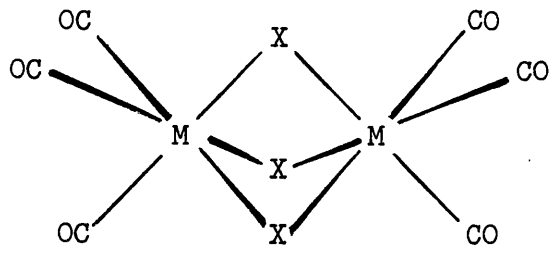

Figure 3.2: Structure of the tri-μ-halogenobridged anions $[M_2(CO)_6(\mu\text{-}X)_3]^-$

Thus apart from $Et_4N[Mn_2(CO)_6(\mu\text{-}Cl)_3]$ which was obtained at best in 19% yield from chloroform and in only 1% yield from diglyme[247], all other pure complexes containing such anions also involve either carbonyl containing cations or very complex porphinium cations. The complexes described in this chapter were prepared in high yield and contained only the simple Et_4N^+ cation which minimised interference in the $\nu(CO)$ region of the vibrational spectra. Because of the high local symmetry and low number of atoms in the anions, a reasonably complete group-theoretical treatment of the vibrational spectra was possible.

EXPERIMENTAL

Details of physical methods and starting materials appear in Appendices 1 and 2. Particular attention was paid to the purification of nitromethane for conductance measurements and chloroform for synthetic work described in this Chapter.

Preparation of $Et_4N[Mn_2(CO)_6(\mu\text{-}X)_3]$, (X = Cl, Br)

(a) The reactions between $Mn(CO)_5X$ (2 mmol) and Et_4NX (1 mmol) were allowed to proceed for 5 h in refluxing chloroform (30 cm^3). After cooling, the pure products were filtered off, washed with a little ethanol and water and dried *in vacuo*. Samples could be recrystallised from acetone-diethyl ether as orange needles although this resulted in a considerable reduction in yield.

(b) $Et_4N[Mn_2(CO)_6(\mu\text{-}X)_3]$, (X = Cl, Br) could also be obtained from the decomposition of $Et_4N[Mn(CO)_4X_2]$ in refluxing chloroform. However separation of the desired products from Et_4NX also formed in the decomposition, by washing with copious amounts of water and subsequent recrystallisation from acetone-diethyl ether, reduced the yield to below 10%.

Preparation of $Et_4N[Re_2(CO)_6(\mu\text{-}X)_3]$, (X = Cl, Br, I)

The reactions between $Re(CO)_5X$ (2 mmol) and Et_4NX (1 mmol) were carried out in refluxing decalin (30 cm^3) for 18 h. The resulting grey solids were filtered off and washed with light petroleum (40 - 60) before dissolution in anhydrous dichloromethane (80 cm^3). The dichloromethane solutions were then filtered and the volume of the filtrates reduced to *ca.* 10 cm^3 to afford colourless crystalline products which were recrystallised from further dichloromethane and dried *in vacuo*.

Yields and elemental analyses of all the above complexes are listed in Table 3.1, together with melting points and conductivity data.

Table 3.1: Yields, Melting Points, Conductivity and Analytical Data

Complex	Yield (%)	M.p. (°C)	Conductivity, Λ_M [b] (S cm^2 mol^{-1})	Elemental Analysis found (calc) (%) C	H	N
$Et_4N[Mn_2(CO)_6(\mu\text{-}Cl)_3]$	91	190[a]	83.7	32.5 (32.7)	4.33 (3.92)	2.52 (2.72)
$Et_4N[Mn_2(CO)_6(\mu\text{-}Br)_3]$	93	196[a]	78.9	26.0 (25.9)	3.24 (3.11)	1.92 (2.16)
$Et_4N[Re_2(CO)_6(\mu\text{-}Cl)_3]$	77	191	74.6	21.6 (21.6)	2.84 (2.59)	1.74 (1.80)
$Et_4N[Re_2(CO)_6(\mu\text{-}Br)_3]$	68	206	74.6	18.7 (18.5)	2.40 (2.21)	1.38 (1.54)
$Et_4N[Re_2(CO)_6(\mu\text{-}I)_3]$	78	>260[a]	73.0	16.1 (16.0)	2.09 (1.92)	1.22 (1.33)

[a] with some decomposition

[b] determined for 10^{-3} Molar solutions at 25°C

RESULTS AND DISCUSSION

The products $Et_4N[Mn_2(CO)_6X_3]$ (X = Cl, Br) were obtained initially by decomposition of $Et_4N[Mn(CO)_4X_2]$ in boiling chloroform (eq. 3.1). Subsequently analytically pure $Et_4N[M_2(CO)_6X_3]$ (M = Mn, X = Cl, Br; M = Re, X = Cl, Br, I) were obtained in high yield by the thermal reactions between $M(CO)_5X$ and Et_4NX in a 2 : 1 molar ratio (eq.3.2).

$$2Et_4N[Mn(CO)_4X_2] \longrightarrow Et_4N[Mn_2(CO)_6X_3] + Et_4NX + 2CO \qquad 3.1$$

$$2M(CO)_5X + Et_4NX \longrightarrow Et_4N[M_2(CO)_6X_3] + 4CO \qquad 3.2$$

Attempts to prepare $Et_4N[Mn_2(CO)_6I_3]$ in order to complete the series proved unsuccessful. As will be shown below the anions contain three bridging halogen atoms and it is therefore reasonable to suppose that the lack of success in preparing $Et_4N[Mn_2(CO)_6I_3]$ is associated with the incompatibility of three bulky iodine bridges linking two small manganese atoms.

The progress of the $M(CO)_5X$ - Et_4NX reactions was monitored by examining changes in the infrared spectra in the $\nu(CO)$ region at various intervals. In addition to bands associated with the starting materials $M(CO)_5X$ and the final products $[M_2(CO)_6X_3]^-$, the predicted four bands assigned to the C_{2v} anions $[M(CO)_4X_2]^-$ were detected during the reaction, as shown in Figure 3.3.

Since the products $Et_4N[Mn_2(CO)_6X_3]$ (X = Cl, Br) were originally obtained by decomposition of $Et_4N[Mn_2(CO)_4X_2]$ in refluxing chloroform, and the latter anions could be detected spectroscopically in the $M(CO)_5$ - Et_4NX reaction mixtures, the reactions employing $M(CO)_5X$ must also proceed *via* $[M(CO)_4X_2]^-$. The reaction may possibly involve the bis-μ-halogeno anions $[M_2(CO)_7X_3]^-$ formed by the rapid combination of $[M(CO)_4X_2]^-$ with further $M(CO)_5X$ before finally affording the complexes $[M_2(CO)_6X_3]^-$ as shown in the reaction

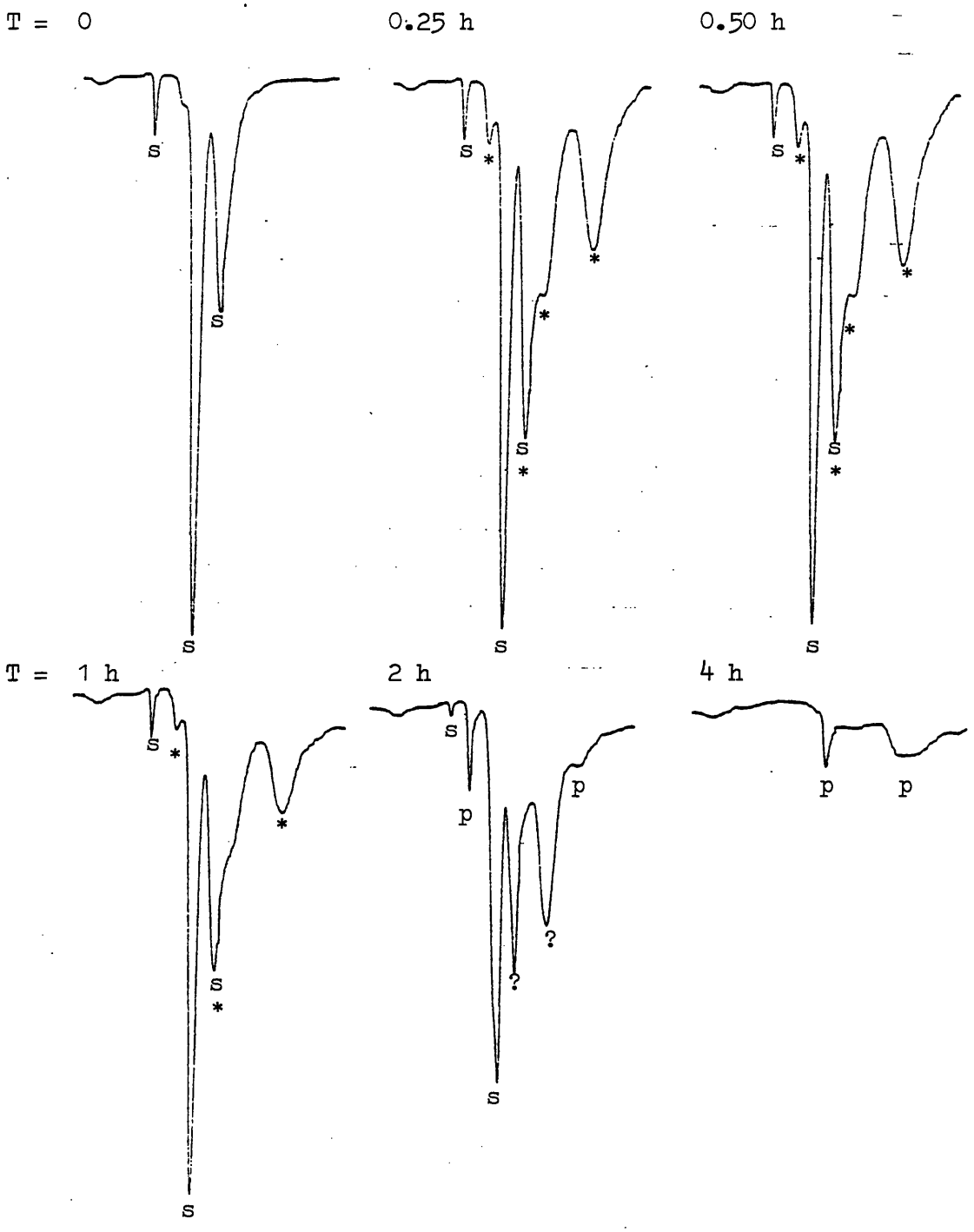

Figure 3.3: Infrared spectra (ν(CO) region in $CHCl_3$) at various intervals during the $Et_4NBr/Mn(CO)_5Br$ reaction

KEY: peaks due to : s, starting material $Mn(CO)_5Br$

*, intermediate $[Mn(CO)_4Br_2]^-$

p, product $[Mn_2(CO)_6(\mu\text{-}Br)_3]^-$ (has low solubility in $CHCl_3$)

sequence of Figure 3.4. Other anions such as $[M(CO)_3X_3]^{2-}$ and $[M_2(CO)_6X_4]^{2-}$ are unlikely to be involved as intermediates as insufficient halide ion is present in the reaction mixture to generate them.

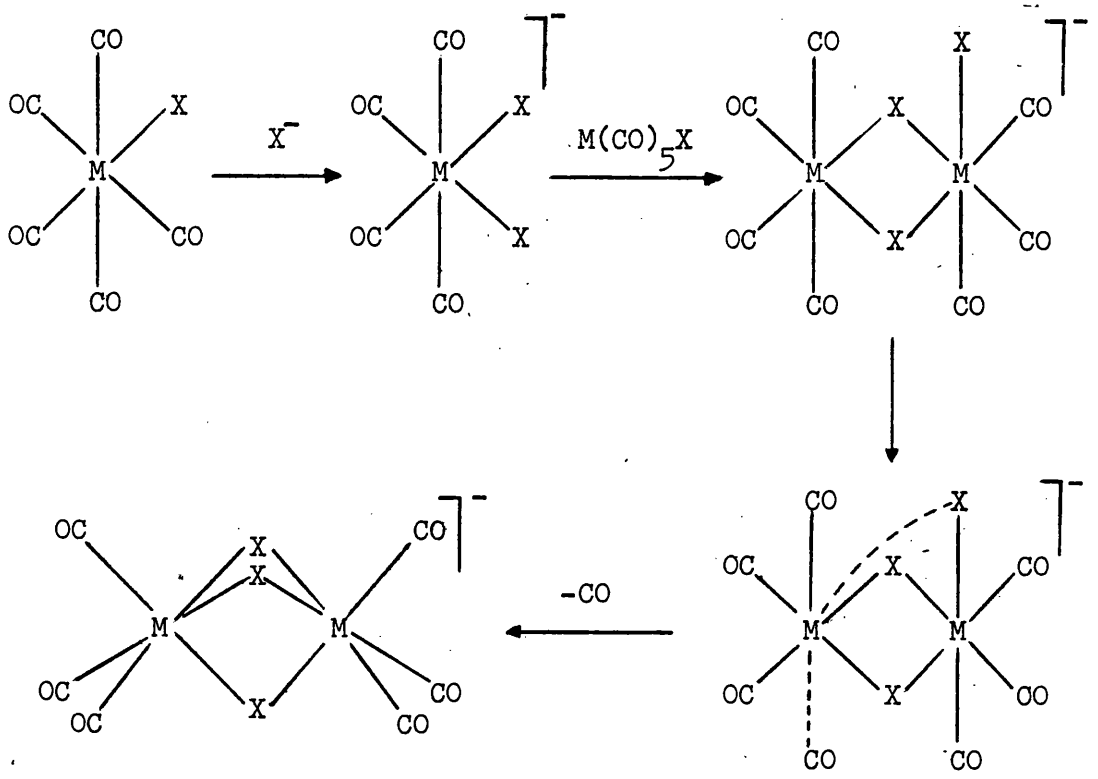

Figure 3.4: Possible mechanism for the formation of the $[M_2(CO)_6X_3]^-$ ion

The complexes are air-stable over a period of some months and may be stored indefinitely under nitrogen. Dichloromethane solutions were stable for at least a few days for the rhenium compounds and a few hours for the manganese compounds, so infrared carbonyl stretching frequencies were obtained in this solvent. Decomposition was found to be more rapid in solvents suitable for conductance measurements (see Figure 3.5). For example, the manganese complexes decomposed almost immediately in acetonitrile and a few minutes after dissolution in nitromethane. The rhenium complexes were generally

less prone to decomposition in polar solvents. Thus, as a result of decomposition, a gradual time dependent increase in the conductance of the complexes in acetonitrile and nitromethane solutions was noticeable and attempts to obtain Onsager plots (Λ vs. $\sqrt{c}$) for the anions was thwarted. However of these two solvents a slower decomposition rate was found in nitromethane, so conductance measurements on 10^{-3} M solutions were made in this solvent at 25°C, the reading being taken as rapidly as possible after solution preparation. The results obtained in this way (Table 3.1) are in good agreement with expectations for uni-valent electrolytes in nitromethane, (75 - 95 S cm^2 mol^{-1} for 10^{-3} M solutions[251]).

The decomposition of these anions in coordinating solvents such as acetonitrile is not unexpected when viewed in the light of known solvolytic reactions of halogenocarbonyl manganese or rhenium complexes[246,252,253]. See for example eqs. 3.3 - 3.6.

$$[Re(CO)_3X_3]^{2-} + MeCN \longrightarrow [Re(CO)_3X_2(MeCN)]^- + X^- \qquad 3.3$$

$$[Re_2(CO)_6X_4]^{2-} + 2MeCN \longrightarrow 2[Re(CO)_3X_2(MeCN)]^- \qquad 3.4$$

$$2[Mn(CO)_5X] + 2MeCN \longrightarrow [Mn_2(CO)_6X_2(MeCN)_2] + 4CO \qquad 3.5$$

$$Re(CO)_5X + 3MeCN + AgPF_6 \longrightarrow [Re(CO)_3(MeCN)_3][PF_6] + AgX + 2CO \qquad 3.6$$

In order to discover more about the solvolysis process the decomposition of $Et_4N[Re_2(CO)_6Br_3]$ in acetontrile solution was briefly studied by monitoring changes in the infrared ν(CO) region, with time (Figure 3.5). Initially the two major ν(CO) bands at 2023 and 1907 cm^{-1} due to the $[Re_2(CO)_6Br_3]^-$ anion were predominant, but after only ten minutes there appeared to be approximately equal

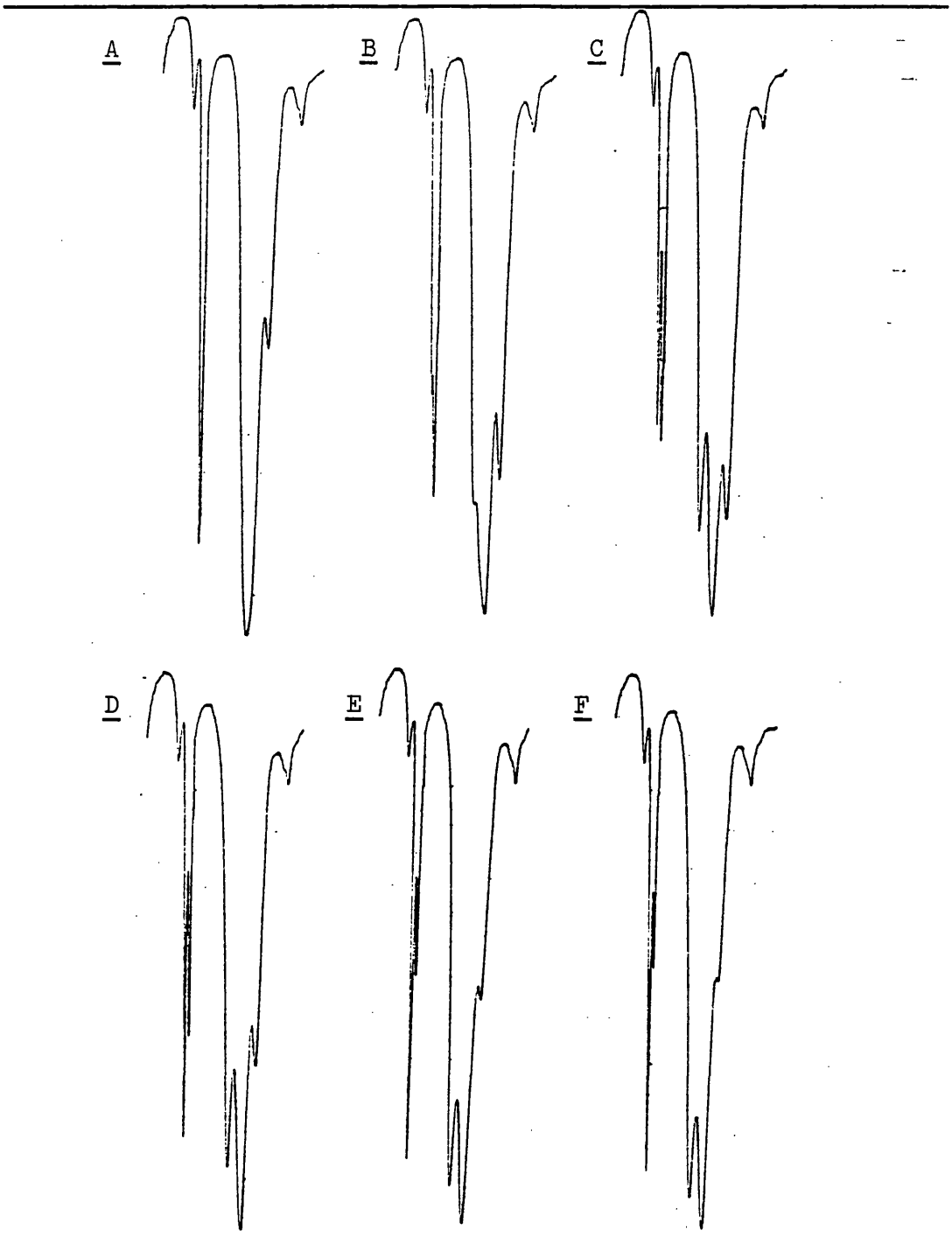

Figure 3.5: Infrared spectra (ν(CO) region) of $Et_4N[Re_2(CO)_6Br_3]$ in acetontrile solution A, 1 min; B, 3 min; C, 10 min; D, 1 h; E, 4 h; F, 18 h.

quantities of the anion and a new species having ν(CO) bands at 2039 1934 and 1882 cm^{-1}. After about four hours, an equilbrium was reached in which the ν(CO) bands due to the new species were the dominant feature of the spectrum. These band positions were

in good agreement with literature values[254] for $[Re(CO)_3Br(MeCN)_2]$ (ν(CO) = 2039, 1916, 1896 cm^{-1}; Nujol mull) so presumably Et_4NBr is liberated (eq. 3.7).

$$Et_4N[Re_2(CO)_6Br_3] + 4MeCN \longrightarrow 2[Re(CO)_3Br(MeCN)_2] + Et_4NBr \qquad 3.7$$

The time dependence of the infrared spectral changes of all the other anions dissolved in acetonitrile followed similar trends and, in agreement with previous observations[253], the manganese complexes had a much faster rate of decomposition. Indeed, two minutes after dissolution in acetonitrile, the spectrum of the complex $Et_4N[Mn_2(CO)_6Br_3]$ contained only three strong bands of the decomposition product at 2042, 1954 and 1932 cm^{-1} (c.f. 2043, 1957 and 1934 cm^{-1} reported[254] for the complex $[Mn(CO)_3Br(MeCN)_2]$). Further support for this initial mode of decomposition was obtained from molecular weight studies on MeCN solutions of the manganese complexes, as determined by vapour pressure osmometry. The determinations were carried out soon after making up the solutions and gave apparent molecular weights of 164 and 223 for the chloro- and bromo- derivatives respectively. The formula weights of these complexes are 514 and 648 respectively and these results, which are approximately one-third of the formula weight ($\frac{1}{3}$ x 514 = 171 and $\frac{1}{3}$ x 648 = 216) are consistent with the presence of at least three particles in solution, and not two as expected for $Et_4N[Mn_2(CO)_6(\mu\text{-}X)_3]$.

If the decomposition followed this route exclusively the conductance in acetonitrile should not markedly change, one univalent electrolyte, the trihalogeno-bridged complex, being replaced by another, Et_4NX. However the conductance slowly increased with time and the ν(CO) region of the infrared spectrum also became more complex (especially for the manganese compounds). This implies

that other electrolyte species were subsequently formed, perhaps by disproportionation. In view of these observations, the published[247] electronic spectrum of $Et_4N[Mn_2(CO)_6Cl_3]$ recorded in acetonitrile seems of doubtful value. Indeed attempts to reproduce the results quoted (46 930 cm^{-1}, ϵ = 41 500 and 26 730 cm^{-1}, ϵ = 2 720) were unsuccessful. It was found in fact that the electronic spectra of the manganese complexes were dependent on both concentration and time. The following values were recorded for 10^{-3} M solutions soon after dissolution and probably represent the solvolysed species. $Et_4N[Mn_2(CO)_6Cl_3]$: λ_{max} = 232 nm (43 100 cm^{-1}), ϵ = 13 930; λ_{max} = 376 nm (26 600 cm^{-1}), ϵ = 1 970 and for $Et_4N[Mn_2(CO)_6Br_3]$: λ_{max} = 229 nm (43 700 cm^{-1}), ϵ = 12 460; λ_{max} = 386 nm (25 900 cm^{-1}), ϵ = 1 220. Both species also exhibited a weak shoulder in the region of 330 nm (30 300 cm^{-1}).

The solution infrared spectra of the complexes in the ν(CO) region are given in Table 3.4 and the solid state infrared spectra below 700 cm^{-1} are presented in Table 3.3. The results are consistent with the presence of a confacial bi-octahedral anion of D_{3h} local symmetry with three bridging halogen atoms (Figure 3.2). Since this type of anion has high local symmetry and the number of atoms involved is low, a reasonably complete vibrational analysis is possible and although the manganese complexes decomposed in the He - Ne laser beam, a satisfactory Raman spectrum of $Et_4N[Re_2(CO)_6(\mu\text{-}Br)_3]$was obtained.

The vibrational representations for an isolated $[M_2(CO)_6(\mu\text{-}X)_3]^-$ anion of D_{3h} symmetry (Figure 3.2) may be derived from a simple group theoretical treatment, which is outlined in Appendix 3. The total vibrational representation is given by:

$$\Gamma_{vib} = 6A_1' + 2A_2' + 8E' + 2A_1'' + 5A_2'' + 7E''$$

This gives the following irreducible representations:

$$\Gamma_{\nu(CO)} = A_1' + E' + A_2'' + E''$$

$$\Gamma_{\nu(MC)} = A_1' + E' + A_2'' + E''$$

$$\Gamma_{\nu(MX)} = A_1' + E' + A_2'' + E''$$

$$\Gamma_{\delta(MCO)} = A_1' + 2E' + A_2'' + 2E''$$

$$\Gamma_{\delta(XMX)} = A_1' + E'$$

$$\left.\begin{matrix}\Gamma_{\delta(XMC)} \\ \Gamma_{\delta(CMC)}\end{matrix}\right\} A' + 2E' + A_2'' + 2E''$$

In D_{3h} symmetry, A_1' and E'' modes are only Raman-active, E' modes are both infrared- and Raman- active, A_2'' modes are only infrared-active, whilst A_2' and A_1'' modes are inactive. The vibrational spectrum of solid $Et_4N[Re_2(CO)_6(\mu\text{-}Br)_3]$ is presented in Table 3.2 together with assignments based on the group theoretical analysis of the anion in Appendix 3.

The assignments of the $\nu(CO)$ bands are straightforward. Thus a strong, sharp band at 2020 cm^{-1} is infrared-active only and is therefore the A_2'' mode, whilst the band which appears at ca. 1900 cm^{-1} in both the Raman and infrared spectra is assigned to the E' mode. This band shows considerable splitting in the solid state but is a broad, unsplit band in dichloromethane solution (Table 3.4). The two remaining $\nu(CO)$ vibrations of $Et_4N[Re_2(CO)_6(\mu\text{-}Br)_3]$ which appear at 2040 and 1951 cm^{-1} in the Raman spectrum only are assigned to A_1' and E'' modes respectively. Unfortunately this complex was not sufficiently soluble in solvents in which it did not undergo solvolysis for Raman polarisation studies. However the A_1' mode is assigned, by analogy with other fac-tricarbonyl species[255-257], to the highest energy band because it involves the simultaneous distortion of all six CO groups.

Table 3.2: Vibrational Spectra of Solid $Et_4N[Re_2(CO)_6(\mu\text{-}Br)_3]$ (cm^{-1})

Infrared	Raman[a]	Proposed Assignments	
	2040 ms	A_1'	ν(CO)
2020 vs		A_2''	
	1951 m	E''	
1915 sh	1909 ms		
1904 vs	1902 ms	E'	
1890 sh	1891 ms		
	671 m	A_1'	δ(MCO)
642 s[b]	642 vw	E'	
629 s	631 vw	E'	
	565 w	E''	
	554 vw	E''	
	520 vs	A_1'	ν(MC)
	512 sh	E''	
506 s	508 ms	E'	
495 s		A_2''	
	212 m	A_1'	ν(MBr)
190 vs		A_2''	
170 vs	170 m	E'	
	not observed	E''	
	123 m	A_1'	δ(BrMBr)
117 s	117 ms	E'	

[a] Other low-energy Raman bands: 110, 104, 98, 91 and 85 cm^{-1}

[b] A_2'' mode may be coincident, (see text).

Assignments in the 680 - 480 cm^{-1} region (Tables 3.2 and 3.3) are less obvious although the δ(MCO) and ν(MC) vibrations do seem to fall into well defined frequency regions. It is generally agreed for other fac-tricarbonyl species such as $[M(CO)_3(\eta^6\text{-arene})]$ (M = Cr, Mo, W)[255,256] and $[Mn(CO)_3(\eta^5\text{-}C_5H_4R)]$ (R = H, Me)[257], that the δ(MCO) modes absorb at higher energies than ν(MC) modes. Group theory predicts three infrared-active δ(MCO) bands and for the manganese complexes these are assigned to the three bands found between 680 - 620 cm^{-1}. However for the rhenium analogues only two such bands are evident in this region. This may be explained in terms of a mass effect on changing from manganese to rhenium, which is known to substantially shift the highest frequency δ(MCO) infrared-active band in, for example, $[M(CO)_6]^+$ [258,259], $[M(CO)_5X]$ [260-262] and $[M(CO)_3(MeCN)_3]^+$ [263], (M = Mn, Re). The magnitude of these shifts are typically about 50 cm^{-1} to lower frequency but for the remaining δ(MCO) bands this effect is much less apparent and may even be reversed[263]. Therefore if the A_2'' δ(MCO) mode found at 680 cm^{-1} for the manganese complexes suffers a similar mass effect for the rhenium analogues, it would become accidentally coincident with the highest infrared-active E' mode, and so only two δ(MCO) infrared bands would be observed for rhenium anions. Inspection of the infrared spectra shows that the highest energy δ(ReCO) bands are indeed somewhat broader than the δ(MnCO) bands of intermediate energy. The E' δ(ReCO) modes at 642 and 629 cm^{-1} in $Et_4N[Re_2(CO)_6(\mu\text{-Br})_3]$ are easily assigned because of their correspondence in the infrared and Raman spectra. The remaining three bands, which appear at 671, 565 and 554 cm^{-1} in the Raman spectrum only, must therefore be the A_1' and 2E'' δ(ReCO) modes, the A_1' mode again being assigned to the band of highest frequency.

Table 3.3: Solid State Infrared Spectra Below 700 cm^{-1}

Complex	δ(MCO) A_2'' + 2E'	ν(MC) A_2'' + E'	ν(MX) A_2'' + E'	δ(XMX) E'	Et_4N^+ Skeletal Deformations
$Et_4N[Mn_2(CO)_6(\mu\text{-}Cl)_3]$	680 s, 633 s, 628 s	504 s, 486 ms	278 s, 239 s	173 s	415 vw, 358 vw
$Et_4N[Mn_2(CO)_6(\mu\text{-}Br)_3]$	673 s, 630 s, 623 s	504 s, 485 ms	212 s, 176 s	161 s	415 w, 350 vw
$Et_4N[Re_2(CO)_6(\mu\text{-}Cl)_3]$	648 s, 635 s	510 sh, 499 s	269 s, 251 s	159 s	414 w, 355 vw
$Et_4N[Re_2(CO)_6(\mu\text{-}Br)_3]$	642 s, 629 s	506 s, 495 s	190 s, 171 s	117 s	414 w[a]
$Et_4N[Re_2(CO)_6(\mu\text{-}I)_3]$	640 s, 630 sh	510 sh, 493 s	156 s, 137 s	100 ms	412 vw, 355 vw

[a] Raman spectrum: 417 m, 413 sh

The infrared spectra of all of the complexes displayed two bands of closely similar frequency at approximately 500 cm^{-1}. In Tables 3.2 and 3.3 these are assigned to the E' and A_2'' ν(MC) modes although it could be argued from a consideration of merely the solid state infrared spectra that the two bands observed could both be assigned to the E' mode split by solid state effects, so leaving the A_2'' mode undetected. However a solution infrared spectrum (recorded in dichloromethane in 1 mm KBr cells) of $Et_4N[Re_2(CO)_6(\mu\text{-}Br)_3]$ in the δ(ReCO) and ν(ReC) region also shows four bands (647, 633, 509, 501 cm^{-1}) thereby supporting these assignments. Two very strong bands, both only Raman-active, at 520 and 512 cm^{-1} in the spectrum of $Et_4N[Re_2(CO)_6(\mu\text{-}Br)_3]$ are assigned A_1' and E'' ν(MC) modes respectively.

Apart from the absence of the E'' Raman-active ν(ReBr) band of $Et_4N[Re_2(CO)_6(\mu\text{-}Br)_3]$, the ν(ReBr) and δ(BrReBr) bands are readily assignable by applying related arguments to those used above. For the series of anions under discussion the bands in this region of the spectra display the expected sensitivity to change of mass of halogen as shown in Figure 3.6. The ν(MBr)/ν(MCl) and ν(MI)/ν(MCl) ratios of 0.67 - 0.74 and 0.55 - 0.58 respectively also give added confidence to the assignments. The frequencies of the ν(MX) bands are in the expected regions for bridging halogen atoms and are of similar frequency to such bands observed[264] for the neutral carbonyl halides, $[M_2(CO)_8(\mu\text{-}X)_2]$ (M = Mn, Re; X = Cl, Br, I).

e.g. $[Mn_2(CO)_8(\mu\text{-}Cl)_2]$; ν(MnCl) = 293 and 243 cm^{-1}.

$[Mn_2(CO)_8(\mu\text{-}Br)_2]$; ν(MnBr) = 216 and 186 cm^{-1}.

$[Re_2(CO)_8(\mu\text{-}Cl)_2]$; ν(ReCl) = 288 and 240 cm^{-1}.

$[Re_2(CO)_8(\mu\text{-}Br)_2]$; ν(ReBr) = 198 and 171 cm^{-1}.

$[Re_2(CO)_8(\mu\text{-}I)_2]$; ν(ReI) = 163 and 142 cm^{-1}.

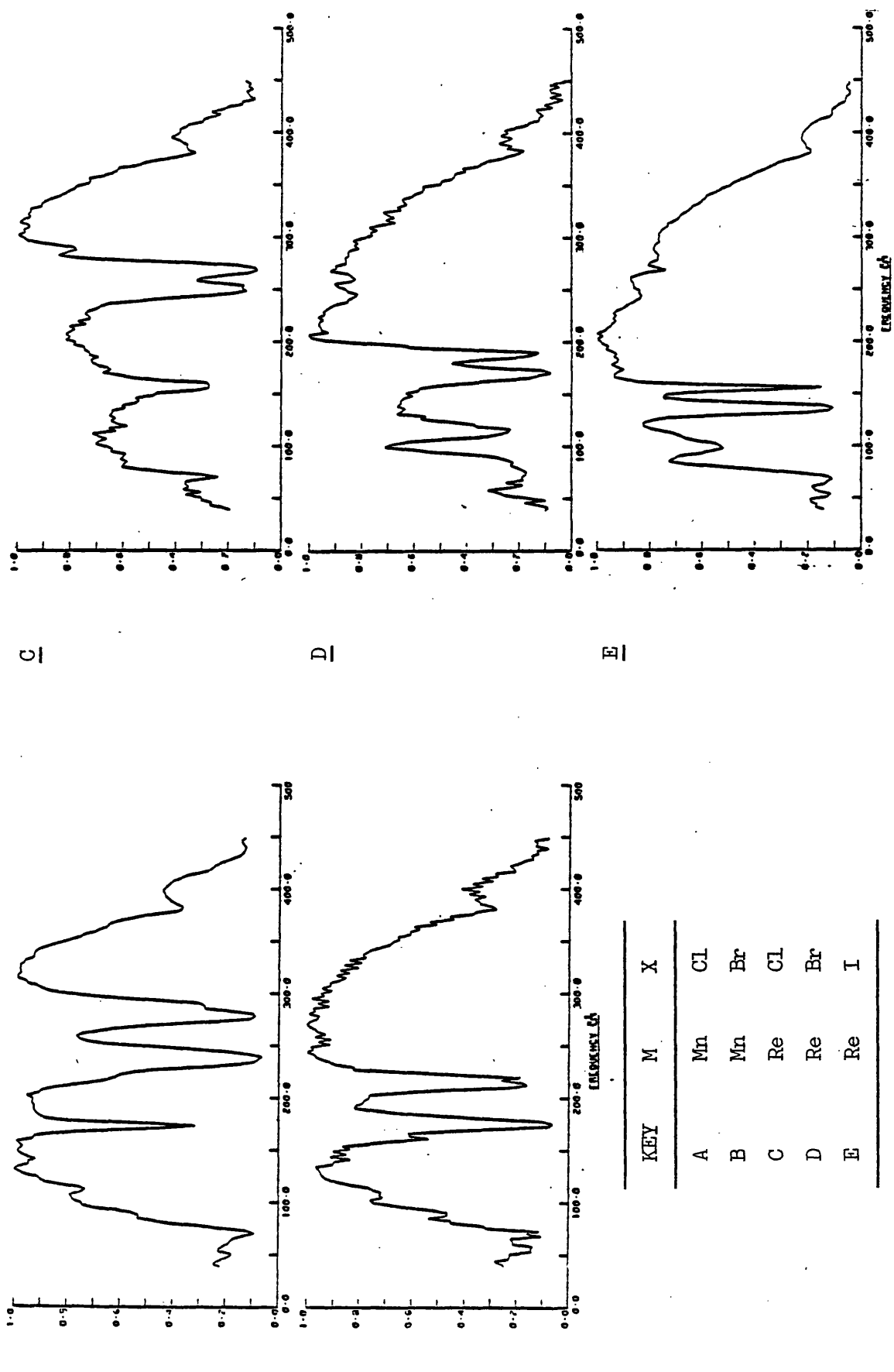

KEY	M	X
A	Mn	Cl
B	Mn	Br
C	Re	Cl
D	Re	Br
E	Re	I

Figure 3.6: Far-infrared spectra of the complexes $Et_4N[M_2(CO)_6(\mu\text{-}X)_3]$

Table 3.4: Infrared Spectra in the ν(CO) Region (cm^{-1})[a]

Complex	CH_2Cl_2 Solution		Nujol Mull			
	A_2''	E'	A_2''	E' [b]		
$Et_4N[Mn_2(CO)_6(\mu\text{-}Cl)_3]$	2030	1936	2020	1948 sh	1935	1912
$Et_4N[Mn_2(CO)_6(\mu\text{-}Br)_3]$	2029	1937	2012	1940 sh	1930	1909
$Et_4N[Re_2(CO)_6(\mu\text{-}Cl)_3]$	2030	1917	2021	1933 sh	1915	1890
$Et_4N[Re_2(CO)_6(\mu\text{-}Br)_3]$	2028	1915	2020	1915 sh	1904	1890 sh
$Et_4N[Re_2(CO)_6(\mu\text{-}I)_3]$	2012	1914	2012	1916 br		1892

[a] All bands strong unless otherwise stated.

[b] Split by solid state effects.

The infrared spectrum of $Et_4N[Mn_2(CO)_6(\mu\text{-}Cl)_3]$ between 3200 - 400 cm^{-1} is illustrated in Figure 3.7. The major infrared spectral features of this and the other anionic complexes have been assigned by analogy with the vibrational analysis of $Et_4N[Re_2(CO)_6(\mu\text{-}Br)_3]$.

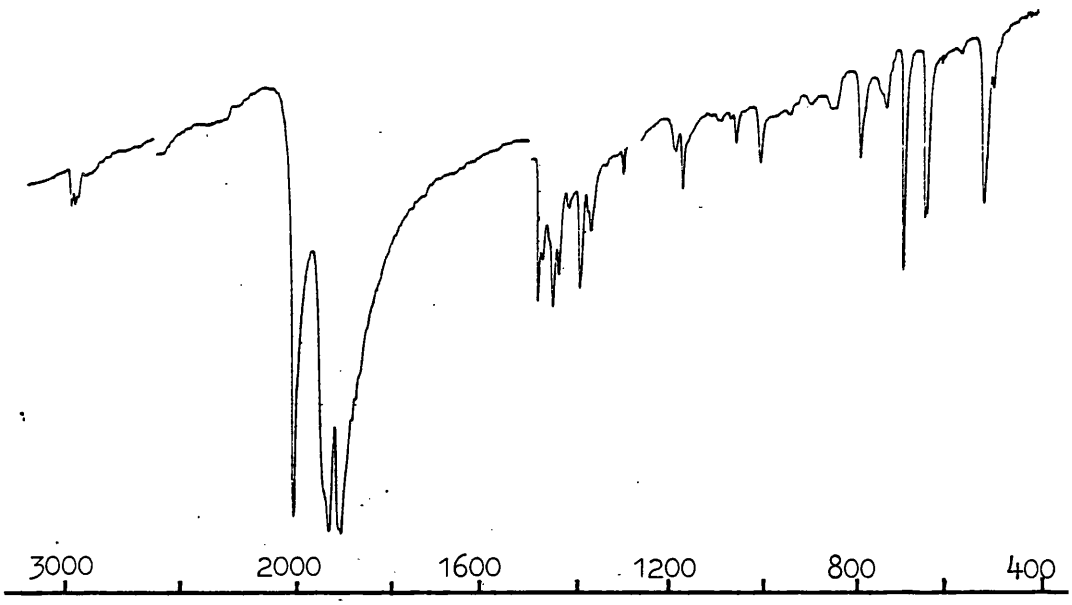

Figure 3.7: Solid state infrared spectrum of the complex $Et_4N[Mn_2(CO)_6(\mu\text{-}Cl)_3]$ (3200 - 400 cm^{-1})

Thus the complexes all display two strong ν(CO) bands (A_2'' + E') in their solution spectra (Table 3.4). In the solid state four or five bands ($2A_2''$ + 3E') assigned to δ(MCO) and ν(MC) and three halogen sensitive bands below 300 cm^{-1}, ν(MX) and δ(XMX) (A_2'' + 2E'), which are typical of bridging halogen atoms, are observed (Table 3.3). The spectra of all the complexes also show bands at approximately 3000, 1480, 1445, 1390, 1300, 1160, 1050, 990 and 780 cm^{-1} in addition to those tabulated which, by comparison with the known[265] spectra of tetraethylammonium halides, may be assigned to vibrations of the Et_4N^+ cation.

As a result of analytical data, conductivities and detailed vibrational analysis, these anions have been established as further examples of the well known structural type $[M_2(CO)_6(\mu\text{-}X)_3]^-$ for Group VII anions (M = Mn, X = N_3, NCO[266]; M = Re, X = H, EtO, i-PrO[267]; M = Re, X = OH, MeO, EtO, n-BuO, t-BuO, CyO[268,269]). They are also isostructural and isoelectronic with the Group VI anions $[M_2(CO)_6(\mu\text{-}X)_3]^{3-}$ (M = Cr, Mo, W; X = F, Cl, Br, I, OH, SCN, N_3, EtO[270] and M = Mo, W; X = Cl[271]), which are known[223] to react with allyl halides according to eq. 3.8.

$$[Et_4N]_3[W_2(CO)_6(\mu\text{-}Cl)_3] + 2C_3H_5Cl + 4MeCN \longrightarrow 2[(\eta^3\text{-}C_3H_5)W(CO)_2(MeCN)_2Cl] + 2CO + 3Et_4NCl \qquad 3.8$$

Since the analogous Group VII anions decomposed in acetonitrile their thermal reactions with allyl halides were investigated in a variety of other solvents including chloroform (bp 62°C), toluene (bp 111°C), diglyme (bp 162°C) and dekalin (bp 187°C) as well as pure allyl chloride (bp 45°C) and allyl bromide (bp 70°C). In each case no reaction occurred, other than the decomposition of the manganese complexes in the higher boiling solvents, except for a remarkable halogen exchange reaction between $Et_4N[Re_2(CO)_6(\mu\text{-}I)_3]$ and allyl bromide (eq. 3.9).

$$Et_4N[Re_2(CO)_6(\mu\text{-}I)_3] \xrightarrow[\text{reflux}]{\text{allylBr}} Et_4N[Re_2(CO)_6(\mu\text{-}Br)_3] \qquad 3.9$$

After only 15 minutes at 70°C the product, isolated in 100% yield, contained only bridging bromines, as indicated by changes in the ν(CO) and ν(ReX) regions of the infrared spectrum. The Group VII anions also failed to react with allyl halides dissolved in dichloromethane and tetrahydrofuran when irradiated with a medium pressure mercury vapour lamp.

Thus, in contrast to their Group VI analogues, these Group VII tri-μ-halogeno anions are unreactive towards allyl halides, with an overriding tendency to retain the triply-bridging structure. Their apparent thermal and photo- stability in non-coordinating solvents does not extend to solvents of greater coordinating power, since it has been shown that a bridge cleavage reaction by σ-donors such as MeCN occurs rapidly.

CHAPTER FOUR

η^1-ALLYLPENTACARBONYL-, η^3-ALLYLTETRACARBONYL- AND PENTACARBONYLMETHYL- RHENIUM(I)

INTRODUCTION

The synthesis of $[(\eta^1\text{-}C_3H_5)Mn(CO)_5]$ from allyl chloride and $Na[Mn(CO)_5]$ and its subsequent decarbonylation to $[(\eta^3\text{-}C_3H_5)Mn(CO)_4]$ exemplifies a classic piece of organometallic chemistry[93,118]. However, as previously noted, the chemistry of Group VII transition metal-allyl complexes is generally very limited and in particular there is only one previous reference[132] to the corresponding η^1-allyl-rhenium complex. This reports the isolation of $[(\eta^1\text{-}C_3H_5)Re(CO)_5]$, in a rather impure state, after the chromatographic work-up of the reaction between allyl chloride and $Na[Re(CO)_5]$. The yield being only ca. 10%. Since decarbonylation of this η^1-allyl complex was evidently not a useful route to $[(\eta^3\text{-}C_3H_5)Re(CO)_4]$[132], the η^3-allyl complex has been prepared[158,159] by reacting $[(\eta^1\text{-}C_3H_5)Sn(CH_3)_3]$ with either $Re(CO)_5Br$ in refluxing tetrahydrofuran or with $Re_2(CO)_{10}$ in diglyme at 150°C for 100 h. A mechanism was proposed on the basis of spectroscopic observations which does not require the involvement of $[(\eta^1\text{-}C_3H_5)Re(CO)_5]$ as an intermediate (see pages 30 - 31).

It is shown in this work that contrary to previous belief pure samples of $[(\eta^1\text{-}C_3H_5)Re(CO)_5]$ can easily be prepared in at least 90% yield from the reaction of allyl chloride with $Na[Re(CO)_5]$ and this complex can be conveniently photodecarbonylated to give $[(\eta^3\text{-}C_3H_5)Re(CO)_4]$ in very reasonable yields (ca. 55%). The preparation of these complexes and their characterisation by NMR, mass and particularly vibrational spectra form the subjects of this chapter.

During the course of this work $[CH_3Re(CO)_5]$ and the isotopically labelled analogues $[CD_3Re(CO)_5]$ and $[^{13}CH_3Re(CO)_5]$ were synthesised for comparative purposes. Since only partial infrared

data was available for these compounds[229,272,273] a detailed vibrational analysis was carried out. These results, which are essentially complementary to those of the η^1-allyl complex, are presented at the end of this chapter.

EXPERIMENTAL

Preparation of $[(\eta^1\text{-}C_3H_5)Re(CO)_5]$

In order to obtain good yields it is necessary to maintain strictly anaerobic conditions throughout the preparation and manipulation of this complex. A solution of $Na[Re(CO)_5]$ was prepared by stirring a solution of $Re_2(CO)_{10}$ (0.326 g/0.5 mmol) in nitrogen saturated anhydrous tetrahydrofuran (10 cm^3) with 0.5% sodium amalgam (2 cm^3) at 0°C for 1 h, under dry nitrogen. After removal of the excess amalgam through a stopcock, allyl chloride (1.0 cm^3) saturated with dry nitrogen, was added. A colourless precipitate of sodium chloride formed quickly, and after 5 min all the $[Re(CO)_5]^-$ had been consumed (as shown by the absence of anion ν(CO) infrared bands). Removal of solvent (15 mm/ 20°C), followed by distillation (0.1 mm/30°C), gave a very pale straw coloured liquid product (Yield: 0.340 g, 92%. Analysis found: C, 26.4; H, 1.39. Calc. for $C_8H_5O_5Re$: C, 26.2; H, 1.37%).

Preparation of $[(\eta^3\text{-}C_3H_5)Re(CO)_4]$

A solution of $[(\eta^1\text{-}C_3H_5)Re(CO)_5]$ (0.260 g/0.7 mmol) in anhydrous n-pentane (75 cm^3) was irradiated for 1 h under dry nitrogen in a conventional water-cooled quartz photochemical reactor. The irradiation source was a 100 watt medium pressure mercury lamp. The reaction was monitored by observing the decay of the ν(CO)

infrared bands of the pentacarbonyl and the growth of bands ascribed to the tetracarbonyl together with weaker bands due to $Re_2(CO)_{10}$. Prolonged irradiation caused no further change. Removal of the solvent (15 mm/20°C) followed by two vacuum sublimations on to a cold finger filled with solid CO_2 gave the product as fine colourless crystals. (Yield: 0.132 g, 55%; m.p. 32°C. Analysis found: C, 24.0; H, 1.38. Calc. for $C_7H_5O_4Re$: C, 24.8; H, 1.49%). Recrystallisation of the residue from carbon-tetrachloride afforded pure $Re_2(CO)_{10}$. Yield 37%.

Preparation of $[CH_3Re(CO)_5]$, $[^{13}CH_3Re(CO)_5]$ and $[CD_3Re(CO)_5]$

A solution of $Re_2(CO)_{10}$ (0.652 g/1 mmol) in tetrahydrofuran was converted to $Na[Re(CO)_5]$ using the same procedure as described previously for the preparation of $[(\eta^1\text{-}C_3H_5)Re(CO)_5]$. Methyl iodide (1 cm^3/16 mmol) was added to this orange solution causing an immediate colour change to very pale yellow. (NaI was precipitated on addition of a few drops of n-pentane). The solvent was removed (15 mm/20°C) and the colourless product twice sublimed on to a solid CO_2-cooled finger. (Yield: 0.400 g, 59%; m.p. 124°C). The deuterated and ^{13}C- isotopically-substituted analogues were prepared in exactly the same manner using CD_3I (1 cm^3/15.6 mmol) or $^{13}CH_3I$ (0.3 cm^3/4.8 mmol) in place of CH_3I. (Yields: $[CD_3Re(CO)_5]$; 0.469 g, 72%; m.p. 117°C and $[^{13}CH_3Re(CO)_5]$; 0.421 g, 62%; m.p. 122°C).

For details of solvents, reagents and a description of the physical methods used see Appendices 1 and 2.

RESULTS AND DISCUSSION

Reaction between $Na[Re(CO)_5]$ and allyl chloride had previously been stated[132] to give a low yield of impure $[(\eta^1\text{-}C_3H_5)Re(CO)_5]$ which was characterised solely by a poorly resolved NMR spectrum. Using basically the same method with variations in reaction times but replacing a chromatographic purification step by vacuum distillation it was found possible to achieve at least a 90% yield of pure $[(\eta^1\text{-}C_3H_5)Re(CO)_5]$.

In addition to the established method of sodium amalgam cleavage of metal-metal bonds, the use of reagents such as $Li[(C_2H_5)_3BH]$ [274,275], potassium hydride[276] and sodium-potassium alloy[277] was explored for this purpose. However, only the alloy is effective in producing $[Re(CO)_5]^-$ in appreciable concentration, but the reaction proceeds very slowly. None of the above reagents is therefore superior to sodium amalgam for the cleavage reaction. The conditions quoted in the literature for sodium amalgam cleavage of $Re_2(CO)_{10}$ [132,277,278] vary considerably, but by continuous monitoring of the infrared $\nu(CO)$ region of the reaction mixture, it was found that the optimum concentration of $[Re(CO)_5]^-$ was achieved after 1 h at 0°C. Solutions of $[Re(CO)_5]^-$ prepared by this method are red-orange in colour and as well as strong $\nu(CO)$ infrared bands at 1911, 1864, 1835 cm^{-1} they also displayed weak $\nu(CO)$ bands at 1969, 1920, 1885 cm^{-1}, indicating the presence of a coloured impurity, possibly $[Re_2(CO)_9]^{2-}$ [277,278]. Extension of the reaction time caused the concentration of $[Re(CO)_5]^-$ to slowly decline.

$[(\eta^1\text{-}C_3H_5)Re(CO)_5]$ is a pale yellow, very air sensitive liquid which easily distils under reduced pressure (0.1 mm/30°C).

Exposure to the atmosphere causes its decomposition to a pale yellow solid within a few minutes. Although this solid was not characterised, mass spectral evidence indicated that it contained a component with Re_2 units. The η^1-allyl complex can be stored at room temperature in sealed ampoules under nitrogen for several months without visible signs of decomposition.

It had been suggested previously[132] that $[(\eta^1\text{-}C_3H_5)Re(CO)_5]$ could not be decarbonylated to give $[(\eta^3\text{-}C_3H_5)Re(CO)_4]$. The evidence now presented however, shows that the η^3-allyl complex can be prepared in acceptable yield by photochemical decarbonylation of $[(\eta^1\text{-}C_3H_5)Re(CO)_5]$. It is much more stable to atmospheric oxidation than its η^1- precursor, forming easily sublimable, colourless needles which may be manipulated freely in air with recourse only to the usual precautions applicable to the handling of toxic substances. The complex may be stored indefinitely under nitrogen at 0^oC. Using the conditions described in the experimental section, the above decarbonylation appears to be in competition with allyl cleavage as $Re_2(CO)_{10}$ is also produced, presumably by coupling of $Re(CO)_5^{\bullet}$ radicals. The ratio of yields of $[(\eta^3\text{-}C_3H_5)Re(CO)_4]$ to $Re_2(CO)_{10}$ obtained from the photochemical reaction decreases if the temperature is allowed to rise. This suggests that the competing reaction is a thermal one and that strict control of temperature is required in order to optimise the yield of the required η^3-allyl complex.

Attempts to widen the scope of the method to include substituted allyl ligands were less successful, only small quantities of η^3-allyl complexes being isolated. The following were identified only by their infrared spectra in n-pentane: $[(\eta^3\text{-}2\text{-}MeC_3H_4)Re(CO)_4]$, $[(\eta^3\text{-}1\text{-}MeC_3H_4)Re(CO)_4]$ and $[(\eta^3\text{-}1\text{-}PhC_3H_4)Re(CO)_4]$, all of which

have ν(CO) bands at approximately 2090 s, 1995 vs, 1980 vs, and 1960 vs (cm^{-1}). No intermediate η^1-allyl complexes were isolated owing to their general instability.

The methyl complexes $[CH_3Re(CO)_5]$,[273,279] $[^{13}CH_3Re(CO)_5]$ and $[CD_3Re(CO)_5]$ were prepared by a similar method to $[(\eta^1\text{-}C_3H_5)Re(CO)_5]$. All are air-stable, colourless solids which sublime readily at room temperature.

^{1}H NMR Results

(a) $[(\eta^1\text{-}C_3H_5)Re(CO)_5]$

The NMR spectrum of $[(\eta^1\text{-}C_3H_5)Re(CO)_5]$, recorded in $CDCl_3$ under low resolution, is of the expected $ABCX_2$ type. It is illustrated in Figure 4.1 and although similar to that reported previously[132]

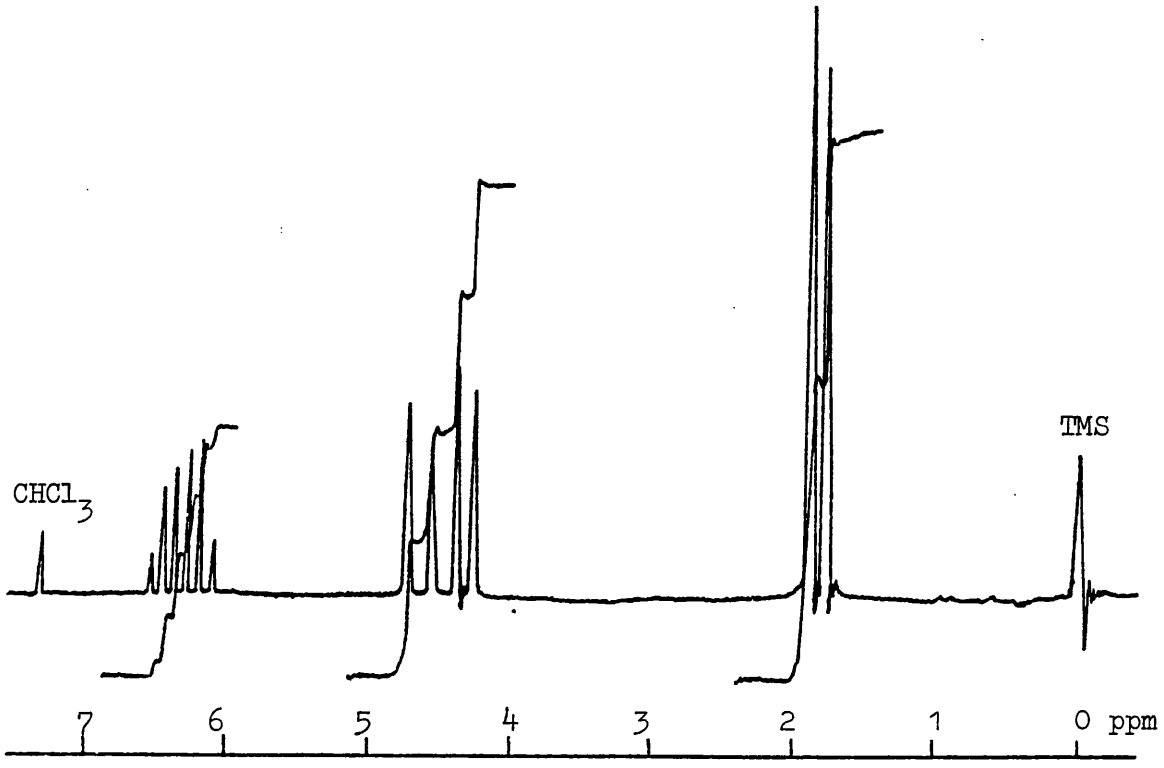

Figure 4.1: ^{1}H NMR spectrum of $[(\eta^1\text{-}C_3H_5)Re(CO)_5]$ in $CDCl_3$ solution

it is of superior quality. Thus an analysis of the spectrum under high resolution enables all possible first order coupling constants

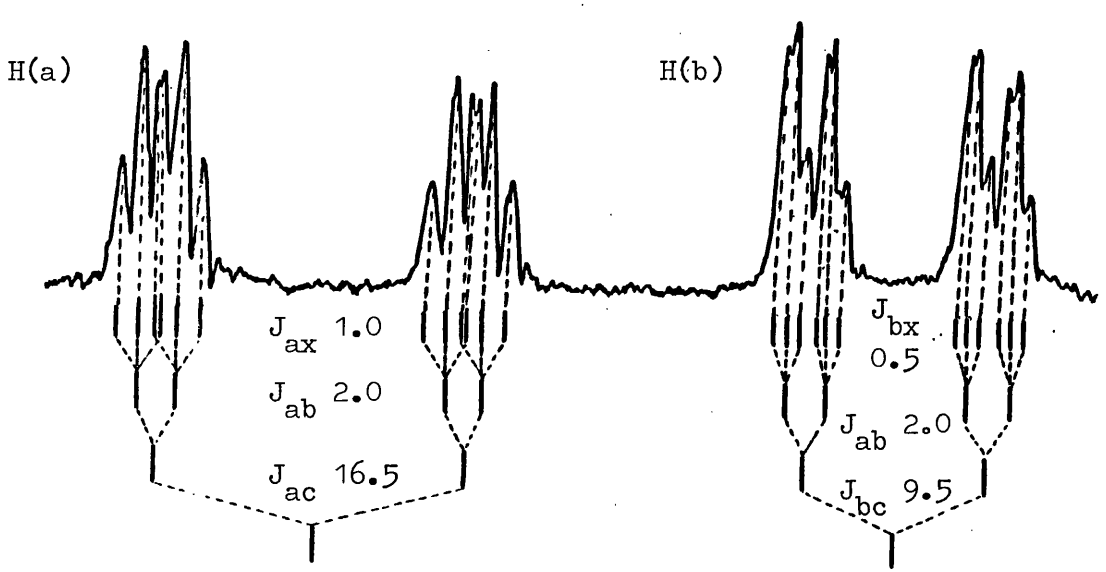

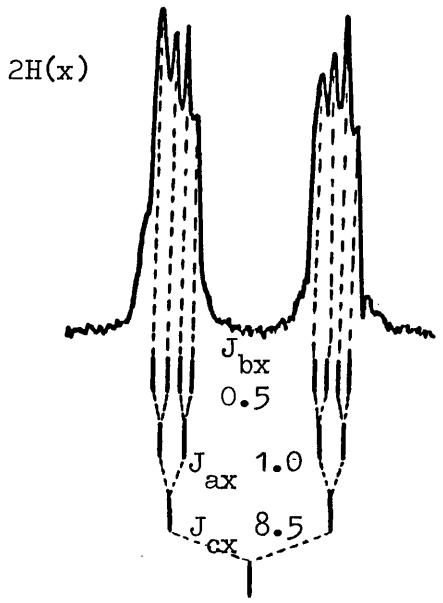

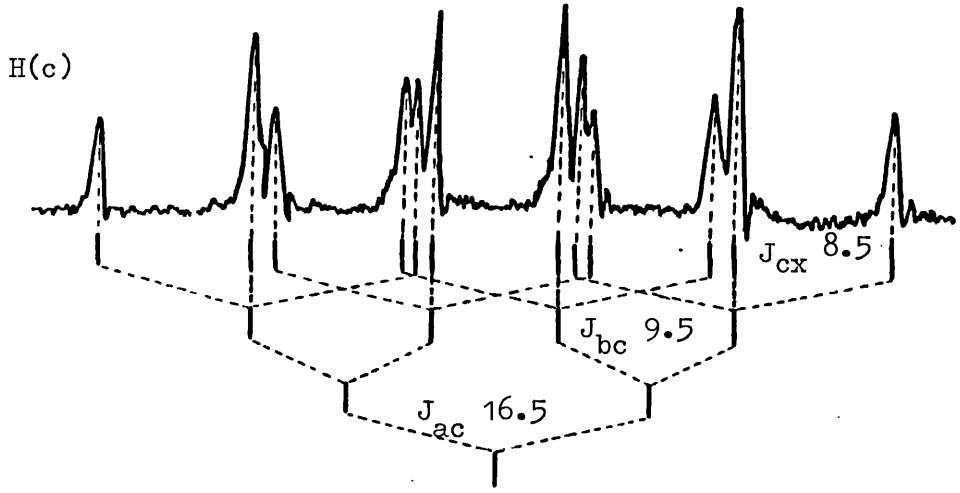

	Chem. shift (δ) (multiplicity)	Assignment (rel. int.)
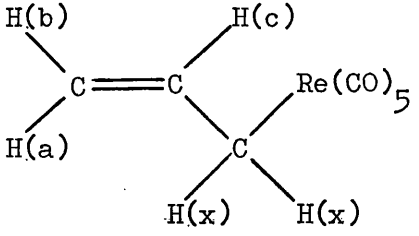	6.34 (12)	H(c) (1)
	4.65 (12)	H(a) (1)
	4.34 (12)	H(b) (1)
	1.85 (8)	H(x) (2)

Figure 4.2: High resolution ^{1}H NMR spectrum of $[(\eta^1\text{-}C_3H_5)Re(CO)_5]$ and coupling constants (Hz)

to be determined (Figure 4.2). The chemical shifts and values so obtained are in good agreement with expectations for an η^1-bonded allyl group (see page 17).

(b) $[(\eta^3\text{-}C_3H_5)Re(CO)_4]$

The ^1H NMR spectrum of $[(\eta^3\text{-}C_3H_5)Re(CO)_4]$ obtained in $CDCl_3$ is indicative of a symmetrical η^3-allyl group, giving a simple AMM'XX' type of spectrum with spectroscopic equivalence of the syn- and anti- protons. The coupling constants and chemical shifts fall within the ranges expected for a typical η^3-allyl group (these are given on page 19). The spectrum, which is illustrated together with assignments and coupling constants in Figure 4.3, agrees well with previous[41,280] results obtained in solution in chloroform. The ^1H NMR spectrum of $[(\eta^3\text{-}C_3H_5)Re(CO)_4]$ has also been measured in a nematic liquid crystal phase[41] and from a consideration of dipolar coupling constants it was concluded that the protons of the η^3-allyl group do not all lie in one plane.

(c) Pentacarbonylmethyl rhenium

The unlabelled pentacarbonylmethyl rhenium exhibited the expected[281] sharp singlet upfield from TMS at -0.20 ppm. The ^1H NMR spectrum of the corresponding ^{13}C labelled complex consisted of a doublet, $J(^{13}CH)$ = 128 Hz, centred around a minor peak due to the ^{12}C isotope at -0.20 ppm. The ratio of the integrals of the major and minor peaks indicated that the isotopic purity of the ^{13}C labelled complex was greater than 90%.

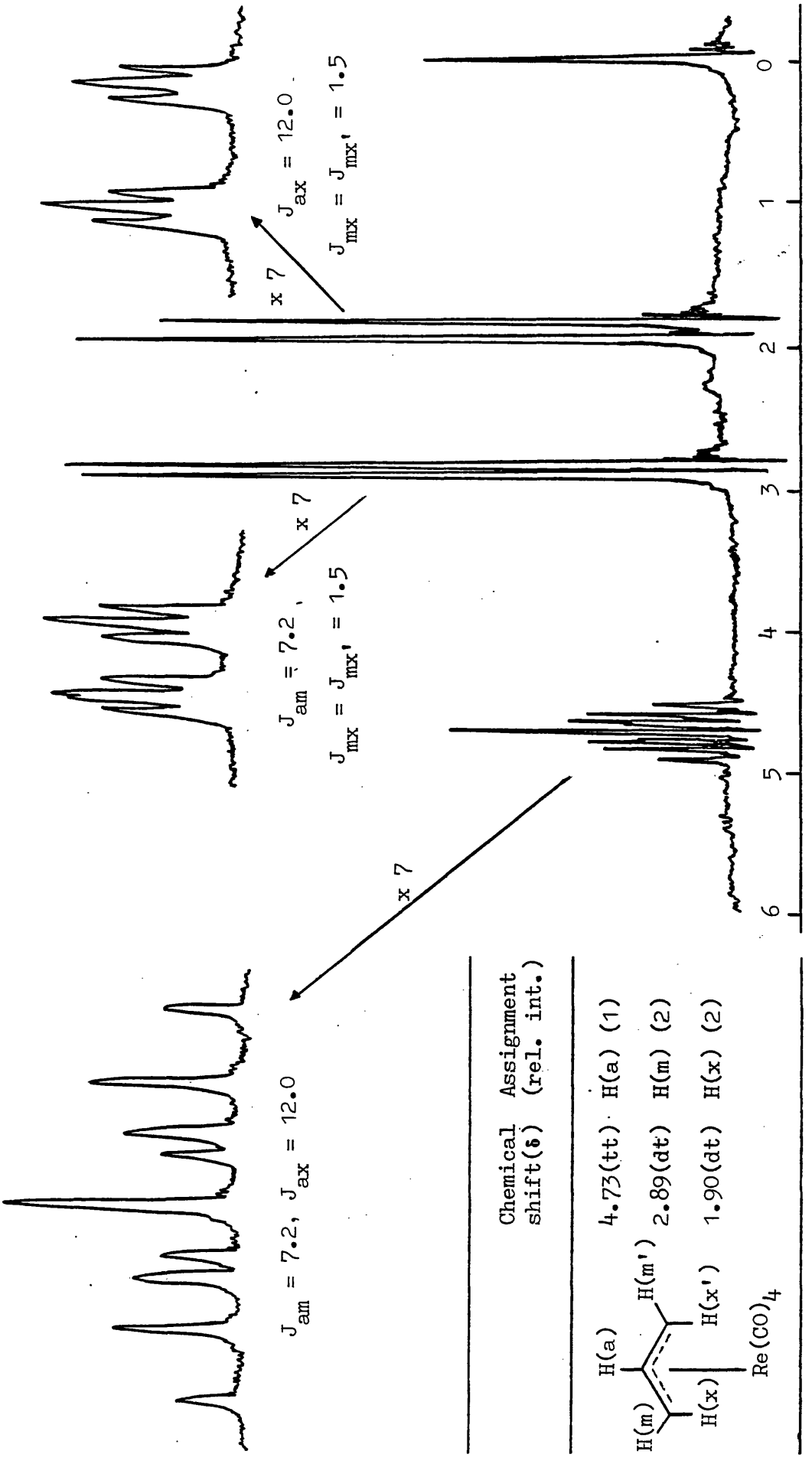

Chemical shift(δ)	Assignment (rel. int.)
4.73(tt)	H(a) (1)
2.89(dt)	H(m) (2)
1.90(dt)	H(x) (2)

Figure 4.3: ^{1}H NMR spectrum of $[(\eta^3\text{-}C_7H_{11})Re(CO)_4]$ and coupling constants (Hz)

Mass Spectra

Metal-containing ions and associated metastables observed in the mass spectra of the allyl and methyl rhenium carbonyl compounds are listed in Tables 4.1 - 4.3. Such ions are clearly identified by the isotopic ratio ^{187}Re : ^{185}Re = 1 : 0.60 (peaks arising from both isotopes are given for each ion in the tables). In each case the ion abundances are quoted relative to a rhenium-containing base peak of 100 units. For convenience of discussion the major ions are classified according to their method of derivation from the molecular ion[282] as follows: (i) loss of carbonyl groups; (ii) loss of the allyl or methyl group; (iii) loss of ligand fragments whilst still attached to rhenium. This is an arbitrary classification and it should be noted that some ions may be derived by more than one process (e.g. $[Re(CO)_4]^+$ from either $[LRe(CO)_4]^+$ or $[Re(CO)_5]^+$).

(a) η^1-Allylpentacarbonylrhenium(I)

Table 4.1 shows that for $[(\eta^1\text{-}C_3H_5)Re(CO)_5]$ the molecular ion is present in relatively high abundance in the mass spectrum. This may be contrasted with, for example, $[(\eta^5\text{-}C_5H_5)(\eta^1\text{-}C_3H_5)Ru(CO)_2]$[132] and many other organometal-carbonyls[283] where only fragments of the molecular ion are observed, the molecular ion itself being undetected. There are two primary fragmentation pathways, both supported by metastables, one involving stepwise loss of CO with final cleavage of the allyl group, the other initiated by loss of allyl followed by stepwise loss of CO. In this respect the spectrum resembles those of $Re(CO)_5X$ (X = Cl, I)[284] where initial loss of CO or X are competing processes. As expected, decarbonylation of the η^1-allyl pentacarbonyl, to give a

Table 4.1: The Mass Spectrum of $[(\eta^1\text{-}C_3H_5)Re(CO)_5]$

m/e	Relative Intensity	Ion
368	28	$[(C_3H_5)Re(CO)_5]^+$
366	16	
340	81	$[(C_3H_5)Re(CO)_4]^+$
338	46	
312	50	$[(C_3H_5)Re(CO)_3]^+$
310	33	
284	46	
282	100	$[(C_3H_5)Re(CO)_2]^+ + [(C_3H_3)Re(CO)_2]^+$
280	44	
256	15	
254	37	$[(C_3H_5)Re(CO)]^+ + [(C_3H_3)Re(CO)]^+$
252	19	
228	9	
226	52	$[(C_3H_5)Re]^+ + [(C_3H_3)Re]^+$
224	37	
188	3	$[ReH]^+$
186	2	
327	35	$[Re(CO)_5]^+$
325	22	
299	65	$[Re(CO)_4]^+$
297	37	
271	61	$[Re(CO)_3]^+$
269	37	
243	20	$[Re(CO)_2]^+$
241	13	
215	11	$[Re(CO)]^+$
213	8	
187	22	$[Re]^+$
185	13	

Metastable supported transitions (Calc. position in parentheses):

368 → 340; m* = 314.0(314.1)
366 → 338; m* = 312.0(312.1)
340 → 312; m* = 286.0(286.3)
338 → 310; m* = 284.0(284.3)
312 → 284; m* = 258.0(258.5)
310 → 282; m* = 256.5(256.5)
327 → 299; m* = 273.0(273.4)
325 → 297; m* = 271.0(271.4)

tetracarbonyl ion (m/e 340) under electron impact occurs readily, resulting in the second most abundant ion in the entire spectrum. Even during a low energy scan (12eV) both the molecular ion M^+ and $[M - CO]^+$ were present in approximately equal abundance, presumably reflecting the stability of $[(\eta^3\text{-}C_3H_5)Re(CO)_4]$ with respect to $[(\eta^1\text{-}C_3H_5)Re(CO)_5]$.

Evaluation of the rhenium isotopic patterns indicates that the peak at m/e 282 (base peak) is associated with both the ions $[(C_3H_5)Re(CO)_2]^+$ and $[(C_3H_3)Re(CO)_2]^+$. The ions $[(C_3H_3)Re(CO)_x]^+$ (x = 2, 1, 0) are of high abundance in the mass spectrum and may arise by the elimination of the relatively common neutral H_2 fragment[132] or by simultaneous loss of 2H and CO possibly as formaldehyde HCHO[134]. The abundance of such ions can be explained by their formulation as η^3-cyclopropenyl-rhenium species. Indeed the formation of similar ions in the mass spectra of allyl complexes is a common occurence and has previously been observed, for example, in the spectra of $[(\eta^3\text{-}C_3H_5)Rh(\mu\text{-}Cl)]_2$[131], $[(\eta^5\text{-}C_5H_5)(\eta^1\text{-}C_3H_5)W(CO)_3]$[132] and $[(\eta^5\text{-}C_5H_5)(\eta^3\text{-}C_3H_5)Mo(CO)_2]$[134]. For the latter two complexes the most abundant metal-containing ions were $[(\eta^5\text{-}C_5H_5)(C_3H_3)M]^+$.

(b) η^3-Allyltetracarbonylrhenium(I)

The mass spectrum of $[(\eta^3\text{-}C_3H_5)Re(CO)_4]$ run using similar operating conditions as employed for the η^1-complex is given in Table 4.2. The molecular ion $[(C_3H_5)Re(CO)_4]^+$ is the second most abundant ion, in line with the reasoning previously used concerning its stability. The fragmentation pathway involving stepwise loss of CO with retention of the allyl group is clearly much favoured over that initiated by loss of allyl. Consequently, in contrast to the η^1-allyl, all the $[Re(CO)_x]^+$ ions (x = 4, 3, 2, 1) are of

Table 4.2: The Mass Spectrum of $[(\eta^3\text{-}C_3H_5)Re(CO)_4]$

m/e	Relative Intensity	Ion
340	65	$[(C_3H_5)Re(CO)_4]^+$
338	39	
312	28	$[(C_3H_5)Re(CO)_3]^+$
310	19	
284	44	
282	100	$[(C_3H_5)Re(CO)_2]^+ + [(C_3H_3)Re(CO)_2]^+$
280	46	
256	14	
254	34	$[(C_3H_5)Re(CO)]^+ + [(C_3H_3)Re(CO)]^+$
252	15	
228	11	
226	40	$[(C_3H_5)Re]^+ + [(C_3H_3)Re]^+$
224	34	
188	3	$[ReH]^+$
186	2	
299	2	$[Re(CO)_4]^+$
297	1	
271	6	$[Re(CO)_3]^+$
269	4	
243	6	$[Re(CO)_2]^+$
241	4	
215	3	$[Re(CO)]^+$
213	2	
187	11	$[Re]^+$
185	7	

Metastable supported transitions:

340 - 312; m* = 286.5(286.3)
338 - 310; m* = 284.2(284.3)
312 - 284; m* = 258.5(258.5)
310 - 282; m* = 256.5(256.5)
282 - 254; m* = 229(228.8)
280 - 252; m* = 227(226.8)

low relative abundance. Again cyclopropenyl-rhenium ions are prominent. The spectrum tabulated was recorded soon after sample insertion, some minor changes being observed with the passage of time. In particular weak peaks were observed at m/e 654 and at

m/e [654 - n(28)] (n = 1 - 10) associated with the formation of $[Re_2(CO)_x]^+$ (x = 10 - 0), in the spectrometer, (m/e for ^{187}Re isotope). In accordance with previous proposals[132,282,285], pyrolysis within the spectrometer may be responsible for the formation of the dinuclear species. Similarly, for example, attempts to obtain the mass spectrum of $[(\eta^5\text{-}C_5H_5)(\eta^3\text{-}C_3H_5)Fe(CO)]$ gave only the spectrum of ferrocene[132].

(c) Methyl, ^{13}C-methyl and d_3-methyl pentacarbonyl rhenium

The mass spectra of the three pentacarbonylmethylrhenium derivatives (Table 4.3) are closely similar. Small variations in abundances may be attributable to factors which are difficult to control[282], such as changes in sample pressure and temperature. The general features of the spectra can therefore be discussed together, using the abbreviation CH_3^* for the $^{12}CH_3$, $^{13}CH_3$ or CD_3 groups as appropriate.

Clearly loss of CO groups with retention of the methyl moiety for these pentacarbonyl derivatives is not a favoured process, the ions $[CH_3^*Re(CO)_x]^+$ (x = 4, 3, 2, 1, 0) being of relatively low abundance. In contrast, initial cleavage of the methyl group with subsequent loss of CO groups is a major fragmentation pathway and is well supported by the observation of the appropriate metastable ions (foot of Table 4.3). Other major ions in the two mass spectra are derived by fragmentation of the methyl group whilst still attached to rhenium, by loss of one, two or three hydrogen (or deuterium) atoms. The ease with which this occurs depends upon the relative energies of $[CH_3^*Re(CO)_n]^+$ and $[CH_{3-x}^*Re(CO)_n]^+$ (x = 1 - 3) as well as upon the neutral fragment released[282]. Evidently, under the conditions prevailing in the mass spectrometer, the 'metalo-carbyne'

Table 4.3: The Mass Spectra of $[CH_3Re(CO)_5]$, $[^{13}CH_3Re(CO)_5]$ and $[CD_3Re(CO)_5]$

$[CH_3Re(CO)_5]$		$[^{13}CH_3Re(CO)_5]$		$[CD_3Re(CO)_5]$		Ion
m/e	Rel.Int.	m/e	Rel.Int.	m/e	Rel.Int.	
342	74	343	58	345	65	$[CH_3^*Re(CO)_5]^+$
340	45	341	40	343	32	
314	2	315	2	317	1	$[CH_{3-x}^*Re(CO)_4]^+$
313	4	314	4	315	3	
312	3	313	3	313	2	
311	2	312	3	311′	1	
310	1	311	2			
286	6	287	7	289	8	$[CH_3^*Re(CO)_3]^+$
				287	6	
284	45	285	42	285	37	$[CH^*Re(CO)_3]^+$
282	26	283	24	283	23	
258	10	259	10	261	14	$[CH_3^*Re(CO)_2]^+$
				259	12	
256	81	257	76	257	82	$[CH^*Re(CO)_2]^+$
254	46	255	46	255	43	

..../cont'd

Table 4.3: Cont'd

$[CH_3Re(CO)_5]$		$[^{13}CH_3Re(CO)_5]$		$[CD_3Re(CO)_5]$		Ion
m/e	Rel.Int.	m/e	Rel.Int.	m/e	Rel.Int.	
230	1	231	2	233	1	$[CH^*_{3-x}Re(CO)]^+$
229	13	230	13	231	8	
228	35	229	37	229	35	
227	16	228	17	227	23	
226	19	227	27	225	4	
225	6	226	5			
202	5	203	7	205	8	$[CH^*_{3-x}Re]^+$
201	18	202	20	203	17	
200	46	201	53	201	48	
199	36	200	33	199	42	
198	26	199	42	197	12	
197	15	198	14			
327	100	327	100	327	100	$[Re(CO)_5]^+$
325	65	325	61	325	60	
299	82	299	78	299	78	$[Re(CO)_4]^+$
297	51	297	47	297	38	
271	89	271	87	271	75	$[Re(CO)_3]^+$
269	55	269	51	269	40	

..../cont'd

Table 4.3: Cont'd

$[CH_3Re(CO)_5]$		$[^{13}CH_3Re(CO)_5]$		$[CD_3Re(CO)_5]$		Ion
m/e	Rel.Int.	m/e	Rel.Int.	m/e	Rel.Int.	
243	36	243	42	243	31	$[Re(CO)_2]^+$
241	20	241	24	241	18	
216	2			217	3	$[H*Re(CO)]^+$
214	1					
215	23	215	28	215	21	$[Re(CO)]^+$
213	15	213	21	213	17	
188	2	188	3	189	4	$[H*Re]^+$
186	2	186	2			
187	47	187	55	187	43	$[Re]^+$
185	29	185	33	185	24	

..../cont'd

Table 4.3: Cont'd (Metastable supported transitions)

$[CH_3Re(CO)_5]$	$[^{13}CH_3Re(CO)_5]$	$[CD_3Re(CO)_5]$
342 → 327; m* = 312.5(312.7)	243 → 327; m* = 311.5(311.7)	345 → 327; m* = 310.0(310.0)
340 → 325; m* = 310.5(310.7)	341 → 325; m* = 309.5(309.7)	343 → 325; m* = 308.0(308.0)
327 → 299; m* = 273.5(273.4)	327 → 299; m* = 273.5(273.4)	327 → 299; m* = 273.5(273.4)
325 → 297; m* = 271.5(271.4)	325 → 297; m* = 271.5(271.4)	325 → 297; m* = 271.5(271.4)
299 → 271; m* = 245.5(245.6)	299 → 271; m* = 246.0(245.6)	299 → 271; m* = 245.5(245.6)
297 → 269; m* = 243.5(243.6)	297 → 269; m* = 244.0(243.6)	297 → 269; m* = 243.5(243.6)
271 → 243; m* = 218.0(217.9)	271 → 243; m* = 218.0(217.9)	271 → 243; m* = 218.0(217.9)
269 → 241; m* = 216.0(215.9)	269 → 241; m* = 216.0(215.9)	269 → 241; m* = 216.0(215.9)
284 → 256; m* = 231.0(230.8)	285 → 257; m* = 232.0(231.8)	285 → 257; m* = 231.5(231.8)
282 → 254; m* = 229.0(228.8)	283 → 255; m* = 230.0(229.8)	283 → 255; m* = 230.0(229.8)
256 → 228; m* = 203.0(203.1)		

ions, $[HC^*Re(CO)_x]^+$ and $[DCRe(CO)_x]^+$ (x = 4, 3, 2, 1, 0), formed by loss of H_2 (or D_2) are relatively stable, as indicated by their high abundance. Indeed a measure of their stability is that the ions $[HC^*Re(CO)_2]^+$ and $[DCRe(CO)_2]^+$ all occur in more than 75% abundance in their respective mass spectra. Other less significant ions at m/e 211 and 209 may be due to $[ReC_2]^+$. Weak peaks at m/e 216 and 188 in the spectrum of $[CH_3^*Re(CO)_5]$ are attributed to $[HRe(CO)]^+$ and $[HRe]^+$, an assignment which is confirmed by comparison with $[CD_3Re(CO)_5]$, where the same peaks occur but shifted to one higher mass unit.

Vibrational Spectra

Apart from a list of $\nu(CO)$ frequencies for the η^3-allyl complex[280], vibrational spectroscopic data were not available for either allylrhenium species. In view of this, fairly extensive infrared and Raman data were obtained for both the η^1- and η^3- allyl compounds. Since $[(\eta^1-C_3H_5)Re(CO)_5]$ is a liquid at room temperature and $[(\eta^3-C_3H_5)Re(CO)_4]$ has a melting point of 32°C, liquid phase spectra of these molecules with Raman polarisation measurements were easily obtained. The results are therefore readily amenable to analysis as correlation and factor group splittings are eliminated. Infrared and Raman spectra of the solid methylrhenium complexes were obtained between 4000 - 40 cm^{-1} and although Raman polarisation measurements were limited by lack of solubility, reasonably complete assignments could be made.

(a) η^1-Allylpentacarbonylrhenium

Because $[(\eta^1-C_3H_5)Re(CO)_5]$ is very air-sensitive in solution, solvents and cells were thoroughly purged with dry nitrogen prior to use. When treated in this way the solution spectra remained

unchanged over a period of some thirty minutes. Liquid film spectra, however, showed signs of decomposition more quickly and at least two samples were required to cover the region 4000 - 200 cm^{-1} during a twelve minute scan.

The vibrational spectra of only a few η^1-allyl compounds have been examined, however useful information is available for $[(\eta^1\text{-}C_3H_5)_4M]$ (M = Si or Sn)[286], $[(\eta^1\text{-}C_3H_5)_2Hg]$[287] and the allyl halides[288]. Of most interest from a comparative point of view is the reported [128] spectrum of $[(\eta^1\text{-}C_3H_5)Mn(CO)_5]$ (Table 1.5) although the absence of Raman polarisation data render some of the assignments questionable.

The vibrational analysis of many organometal carbonyls has often employed the concept of local symmetry. Thus for $[(\eta^1\text{-}C_3H_5)Re(CO)_5]$ the local symmetry of the $Re(CO)_5$ unit is C_{4v} and that of the allyl group is C_s. Tables 4.4 and 4.8 list the numbers and symmetries of the normal modes for the $Re(CO)_5X$ unit (X = bonded C of the η^1-allyl group) and for the allyl group respectively.

Table 4.4: Vibrations of an $XRe(CO)_5$ Unit in C_{4v} Symmetry

Vibrational Mode	C_{4v} Symmetry Species	Raman(R) or Infrared(IR) Activity[a]
ν(CO)	$2A_1 + B_1 + E$	4R(2 pol) + 3IR
ν(ReC)	$2A_1 + B_1 + E$	4R(2 pol) + 3IR
ν(ReX)	A_1	1R(pol) + 1IR
δ(ReCO)	$A_1 + A_2 + B_1 + B_2 + 3E$	6R(1 pol) + 4IR
δ(CReC)	$A_1 + B_1 + B_2 + 2E$	5R(1 pol) + 3IR
δ(CReX)	E	1R + 1IR

[a] A_2 modes inactive

Although group theory (Appendix 3) allows the formal derivation of such modes it must be borne in mind when discussing vibrational spectra that these are only approximate descriptions. In reality some mixing of modes is often likely and may be extensive, especially when vibrations of like symmetry, which are close in frequency, are considered.

(i) The ν(CO) region

The ν(CO) bands are listed in Table 4.5. The assignments are in line with those reported for other $LM(CO)_5$ systems in that the frequencies decrease in the order $A_1(eq) > B_1 > E > A_1(ax)$ (Figure 4.4).

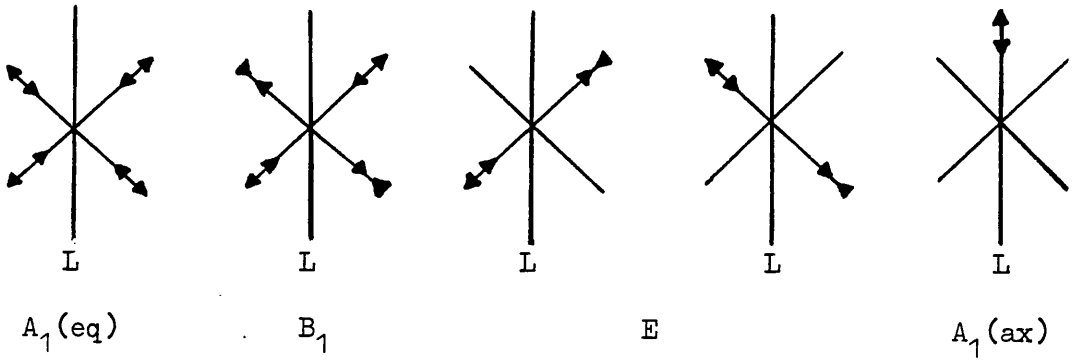

Figure 4.4: Normal ν(CO) modes of $LM(CO)_5$ in C_{4v} symmetry

In the infrared spectrum the band intensities decrease in the expected[229] order $E > A_1(ax) \gg A_1(eq) \gg B_1$, the B_1 mode being formally infrared-inactive. Its appearance is indicative of a small perturbation from C_{4v} symmetry due to the presence of the allyl group[233]. The intensity order in the Raman spectrum is $A_1(eq) > B_1 > A_1(ax) \gg E$, thus bands which are strong in the infrared are weak in the Raman and vice-versa. Both $A_1(eq)$ and $A_1(ax)$ bands are polarised thereby confirming their assignments. A weak band at 1943 cm^{-1} is attributed to the ^{13}C satellite of the $A_1(ax)$ mode. The observed ratio $\nu(^{12}CO)/\nu(^{13}CO)$ (0.978) is very

close to the expected value of 0.977[233].

Table 4.5: Vibrational Spectra of $[(\eta^1\text{-}C_3H_5)Re(CO)_5]$ in the Carbonyl Region

Infrared (pentane)	Raman (benzene)	Infrared (liquid)	Raman (liquid)	Assignment
2131 w	2127 vs, pol	2129 s	2127 vs, pol	A_1(eq)
2050 w	2052 s, dp	2050 m, sh	2051 s, dp	B_1
2020 vs	2020 vw	2020 vs, vbr	2020 vvw	E
1986 s	1972 m, pol	1970 vs	1970 m, pol	A_1(ax)
1943 w				$\nu(^{13}CO)$

These results confirm the view that the local symmetry approach is justified since if C_{2v} symmetry were more appropriate (pairs of equatorial CO groups being perturbed by allyl) five ν(CO) bands should be observed in both the infrared and Raman spectra ($3A_1 + B_1 + B_2$, 3 pol). Alternatively if the molecule possessed overall C_s symmetry five ν(CO) bands (4A' + A") would be expected, of which four should be polarised. The results are clearly best explained in terms of C_{4v} local symmetry.

The solution ν(CO) frequencies were used to calculate simple Cotton-Kraihanzel (CK) force constants (Appendices 4 and 5) and the values obtained were: K_{ax}, 16.09; K_{eq}, 17.07; K_i, 0.29 mdyne Å^{-1}. Using literature ν(CO) frequencies[128] the CK force constants for $[(\eta^1\text{-}C_3H_5)Mn(CO)_5]$ were also calculated (K_{ax}, 16.20; K_{eq}, 16.88; K_i, 0.24 mdyne Å^{-1})and for comparison use of the ν(CO) frequencies of the methyl compounds (Table 4.16 and reference 289) gave CK force constants as follows: $[CH_3Re(CO)_5]$ (K_{ax}, 16.08; K_{eq}, 17.04; K_i, 0.30 mdyne Å^{-1}) and $[CH_3Mn(CO)_5]$ (K_{ax}, 16.13; K_{eq}, 16.83;

K_i, 0.25). The K_{ax} values are marginally lower and K_{eq} and K_i values marginally higher for the rhenium compounds when like pairs are considered, but the variations, although consistent, are within the experimental error of the method and are therefore barely significant. The results suggest that the manganese and rhenium atoms in these compounds show very similar π-acceptor and σ-donor capacities and that the σ-bonding abilities of the methyl and η^1-allyl groups and their inductive effects are indistinguishable (c.f. pages 10 and 11). Finally it is noticeable that although the A_1(eq), E and A_1(ax) ν(CO) frequencies alter by +21, +6 and -8 cm^{-1} on changing from $[(\eta^1\text{-}C_3H_5)Mn(CO)_5]$ to $[(\eta^1\text{-}C_3H_5)Re(CO)_5]$, the B_1 frequency only changes by +1 cm^{-1}. This is in line with the expectation that the B_1 mode should be insensitive to changes in the mass of the metal atom[260].

(ii) The δ(ReCO) and ν(ReC) region

The δ(ReCO) and ν(ReC) vibrations are expected to lie in the 700 - 300 cm^{-1} region[290-292] and the former generally, but not invariably, appear at the higher frequencies[293]. One of the problems in assigning such vibrations is that extensive mixing of modes of the same symmetry will occur owing to the small frequency differences between δ(MCO) and ν(MC) fundamentals[294]. As an assignment aid it is well known that δ(MCO) bands are normally much more intense in the infrared than in the Raman, the reverse being true of ν(MC) bands. Thus, in contrast to the ν(CO) region, assignment of δ(MCO) and ν(MC) vibrations is not so obvious, frequently leading to uncertain and sometimes ambiguous results. However the method of symmetry correlation between these vibrations and those of an appropriate metal carbonyl, for which the assignments are unequivocal, has often been successfully applied. For example,

the δ(MCO) and ν(MC) vibrations of $Mn(CO)_5Br$ were assigned by correlation with $Cr(CO)_6$[290] and those of $[M(CO)_5(PH_3)]$ by correlation with $M(CO)_6$; (M = Cr, Mo, W)[295]. The derivation of correlation tables for the species of a group and its subgroups is treated in detail in several texts[226,232,296] and the correlation required in this case, namely that between O_h and C_{4v} symmetries, is given in Table 4.6.

Table 4.6: Correlation Between the O_h and C_{4v} Groups via the Intermediate D_{4h} Group

O_h	D_{4h}	C_{4v}
A_{1g}	A_{1g}	A_1
A_{2g}	B_{1g}	B_1
E_g	$A_{1g} + B_{1g}$	$A_1 + B_1$
T_{1g}	$A_{2g} + E_g$	$A_2 + E$
T_{2g}	$B_{2g} + E_g$	$B_2 + E$
A_{1u}	A_{1u}	A_2
A_{2u}	B_{1u}	B_2
E_u	$A_{1u} + B_{1u}$	$A_2 + B_2$
T_{1u}	$A_{2u} + E_u$	$A_1 + E$
T_{2u}	$B_{2u} + E_u$	$B_1 + E$

The well documented[258] spectrum of $[Re(CO)_6]^+$ was chosen for symmetry correlation with $[(\eta^1\text{-}C_3H_5)Re(CO)_5]$ although that of $W(CO)_6$ [297,298] could equally well have been used. Assignments for the $Re(CO)_5X$ unit (X = bonded C of the η^1-allyl group) based on this correlation are proposed in Table 4.7.

Table 4.7: Assignment of δ(ReCO) and ν(ReC) Bands (cm^{-1}) of $[(\eta^1\text{-}C_3H_5)Re(CO)_5]$ and Symmetry Correlation with $[Re(CO)_6]^+$

$[Re(CO)_6]^+$		$[(\eta^1\text{-}C_3H_5)Re(CO)_5]$		
Frequency	Assignment (O_h)	Assignment (C_{4v})	Infrared (liquid)	Raman (liquid)
584	T_{1u} δ(ReCO)	A_1	600 vs	603 w
		E	585 vs	590 vw
522	T_{2u} δ(ReCO)	E	531 ms	533 vw
		B_1		522 vw
486	T_{2g} δ(ReCO)	B_2	505 vw	503 vw
441	A_{1g} ν(ReC)	A_1(eq)	465 w, sh	463 vs, pol
426	E_g ν(ReC)	A_1(ax)	446 ms	445 ms, pol?
		B_1	430 w, sh	430 m, dp?
356	T_{1u} ν(ReC)	E	373 vs[a]	
		A_1 ν(ReX)[b]		370 s, pol[a]
354	T_{1g} δ(ReCO)	A_2	inactive	
		E	350 m	

[a] may be accidentally degenerate bands, see text

[b] X = bonded C of η^1-allyl group

Using the assignment of the infrared active T_{1u} δ(ReCO) mode of $[Re(CO)_6]^+$ to a band at 584 cm^{-1}, it follows that the two highest energy very strong infrared bands of $[(\eta^1\text{-}C_3H_5)Re(CO)_5]$ are the A_1 + E δ(ReCO) vibrations. The A_1 band is too weak in the Raman spectrum for a polarisation measurement. The B_1 and B_2 δ(ReCO) vibrations should be Raman-active only and are assigned to weak bands at 522 and 503 cm^{-1}. The weakness of B_1 is expected since

it correlates with the formally inactive T_{2u} δ(ReCO) mode of $[Re(CO)_6]^+$. The two remaining bands assigned to δ(ReCO) vibrations are the E modes which are, as expected, of high intensity in the infrared but at best very weak in the Raman. One of these bands at 531 cm^{-1} correlates with T_{2u} δ(ReCO) and the other which appears at the very low frequency of 350 cm^{-1} is in line with the T_{1g} mode of $[Re(CO)_6]^+$ found at 354 cm^{-1}.

The symmetry correlation method also allows a sensible assignment of the ν(ReC) modes of the η^1-allyl complex. Thus the A_{1g} mode of $[Re(CO)_6]^+$ at 441 cm^{-1} correlates with the A_1(eq) mode of the C_{4v} allyl, and can readily be assigned to a very strong, polarised Raman band at 463 cm^{-1} which appears only as a weak shoulder in the infrared spectrum. The A_1(ax) mode is assigned to a medium intensity Raman and infrared band at 445 cm^{-1}. The polarisation of this band could not be accurately measured owing to the closeness of the very intense A_1(eq) band. However the intensity relationship between these two bands is in accordance with the prediction that the equatorial mode should develop almost zero change in dipole moment but a very large change in polarisability. Due to the intensity of A_1(eq) the B_1 mode, which is assigned to a band at 430 cm^{-1}, and the A_1(ax) band are only clearly visible in parallel polarisation resulting in uncertain polarisation measurements. Similar behaviour was noted for the E_g ν(MC) modes of $[Re(CO)_6]^+$ [258] and $M(CO)_6$ (M = Cr, Mo and W), which correlate with A_1(ax) and B_1 modes of $[(\eta^1\text{-}C_3H_5)Re(CO)_5]$. Using the assignments for $[Re(CO)_6]^+$ and correlating E_g(Raman) → B_1 and T_{1u}(infrared) → E, the remaining E mode should occur as a strong infrared band but a weak Raman band at lower energy than B_1. The only remaining very strong infrared band is found at 373 cm^{-1} and

so is assigned accordingly. However the Raman spectrum also contains a strong polarised band at 370 cm^{-1} which cannot be assigned to the E ν(ReC) mode and therefore indicates that these bands do not arise from the same vibration but are accidentally almost degenerate. Since a strong, polarised band in the spectrum of $[(\eta^5\text{-}C_5H_5)(\eta^1\text{-}C_3H_5)W(CO)_3]$ at 353 cm^{-1} was assigned to ν(WX) it seems likely that one other band that is expected in this region is the ν(Re-X) mode (X = bonded C of η^1-allyl) and so this is assigned to the strong polarised Raman band at 370 cm^{-1}. A further difficulty arises in that previous workers[286,287] have for $[(\eta^1\text{-}C_3H_5)_4Si]$ and for $[(\eta^1\text{-}C_3H_5)_2Hg]$ assigned a band in this region to an A"(CC=C) out-of-plane deformation. However no such assignment is made for $[(\eta^1\text{-}C_3H_5)Re(CO)_5]$ and some comments on this point are made below.

In the reported[128] spectrum of $[(\eta^1\text{-}C_3H_5)Mn(CO)_5]$ all the observed bands in the 700 - 300 cm^{-1} region were assigned to A_1 and E modes but even though benzene solution Raman spectra were recorded no polarisation data were included. As a result some of the assignments appear to be erroneous. Thus a Raman band at 479 cm^{-1} is listed as coincident with an infrared band at 456 cm^{-1} and assigned to A_1(ax) ν(MnC) whereas these are more likely associated with A_1(ax) and E ν(MnC) modes respectively. The energy order of the ν(MnC) bands is given as $E > A_1(ax) > A_1(eq)$ which does not agree with the order proposed above for the analogous η^1-allyl-rhenium complex. Finally although the assignment of the two highest energy δ(MnCO) to A_1 + E is reasonable no regard was paid to the fact that an A'(CC=C) in-plane deformation of the allyl group should appear in this region.

(iii) η^1-Allyl vibrations

A simple group theoretical treatment of the η^1-C_3H_5 unit in C_s symmetry shows that eighteen normal modes of vibration are expected for an isolated η^1-allyl group (8 atoms). The derivation of these modes appears in Appendix 3 and approximate descriptions of the vibrations, together with the C_s symmetry labels so obtained, are listed in Table 4.8.

Table 4.8: Vibrations of an Isolated η^1-Allyl Group in C_s Symmetry

Vibrational Mode[a]	C_s Symmetry Species[b]	Vibrational Mode[a]	C_s Symmetry Species[b]
$\nu(CH_2)$vinyl	2A'	$\rho_w(CH_2)$vinyl	A''
ν(CH)vinyl	A'	δ_r(CH)vinyl in-plane	A'
$\nu(CH_2)$methylene	A' + A''	$\delta_s(CH_2)$methylene	A'
ν(C=C)	A'	$\rho_w(CH_2)$methylene	A'
ν(CC)	A'	$\rho_t(CH_2)$methylene	A''
$\delta_s(CH_2)$vinyl	A'	$\rho_r(CH_2)$methylene	A''
$\rho_r(CH_2)$vinyl	A'	δ(CC=C)in plane	A'
$\rho_t(CH_2)$vinyl	A''	π(CCH=C)out-of-plane	A''

[a] All modes infrared and Raman active

[b] A' polarised in the Raman

Previously[286] nineteen normal modes of vibration have been ascribed to the allyl group, including a vinyl (CH) out-of-plane wag (A'') and a (CC=C) out-of-plane deformation (A''). However whilst due regard must be paid to the approximate nature of these descriptions, the combination of these two modes to give one A'' vibration is preferable. This vibration can be described as an out-of-plane π(CCH=C) deformation or more simply as a skeletal

deformation[288]. Support for this approach comes from the fact that although nineteen modes were predicted previously, assignments for both the vinyl (CH) out-of-plane wag and the (CC=C) out-of-plane deformation proved to be elusive, assignments being made only after all other modes had been eliminated. Bearing in mind the above comments, the A' and A'' modes of the allyl group in $[(\eta^1\text{-}C_3H_5)Re(CO)_5]$ have been assigned using the reported spectra of $[(\eta^1\text{-}C_3H_5)_4M]$ (M = Si, Sn) and the allyl halides as a guide.

The fundamental frequencies and probable assignments for the allyl group are summarised in Table 4.9. Three ν(CH) and $\nu(CH_2)$ stretching vibrations associated with the vinyl part of the allyl group give rise to the highest energy fundamentals[99,286,288] and are assigned to medium intensity bands at 3078, 2987 and 2964 cm^{-1}. Two medium intensity bands of lower energy are assigned to the $\nu(CH_2)$methylene asymmetric and symmetric stretches at 2915 and 2855 cm^{-1} respectively. The ν(C=C) stretch is easily assigned to an intense sharp feature at 1616 cm^{-1}, in close agreement with many other η^1-allyl-metal compounds (page 23). The observation of this band is a simple diagnostic test for the presence of an η^1-bonded allyl group.

By analogy with the allyl halides[288] and vinyl and methylene groups in many other chemical environments[99,286], the methylene and vinyl scissors deformations are assigned to medium intensity bands at 1434 and 1398 cm^{-1} respectively. Two rocking deformations of the CH and CH_2 groups are found at 1295 and 1095 cm^{-1} respectively. The latter is very strong in the Raman spectrum (1099 cm^{-1}) and corresponds with a similar very strong $\rho_r(CH_2)$ band in $[Sn(\eta^1\text{-}C_3H_5)_4]$ at 1094 cm^{-1} [286]. The methylene wagging vibration is expected to give rise to a sharp, medium to

Table 4.9: Allyl Vibrations of $[(\eta^1\text{-}C_3H_5)Re(CO)_5]$

Frequency (cm^{-1})		Assignment	
Infrared	Raman	Description	Symmetry
3078 m	3075 vw, br	$\nu_a(CH_2)$vinyl	A'
2989 w	2987 m	ν(CH)vinyl	A'
2964 m		$\nu_s(CH_2)$vinyl	A'
2925 m		$\nu_a(CH_2)$methylene	A''
2854 w	2855 m	$\nu_s(CH_2)$methylene	A'
1616 s	1617 s	ν(C=C)	A'
1434 m	1430 vw	$\delta_s(CH_2)$methylene	A'
1398 m	1397 m	$\delta_s(CH_2)$vinyl	A'
1295 m	1293 m	δ_r(CH)vinyl	A'
1200 ms	1202 w	$\rho_w(CH_2)$methylene	A'
1095 m	1099 vs	$\rho_r(CH_2)$vinyl	A'
1037 ms	1041 vw	$\rho_t(CH_2)$methylene	A''
991 ms		$\rho_t(CH_2)$vinyl	A''
954 ms	961 w	ν(CC)	A'
875 s	874 w	$\rho_w(CH_2)$vinyl	A''
755 m	752 w	$\rho_r(CH_2)$methylene	A''
678 ms	678 m, pol	δ(CC=C)in-plane	A'
637 w		π(CCH=C)out-of-plane	A''

strong infrared band between 1200 and 1180 cm^{-1} and the corresponding twisting mode should appear at lower frequency as a medium intensity infrared band. Both should have weak Raman counterparts and are assigned to bands at 1200 and 1037 cm^{-1} respectively. In the allyl halides, $[Si(\eta^1\text{-}C_3H_5)_4]$ and $[Sn(\eta^1\text{-}C_3H_5)_4]$ the vinyl twisting mode occurs consistently within the range 995 - 980 cm^{-1} as a

medium-strong infrared band with a weaker or absent Raman counterpart. Thus a medium-strong band at 991 cm^{-1} in the infrared spectrum of $[(\eta^1\text{-}C_3H_5)Re(CO)_5]$ is assigned to the $\rho_t(CH_2)$ vinyl mode.

The ν(CC) stretch is assigned to a medium-strong infrared band at 954 cm^{-1} rather than to the weaker band at 933 cm^{-1} which is believed to originate from an overtone of the A_1 ν(ReC) vibration at 465 cm^{-1}. The corresponding ν(CC) band in $[Sn(\eta^1\text{-}C_3H_5)_4]$ occurs at 930 cm^{-1}. This leaves strong infrared bands with weak Raman counterparts at 875 and 755 cm^{-1} to be assigned to the vinyl (CH_2) wag and the methylene (CH_2) rocking mode. The latter vibrations occur over a wide frequency range (800 - 720 cm^{-1}) depending on the nature of the compound[286]. The (CC=C) in-plane deformation is assigned to a medium intensity band at 678 cm^{-1}, polarised in the Raman spectrum. Strong, polarised Raman bands at 678 and 670 cm^{-1} were similarly assigned for $[Si(\eta^1\text{-}C_3H_5)_4]$ and $[Sn(\eta^1\text{-}C_3H_5)_4]$ respectively. Finally the π(CCH=C) skeletal deformation is assigned to the only remaining band above the δ(ReCO) region at 637 cm^{-1}.

(iv) Overtone and combination vibrations

The above three sections account for all the major features in the vibrational spectra of $[(\eta^1\text{-}C_3H_5)Re(CO)_5]$. The remaining weak or very weak peaks are listed in Table 4.10 and their possible origin as overtones or combinations of the fundamental vibrations is suggested.

Table 4.10: Overtones and Combinations

Observed Frequency (cm^{-1})		Possible Origin
Infrared	Raman	
3027 w	3033 vw	1616 + 1434
2911 m	2909 vw	1616 + 1295
2823 w		1434 + 1398
2565 w		1970 + 600, 2129 + 430
2500 w		2129 + 370
2434 w		1970 + 465
1463 vw		1095 + 370
1750 w		2 x 875
1366 m		2 x 678
1268 w		600 + 678
933 w	935 mw	2 x 465
912 w		465 + 446

(b) η^3-Allyltetracarbonylrhenium

The vibrational spectra of several η^3-allyl complexes of the transition metals have been reported and extensive studies carried out on, for example, $[(\eta^3\text{-}C_3H_5)PdX]_2$ (X = Cl, Br)[125] and $[(\eta^3\text{-}C_3H_5)Co(CO)_3]$[300]. The former compound (X = Cl) is of interest in that it was the subject of a recent study[301] in which incoherent inelastic neutron scattering was used to obtain information about the low frequency vibrations. The study most relevant to this work is that on $[(\eta^3\text{-}C_3H_5)Mn(CO)_4]$[40] (see Chapter 1, pages 24 - 26).

The evidence presented below shows that unlike $[(\eta^1\text{-}C_3H_5)Re(CO)_5]$, but in agreement with the findings on $[(\eta^3\text{-}C_3H_5)Mn(CO)_4]$, the

concept of local symmetry cannot be applied to the assignment and interpretation of the vibrational spectrum of $[(\eta^3\text{-}C_3H_5)Re(CO)_4]$. Instead the overall C_s symmetry of the molecule must be used with the comformation of the molecule being that shown in Figure 4.5(a) (with a σ_v plane) rather than the alternative conformation shown in Figure 4.5(b) (with a σ_d plane).

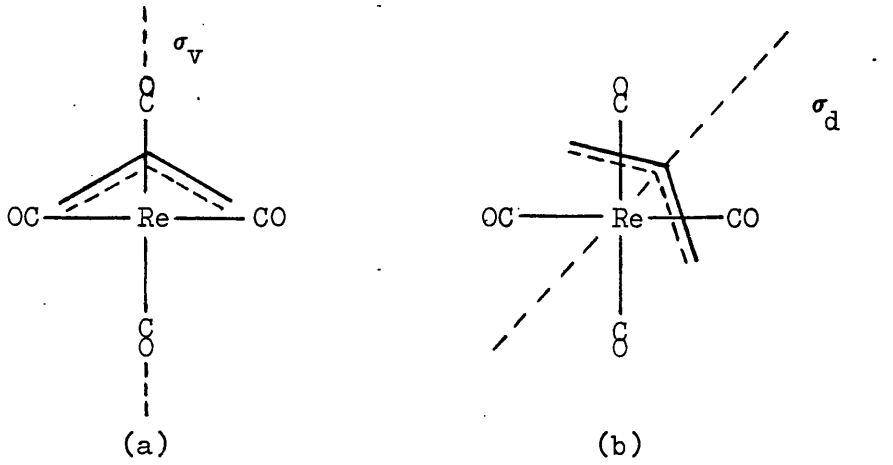

Figure 4.5: Alternative conformations of $[(\eta^3\text{-}C_3H_5)Re(CO)_4]$

(i) The ν(CO) region

The ν(CO) vibrational modes, infrared and Raman activities and numbers of polarised bands predicted for several alternative symmetries of the $Re(CO)_4$ unit are listed in Table 4.11.

Table 4.11: Predicted Numbers and Symmetries of the ν(CO) Vibrational Modes of the $Re(CO)_4$ Unit

Local Symmetry	ν(CO) Modes Predicted	Infrared(IR) or Raman(R) activity	Polarised Bands
C_{4v}	$A_1 + B_1 + E$	2IR, 3R	A_1
C_{2v}	$2A_1 + B_1 + B_2$	4IR, 4R	$2A_1$
$C_s(\sigma_d)$	2A' + 2A''	4IR, 4R	2A'
$C_s(\sigma_v)$	3A' + A''	4IR, 4R	3A'

Solution infrared spectra in the ν(CO) region in various solvents are presented in Table 4.12 and the band positions obtained from the infrared and Raman spectra of molten samples are listed in Table 4.13. The infrared results are in good agreement with those quoted previously for $[(\eta^3\text{-}C_3H_5)Re(CO)_4]$ (2091, 1996, 1982, 1963 cm^{-1})[280].

Table 4.12: Solution Infrared Spectra of $[(\eta^3\text{-}C_3H_5)Re(CO)_4]$ (cm^{-1})

n-pentane	chloroform	Nujol (solution)	ν(CO) Assignment[a]
2093 m	2090 s	2094 s	A'
1997 vs	1995 vs	1994 vs	A'
1983 vs	1978 vs	1980 vs	A''
1963 vs	1949 vs	1959 vs	A'
1945 w			$\nu(^{13}CO)$

[a] Supported by Raman polarisation measurements

Both the infrared and Raman spectra show four ν(CO) bands and therefore a description utilising the concept of C_{4v} local symmetry is inadequate. Furthermore, three bands are polarised in the Raman effect whilst only one is depolarised. These results are in accord with the selection rules for overall C_s symmetry with the most likely conformation being that containing a σ_v symmetry plane (Figure 4.5(a)).

Cotton-Kraihanzel force constants were also calculated (K_1 = 15.83, K_2 = 16.76, K_i = 0.33 mdyne $Å^{-1}$). Using literature ν(CO) frequencies[40] for $[(\eta^3\text{-}C_3H_5)Mn(CO)_4]$, the corresponding force constants were calculated for comparison (K_1 = 15.78, K_2 = 16.64, K_i = 0.27 mdyne $Å^{-1}$). Clearly, as for the $[(\eta^1\text{-}C_3H_5)M(CO)_5]$, (M = Mn, Re), pair there is little significant difference in the

electron availability at the two metal centres.

(ii) The δ(ReCO), ν(ReC) and ν(Re-allyl) region

The infrared and Raman spectra in the 620 - 320 cm^{-1} region (Table 4.13) are, as anticipated, very rich in bands and although the observations do not permit a distinction to be made between the possible C_s symmetries (Figure 4.5) it is again clear that the results are inconsistent with C_{4v} local symmetry. For example, three polarised Raman bands at 608, 594 and 546 cm^{-1} must be assigned to A' δ(ReCO) modes whereas for C_{4v} symmetry only the single A_1 vibration of the $A_1 + A_2 + B_1 + B_2 + 2E$ δ(ReCO) set should be polarised. Likewise the presence of at least two polarised Raman bands (477, 459 cm^{-1}), assignable to ν(ReC) vibration, rules out C_{4v} symmetry since only a single A_1 vibration of the $A_1 + B_1 + E$ ν(ReC) set should be polarised. Since the evidence from the ν(CO) region clearly favours the conformation involving a σ_v plane, the results for the lower frequency region have also been analysed from this standpoint. Thus the total number of modes expected (9A' + 6A") are as follows:

$\Gamma_{\delta(ReCO)} = 4A' + 4A''$

$\Gamma_{\nu(ReC)} = 3A' + A''$

$\Gamma_{\nu(Re\text{-}allyl)} = 2A' + A''$

Eleven bands have been observed of which seven are polarised so clearly A' in type.

Four δ(Re CO) bands are observed (three only in the infrared), whereas eight are predicted for C_s symmetry, and as expected they are very strong in the infrared but weak in the Raman. Three of the bands are polarised and must therefore be assigned to A' modes. Two Raman bands, at 477 and 459 cm^{-1}, are very intense and polarised so are assigned to A' ν(ReC) modes. They have weaker

Table 4.13: Vibrational Frequencies (cm^{-1}) of $[(\eta^3-C_3H_5)Re(CO)_4]$ Excluding Allyl Bands

Infrared (melt)	Raman (melt)	Assignment (C_s)	
2094 s	2091 ms, pol	ν(CO)	A'
1994 vs	1990 m, pol	ν(CO)	A'
1980 vs	1979 mw, dp	ν(CO)	A''
1959 vs	1953 mw, pol	ν(CO)	A'
610 vs	608 vw, pol	δ(ReCO)	A'
591 vs	594 w, pol	δ(ReCO)	A'
547 s	546 m, pol	δ(ReCO)	A'
	501 vw, dp?	δ(ReCO)	A''
471 s	477 vs, pol	ν(ReC)	A'
455 vw, sh	459 vs, pol	ν(ReC)	A'
442 m		ν(ReC)	A'?
395 m, sh	394 m, pol	ν_t(Re-allyl)	A'
377 vs	377 w, dp	ν(ReC)	A''
332 m	331 s, pol	ν_s(Re-allyl)	A'
	314 ms, dp	ν_t(Re-allyl)	A''
	217 ms, pol		
	142 m, dp	δ(CReC)	A''
	100 s, pol	δ(CReC)	A'

infrared counterparts. The three ν(Re-allyl) vibrations have been assigned by a consideration of polarisation data and also in the knowledge that these bands are found between 400 and 300 cm^{-1} in such compounds as $[(\eta^3-C_3H_5)Mn(CO)_4]$[40], $[(\eta^3-C_3H_5)PdX]_2$ (X = Cl, Br)[125], $[(\eta^3-C_3H_5)Co(CO)_3]$[300] and $[(\eta^3-C_3H_5)NiBr]_2$[301].

These vibrations may be described as one stretch ν_s(Re-allyl) A' and two tiliting motions ν_t(Re-allyl) A' + A" (see page 25). Analysis of the spectra of several η^3-allyl-metal compounds has shown[38] that the frequency of the A" vibration can occupy any of the three possible positions in relation to the other two A' vibrations. On these grounds the bands at 394, 331 and 314 cm^{-1} are assigned to these vibrations, the two highest in energy being polarised and hence A' in type. The weaker depolarised Raman band with no infrared counterpart at 314 cm^{-1} is assigned to the ν_t(Re-allyl) A" vibration by analogy with other η^3-allyl-metal systems[38,40,125], in which it also occurs as a medium-weak infrared and Raman feature. The very strong infrared band at 377 cm^{-1} is tentatively assigned to the only ν(ReC) A" vibration. These assignments are by no means secure however as the two A" assignments at 377 and 314 cm^{-1} could quite conceivably be interchanged. A final τ(Re-allyl) A" torsion has not been assigned but would be of low energy and weak intensity in both infrared and Raman spectra. Other low energy Raman bands of medium-strong intensity at 142 and 100 cm^{-1} are more likely to be due to δ(CReC) deformations.

(iii) η^3-Allyl vibrations

Table 1.4 (page 24) and Appendix 3 show that for an η^3-allyl group of C_s symmetry there are eighteen normal modes of vibration (10A' + 8A"). In Table 4.14 nine A' and seven A" modes have been assigned for $[(\eta^3\text{-}C_3H_5)Re(CO)_4]$, no bands being found in the 2950 and 520 cm^{-1} regions which could be assigned to the $\nu(CH_2)$ A" and δ(CCC) A' vibrations respectively. The $\nu(CH_2)$ A" vibration could likewise not be found for either $[(\eta^3\text{-}C_3H_5)Co(CO)_3]$[300] or $[(\eta^3\text{-}C_3H_5)PdX]_2$ (X = Cl, Br)[125]. The assignments in Table 4.14

are based largely on those presented for $[(\eta^3\text{-}C_3H_5)Mn(CO)_4]$[40] (see Table 1.5, page 26), $[(\eta^3\text{-}C_3H_5)PdX]_2$[125] and $[(\eta^3\text{-}C_3^*H_5)Fe(CO)_2NO]$ ($^*H = {}^1H, {}^2H$)[122] and whilst general agreement is good with only a few minor variations in assignments, the approximate nature of the descriptions must always be kept in mind.

Table 4.14: Allyl Vibrations of $[(\eta^3\text{-}C_3H_5)Re(CO)_4]$

Frequency (cm^{-1})		Assignment	
Infrared (melt)	Raman (melt)	Description	Symmetry
3075 w	3077 vw, dp	$\nu(CH_2)$	A''
3015 w	3019 w, pol	$\nu(CH)$	A'
2965 vw	2964 vw, pol	$\nu(CH_2)$	A'
2935 vw		$\nu(CH_2)$	A'
1495 m	1495 vw, dp	$\nu(CCC) + \delta(CH_2)$	2A''
1397 w	1396 w, dp		
1463 m	1463 vw, pol	$\delta(CH_2)$	A'
1214 m	1219 m, pol	$\pi(CH)$	A'
1140 w	1138 vw, dp?	$\delta(CH)$	A''
1025 vw	1023 m, pol	$\nu(CCC)$	A'
1004 m	1003 ms, pol	$\rho_t(CH_2)$	A'
978 vw		$\rho_t(CH_2)$	A''
923 m	923 m, pol	$\rho_w(CH_2)$	A'
872 m	871 vw, dp	$\rho_w(CH_2)$	A''
797 w	791 mw, pol	$\rho_r(CH_2)$	A'
774 vw	762 mw, dp	$\rho_r(CH_2)$	A''

Perhaps the most obvious difference of opinion arises from the assignment of the three bands at ca. 1500, 1470 and 1390 cm^{-1}.

Since the first tentative assignments for allyl-metal systems in 1961[126], various authors[40,120-125,300] have used all possible alternatives in assigning these three bands. However, more recently, the availability of Raman data has led to general agreement that the band of intermediate frequency (ca. 1470 cm^{-1}) is polarised and must therefore be assigned to the $\delta(CH_2)$ A' vibration. Differences remain however in the assignment of the two depolarised bands at ca. 1500 and 1390 cm^{-1}. Thus the order $\delta(CH_2)A'' > \delta(CH_2)A' > \nu(CCC)A''$ has been used in the assignments for $[(\eta^3\text{-}C_3H_5)Mn(CO)_4]$[40], $[(\eta^3\text{-}C_3H_5)Co(CO)_3]$[300] and $[(\eta^3\text{-}RC_3H_4)PdX]_2$ (R = H, CH_3; X = Cl, Br)[125]. For the first of these complexes the assignments are based mainly on the argument that the high ν(Mn-allyl) frequencies indicate a considerable perturbation of the bonding within the allyl group and that the 1390 cm^{-1} frequency band is too low to be assigned to the $\delta(CH_2)$ A'' mode[114]. Comparisons with the spectra of coordinated ethene in Zeise's salt[302] also support this view. The alternative order $\nu(CCC)A'' > \delta(CH_2)A' > \delta(CH_2)A''$ has been employed in the assignments for $[(\eta^3\text{-}C_3H_5)Co(CO)_3]$[123], $[(\eta^3\text{-}RC_3H_4)PdX]_2$ (R = H, CH_3; X = Cl, Br)[124] and $[(\eta^3\text{-}C_3H_5)Fe(CO)_2NO]$[122]. The major reason for assigning the highest frequency band to ν(CCC) A'' was its insensitivity to deuteration in the vibrational spectrum of $[(\eta^3\text{-}C_3D_5)Fe(CO)_2NO]$[122].

Although no final agreement has been possible between the two alternative assignments, this is of little importance since detailed calculations[303] show that two bands at ca. 1500 and 1240 cm^{-1} in ethene complexes must be assigned together to the strongly coupled ν(C=C) and $\delta(CH_2)$ vibrations. These results indicate that the ν(CCC) A'' and $\delta(CH_2)$ A'' vibrations of the allyl ligand are also likely to be appreciably mixed. Thus no absolute distinction

can be made as to which mode makes the major contribution to the highest frquency band and for $[(\eta^3\text{-}C_3H_5)Re(CO)_4]$ these modes are assigned together.

In view of these difficulties it is not surprising to find that minor ambiguities exist in almost all of the reported η^3-allyl spectra. However, as already pointed out, the approximate nature of the descriptions allows only a tentative assignment of the mode which makes the major contribution to a particular frequency. In addition to the assignments available for η^3-allyl complexes, the spectra of free ethene[304] and coordinated ethene[302] are also helpful in assisting the assignments given in Table 4.14.

Thus, in agreement with most previous results, the two bands at 1214 and 1140 cm^{-1} are assigned to the out-of-plane $\pi(CH)A'$ and in-plane $\delta(CH)A''$ deformations respectively. The next two medium intensity Raman bands at 1023 and 1003 cm^{-1} are both polarised and therefore assigned to the $\nu(CCC)A'$ and $\rho_t(CH_2)A'$ vibrations which are expected in this region. There is no reason to suppose that the assignments given are definitive however, and the reverse is equally likely. Assignments for the two wagging and two rocking allyl modes are in good agreement for most of the reported spectra. Consequently four medium-weak infrared and Raman bands of $[(\eta^3\text{-}C_3H_5)Re(CO)_4]$ are similarly assigned as follows:- $\rho_w(CH_2)A'$, 923; $\rho_w(CH_2)A''$, 872; $\rho_r(CH_2)A'$, ca. 794; $\rho_r(CH_2)A''$, 768 cm^{-1}. Finally the only band of reasonable frequency remaining for the assignment of the $\rho_t(CH_2)A''$ twisting mode is a very weak infrared band at 978 cm^{-1}. This assignment is in line with most previous studies apart from that on $[(\eta^3\text{-}C_3H_5)Fe(CO)_2NO]$[122] for which a band at 722 cm^{-1} was so assigned.

(iv) Overtone and combination vibrations

As with the η^1-allyl complex the remaining very weak bands in the infrared spectrum may be assigned to overtones or combinations of the fundamental vibrations, these being listed in Table 4.15. The totally symmetric ν(CO) vibration, which always occurs at the highest frequency, commonly combines with most other fundamentals [233] and this is clearly seen in the combination spectrum of the ν(CO)A' band at 2094 cm^{-1} in $[(\eta^3\text{-}C_3H_5)Re(CO)_4]$ (Table 4.15).

Table 4.15: Overtones and Combinations

Observed Frequency (cm^{-1})		Possible Origin
Infrared	Raman	
2675 vw		2094 + 591, 1463 + 1214
2568 vw		2094 + 471, 1959 + 610
2465 w		2094 + 377, 1994 + 471
2418 w		2094 + 332, 2 x 1214
2193 w		2094 + 100
1840 mw		1463 + 377, 2 x 923
1790 w		1463 + 332, 923 + 872
1745 w		2 x 872
1323 vvw	1326 vw, dp?	872 + 455
1260 vvw		872 + 395
	1101 vw, dp?	1003 + 100, 608 + 501
1090 w	1087 vw, pol	2 x 546
1047 w		546 + 501

(c) Pentacarbonylmethylrhenium

(i) ν(CO), δ(MCO) and ν(MC) vibrations

The solid state vibrational spectra of pentacarbonylmethylrhenium and its isotopically lalelled analogues, in the ν(CO), δ(ReCO) and ν(ReC) regions, are listed in Table 4.16. As expected, the frequencies observed for the $XRe(CO)_5$ unit (X = bonded C of methyl) follow a closely similar pattern to those of $[(\eta^1\text{-}C_3H_5)Re(CO)_5]$. The assignments (Table 4.16) of most of the bands are therefore based on the same rationale of C_{4v} local symmetry and warrant little further comment.

The ^{13}C and ^{2}H labelled compounds were originally synthesised in the hope that the position of the $\nu(ReC_{methyl})$ stretching vibration could be unequivocally established by examining isotopic shifts in the vibrational spectra. Unexpectedly, a small shift (ca. 10 cm^{-1}) with respect to the unlabelled compound is observed for several bands in the 610 - 350 cm^{-1} region for both labelled compounds. However, the most significant change observed is the appearance of new medium-strong intensity Raman bands at 442 and 425 cm^{-1}, in the spectra of the ^{13}C and ^{2}H labelled compounds respectively. This is accompanied by concurrent loss of intensity of the band at ca. 450 cm^{-1} when compared with the unlabelled compound and is illustrated in Figure 4.6. To account for these observations it is suggested that the $\nu(ReC_{methyl})A_1$ vibration, of unlabelled $[CH_3Re(CO)_5]$, contributes to the intensity of the $\nu(ReC)A_1(ax)$ band at 450 cm^{-1}. The new bands at 442 and 425 cm^{-1} are then tentatively assigned to the $\nu(Re^{13}CH_3)A_1$ and $\nu(ReCD_3)A_1$ vibrations respectively. However since the δ(ReCO) bands at ca. 590 and 530 cm^{-1}, and the $\nu(ReC)A_1(eq)$ band at ca. 470 cm^{-1} are also significantly influenced by isotopic substitution it seems, as

Table 4.16: Vibrational Spectra[a] of Isotopically Labelled Pentacarbonylmethylrhenium in the ν(CO), δ(ReCO) and ν(ReC) Regions

$[CH_3Re(CO)_5]$		$[^{13}CH_3Re(CO)_5]$		$[CD_3Re(CO)_5]$		Assignment
IR	R	IR	R	IR	R	(C_{4v})
2130 m	2126 vs	2130 m	2128 vs	2129 sh	2128 vs	ν(CO) A_1(eq)
	2049 m, sh		2054 m, sh		2050 m, sh	ν(CO) B_1
2047 sh[b]	2041 vvs	2045 sh[b]	2043 vvs	2046 sh[b]	2041 vvs	
2017 vs[b]	2024 vw, sh	2017 vs[b]	2020 vw, sh	2020 vs[b]	2025 vw, sh	ν(CO) E
1985 s[b]	1970 m, sh	1985 s[b]	1969 m, sh	1984 s[b]	1968 m, sh	ν(CO) A_1(ax)
	1956 m		1955 m		1953 m	
1941 w[b]		1942 w[b]		1941 w[b]		ν(^{13}CO)
601 vs	605 vw	603 vs	605 vw	604 vs	602 vw	δ(ReCO) A_1
591 vs	590 vw	584 vs	591 vw	580 vs	576 vw	δ(ReCO) E
560 w, sh				560 w, sh		δ(ReCO) B_1?
537 m	531 vw	532 m	533 vw	525 m	525 vw	δ(ReCO) E
506 vw	502 m	504 vw	503 w	507 vw	504 mw	δ(ReCO) B_2
	484 sh		483 sh		473 sh	

..../cont'd

Table 4.16: Cont'd

$[CH_3Re(CO)_5]$		$[^{13}CH_3Re(CO)_5]$		$[CD_3Re(CO)_5]$		Assignment
IR	R	IR	R	IR	R	(C_{4v})
474 w	472 vvs	466 w	466 vvs	466 w	462 vvs	ν(ReC) A_1(eq)
453 m	450 vs	451 m	449 ms	452 m	448 sh	ν(ReC) A_1(ax)
	450?		442 ms		425 m	$\nu(ReC_{methyl})$ A_1
437 w		435 w		434 w		ν(ReC) B_1
380 vs	384 w, sh	378 vs	384 w, sh	381 vs	385 w, sh	ν(ReC) E
360 sh?	377 m	350 sh?	375 m		375 m	δ(ReCO) E
	193 m		195 m			
	139 s		142 w		139 w	
	106 vs, br		109 vs, br		107 vs, br	δ(CReC) and lattice modes
	88 s		92 sh		90 sh	
	75 s		78 m		75 m	
	40 s		38 vs		32 vs	

[a] Recorded for solid samples; Infrared (IR) and Raman (R) frequencies in cm^{-1}

[b] Tabulated values refer to n-pentane solution spectra, as the Nujol mull spectra gave one very intense, very broad absorption ca. 2040 - 1940 cm^{-1}

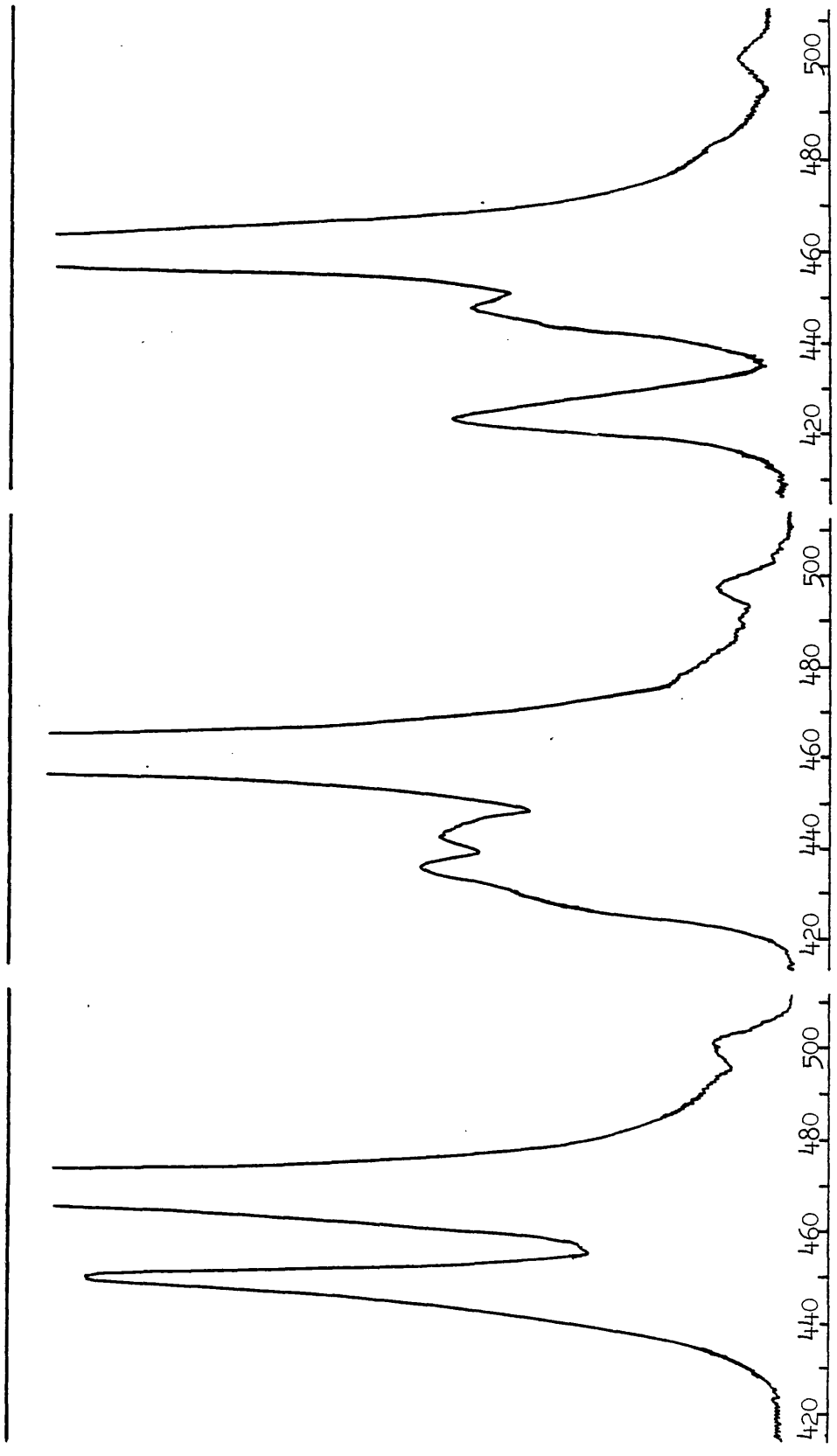

Figure 4.6: Raman spectra (410 - 510 cm^{-1}) of the pentacarbonylmethylrhenium derivatives

suggested previously, that some mixing of modes occurs. Added confidence in these assignments is gained by plotting the frequency of the ν(ReX) vibration against the reciprocal root atomic mass ($1/\sqrt{M_x}$) for the series of compounds $[H_3XRe(CO)_5]$ (X = ^{12}C, ^{13}C, Si, Ge) (Figure 4.7).

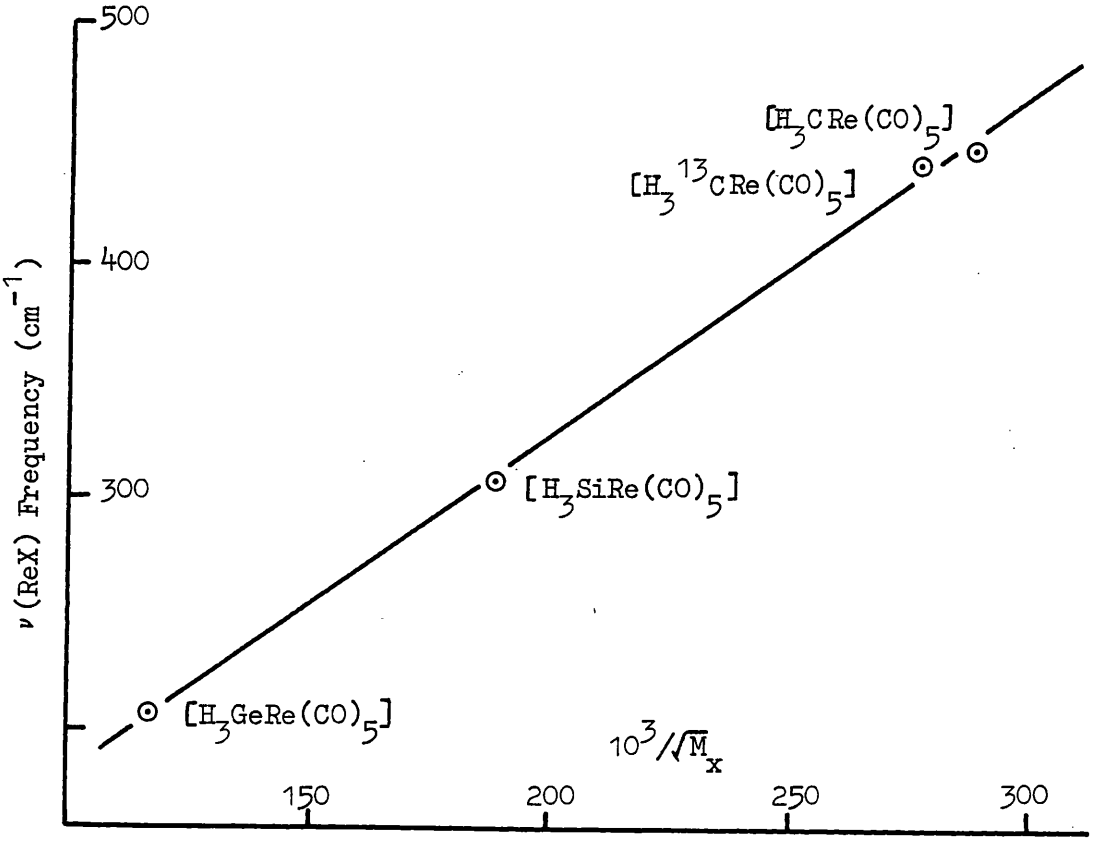

Figure 4.7: Correlation between ν(ReX) and $1/\sqrt{M_x}$ for $[H_3XRe(CO)_5]$ (X = Ge, Si, ^{13}C, ^{12}C)

Thus, using the literature[305] values of ν(ReX), (X = Ge, Si) and the proposed values for ν(Re*C) (*C = ^{12}C, ^{13}C) a linear correlation is obtained. Such a correlation must naturally be treated with certain reservations, however it does show that the $\nu(ReC_{methyl})$ vibrations are expected in the 430 cm^{-1} region. The corresponding ν(W-CH_3) and ν(W-CD_3) vibrations in $[(\eta^5\text{-}C_5H_5)W(R)(CO)_3]$ (R = CH_3, CD_3) were assigned to bands at 430 and 407 cm^{-1} respectively. From the results presented above, it is clear that the ν(MC) frequencies are also influenced by substitution of deuterium for hydrogen.

This is a further indication that it is only an approximation to regard such frequencies as 'pure' metal-carbon stretches.

The remaining low frequency bands vary little for each compound and are generally assigned to δ(CReC) and lattice vibrations. Raman polarisation measurements were severely limited by the low solubility of the methyl complexes, however the very strong bonds at ca. 2125, 1970 and 470 cm^{-1} were polarised in CS_2 solution, thereby confirming their assignment as A_1 modes.

(ii) Vibrations of the methyl group

The assignment of the methyl modes in $[(\eta^5\text{-}C_5H_5)W(R)(CO)_3]$ (R = CH_3, CD_3)[306,307] indicated that the CH_3W group has effective C_{3v} symmetry. The local symmetry approach was also used successfully in neutron diffraction structure determinations on $[H_3X(CO)_5]$ (M = Mn, Re; X = C, Si, Ge)[308-310] and in vibration/rotation studies on $[CH_3^*Mn(CO)_5]$[311] (methyl groups labelled * refer to the appropriate isotope throughout this section). In the light of these results it therefore seems reasonable to treat the CH_3^*Re group in $[CH_3^*Re(CO)_5]$ in a similar manner. The vibrational modes expected (Appendix 3) for a CH_3M group of C_{3v} symmetry together with a summary of the frequency ranges in which they occur in methyl and deuterated methyl derivatives[129] are listed in Table 4.17.

Table 4.18 lists the bands observed in the vibrational spectra (excluding ν(CO) bands) of the three methyl complexes, $[CH_3^*Re(CO)_5]$, between 4000 - 610 cm^{-1}. Clearly there are more than the five bands predicted for the internal modes of a methyl group of C_{3v} symmetry. However using the reported spectra of $[(\eta^5\text{-}C_5H_5)W(R)(CO)_3]$[306,307], $[CH_3^*Mn(CO)_5]$[311] and CH_3^*X (X = halogen)[312] as a guide the vibrations of the methyl group may be tentatively assigned whilst

the remaining bands are accounted for as overtones and combinations of the $Re(CO)_5$ unit.

Table 4.17: Frequency Ranges for Terminal Methyl and Deuterated Methyl Modes (cm^{-1})

Mode	CH_3	CD_3
ν_a	3050 - 2810	2275 - 2035
ν_s	2950 - 2750	2175 - 2000
δ_a	1475 - 1300	1125 - 960
δ_s	1350 - 1100	1000 - 870
ρ_r	975 - 620	750 - 475

Two $\nu(CH_3)$ stretches are predicted for C_{3v} symmetry however all of the methyl derivatives display three medium-strong infrared absorptions which are definitely associated with the methyl group since they shift dramatically in the spectrum of the deuterated compound. The two bands at highest frequency are assigned to the asymmetric $\nu_a(CH_3)E$ and symmetric $\nu_s(CH_3)A_1$ vibrations respectively, whilst the third medium intensity band in the $\nu(CH_3)$ region is assigned to the first overtone of the $\delta_a(CH_3)E$ asymmetric deformation. The presence of three bands is almost a universal feature of methyl compounds[312] and the usually weak overtone probably gains some intensity from a Fermi resonance interaction with the $\nu_s(CH_3)A_1$ vibration. The $\delta_a(CH_3)E$ mode is assigned to a weak infrared band in the 1425 cm^{-1} region for the CH_3 and $^{13}CH_3$ compounds but no comparable feature is observed in the spectrum of the deuterated analogue. However since a band at 2060 cm^{-1} is assigned to $2\delta_a(CD_3)E$ and by analogy with previous assignments for deuterated methyl compounds[307,312] it is suggested that this band

Table 4.18: The Infrared[a] Spectra of $[CH_3Re(CO)_5]$ Derivatives (4000 - 610 cm^{-1}) Excluding $\nu(CO)$ Modes

$[CH_3Re(CO)_5]$	$[^{13}CH_3Re(CO)_5]$	$[CD_3Re(CO)_5]$	Assignment[b]
2963 m, br	2955 m br	2224 m, br (2223 vw)	$\nu_a(CH_3)$ E
2909 s (2906 vw)	2904 s (2902 m)	2119 s (2119 vw, sh)	$\nu_s(CH_3)$ A_1
2829 m	2824 m	2060 m	$2\delta_a(CH_3)$ E
2508 w	2506 w	2509 w	2130 + 380
2441 m	2438 m	2436 m	1985 + 453
2363 vw	2360 vw	2364 vw	1985 + 380
2223 vw	2220 vw		2130 + 88
1427 vw	1421 vw	1031?	$\delta_a(CH_3)$ E
1262 w (1263 w)	1260 w		
1196 m (1192 ms)	1187 m (1189 ms)	902 m (903 ms)	$\delta_s(CH_3)$ A_1
1140 vw	1138 vw	1121 vw	601 + 537

..../cont'd

Table 4.18: Cont'd

$[CH_3Re(CO)_5]$	$[^{13}CH_3Re(CO)_5]$	$[CD_3Re(CO)_5]$	Assignment [b]
1088 w	1087 w	1076 w	591 + 506
1065 vw	1063 vw		2 x 537; 591 + 474
1037 m	1034 m	1031 m	537 + 506
		980 w	
957 m	955 m	959 sh	506 + 453
		948 m	
903 vw	902 vw	894 vw	2 x 453, 474 + 437
779 w	774 w		$\rho_r(CH_3)$ E

[a] Figures in parenthesis indicate Raman frequencies

[b] Possible combinations and overtones given refer only to the unlabelled compound

occurs at approximately 1031 cm^{-1} and is coincident with a medium intensity combination band. The symmetric $\delta_s(CH_3)$ A_1 deformation is more easily assigned to a medium intensity infrared band at ca. 1190 cm^{-1} which shifts to 902 cm^{-1} on deuteration. These bands all have quite strong Raman counterparts as expected for such a mode[307]. Finally the $\rho_r(CH_3)$ E rocking vibration is assigned to a weak feature at ca. 780 cm^{-1} which is absent in the spectrum of the deuterated complex, probably as a result of it being obscured by the very strong δ(ReCO) bands.

A summary of the proposed vibrational assignments for the methyl vibrations together with the $^{12}CH_3/^{12}CD_3$ frequency ratios is given in Table 4.19. The frequency ratio for H to D substitution normally lies in the range 1.33 - 1.40[31,312] thus the suggested assignments may be viewed with added confidence. It is also noteworthy that all the bands assigned to methyl vibrations in the ^{13}C substituted complex suffer a small (4 - 9 cm^{-1}) shift to lower wavenumbers when compared with results for the unlabelled complex.

Table 4.19: Summary of Methyl Frequencies (cm^{-1}) for $[CH_3^*Re(CO)_5]$

$^{12}CH_3$	$^{13}CH_3$	CD_3	Assignment	$^{12}CH_3/^{12}CD_3$ Ratio
2963	2955	2224	$\nu_a(CH_3)$ E	1.33
2909	2904	2119	$\nu_s(CH_3)$ A_1	1.37
1427	1421	1031	$\delta_a(CH_3)$ E	1.38
1196	1187	902	$\delta_s(CH_3)$ A_1	1.33
779	774	not observed	$\rho_r(CH_3)$ E	

CHAPTER FIVE

η^3-ALLYL COMPLEXES OF MANGANESE AND RHENIUM WITH GROUP V DONOR LIGANDS

INTRODUCTION

As indicated in Chapter One (pages 39 - 42), the number of known ligand substituted allyl complexes of the Group VII metal carbonyls are very few. However two very recent publications[11,219], which report the preparation of phosphine and phosphite derivatives show that this is an area of some current interest, particularly since the combination of η^3-allyl and phosphine or phosphite ligands has proved to be especially effective for oxidative-addition reactions[11,16]. For example, the corresponding allyl-cobalt complexes are highly selective catalysts for the cis-hydrogenation of arenes[10,316,317]. The mechanism proposed[334] for these reactions involves a rapid $\pi \rightleftharpoons \sigma$ interconversion as the first step (eq. 5.1).

$$[(\eta^3\text{-}C_3H_5)Co\{P(OMe)_3\}_3] \rightleftharpoons [(\eta^1\text{-}C_3H_5)Co\{P(OMe)_3\}_3] \qquad 5.1$$

This is then followed by the formation of a cis-dihydride (eq. 5.2), the presence of which is confirmed by low temperature NMR studies in cyclohexane. If no arene is present then cis-elimination of propene terminates the cycle (eq. 5.3).

$$[(\eta^1\text{-}C_3H_5)Co\{P(OMe)_3\}_3] + H_2 \rightleftharpoons [(\eta^1\text{-}C_3H_5)CoH_2\{P(OMe)_3\}_3] \qquad 5.2$$

$$[(\eta^1\text{-}C_3H_5)CoH_2\{P(OMe)_3\}_3] \longrightarrow C_3H_6 + [HCo\{P(OMe)_3\}_3] \qquad 5.3$$

However in the presence of arenes it is thought that two moles of $P(OMe)_3$ dissociate, allowing the complex to interact with the arene molecule (eqs. 5.4 and 5.5).

$$[(\eta^1\text{-}C_3H_5)CoH_2\{P(OMe)_3\}_3] \rightleftharpoons [(\eta^3\text{-}C_3H_5)CoH_2\{P(OMe)_3\}_2] + P(OMe)_3$$
$$\rightleftharpoons [(\eta^3\text{-}C_3H_5)CoH_2P(OMe)_3] + P(OMe)_3 \qquad 5.4$$

$$[(\eta^3\text{-}C_3H_5)CoH_2P(OMe)_3] + \text{arene} \rightleftharpoons$$
$$[(\eta^1\text{-}C_3H_5)CoH_2(\eta^4\text{-arene})P(OMe)_3] \qquad 5.5$$

Stepwise hydrogenation may then proceed almost exclusively on the endo-face of the arene. The cycle is completed by dissociation of the product and recombination of the phosphite ligands leading to the complex shown in eq. 5.1.

At the time of these reports the related allylcarbonyl manganese complexes described in this Chapter, had already been isolated and fully characterised. In addition the first two examples of ligand substituted allyl-rhenium complexes have been prepared and a single crystal X-ray structure determination on a representative manganese complex, namely $[(\eta^3\text{-}C_3H_5)Mn(CO)_2\{P(OMe)_3\}_2]$, carried out.

EXPERIMENTAL

Details of the physical methods employed for the preparation and characterisation of the complexes described below are given in Appendix 1. The starting materials $[(\eta^3\text{-}C_3H_5)Mn(CO)_4]$[93,118] (Appendix 2) and $[(\eta^3\text{-}C_3H_5)Re(CO)_4]$ (Chapter 4) were prepared as described previously and their purity checked by infrared and ^{1}H NMR spectroscopic measurements. Liquid phosphines and phosphites were stored over molecular sieves and vacuum distilled before use. Solid ligands were used without further purification.

I. η^3-Allyltricarbonyl(triphenylphosphine)manganese(I)[171,219]

A solution of $[(\eta^3\text{-}C_3H_5)Mn(CO)_4]$ (0.42 g/2 mmol) and PPh_3 (0.52 g/2 mmol) in cyclohexane (25 cm^3) was heated under reflux for 3 h. The solvent was removed (25°C/15 mm) and the pale yellow solid residue dissolved in the minimum volume of a 12:1 light petroleum (60° - 80°C)- diethyl ether mixed solvent. Chromatography on a

Florisil column (30 x 2 cm), using the same mixed solvent for elution under nitrogen, followed by immediate removal of the solvent, gave pale yellow crystals of the complex $[(\eta^3\text{-}C_3H_5)Mn(CO)_3PPh_3]$

II. η^3-Allyltricarbonyl(triphenylarsine)manganese(I)

Reaction between $[(\eta^3\text{-}C_3H_5)Mn(CO)_4]$ (0.42 g/2 mmol) and $AsPh_3$ (1.20 g/4 mmol) for 8 h in refluxing cyclohexane (25 cm^3), followed by removal of solvent and chromatography as above gave two fractions. The first yielded unchanged tetracarbonyl and the second gave pale yellow crystals of the substituted allyl derivative, which could be recrystallised from n-pentane.

III. η^3-Allyltricarbonyl(tricyclohexylphosphine)manganese(I)

The reaction between $[(\eta^3\text{-}C_3H_5)Mn(CO)_4]$ (0.42 g/2 mmol) and PCy_3 (0.84 g/3 mmol) in refluxing cyclohexane (25 cm^3) for 4 h, followed by work-up procedures similar to those above gave product III as pale yellow crystals.

IV. η^3-Allyltricarbonyl(tri-n-butylphosphine)manganese(I)

A mixture of $[(\eta^3\text{-}C_3H_5)Mn(CO)_4]$ (0.42 g/2 mmol) and PBu^n_3 (0.41 g/2 mmol) was heated in refluxing cyclohexane for 20 minutes. (Longer reaction times led to mixtures of $[(\eta^3\text{-}C_3H_5)Mn(CO)_{4-x}(PBu^n_3)_x]$ (x = 1 - 3) as indicated by infrared spectra in the ν(CO) region). The solution was reduced in volume to ca. 5 cm^3 and initially chromatographed on a Florisil column using cyclohexane as eluant. Removal of the cyclohexane left an oily residue which was dissolved in the minimum volume of dichloromethane and subjected to a further chromatographic separation. A yellow fraction eluted with dichloromethane gave a yellow hygroscopic liquid (IV) on removal of solvent.

V. η^3-Allyltricarbonyl(methyldiphenylphosphine)manganese(I)

Using a conventional reaction vessel fitted with a quartz water-cooled immersion well, a reflux condenser and a cannula for admission of dry nitrogen, a solution of $[(\eta^3\text{-}C_3H_5)Mn(CO)_4]$ (0.42 g/2 mmol) and $PMePh_2$ (0.40 g/2 mmol) in cyclohexane (75 cm^3) was photolysed at ambient temperature for 20 h. Infrared evidence indicated that, although some unchanged tetracarbonyl remained after this time, prolonged photolysis led to lower yields of the complex (V), the related dicarbonyl being formed (see below), together with decomposition products. The solution was filtered, reduced in volume and chromatographed on a Florisil column eluted with cyclohexane. The initial fraction contained unreacted starting materials. Changing to a 12:1 light petroleum (60° - 80°C)-diethyl ether mixed solvent allowed the elution of a yellow band which gave an oily residue on removal of the solvent. The product was obtained as a yellow hygroscopic liquid by dissolving the residue in n-pentane, followed by rapid filtration under nitrogen, and removal of solvent under high vacuum.

VI. η^3-Allyldicarbonylbis(methyldiphenylphosphine)manganese(I)

A similar photolysis reaction to that above using 1.60 g (8 mmol) of $PMePh_2$ and a reaction time of 72 h, followed by removal of the solvent, gave an oily residue. This was dissolved in n-pentane (300 cm^3), filtered and the volume of the filtrate reduced until crystallisation was evident. The filtrate was then left at 0°C for several hours and gave bright yellow crystals of the product (VI), which were filtered off, washed with n-pentane and dried *in vacuo*.

VII. η^3-Allyldicarbonyl{bis(diphenylphosphino)methane}manganese(I)

A mixture of $[(\eta^3\text{-}C_3H_5)Mn(CO)_4]$ (0.83 g/4 mmol) and dppm (1.54 g/4 mmol) was heated in refluxing light petroleum (80° - 100°C boiling range, 50 cm^3) for 18 h. After filtering the hot solution, removal of the solvent left a solid which was recrystallised from a dichloromethane-ethanol mixture to give orange crystals of the product (VII).

VIII. η^3-Allyldicarbonylbis(trimethylphosphite)manganese(I)

A solution of $[(\eta^3\text{-}C_3H_5)Mn(CO)_4]$ (0.63 g/3 mmol) and $P(OMe)_3$ (0.75 g/6 mmol) in cyclohexane (25 cm^3) was heated under reflux for 1.5 h. The solvent was removed and the resulting yellow oil transferred to a column packed with Florisil. Elution with 12:1 light petroleum (60° - 80°C)-diethyl ether mixed solvent gave a pale yellow fraction which, when reduced in volume and kept at -20°C, yielded the product (VIII) as pale yellow platelets.

IX. η^3-Allyldicarbonylbis(triethylphosphite)manganese(I)

Using a similar procedure to that above for the $P(OMe)_3$ complex, the product (IX) was isolated as a yellow oil after chromatography. Very pale yellow crystals were obtained from the oil by recrystallisation six times from n-pentane at -78°C.

X. η^3-Allyltricarbonyl(triphenylphosphine)rhenium(I)

A mixture of $[(\eta^3\text{-}C_3H_5)Re(CO)_4]$ (0.34 g/1 mmol) and PPh_3 (0.52 g/2 mmol) was heated under reflux in cyclohexane (25 cm^3) for 85 h during which time the ν(CO) region of the infrared spectrum was monitored. The intensity of the ν(CO) bands of the tricarbonyl product (X) reached a maximum after 85 h, although some unchanged

tetracarbonyl as well as some dicarbonyl product were also present. Removal of the solvent left a white solid residue which was dissolved in warm light petroleum (60 - 80°C)-diethyl ether and the solution eluted with the same solvent on a Florisil column. Further monitoring by infrared spectroscopy allowed the separation of the product (X), obtained as a white powder after removal of solvent.

XI. η^3-Allyldicarbonylbis(triphenylphosphine)rhenium(I)

A mixture of $[(\eta^3\text{-}C_3H_5)Re(CO)_4]$ (0.34 g/1 mmol) and PPh_3 (1.57 g/ 6 mmol) were reacted together in refluxing cyclohexane (80 cm^3) for 22 days. By monitoring the course of the reaction by infrared spectroscopy it was clear that the major species in solution was the monosubstituted product (X). However after 6 days a solid began to form and the reaction was allowed to proceed until no further change in the infrared spectrum was observed. After cooling, the solid was filtered off and dissolved in hot dichloromethane - light petroleum (80 - 100°C) mixture, which was then allowed to evaporate slowly until crystals began to form. After standing at 0°C for several hours the colourless crystalline product (XI) was collected, washed with n-pentane and dried in vacuo.

The yields, melting points and analyses obtained for all the complexes I - XI appear in Table 5.1. Their infrared and ^1H NMR spectra are listed in Tables 5.3 and 5.4 respectively.

Structure Determination

A sample of $[(\eta^3\text{-}C_3H_5)Mn(CO)_2\{P(OMe)_3\}_2]$, prepared as above, was recrystallised three times from n-pentane at -20°C to provide

crystals suitable for an X-ray single crystal structure determination. A crystal with dimensions 0.2 x 0.5 x 1.5 mm was mounted with the (101) planes perpendicular to the instrument axis of a General Electric XRD 5 diffractometer, which was equipped with a manual goniostat, scintillation counter and pulse-height discriminator. Zirconium filtered molybdenum X-radiation was used. 1742 independent reflections with $2\theta < 40^{\circ}$ were measured by the stationary-counter-stationary-crystal method, using a take off angle of 4° and a counting time of 10 s. Of these 1348 reflections with intensities $(I) > 2\sigma(I)$ were used in subsequent calculations. Individual backgrounds were taken as a function of 2θ. Several standard reflections were measured repeatedly during the course of the experiment but no significant change in I was detected. Neither an absorption nor an extinction correction was applied.

Crystal data: $C_{11}H_{23}MnO_8P_2$, M = 400.19, Monoclinic, a = 18.618(11), b = 9.218(7), c = 10.607(11) Å, β = 102.1(1)°, U (volume of the unit cell) = 1780.0 $Å^3$, D_c = 1.49, Z = 4 (number of molecules in the unit cell), (Mo-K_α) = 0.7107 Å, μ (absorption factor) = 9.90 cm^{-1}, F(ooo) (number of electrons in the unit cell) = 832, space group $P2_1/a$ from systematic absences h0l, h = 2n + 1; 0k0, k = 2n + 1.

Solution and refinement

The positions of the manganese atoms were obtained from the Patterson map and subsequent Fourier syntheses gave all the remaining non-hydrogen atom positions. These were refined and then a difference Fourier map was calculated which enabled all the hydrogen atoms to be located. The positions of the allyl hydrogen atoms were allowed to refine, whilst those of the methyl groups were fixed in tetrahedral positions. Isotropic thermal parameters

were refined for all the hydrogen atoms. All other atoms were given anisotropic thermal parameters and the structure was refined by full-matrix least squares to R = 0.059. The weighting scheme employed was chosen to give similar values of $w\Delta^2$ over ranges of F_o and sin θ/λ and was $\sqrt{w} = 1$ for $F_o < 40$ and $40/F_o$ for $F_o > 40$. Calculations were made using the Shelx 76[318] system of programs at the University of London Computer Centre. Scattering factors and dispersion corrections were obtained from reference 319. The final list of atomic positions is given in Table 5.6 and the bond lengths and angles appear in Table 5.7. The final difference Fourier map showed no significant peaks and the 394 zero weighted reflections showed no large discrepancies. A list of the structure factors, together with thermal parameters, are given in Appendix 6.

Table 5.1: Yields, Melting Points and Analytical Data

Complex (Ref No.)	Yield (%)	M.p. (°C)	Analysis found C	H
$[(\eta^3\text{-}C_3H_5)Mn(CO)_3PPh_3]$ (I)	53	159[a]	65.2 (65.2)	4.67 (4.56)
$[(\eta^3\text{-}C_3H_5)Mn(CO)_3AsPh_3]$ (II)	31	157[a]	59.1 (59.3)	4.02 (4.15)
$[(\eta^3\text{-}C_3H_5)Mn(CO)_3PCy_3]$ (III)	33	178[a]	62.6 (62.6)	8.24 (8.32)
$[(\eta^3\text{-}C_3H_5)Mn(CO)_3PBu^n_3]$ (IV)	49		56.2 (56.5)	8.54 (8.44)
$[(\eta^3\text{-}C_3H_5)Mn(CO)_3PMePh_2]$ (V)	36		61.0 (60.0)	4.83 (4.77)
$[(\eta^3\text{-}C_3H_5)Mn(CO)_2(PMePh_2)_2]$ (VI)	32	154[a]	66.8 (67.4)	5.58 (5.66)
$[(\eta^3\text{-}C_3H_5)Mn(CO)_2$dppm] (VII)	25	204[a]	66.4 (67.2)	5.16 (5.07)
$[(\eta^3\text{-}C_3H_5)Mn(CO)_2\{P(OMe)_3\}_2]$ (VIII)	66	46	33.5 (33.0)	5.80 (5.79)
$[(\eta^3\text{-}C_3H_5)Mn(CO)_2\{P(OEt)_3\}_2]$ (IX)	41	24	42.0 (42.2)	7.01 (7.28)
$[(\eta^3\text{-}C_3H_5)Re(CO)_3PPh_3]$ (X)	35	168	50.6 (50.3)	3.94 (3.51)
$[(\eta^3\text{-}C_3H_5)Re(CO)_2(PPh_3)_2]$ (XI)	56	260[a]	60.9 (61.0)	4.47 (4.37)

[a] Melting occured with decomposition

RESULTS AND DISCUSSION

General Properties

The complexes $[(\eta^3\text{-}C_3H_5)M(CO)_3L]$ (M = Mn, L = PPh_3, $AsPh_3$, PCy_3, PBu^n_3, $PMePh_2$; M = Re, L = PPh_3) and $[(\eta^3\text{-}C_3H_5)M(CO)_2L_2]$ (M = Mn, L = $PMePh_3$, $P(OMe)_3$, $P(OEt)_3$, $\frac{1}{2}$dppm; M = Re, L = PPh_3) have been prepared by carbonyl displacement reactions employing the readily available $[(\eta^3\text{-}C_3H_5)M(CO)_4]$ complexes as starting materials. Of these complexes only $[(\eta^3\text{-}C_3H_5)Mn(CO)_3PPh_3]$[171,219] and $[(\eta^3\text{-}C_3H_5)Mn(CO)_2\{P(OMe)_3\}_2]$[11] have been previously reported. There are considerable disparities in the melting point of the PPh_3 complex, reported as 120 - 125°C (d)[219] or 140 - 142°C (d)[171] in the literature but found to be 159°C in this work. The probable cause for such disagreement lies in the method adopted for the determination. Thus in conventional melting point determinations of unstable compounds the onset of decomposition probably occurs well below the true melting point whereas use of the hot stage apparatus gives an 'instantaneous temperature' which often allows melting to precede decomposition.

In agreement with recent observations[11], most of the complexes (I - XI) could be prepared both thermally and photochemically, however the thermal method proved to be the most effective for all but the two methyldiphenylphosphine complexes V and VI. For example, the two rhenium complexes X and XI can also be prepared by the photochemical method but the yields (19% and 13% respectively) are considerably poorer than those attained in thermal reactions. The complexes V and VI were best synthesised by a photochemical method as thermal reactions gave mixtures of products separable only with difficulty. In a number of similar reactions, infrared evidence from the ν(CO) region indicated the formation of several

analgous products. Thus $[(\eta^3\text{-}C_3H_5)M(CO)_3L]$ (M = Mn, L = unidentate dppm, unidentate dppe, $P(OMe)_3$; M = Re, L = PCy_3, $P(OMe)_3$, $[(\eta^3\text{-}C_3H_5)M(CO)_2L_2]$ (M = Mn, L = PBu^n_3, $\frac{1}{2}$dppe; M = Re, L = PCy_3, $P(OMe)_3$) and $[(\eta^3\text{-}C_3H_5)M(CO)(PBu^n_3)_3]$ are clearly present in solution but have not been isolated as pure solid products because of difficulties associated with their separation from starting materials and other products formed in the reactions. Table 5.2 lists these complexes and the ν(CO) infrared bands attributed to them. Apart from the preparation of $[(\eta^3\text{-}C_3H_5)Mn(CO)_3AsPh_3]$, all the complexes isolated contain phosphorus donor ligands and attempts to use the nitrogen donor ligands, pyridine, 2,2'-bipyridine or 1,2-diaminoethane, in analogous reactions produced only complex mixtures which could not be separated.

The substitution reactions proceed at a much slower rate for rhenium than for manganese in line with general expectations for these Group VII metals (see Chapter 3, pages 76 - 79). It is also noticeable that within the manganese series the ease with which substitution occurs is dictated to some extent by the steric bulk of the incoming ligand although other factors such as σ-donor and π-acceptor abilities undoubtedly also play a part. The following series, in order of decreasing ease of substitution, which may be derived from purely qualitative observations on reaction rates, bears this out: $P(OMe)_3 > P(OEt)_3 > PBu^n_3 > PMePh_2 >$ dppm $> PPh_3 \simeq PCy_3 > AsPh_3$.

The manganese complexes I, II, III, VIII and IX are pale yellow crystalline solids, VI and VII are orange-yellow solids, whilst IV and V are deep yellow liquids. All are markedly susceptible to atmospheric oxidation particularly in solution giving rise to brown, non-carbonyl containing, paramagnetic decomposition products.

Table 5.2: Complexes Present in Reaction Mixtures

Complex	Synthetic Method[a]	Infrared Spectra ν(CO) Region (cm^{-1})				Solvent
$[(\eta^3\text{-}C_3H_5)Mn(CO)_3dppm]$	T	2000 s	1930 s	1900 s		CCl_4
	P	2006 s	1934 s	1903 s		C_6H_{12}
$[(\eta^3\text{-}C_3H_5)Mn(CO)_3dppe]$	T	1996 s	1927 s	1998 s		CCl_4
$[(\eta^3\text{-}C_3H_5)Mn(CO)_3P(OMe)_3]$	T	2014 s	1937 s	1908 s		CH_2Cl_2
$[(\eta^3\text{-}C_3H_5)Re(CO)_3PCy_3]$	T	2016 m	1925 sh	1918 s	1903 s	C_6H_{12}
$[(\eta^3\text{-}C_3H_5)Re(CO)_3P(OMe)_3]$	T, P	2030 s	1945 s	1923 s		$n\text{-}C_5H_{12}$
$[(\eta^3\text{-}C_3H_5)Mn(CO)_2(PBu^n_3)_2]$	T, P	1909 s	1839 vs			C_6H_{12}
$[(\eta^3\text{-}C_3H_5)Mn(CO)_2dppe]$	T	1929 vs	1865 s			CCl_4
$[(\eta^3\text{-}C_3H_5)Re(CO)_2(PCy_3)_2]$	T	1926 s	1875 s			C_6H_{12}
$[(\eta^3\text{-}C_3H_5)Re(CO)_2\{P(OMe)_3\}_2]$	T, P	1952 s	1881 s			$n\text{-}C_5H_{12}$
$[(\eta^3\text{-}C_3H_5)Mn(CO)(PBu^n_3)_3]$	P	1898 vs				$n\text{-}C_5H_{12}$

[a] T = Thermal reaction, P = photochemical reaction

They can however be stored for long periods in sealed, nitrogen flushed, ampoules. In contrast the two rhenium complexes X and XI appear to be air-stable as solids and much less prone to oxidation in solution.

In a number of cases manganese complexes were also prepared by the more direct thermal reactions between $[(\eta^1\text{-}C_3H_5)Mn(CO)_5]$ and the appropriate phosphorus donor ligand in refluxing cyclohexane. Thus it would appear that prior decarbonylation of the η^1-allyl complex and isolation of $[(\eta^3\text{-}C_3H_5)Mn(CO)_4]$ is not essential since facile decarbonylation <u>in situ</u> probably precedes the carbonyl substitution step when using $[(\eta^1\text{-}C_3H_5)Mn(CO)_5]$. The corresponding reactions between $[(\eta^1\text{-}C_3H_5)Re(CO)_5]$ and phosphorus donor ligands did not however lead to the formation of substituted η^3-allyl-rhenium analogues. Presumably this is because $[(\eta^1\text{-}C_3H_5)Re(CO)_5]$ can only be successfully decarbonylated photolytically to give $[(\eta^3\text{-}C_3H_5)Re(CO)_4]$ as found previously (Chapter 4, page 96). In view of the rather lengthy reaction times involved in the synthesis of the allyl-rhenium derivatives two other potential routes via substituted anionic rhenium carbonyls were investigated. If such anions could be prepared they are expected to be very reactive towards allyl halides. The first route involved the use of $[Re_2(CO)_8(PPh_3)_2]$[313] as starting material (Appendix 2) in the attempted preparation of the $[Re(CO)_4PPh_3]^-$ anion. However in contrast to the corresponding manganese complex[320-322] but in agreement with previous observations[322] the $[Re_2(CO)_8(PPh_3)_2]$ dimer resisted all attempts to cleave the Re-Re bond under a variety of reaction conditions, using reagents such as Na/Hg, Pb/Na and $Li[Et_3BH]$. These results are consistent with the difficulties experienced in cleaving the Re-Re bond of $Re_2(CO)_{10}$ (see Chapter 4, page 95).

The second route investigated attempts to synthesise $[Re(CO)_3(PPh_3)_2]^-$ by reduction of fac-$[Re(CO)_3(PPh_3)_2Br]$[314,315] (Appendix 2) again using a variety of reaction conditions and reducing reagents. Although analogous reactions employing manganese complexes are known to proceed to the desired anions[323] the reactions involving fac-$[Re(CO)_3(PPh_3)Br]$ led only to the formation of complex mixtures of products as indicated by the infrared spectra in the $\nu(CO)$ region.

Thus this approach to the potential synthesis of ligand substituted allyl-rhenium derivatives is limited by the availability of suitable anionic species. One group of anions which were not investigated but do look promising however are the recently reported[324,325] highly reduced tetracarbonyl trianions of manganese and rhenium. As expected these are extremely nucleophilic reagents and react with a wide variety of halides such as Ph_3PAuCl or Me_3SnCl forming neutral seven-coordinate derivatives or disubstituted monoanions[325] (eqs. 5.6 and 5.7).

$$Na_3[Re(CO)_4] + 3Ph_3PAuCl \xrightarrow{HMPA} [(Ph_3PAu)_3Re(CO)_4] + 3NaCl \qquad 5.6$$

$$Na_3[Mn(CO)_4] + 2Me_3SnCl \xrightarrow[Ph_4AsCl]{HMPA} [Ph_4As][(Me_3Sn)_2Mn(CO)_4] + 3NaCl \qquad 5.7$$

Such trianions would undoubtedly react with allyl halides and in the presence of suitable ligands may produce novel substituted allyl complexes of manganese and rhenium.

Infrared Spectra

The observed $\nu(CO)$ band patterns (Table 5.3) may be rationalised if the complexes are considered to be pseudo-octahedral with the η^3-allyl group acting as a bidentate ligand with a small normalised bite[11,39,54,57,336]. (The 'normalised bite' of a bidentate ligand,

having atoms A and B bonded to a metal M, is defined as the distance between A and B divided by the mean of the distances AM and BM.) The determination of the molecular structure of $[(\eta^3\text{-}C_3H_5)Mn(CO)_2\{P(OMe)_3\}_2]$, described at the end of this chapter, supports this view.

A consideration of the local symmetry of the carbonyl groups and the nature of the other ligands, but ignoring possible orientations of the η^3-allyl group, shows that the tricarbonyl complexes (I, II, III, IV, V, X) could exist in two isomeric forms with the three carbonyl ligands adopting either fac- or mer- arrangements (Figure 2.1). The way in which infrared spectroscopy is capable of differentiating between these two alternatives has been discussed in Chapter 2 (pages 48-50).

In solution or as liquid films all the tricarbonyl complexes show three strong infrared absorptions of approximately equal intensity indicating the isolation of a facial isomer. In addition the complexes $[(\eta^3\text{-}C_3H_5)Mn(CO)_3PCy_3]$ (III) and $[(\eta^3\text{-}C_3H_5)Mn(CO)_3PBu^n_3]$ (V) consistently show a weak shoulder on the band of intermediate frequency. The Nujol mull spectra of the tricarbonyl complexes likewise have three major ν(CO) bands but also an additional pronounced shoulder presumably associated with solid state splitting effects as this shoulder is lost on dissolution. The spectrum of a typical example, $[(\eta^3\text{-}C_3H_5)Re(CO)_3PPh_3]$, is illustrated in Figure 5.1.

All the dicarbonyl complexes (VI, VII, VIII, IX, XI) display two strong ν(CO) absorptions consistent with a cis-dicarbonyl arrangement. In all the complexes, except $[(\eta^3\text{-}C_3H_5)Mn(CO)_2dppm]$, the lower frequency asymmetric stretching mode is the more intense

Table 5.3: Infrared Data

Complex Number	ν(CO), solution[a] (cm^{-1})	ν(CO), solid[b] (cm^{-1})	ν(allyl)[c] (cm^{-1})	Approximate Angle ($2\theta^{o}$)
I	2004 s 1930 s 1908 vs	1996 s 1926 s 1865 w, sh	1508 vw	
II	2005 s 1930 s 1910 s	1994 s 1918 s 1896 s 1862 w, sh	1502 w	
III	2002 m 1926 w, sh 1916 s 1903 s	1996 s 1912 s, sh 1899 vs 1882 vs	1501 vw	
IV	2003 s 1929 s 1921 m, sh 1905 vs	1997 s ‡ 1921 s 1898 s	1501 vw	
V	2011 s 1931 s 1909 vs	1996 s ‡ 1919 s 1889 s	1502 w	
VI	1917 s 1851 vs	1901 s 1844 s		97
VII	1930 vs* 1866 s	1912 s 1847 s	1500 vw	80
VIII	1943 s 1872 vs	1936 s 1867 vs	1496 w	102
IX	1939 s 1867 vs	1937 s 1866 vs	1496 w	102
X	2026 s 1940 s 1915 s	2015 s 1934 s 1897 s 1870 w, sh	1497 w	
XI	1926 s** 1849 vs	1931 s 1856 vs		99

[a] Determined for n-pentane solutions except *CCl_4 and **$CHCl_3$.

[b] Determined for Nujol Mulls except ‡ liquid films.

[c] Determined for hexachlorobutadiene mulls.

band. Thus for these compounds the OC-M-CO angle must be greater than 90° since the relative intensities of the two bands are dependent upon the angle 2θ between the two CO bonds[326-328], according to $I_a/I_s = \tan^2\theta$. The intensities of the symmetric (I_s) and asymmetric (I_a) bands of the dicarbonyl complexes were assessed by measuring the areas under the peaks obtained from solution spectra in n-pentane. The angles so calculated are given in Table 5.3. For example, a value of 102° was calculated for $[(\eta^3\text{-}C_3H_5)Mn(CO)_2\{P(OMe)_3\}_2]$ and compares with the value of 97.7° obtained from the single-crystal structure determination. Since this bis-phosphite complex contains mutually trans-phosphite ligands, the carbonyl groups are trans to the small-bite chelating η^3-allyl moiety (C_1-Mn-C_3 angle, 67.0°), so it is to be expected that 2θ will exceed 90°. There is no reason to suppose that this stereochemistry is different for the other dicarbonyl complexes, apart from $[(\eta^3\text{-}C_3H_5)Mn(CO)_2dppm]$. Certainly multinuclear NMR evidence[11] favours this ligand arrangement for $[(\eta^3\text{-}C_3H_5)Mn(CO)_2\{P(OPr^i)_3\}_2]$. In the complex $[(\eta^3\text{-}C_3H_5)Mn(CO)_2dppm]$ however, a mutually trans arrangement of phosphorus atoms is not possible because the bis-phosphine is chelating. Since the carbonyl groups are still evidently cis to each other, one must be trans to a Ph_2P moiety whilst the other is essentially trans to a terminal carbon of the η^3-allyl ligand. Therefore the angle 2θ will be expected to be smaller than for the other dicarbonyl complexes. Indeed for this complex only the intensity of the higher frequency symmetric mode is greater than that of the lower frequency asymmetric mode implying a 2θ value of less than 90° and a value of 80° was determined from CCl_4 solution data. Both the solution and solid state infrared ν(CO) frequencies are listed in Table 5.3, together with weak bands at ca. 1500 cm^{-1} which, when

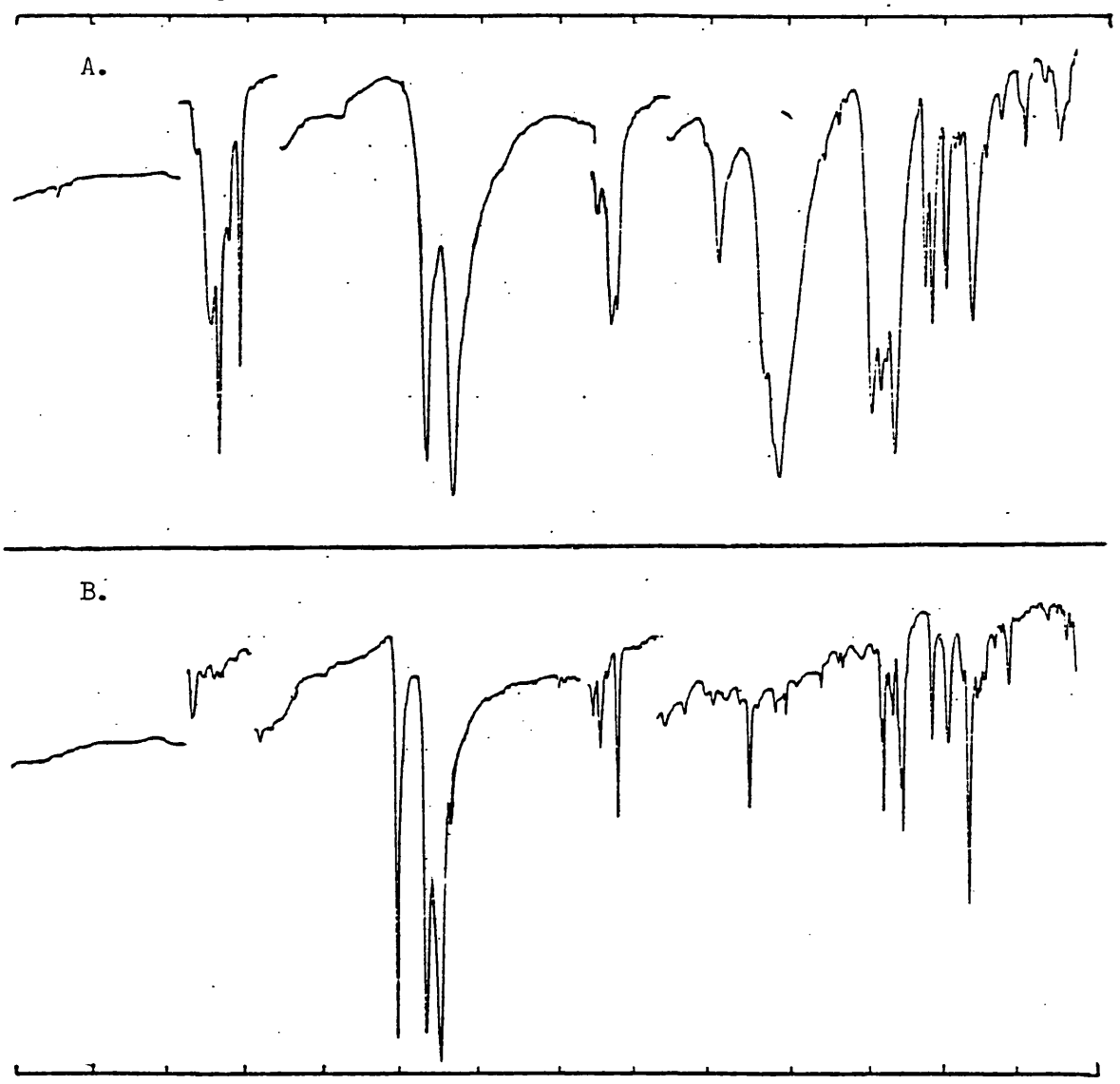

Figure 5.1: Solid state infrared spectra (4000 - 200 cm^{-1})
A. $[(\eta^3\text{-}C_3H_5)Mn(CO)_2\{P(OMe)_3\}_2]$(VIII)
B. $[(\eta^3\text{-}C_3H_5)Re(CO)_3PPh_3]$(X)

observed, are found at frequencies characteristic of $\delta_a(CH)_2$ + $\nu_a(CCC)$ in η^3-allyl groups (see Chapter 4, pages 129-131). The analogous allyl bands of $[(\eta^3\text{-}C_3H_5)M(CO)_4]$ are found at 1500 cm^{-1} (M = Mn)[40] and 1495 cm^{-1} (M = Re).

Figure 5.1 illustrates the infrared spectra of two typical complexes (VIII and X). As expected, absorptions due to the coordinated phosphorus (or arsenic) donor ligands are a predominant

feature in the infrared spectra of all these complexes. By comparing their infrared spectra, it is clear that below 1600 cm^{-1} most of the intense absorptions occur at frequencies closely similar to those of the uncoordinated ligands. For example, the complex $[(\eta^3\text{-}C_3H_5)Mn(CO)_2\{P(OMe)_3\}_2]$ displays medium-strong bands at 2980, 2945, 2840, 1455, 1174, 1017 br, 776, 718, 517 cm^{-1} due to coordinated $P(OMe)_3$, and $[(\eta^3\text{-}C_3H_5)Re(CO)_3PPh_3]$ exhibits similar intensity bands at 3050, 1480, 1435, 1094, 846, 795, 524, 425 cm^{-1}, which can be assigned to coordinated PPh_3. Thus apart from the very weak feature at ca. 1500 cm^{-1} and the strong $\nu(CO)$ absorptions no other bands could be confidently assigned to vibrations of the allyl or carbonyl fragments of these complexes, although the occurence of at least one additional strong band in the 700 - 500 cm^{-1} region in every case can probably be attributed to a metal-carbon-oxygen deformation.

^1H NMR Spectra

Details of the 100 MHz ^1H NMR spectra of these complexes, measured at ambient temperatures, are listed in Table 5.4. Some difficulties were encountered in obtaining good spectra and for complexes VI and VII only broad featureless bands were observed. Indeed if the solutions were prepared without taking precautions the peaks in the resulting spectra were often broad band envelopes without fine structure. Since both metals have large nuclear spins and quadrupole moments it is possible that hetero-nuclear coupling and adverse relaxation effects could cause line broadening. However good quality spectra, showing coupling between allyl syn- (H_m) and anti- (H_x) protons or between ^{31}P nuclei and allyl syn- protons of the order of 1 Hz, can be obtained for many of the complexes once the samples have been freshly recrystallised or

purified by chromatography and precautions taken in their dissolution in NMR solvents. It seems therefore that oxidation to paramagnetic impurities is the major reason for the poor quality of some spectra.

Table 5.4: ^{1}H NMR Data

Complex No. (Solvent)	Chemical Shift (δ ppm)	Assignment* (Rel.Int.)	Coupling Consts.‡ (Hz)
I($CDCl_3$)	7.38 d	PPh_3 (15)	J_{Pa} = 12.0
	3.85 m	H_a (1)	J_{ax} = 12.0
	2.21 d	H_m (2)	J_{am} = 7.0
	1.80 dd	H_x (2)	J_{Px} = 4.0
I(CS_2)	7.35 d	PPh_3 (15)	J_{Pa} = 12.4
	3.78 m	H_a (1)	J_{ax} = 12.0
	2.08 qt**	H_m (2)	J_{am} = 7.2
	1.69 qt	H_x (2)	J_{Px} = 3.8
			J_{Pm} = 1.2
			$J_{mx} = J_{mx'}$ = 1.2
II($CDCl_3$)	7.36 s	$AsPh_3$ (15)	J_{ax} = 12.0
	4.02 tt	H_a (1)	J_{am} = 7.0
	2.42 d	H_m (2)	
	1.84 d	H_x (2)	
III(CD_2Cl_2)	4.56 m	H_a (1)	J_{Pa} = 12.2
	2.59 dd	H_m (2)	J_{ax} = 12.0
	2.20 dd	H_x (2)	J_{am} = 7.0
	1.84 m, br }	PCy_3 (33)	J_{Px} = 6.0
	1.26 m, br }		J_{Pm} = 1.0
IV($CDCl_3$)	3.92 m	H_a (1)	J_{ax} = 12.0
	2.38 dd	H_m (2)	J_{am} = 7.0
	1.73 dd	H_x (2)	J_{Px} = 5.0
	1.39 m, br	$3(CH_2)_3$ (18)	J_{Pm} = 1.0
	0.92 m, br	$3(CH_3)$ (9)	

..../cont'd

Table 5.4: Cont'd

Complex No. (Solvent)	Chemical Shift (ppm)	Assignment* (Rel.Int.)	Coupling Consts.† (Hz)
V(CS_2)	7.34 m	PPh_2 (10)	J_{Pa} = 12.0
	3.60 m	H_a (1)	J_{ax} = 11.8
	2.03 dq	H_m (2)	J_{am} = 7.0
	1.63 d	PCH_3 (3)	J_{PCH_3} = 7.0
	1.62 qt	H_x (2)	J_{Px} = 5.0
			$J_{mx} = J_{mx'}$ = 1.2
			J_{Pm} = 1.0
VI($CDCl_3$)	7.25 m	2(PPh_2) (20)	
	3.80 m	H_a (1)	
	2.20, 1.65 m	2(CH_3), H_m, H_x, (10)	
VII(CD_2Cl_2)	7.40 m	2(PPh_2) (20)	
	4.44 m	CH_2 (2)	
	3.70 m	H_a (1)	
	2.46 m	H_m (2)	
	1.80 m	H_x (2)	
VIII($CDCl_3$)	4.56 m	H_a (1)	J_{Px} = 14.0
	3.60 t	2(OCH_3)$_3$ (18)	J_{Pa} = 12.0
	2.18 dm	H_m (2)	J_{ax} = 11.5
	1.38 m	H_x (2)	$^3J_{POMe}$ = 10.5
			J_{am} = 7.0
			J_{Pm} = 1.0
			$J_{mx} = J_{mx'}$ = 0.5
IX($CDCl_3$)	4.54 m	H_a (1)	J_{Px} = 12.0
	3.96 m	2(OCH_2)$_3$ (12)	J_{am} = 7.0
	2.13 d, br	H_m (2)	
	1.26 m	H_x + 2(CH_3)$_3$ (20)	

..../cont'd

Table 5.4: Cont'd

Complex No. (Solvent)	Chemical Shift (δ ppm)	Assignment* (Rel. Int.)	Coupling Consts.† (Hz)
X($CDCl_3$)	7.32 d	PPh_3 (15)	J_{ax} = 12.0
	3.82 m	H_a (1)	J_{Pa} = 10.8
	2.32 dt, br	H_m (2)	J_{Px} = 4.0
	2.06 dm	H_x (2)	J_{mx} = $J_{mx'}$ = 1.2
XI(CD_2Cl_2)	7.57 m	2(PPh_3) (30)	J_{am} = 7.0
	4.14 m	H_a (1)	
	1.99 d, br	H_m (2)	
	0.84 m	H_x (2)	

* The allyl protons are labelled according to Figure 1.7 (page 18). i.e. m and m' are the syn- protons and x and x' are the anti- protons.

† All spectra display the simple AM_2X_2 or AMM'XX' patterns when broad-band phosphorus decoupled.

** Two sets of triplets overlap.

The room temperature spectra show the characteristic features of a η^3-bonded allyl ligand which is coupled to ^{31}P and may be analysed as either AM_2X_2 or AMM'XX' spin systems on ^{31}P decoupling (see pages 18-20). A typical example, $[(\eta^3\text{-}C_3H_5)Mn(CO)_3PPh_3]$, is illustrated in Figure 5.2. As expected, J_{ax} (ca. 12 Hz) is always larger than J_{am} (ca. 7 Hz).

For the phosphine complexes strong coupling (ca. 5 Hz) between ^{31}P and H_x is also observed whereas J_{Pm} is much weaker (ca. 1 Hz). These couplings are of the opposite order to those found for the Group VI complexes $[(\eta^3\text{-}C_3H_5)MX(CO)_2L_2]$ (M = Mo, W; X = Cl, Br; L_2 = dppm, dppe)[188] and $[(\eta^3\text{-}C_3H_5)MoCl(CO)_2\{P(OMe)_3\}_2]$[34] where J_{Px} values are less than 1 Hz and often not observed at all, whereas J_{Pm} values are all ca. 3 Hz. The central allyl proton H_a

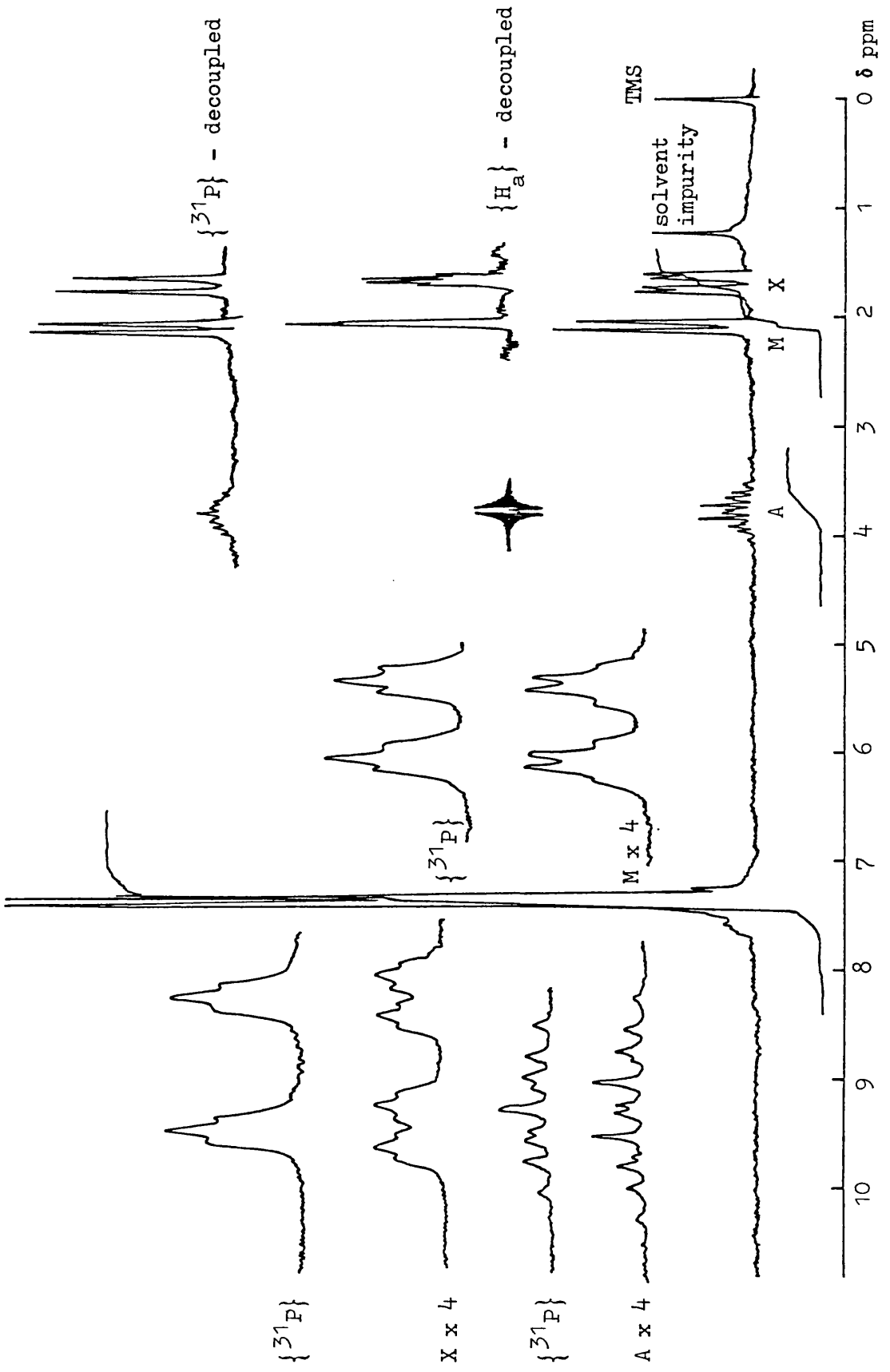

Figure 5.2: ^{1}H NMR Spectrum of $[(\eta^{3}\text{-}C_{3}H_{5})Mn(CO)_{3}PPh_{3}]$ (CS_{2} solution)

is also strongly coupled to ^{31}P (ca. 12 Hz), however detailed measurements were also hindered by the complexity of this resonance.

Analysis of the spectra of the two phosphite derivatives (VIII and IX) is not quite so straightforward and they differ from the phosphine compounds in a number of respects. Although well resolved spectra were obtained for both compounds, detailed analysis for the $P(OEt)_3$ complex (IX) was not possible because the CH_3 resonances of the ethyl groups obscured most of the region of interest. However it is reasonable to assume that the following comments on the spectrum of $[(\eta^3\text{-}C_3H_5)Mn(CO)_2\{P(OMe)_3\}_2]$ (VIII) are also applicable to that of $[(\eta^3\text{-}C_3H_5)Mn(CO)_2\{P(OEt)_3\}_2]$ (IX).

The 100 MHz ^1H NMR spectrum of VIII, measured at 29°C, is illustrated in Figure 5.3. The first notable difference compared with the phosphine analogues is the magnitude of J_{Px} (ca. 14 Hz) which is greater than J_{ax} and much greater than J_{Px} of the phosphine complexes. Secondly Figure 5.3 shows the methoxy protons as a slightly split, deceptively simple triplet. It has been shown[329] that for an $X_9AA'X'_9$ (X = H; A = P) spin system of this type, with the X nuclei magnetically equivalent, a simple 1 : 2 : 1 triplet will be observed when $J_{AA'} \gg |J_{AX} - J_{AX'}|$. Thus initially it seems reasonable to explain this feature on the basis of virtual coupling with the two mutually trans-phosphorus nuclei coupling strongly with each other and the methoxy protons coupling equally with both ^{31}P nuclei. The spectra of several bis-phosphine and bis-phosphite complexes e.g. trans-$[M(CO)_4\{P(OMe)_3\}_2]$[330,331] (M = Cr, Mo, W) and trans-$[MX_2(PMe_3)_2]$[332] (M = Pd, Pt; X = halide) have been assigned in this manner. The methoxy protons of the closely related complex $[Mn(CO)_2\{P(OMe)_3\}_2(oxinate)]$ (oxine = 8 - hydroxyquinoline) also appear as a triplet[333].

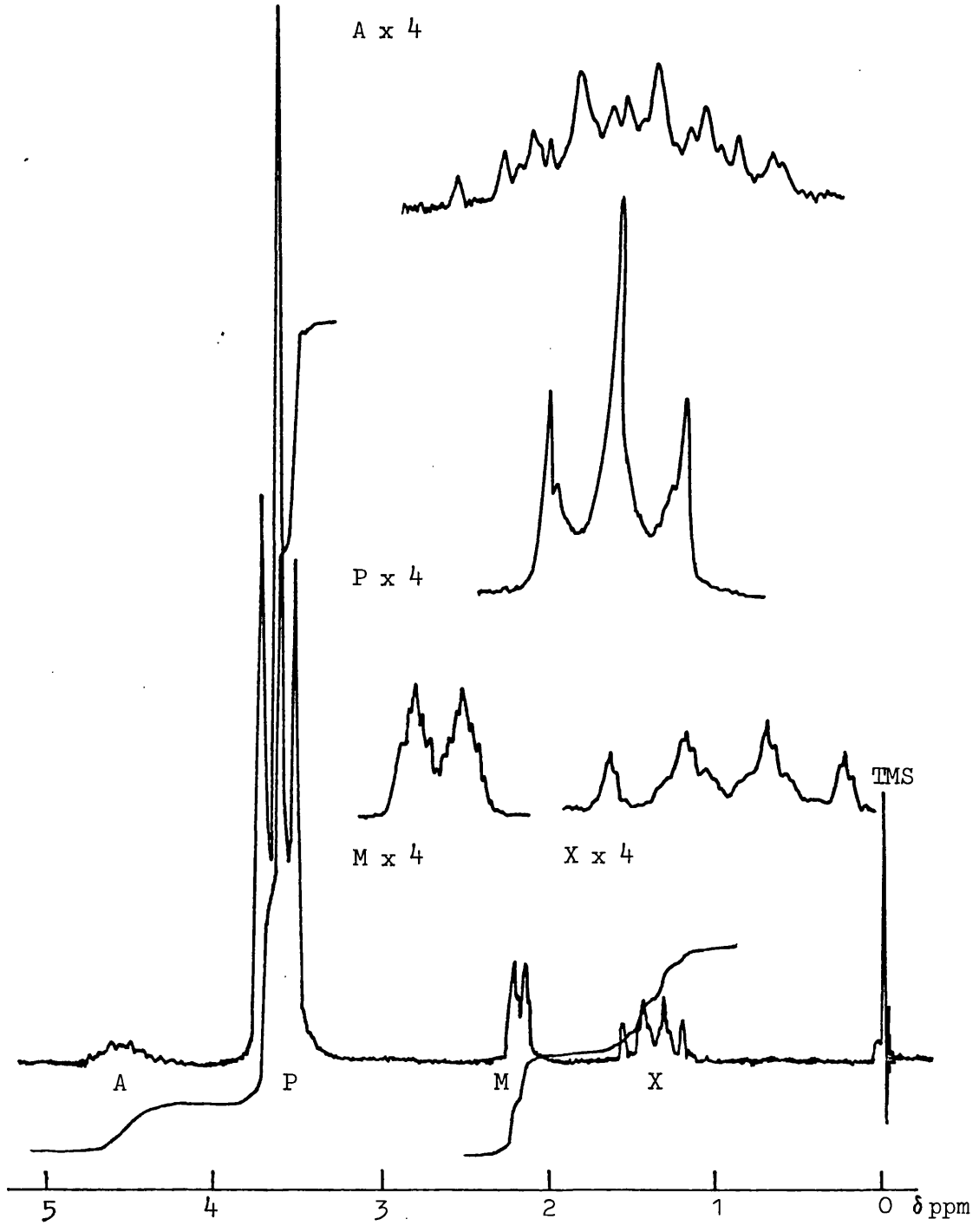

Figure 5.3: ^{1}H NMR spectrum of $[(\eta^{3}\text{-}C_{3}H_{5})Mn(CO)_{2}\{P(OMe)_{3}\}_{2}]$ in $CDCl_{3}$ solution

A more detailed study of the spectrum of VIII however, suggests that virtual coupling need not be invoked. Thus the ^{31}P-decoupled 100 MHz spectra recorded at -80°C and at +29°C do not show a singlet for the methoxy protons, as would be expected for a virtually coupled system, but rather a 1 : 1 doublet of separation 10 Hz. This is indicative of two different environments for the phosphite ligands with respect to the η^3-allyl group, in agreement with the solid state structure (vide infra). Furthermore, a 60 MHz spectrum, measured at ambient temperature (Figure 5.4), is composed of two 1 : 1 doublets for the methoxy protons ($^3J_{POMe}$ = 10.5 Hz) showing that the central line of the 100 MHz spectrum 1 : 2 : 1 triplet is produced by the adventitious overlap of two of these four lines.

The 100 MHz ^{1}H NMR spectrum of VIII was determined at several temperatures within the range -80° to +50°, with the methoxy resonances proving to be the most temperature dependent as shown in Figure 5.4. Thus at -80°C each line of the triplet is clearly split into a doublet (separation ca.2 Hz), such splitting being just apparent at +29°C but absent at +50°C. Also at +50°C in the ^{31}P-decoupled spectrum the methoxy protons doublet is very broad tending to collapse towards a singlet. Using first-order coupling rules these observations are best explained as follows: At -80°C the complex is stereochemically rigid, with the two sets of methoxy resonances being split into overlapping doublets by the nearest ^{31}P nucleus ($^3J_{POMe}$ = 10.5 Hz), and each line being further split by coupling to the more distant ^{31}P nucleus, ($^5J_{POMe}$ = 2 Hz). On warming, the phosphite ligands tend to lose their inequivalence with respect to the η^3-allyl ligand presumably by a fast rearrangement of the allyl group. Evidence supporting this suggestion comes from the observation that the allyl proton signals

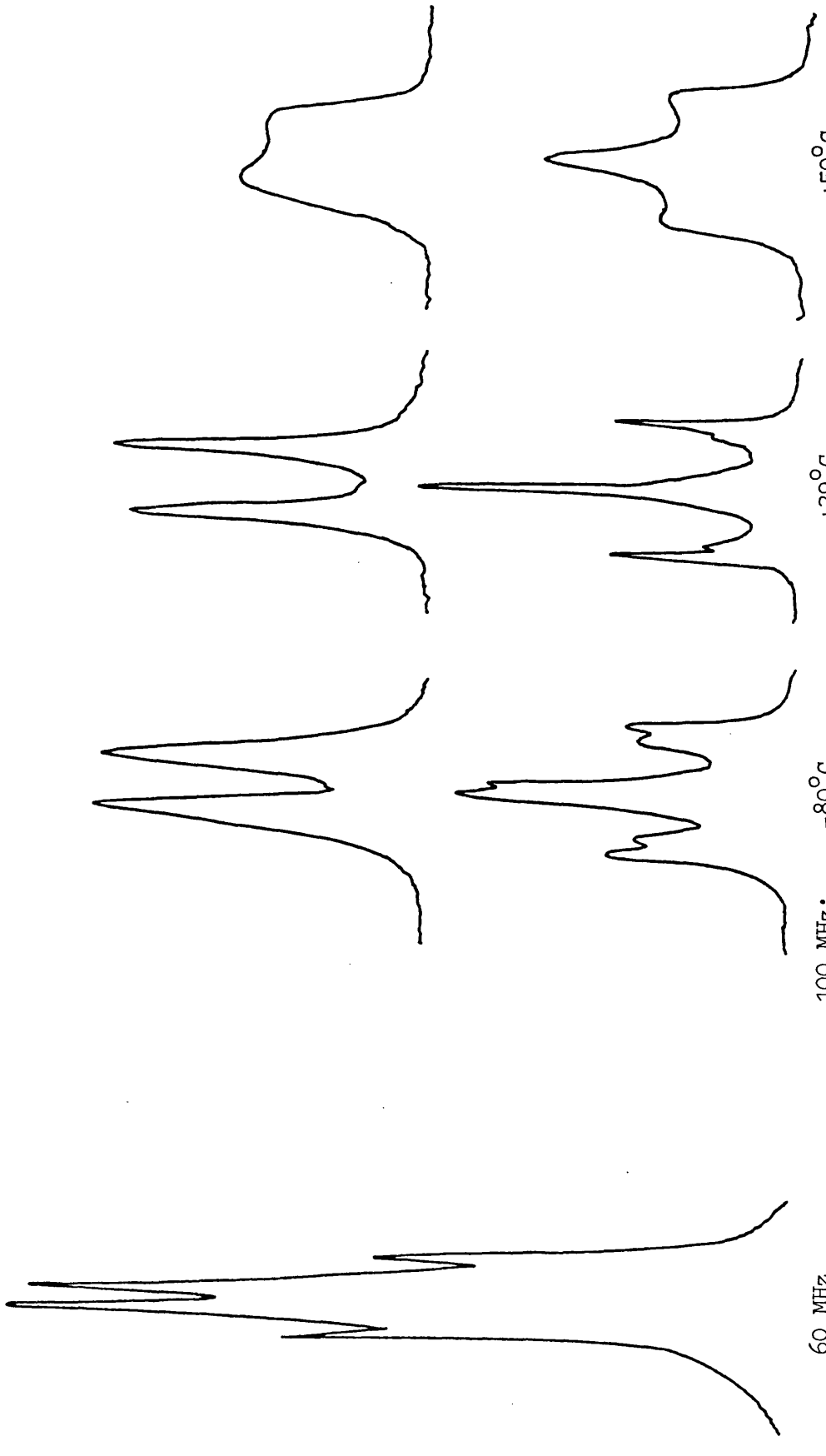

Figure 5.4: 60 MHz and Variable temperature 100 MHz ^{1}H NMR spectra for the methoxy protons of the complex $[(\eta^{3}\text{-}C_7H_{11})Mn(CO)_2\{P(OMe)_3\}_2]$ in CD_2Cl_2 solution (top spectra ^{31}P decoupled)

are noticeably sharper at +50°C. Thus this complex is probably stereochemically non-rigid above room temperature, but a study above +50°C could not be carried out because of the onset of decomposition.

Mass Spectra

The mass spectrum of each complex has been obtained and the metal-containing ions observed are listed in Table 5.5, together with the observed metastable ions. Each spectrum also contains many ions, often of high intensity, generated by ligand fragmentations. These have not been considered in detail so that the individual ion abundances quoted in the Table do not approximate to the percentage of ion current carried. As before (Chapter 4) the rhenium-containing ions are easily identified by the ^{185}Re : ^{187}Re isotopic ratio of 1 ; 0.59, but this is not possible for the manganese ions as ^{55}Mn is 100% abundant. Intensities are given relative to a metal-containing base peak of 100 units. The molecular ion is observed for all the complexes except $[(\eta^3\text{-}C_3H_5)Mn(CO)_2(PMePh_2)_2]$(VI), but is of high relative intensity only for $[(\eta^3\text{-}C_3H_5)Re(CO)_3PPh_3]$ (X).

The manganese tricarbonyl complexes show very few metal-containing ions and there is little evidence of the expected stepwise carbonyl ligand loss. Indeed analysis of the metastable ions shows that all three carbonyl groups can be lost in a single step, resulting in the formation of $[(C_3H_5)MnL]^+$ fragments, which are by far the most abundant metal-containing ions for each complex. Also there is no evidence for $[Mn(CO)_{3-x}L]^+$ (x = 0 - 2) fragment ions, so it seems that loss of allyl prior to carbonyl fragmentation is not a favoured process.

Table 5.5: Mass Spectra[a] of the Complexes $[(\eta^3\text{-}C_3H_5)M(CO)_{4-x}L_x]$

I. $[(\eta^3\text{-}C_3H_5)Mn(CO)_3PPh_3]$[b]

m/e	R.I.	Ion
442	7	$[C_3H_5Mn(CO)_3PPh_3]^+$
358	100	$[C_3H_5MnPPh_3]^+$
317	47	$[MnPPh_3]^+$

Metastables[c]: 358 → 317; m* = 281.0(280.7)

II. $[(\eta^3\text{-}C_3H_5)Mn(CO)_3AsPh_3]$[b]

m/e	R.I.	Ion
486	5	$[C_3H_5Mn(CO)_3AsPh_3]^+$
458	5	$[C_3H_5Mn(CO)_2AsPh_3]^+$
402	100	$[C_3H_5MnAsPh_3]^+$
381	12	$[C_3H_5Mn(CO)_2AsPh_2]^+$
361	33	$[MnAsPh_3]^+$

Metastables: 486 → 402; m* = 332.0(332.5)

III. $[(\eta^3\text{-}C_3H_5)Mn(CO)_3PCy_3]$[b]

m/e	R.I.	Ion
460	4	$[C_3H_5Mn(CO)_3PCy_3]^+$
376	100	$[C_3H_5MnPCy_3]^+$
335	10	$[MnPCy_3]^+$

IV. $[(\eta^3\text{-}C_3H_5)Mn(CO)_3PBu^n_3]$[b]

m/e	R.I.	Ion
382	10	$[C_3H_5Mn(CO)_3PBu^n_3]^+$
298	100	$[C_3H_5MnPBu^n_3]^+$
257	8	$[MnPBu^n_3]^+$

Metastables: 382 → 298; m* = 232.5(232.5)
298 → 257; m* = 221.5(221.5)
298 → 256; m* = 220.0(219.9)
298 → 255; m* = 218.0(218.2)

..../cont'd

Table 5.5: Cont'd

V. $[(\eta^3\text{-}C_3H_5)Mn(CO)_3PMePh_2]$[b]

m/e	R.I.	Ion
380	10	$[C_3H_5Mn(CO)_3PMePh_2]^+$
224	3	$[C_3H_5Mn(CO)PMePh_2]^+$
296	100	$[C_3H_5MnPMePh_2]^+$
255	28	$[MnPMePh_2]^+$

Metastables: 380 → 324; m* = 276.0(276.2)
324 → 296; m* = 270.5(270.4)
296 → 255; m* = 219.5(219.7)
255 → 200; m* = 157.0(156.9) (m/e 200 = $PMePh_2$)

VI. $[(\eta^3\text{-}C_3H_5)Mn(CO)_2(PMePh_2)_2]$[b]

m/e	R.I.	Ion
552	not obs.	$[C_3H_5Mn(CO)_2(PMePh_2)_2]^+$
496	0.1	$[C_3H_5Mn(PMePh_2)_2]^+$
481	0.1	$[C_3H_5Mn(PPh_2)(PMePh_2)]^+$
455	0.1	$[Mn(PMePh_2)]^+$
440	0.1	$[Mn(PPh_2)(PMePh_2)]^+$
380	5	$[C_3H_5Mn(CO)_3PMePh_2]^+$
324	5	$[C_3H_5Mn(CO)PMePh_2]^+$
296	100	$[C_3H_5MnPMePh_2]^+$
255	18	$[MnPMePh_2]^+$

VII. $[(\eta^3\text{-}C_3H_5)Mn(CO)_2dppm]$[b]

m/e	R.I.	Ion
536	1	$[C_3H_5Mn(CO)_2dppm]^+$
480	100	$[C_3H_5Mndppm]^+$
439	18	$[Mndppm]^+$

Metastables: 536 → 480; m* = 430.0(429.8)
480 → 439; m* = 401.5(401.5)

..../cont'd

Table 5.5: Cont'd

VIII. $[(\eta^3\text{-}C_3H_5)Mn(CO)_2\{P(OMe)_3\}_2]^b$

m/e	R.I.	Ion
400	11	$[C_3H_5Mn(CO)_2\{P(OMe)_3\}_2]^+$
369	2	$[C_3H_5Mn(CO)_2\{P(OMe)_3\}\{P(OMe)_2\}]^+$
344	8	$[C_3H_5Mn\{P(OMe)_3\}_2]^+$
313	7	$[C_3H_5Mn\{P(OMe)_3\}\{P(OMe)_2\}]^+$
303	1	$[Mn\{P(OMe)_3\}_2]^+$
288	1	$[Mn\{P(OMe)_3\}\{PO(OMe)_2\}]^+$
248	1	$[C_3H_5Mn(CO)P(OMe)_3]^+$
220	100	$[C_3H_5MnP(OMe)_3]^+$
179	37	$[MnP(OMe)_3]^+$

Metastables: 400 → 369; m* = 340.5(340.4)
400 → 344; m* = 295.5(295.8)
369 → 313; m* = 265.0(265.5)
344 → 220; m* = 140.5(140.7)
220 → 179; m* = 145.5(145.6)

IX. $[(\eta^3\text{-}C_3H_5)Mn(CO)_2\{P(OEt)_3\}_2]^b$

m/e	R.I.	Ion
484	9	$[C_3H_5Mn(CO)_2\{P(OEt)_3\}_2]^+$
439	2	$[C_3H_5Mn(CO)_2\{P(OEt)_2\}\{P(OEt)_3\}]^+$
428	7	$[C_3H_5Mn\{P(OEt)_3\}_2]^+$
387	1	$[Mn\{P(OEt)_3\}]^+$
383	4	$[C_3H_5Mn\ P(OEt)_2\{P(OEt)_3\}]^+$
354	1	[383 - Et]
309	1	[383 - OEt]
262	100	$[C_3H_5MnP(OEt)_3]^+$
221	14	$[MnP(OEt)_3]^+$

Metastables: 484 → 428; m* = 379.0(378.5)
428 → 262; m* = 160.5(160.4)
262 → 221; m* = 187.0(186.4)

..../cont'd

X. $[(\eta^3\text{-}C_3H_5)Re(CO)_3PPh_3]^d$

m/e	R.I.	Ion
574	90	$[C_3H_5Re(CO)_3PPh_3]^+$
546	97	$[C_3H_5Re(CO)_2PPh_3]^+$
533	100	$[Re(CO)_3PPh_3]^+$
518	61	$[C_3H_5Re(CO)PPh_3]^+$
505	32	$[Re(CO)_2PPh_3]^+$
504	23	
490	38	$[C_3H_5RePPh_3]^+$
474	43	
449	88	$[RePPh_3]^+$
448	66	
444	23	
372	37	$[RePPh_2]^+$

Metastables: 574 → 546; m* = 519.0(519.3)
574 → 533; m* = 495.0(494.9)
546 → 518; m* = 491.5(491.4)
533 → 505; m* = 478.5(478.5)
518 → 490; m* = 463.5(463.5)

XI. $[(\eta^3\text{-}C_3H_5)Re(CO)_2(PPh_3)_2]^d$

m/e	R.I.	Ion
808	3	$[C_3H_5Re(CO)_2(PPh_3)_2]^+$
767	7	$[Re(CO)_2(PPh_3)_2]^+$
739	8	$[Re(CO)(PPh_3)_2]^+$
711	4	$[Re(PPh_3)_3]^+$
634	3	$[Re(PPh_2)(PPh_3)]^+$
574	38	$[C_3H_5Re(CO)_3PPh_3]^+$
546	100	$[C_3H_5Re(CO)_2PPh_3]^+$
533	44	$[Re(CO)_3PPh_3]$

..../cont'd

Table 5.5: Cont'd

m/e	R.I.	Ion
518	40	$[C_3H_5Re(CO)PPh_3]^+$
505	16	$[Re(CO)_2PPh_3]^+$
504	18	
490	38	$[C_3H_5RePPh_3]^+$
474	39	
449	50	$[RePPh_3]^+$
448	58	
Metastable: 739 → 711; m* = 684.0(684.1)		

[a] Metal containing ions only.

[b] Ions at m/e 96 $[MnC_3H_5]^+$ and 55 $[Mn]^+$ always highly abundant and often linked by m* = 31.5, they are not tabulated because they undoubtedly contain contributions from ligand fragments.

[c] Calculated position in parenthesis.

[d] Based on ^{187}Re isotope.

Since loss of allyl prior to carbonyl fragmentation is not a favoured process for the manganese tricarbonyl complexes, fragments of the type $[MnL]^+$ must therefore arise from the process:-

$$[(C_3H_5)MnL]^+ \longrightarrow [MnL]^+ + C_3H_5^{\cdot}$$

This is confirmed by the observation of the appropriate metastable peaks.

The mass spectrum of $[(\eta^3\text{-}C_3H_5)Re(CO)_3PPh_3]$ is however markedly different to those of the manganese tricarbonyl complexes. Thus stepwise loss of carbonyl groups is a favoured process, each fragment ion being of high relative intensity with all three metastable ions present. Unlike the manganese analogues, $[(C_3H_5)ReL]^+$ is not the most abundant metal-containing ion, the

base peak in this case being $[Re(CO)_3L]^+$. The appearance of the appropriate metastable ion shows that the allyl loss,

$$[(C_3H_5)Re(CO)_3PPh_3]^+ \longrightarrow [Re(CO)_3PPh_3]^+ + C_3H_5^{\bullet},$$

is a major fragmentation process in competition with that of initial carbonyl loss. Subsequent stepwise loss of carbonyl groups then occurs. Thus the highly abundant $[RePPh_3]^+$ ion arises from two alternative fragmentation pathways. Ligand fragmentation whilst still attached to the metal is not a favoured process for these tricarbonyl complexes although $[(C_3H_5)Mn(CO)_2AsPh_2]^+$ is observed as a moderately abundant peak in the spectrum of the $AsPh_3$ complex II.

Consideration of the metastable ions detected in the spectra of the manganese dicarbonyl complexes $[(\eta^3\text{-}C_3H_5)Mn(CO)_2L_2]$ (L = $PMePh_2$, $P(OMe)_3$, $P(OEt)_3$), indicates that initial simultaneouus loss of both carbonyl groups, followed by loss of one ligand molecule before final elimination of the allyl group, is the major fragmentation pathway. The ion $[(C_3H_5)Mn(CO)L_2]^+$ was not detected in any of the spectra. As for the tricarbonyl complexes, the most abundant metal-containing ion in each of these three spectra is $[(C_3H_5)MnL]^+$ showing that loss of only one mole of ligand is a favoured process. However there is evidence for other ions such as $[(C_3H_5)Mn(CO)L]^+$, albeit in low abundance, showing that carbonyl and ligand loss may be competitive processes. The following scheme summarises the fragmentation processes (unbroken arrows indicate the major pathway):-

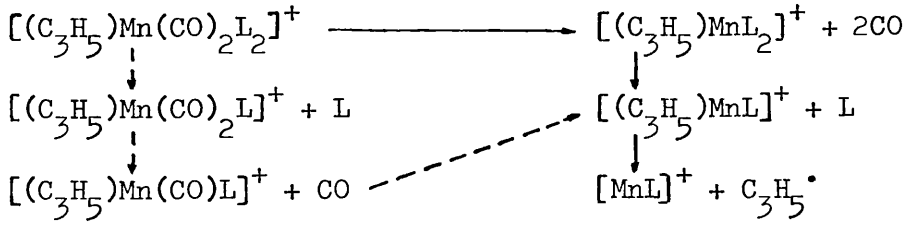

The mass spectrum of $[(\eta^3\text{-}C_3H_5)Mn(CO)_2dppm]$ is, as expected, somewhat different in that the chelating ligand prevents loss of one bonded phosphorus without ligand cleavage. The fragmentation pattern, which is confirmed by the observation of the appropriate metastable ions, thus follows the more simple sequence:-

$$[(C_3H_5)Mn(CO)_2dppm]^+ \longrightarrow [(C_3H_5)Mndppm]^+ + 2CO$$
$$\downarrow$$
$$[Mndppm]^+ + C_3H_5^{\bullet}$$

As for the tricarbonyl series, the rhenium dicarbonyl complex $[(\eta^3\text{-}C_3H_5)Re(CO)_2(PPh_3)_2]$ (XI) does not follow the same fragmentation pattern as the manganese dicarbonyl complexes. The base metal-containing peak is $[(C_3H_5)Re(CO)_2PPh_3]^+$ and generally the most abundant ions are derived from this peak by successive loss of carbonyl groups. Although the loss of one phosphine ligand is again favoured, initial loss of the allyl group must be a competing pathway for this dicarbonyl complex, since all possible $[Re(CO)_{2-x}(PPh_3)_2]^+$ (x = 0-2) ions as well as $[Re(CO)_2(PPh_3)]^+$ are detected. In contrast to the tricarbonyl rhenium complex, X, initial loss of carbonyl groups appears to be insignificant for this complex as the ions $[(C_3H_5)Re(CO)_{2-x}(PPh_3)_2]^+$ (x = 1, 2) are not detected. The suggested fragmentation sequence is summarised in the following scheme:-

$$\begin{array}{lll}
[(C_3H_5)Re(CO)_2(PPh_3)_2]^+ & \longrightarrow & [(C_3H_5)Re(CO)_2PPh_3]^+ + PPh_3 \\
\downarrow & & \downarrow \\
[Re(CO)_2(PPh_3)_2]^+ + C_3H_5 & & [(C_3H_5)Re(CO)PPh_3]^+ + CO \\
\downarrow & & \downarrow \\
[Re(CO)(PPh_3)_2]^+ + CO & & [(C_3H_5)RePPh_3]^+ + CO \\
\downarrow & & \downarrow \\
[Re(PPh_3)_2]^+ + CO & \longrightarrow & [RePPh_3]^+ + C_3H_5^{\bullet}
\end{array}$$

Unlike the tricarbonyl complexes, ligand fragmentation whilst still attached to the metal is a significant feature in the mass spectra of the dicarbonyls, particularly for the bis-phosphite complexes where ions such as $[(C_3H_5)Mn(CO)_{2-x}P(OR)_3P(OR)_2]^+$ (x = 0, 2; R = Me, Et) are of at least moderate relative intensity. The fragmentation pathway,

$$[(C_3H_5)Mn(CO)_2\{P(OMe)_3\}_2]^+ \longrightarrow [(C_3H_5)Mn(CO)_2P(OMe)_3P(OMe)_2]^+ + OMe^\bullet$$
$$\downarrow$$
$$[(C_3H_5)MnP(OMe)_3P(OMe)_2]^+ + 2CO,$$

is established for the complex VIII by observation of the appropriate metastable ions.

Finally, it is noticeable that no ions are observed which correspond to the loss of two hydrogen atoms from the allyl group whilst still bound to the metal. Such ions, e.g. $[(C_3H_3)Re(CO)_x]^+$ (x = 0-2), are however of high abundance in the mass spectra of both $[(\eta^1\text{-}C_3H_5)Re(CO)_5]$ and $[(\eta^3\text{-}C_3H_5)Re(CO)_4]$ (see Chapter 4).

The Crystal and Molecular Structure of $[(\eta^3\text{-}C_3H_5)Mn(CO)_2\{P(OMe)_3\}_2]$

The crystal and molecular structure of the title compound described in this section was determined in collaboration with Dr. M.G.B. Drew at the University of Reading. Plate 5.1 illustrates the structure which consists of discrete molecules of $[(\eta^3\text{-}C_3H_5)Mn(CO)_2\{P(OMe)_3\}_2]$ separated by the usual van der Waals contacts and a diagrammatic view with the atom numbering scheme is given in Figure 5.5. Table 5.6 lists the final atomic positions whilst the important bond lengths and angles are presented in Table 5.7.

The metal atom is bonded to two mutually trans phosphorus atoms [Mn-P 2.175(5), 2.219(5) Å], two cis carbonyl groups [Mn-C 1.75(2), 1.83(2) Å] and a η^3-allyl ligand [Mn-C 2.223(17), 2.114(14), 2.229(13) Å].

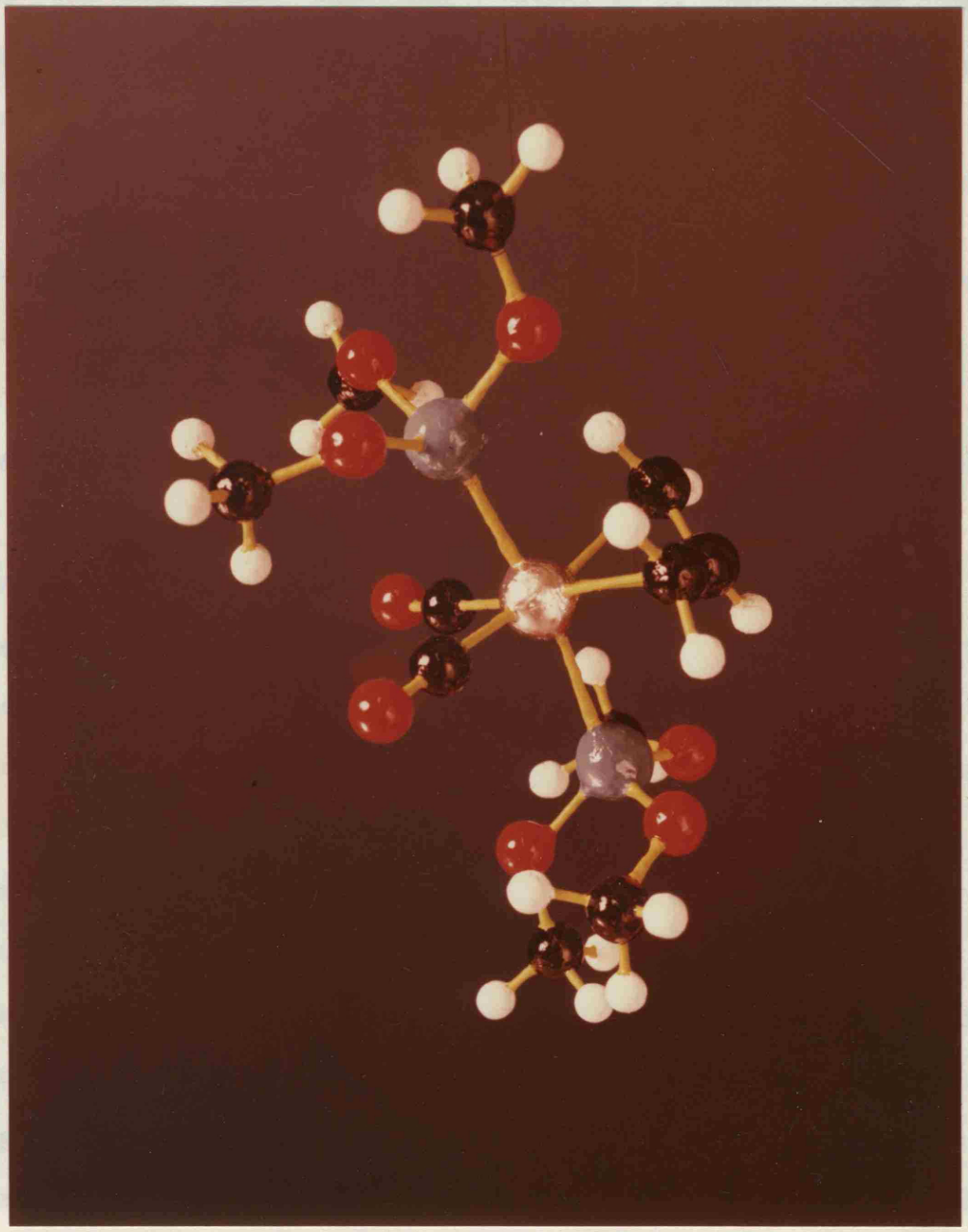

Plate 5.1: The Structure of $[(\eta^3\text{-}C_3H_5)Mn(CO)_2\{P(OMe)_3\}_2]$

If the allyl group is looked upon as a bidentate ligand, the metal atom may then be considered to possess a distorted octahedral environment. This is of course merely a matter of convenience and the reverse situation where the allyl group is considered to occupy only one coordination site often applies. For example, the Group VI complexes $[(\eta^3\text{-}RC_3H_4)MX(CO)_2L_2]$ discussed in Chapter Two possess a pseudo-octahedral structure only if the allyl group is monodentate.

The distortion in the present complex is considerably greater than that found in the related compound $[Mn(CO)_2(PPh_3)_2(O_2CCH_3)]$[335], which contains a chelating acetato-group, even though the O-Mn-O angle in the acetate is only $61.6(3)^\circ$ compared with C(12)-Mn-C(14) of $67.0(6)^\circ$ in the allyl. This cannot be ascribed to the difference in 'normalised bite' between the allyl and acetate ligands since they are both very similar in this respect (allyl 1.1, acetate 1.0). However in the former complex the allyl hydrogens and indeed C(13) are close to the coordination sphere of the metal whilst in the latter complex only the two oxygen atoms of the acetate group affect the position of the other atoms. A further cause of distortion from octahedral symmetry is derived from the close contacts involving the oxygen atoms of the trimethylphosphite groups and atoms in the metal coordination sphere. Thus it is significant that torsion angles of the type L-Mn-P-O are different for the two phosphorus atoms, the three smallest all involving P(2) rather than P(1) i.e. [C(8)-Mn-P(2)-O(6) -6.0, C(12)-Mn-P(2)-O(4) 17.1, C(13)-Mn-P(2)-O(4) -17.5°].

It has already been mentioned that the ^1H NMR spectra of the complex at several temperatures (page 169) indicate that the $P(OMe)_3$ ligands are in different environments. Likewise in the solid state, as illustrated qualitatively in Plate 5.1, the methoxy

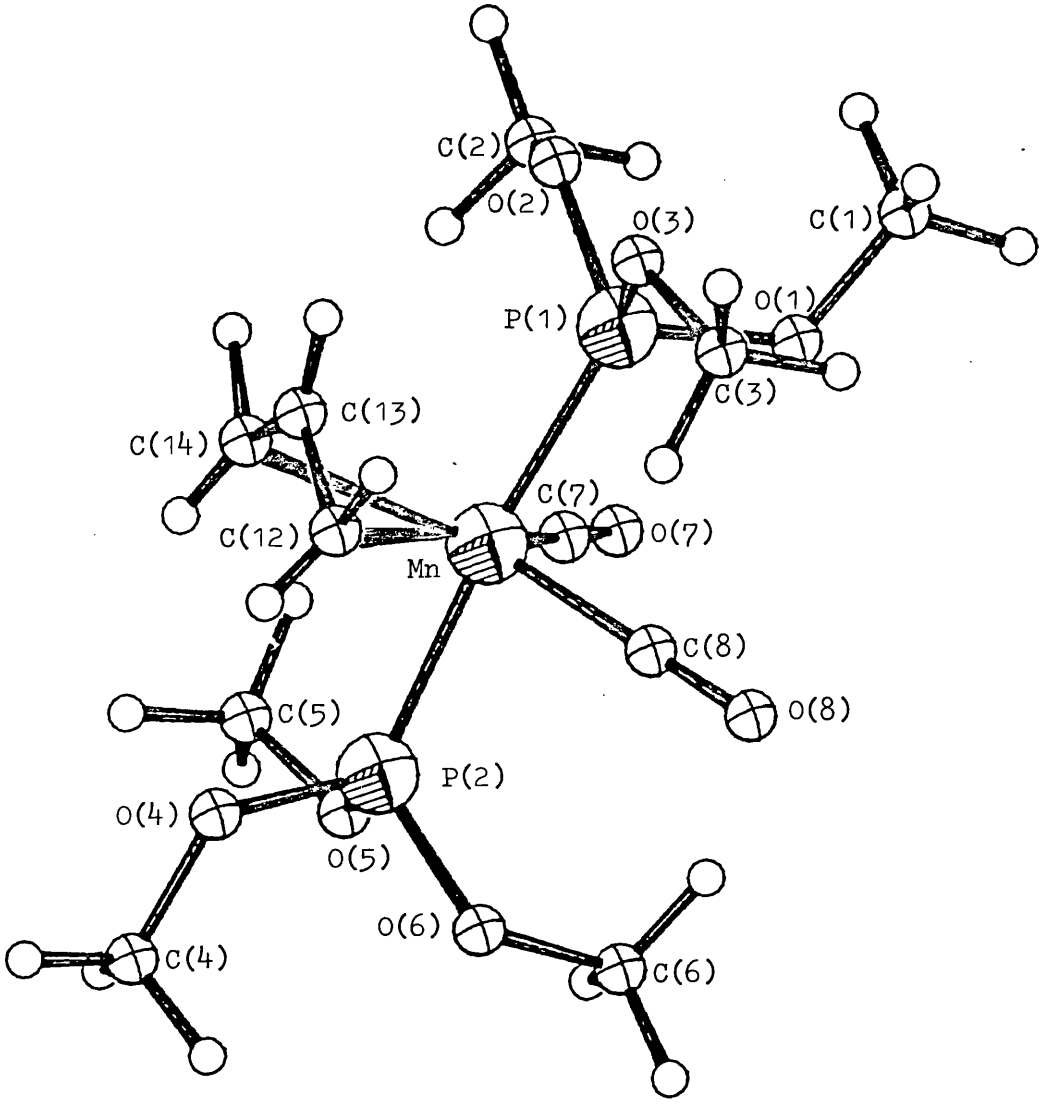

Figure 5.5: Diagram of the molecule with atom numbering scheme

groups of the 'lower' $P(OMe)_3$ ligand, P(1), do not adopt the regular 'propeller' configuration but rather are twisted away from the central allyl CH. Thus P(1) is further from C(12) and C(14) [P(1)-Mn-C(12) 96.0(5), P(1)-Mn-C(14) 99.2(4)°] than P(2) [90.6(5), 85.9(4)°] and the central allyl carbon which is on the opposite side of the equatorial plane (defined by Mn, C(7) and C(8)) is closer to P(1) [P(1)-Mn-C(13) 81.9(5)°] than P(2) [105.1(5)°]. The P(1)-Mn-P(2) angle of 172.8(2) also shows that the phosphite ligands are forced away from the allyl group, being reduced from the ideal trans angle of 180°.

Table 5.6: Atomic Coordinates ($\times 10^4$) with Estimated Standard Deviations in Parenthesis

Atom	X	Y	Z
Mn	1454(1)	1852(3)	2540(2)
P(1)	760(2)	2893(5)	3688(4)
P(2)	2040(2)	620(5)	1266(4)
O(1)	-91(5)	2438(12)	3199(10)
O(2)	918(5)	2683(13)	5213(9)
O(3)	731(6)	4632(12)	3793(11)
O(4)	2848(5)	1140(13)	1256(10)
O(5)	2111(7)	-1106(13)	1416(11)
O(6)	1688(6)	609(14)	-259(9)
C(1)	-653(9)	2972(23)	3819(17)
C(2)	920(11)	1263(24)	5741(17)
C(3)	463(11)	5512(20)	2659(19)
C(4)	3297(10)	494(26)	452(18)
C(5)	2448(12)	-1810(23)	2576(20)
C(6)	1014(10)	-196(24)	-776(17)
C(7)	988(8)	242(18)	2738(13)
O(7)	669(7)	-824(14)	2876(13)
C(8)	812(9)	2529(17)	1112(16)
O(8)	426(7)	2974(14)	227(11)
C(12)	2254(9)	3664(18)	2665(17)
C(13)	2485(8)	2981(18)	3835(14)
C(14)	2460(8)	1520(18)	4074(14)
H(11)	-1179(9)	2537(23)	3342(17)
H(12)	-670(9)	4142(23)	3764(17)
H(13)	-535(9)	2640(23)	4818(17)
H(21)	1035(11)	1329(24)	6781(17)
H(22)	1337(11)	617(24)	5439(17)
H(23)	389(11)	766(24)	5404(17)
H(31)	486(12)	6643(20)	2928(19)
H(32)	-98(12)	5216(20)	2244(19)
H(33)	800(12)	5331(20)	1961(19)
H(41)	3824(10)	1033(26)	617(18)
H(42)	3028(10)	608(26)	-549(18)
H(43)	3377(10)	-643(26)	685(18)
H(51)	2428(12)	-2971(23)	2430(20)
H(52)	2161(12)	-1532(23)	3328(20)
H(53)	3014(12)	-1467(23)	2855(20)
H(61)	871(10)	-66(24)	-1811(17)
H(62)	574(10)	212(24)	-357(17)
H(63)	1100(10)	-1334(24)	-545(17)
H(121)	2615(68)	3447(89)	2322(84)
H(122)	2094(65)	4854(89)	2738(83)
H(13)	2155(65)	3636(88)	4390(84)
H(141)	2414(58)	1055(81)	5071(80)
H(142)	2784(67)	1050(87)	3753(83)

Table 5.7: Interatomic Distances and Angles with Standard Deviations in Parenthesis

Distance (Å)		Angle (°)	
Coordination sphere			
Mn-P(1)	2.175(5)	P(1)-Mn-P(2)	172.8(2)
Mn-P(2)	2.219(5)	P(1)-Mn-C(7)	86.6(6)
Mn-C(7)	1.75(2)	P(1)-Mn-C(8)	87.2(6)
Mn-C(8)	1.83(2)	P(1)-Mn-C(12)	96.0(5)
Mn-C(12)	2.223(17)	P(1)-Mn-C(13)	81.9(5)
Mn-C(13)	2.114(15)	P(1)-Mn-C(14)	99.2(4)
Mn-C(14)	2.229(13)	P(2)-Mn-C(7)	87.6(6)
		P(2)-Mn-C(8)	89.4(6)
		P(2)-Mn-C(12)	90.6(5)
		P(2)-Mn-C(13)	105.1(5)
		P(2)-Mn-C(14)	85.9(4)
		C(7)-Mn-C(8)	97.7(7)
		C(7)-Mn-C(12)	166.1(6)
		C(7)-Mn-C(14)	99.1(6)
		C(8)-Mn-C(12)	96.1(7)
		C(8)-Mn-C(14)	162.4(7)
		C(12)-Mn-C(14)	67.0(6)
Allyl ligand			
C(12)-C(13)	1.38(2)	C(12)-C(13)-C(14)	124.5(15)
C(13)-C(14)	1.40(2)		
Carbonyl groups			
C(7)-O(7)	1.17(2)	Mn-C(7)-O(7)	179.1(15)
C(8)-O(8)	1.13(2)	Mn-C(8)-O(8)	178.3(15)

..../cont'd

Table 5.7: Cont'd

Distance (Å)		Angle (°)	
Trimethylphosphite ligands			
P(1)-O(1)	1.62(1)	Mn-P(1)-O(1)	111.3(4)
P(1)-O(2)	1.59(1)	Mn-P(1)-O(2)	120.6(4)
P(1)-O(3)	1.61(1)	Mn-P(1)-O(3)	120.7(5)
P(2)-O(4)	1.58(1)	Mn-P(2)-O(4)	116.1(5)
P(2)-O(5)	1.6o(1)	Mn-P(2)-O(5)	119.2(5)
P(2)-O(6)	1.61(1)	Mn-P(2)-O(6)	117.8(5)
O(1)-C(1)	1.43(2)	P(1)-O(1)-C(1)	121.6(10)
O(2)-C(2)	1.42(2)	P(1)-O(2)-C(2)	119.7(10)
O(3)-C(3)	1.45(2)	P(1)-O(3)-C(3)	120.7(10)
O(4)-C(4)	1.44(2)	P(2)-O(4)-C(4)	123.3(11)
O(5)-C(5)	1.42(2)	P(2)-O(5)-C(50	123.6(11)
O(6)-C(6)	1.46(2)	P(2)-O(6)-C(6)	121.0(11)
		O(1)-P(1)-O(2)	104.7(6)
		O(1)-P(1)-O(3)	103.6(6)
		O(2)-P(1)-O(3)	93.0(6)
		O(4)-P(2)-O(5)	104.0(7)
		O(4)-P(2)-O(6)	100.5(6)
		O(5)-P(2)-O(6)	95.8(6)

Probably as a result of different O...C contacts the two Mn-P distances (Table 5.7) differ significantly [Mn-P(1)>Mn-P(2)] by 0.044(5) Å. Furthermore both are appreciably shorter than those found in a number of other manganese(I) bis-phosphine and bis-phosphite complexes e.g. 2.260(3), 2.275(3) Å in $[Mn(CO)_2(PPh_3)_2(O_2CCH_3)]$[335]; 2.278(5), 2.279(5) Å in $[Mn(CO)_2(PPh_3)_2NO]$[336]; 2.260(8), 2.279(8) Å in fac-

$[Mn(CO)_3Br\{P(OMe)_2Ph\}_2]$[231]. Such shortening of Mn-P bond lengths may be attributed to the greater Lewis acidity of the trimethylphosphite ligands[231].

The Mn-C(carbonyl) bond lengths [Mn-C(7) 1.75(2), Mn-C(8) 1.83(2) Å] fall within the expected range for manganese(I) carbonyl complexes and may be compared with similar distances in, for example, $[Mn(CO)_2(PPh_3)_2(O_2CCH_3)]$ (1.70 - 1.76)[335], $[Mn(CO)_3(PPh_3)NO]$ (1.76 - 1.83 Å)[337], $[Mn(CO)_4(PPh_3)(SnPh_3)]$ (1.74 - 1.85 Å)[338], $[Mn(CO)_4(PPh_3)Cl]$ (1.75 - 1.86 Å)[339], $[(\eta^5\text{-}C_5H_5)Mn(CO)_2(PPh_3)]$ (1.74 - 1.77 Å)[340] and cis-$[Mn(CO)_2\{P(OMe)_2Ph\}_4]^+$ (1.78)[341]. The difference in Mn-C(carbonyl) distances (0.08(2) Å) [Mn-C(8) > Mn-C(7)] is not easily explained in this fairly symmetrical structure however it may be a direct result of the close contact between C(8) and O(6) mentioned previously. The C(7)-Mn-C(8) angle [97.7(7)°] is greater than the octahedral angle 90° (c.f. 89.3(5)° in $[Mn(CO)_2(PPh_3)_2(O_2CCH_3)]$) as predicted from infrared ν(CO) band intensity measurements for this complex (page 160). As expected the manganese carbonyl units are almost linear [Mn-C(7)-O(7) 179.1(15), Mn-C(8)-O(8) 178.3(15)°] and the C-O bond lengths [1.17(2), 1.13(2) Å] are typical of metal carbonyls generally.

The Mn-C(allyl) bond lengths [2.223(17), 2.214(15), 2.229(13) Å] and allyl C-C distances [1.38(2), 1.40(2)] show that the allyl group is a symmetrically bound trihapto-ligand with the shortest Mn-C bond to the unique central carbon C(13). The C(12)-Mn-C(14) angle of 67.0(6)° and the C(12)-C(13)-C(14) angle of 124.5(15)° are typical of many η^3-allyl complexes[57] and may be compared with, for example, analogous angles of 69.5(2)° and 118.8(5)° found in the complex $[(\eta^3\text{-}C_3H_5)Co(CO)_2(PPh_3)]$[342]. The plane of the allyl

carbons [C(12), C(13), C(14)] intersects the equatorial plane [Mn, C(7), C(8)] at an angle of 71.0°. Alternatively, using the convention given in Chapter 1, the dihedral 'allyl tilt' angle, X, is 109.0° as shown in Figure 5.6.

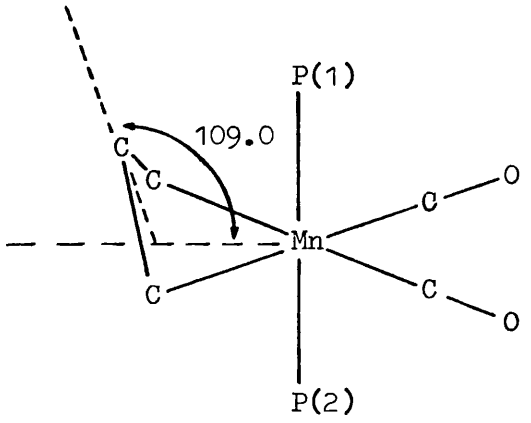

Figure 5.6: Schematic drawing of the coordination sphere in $[(\eta^3\text{-}C_3H_5)Mn(CO)_2\{P(OMe)_3\}_2]$ showing the 'allyl tilt'

In the solid state the allyl group in $[(\eta^3\text{-}C_3H_5)Mn(CO)_2\{P(OMe)_3\}_2]$ is slightly twisted with respect to the equatorial plane. Thus C(12) lies 0.07 Å below the Mn, C(7), C(8) plane whereas C(14) lies 0.21 Å below. The central allyl carbon lies 0.47 Å above the plane.

Although there are no structure determinations involving the $[(\eta^3\text{-}C_3H_5)Mn]$ unit available for direct comparison of the bond lengths and angles, the features described above are common amongst η^3-allyl complexes in general[57] (see Chapter 1, pages 5 - 10). The only other crystal structure determination reported[343] in which an η^3-moiety is bonded to manganese is for the complex $[Mn_2(CO)_6(As_3Me_6F_5C_4)]$. The structure is illustrated in Figure 5.7. This complex has Mn-C(allyl) bond lengths of 2.09(2), 2.07(2) and 2.13(2) Å and the angle subtended at the central carbon atom is 122(2)°. However the η^3-moiety in this compound is substituted

(by two As atoms, two F atoms and a CF_3 group) and is also part of a cyclic system and therefore comparison with the bis-phosphite complex under discussion is not strictly valid.

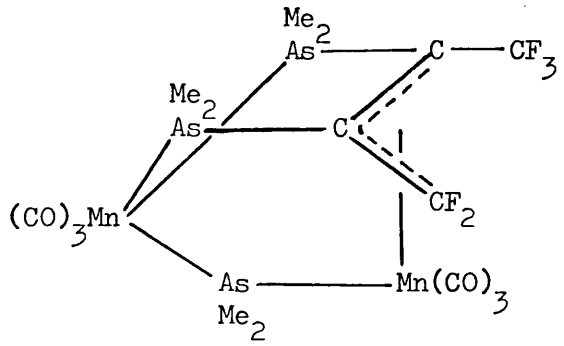

Figure 5.7: The structure of $[Mn_2(CO)_6(As_3Me_6C_4F_5)]$

In conclusion it is clear that, in solution, the spectroscopic properties of the closely related dicarbonylbis- phosphine and phosphite complexes described in this Chapter are best explained in terms of a pseudo-octahedral structure. Such a structure has been established for the complex $[(\eta^3\text{-}C_3H_5)Mn(CO)_2\{P(OMe)_3\}_2]$ in the solid state by X-ray crystallography. Thus the solid state structure and the solution properties are in good agreement.

APPENDICES

APPENDIX 1

PHYSICAL METHODS AND INSTRUMENTATION

^{1}H NMR Spectra

^{1}H NMR spectra were measured on a JEOL PS 100 spectrometer, together with the associated variable temperature controller, using tetramethylsilane (TMS) as internal reference. Samples were dissolved under nitrogen to give 5-10% solutions and held in 4 mm silica tubes. The spectrograde solvents CD_2Cl_2, $CDCl_3$, CCl_4, CS_2 and SO_2 were used as received without further purification.

Infrared Spectra

Infrared spectra in the 4000-200 cm^{-1} region were obtained on a Hilger-Watts Infrascan H 1200 or on Perkin-Elmer 735 and 597 spectrophotometers. Samples were prepared as Nujol or hexachlorobutadiene mulls and liquid films held between CsI plates or as solutions in a Beckmann-RIIC FS 125 0.1 mm KBr cell. Wavenumber calibration at several points for each spectrum was achieved by reference to known absorptions in the spectra of polystyrene or polytetrafluoroethene. Far infrared spectra of samples dispersed in pressed polythene discs were recorded between 400-40 cm^{-1} using a Beckmann-RIIC FS 720 interferometer. Fourier transforms of the interferograms were computed on an ICL 4-50 computer by means of a Fortran IV programme.

Raman Spectra

Raman spectra of solid, liquid or solution samples held in capillary tubes were measured using a Spex 1401 spectrometer in conjunction with a Spectra-Physics He-Ne laser having an output of ca. 50 mW at 632.8 nm. Spectra were calibrated by means of several lines in the neon gas emission spectrum[202] and from known indene peaks.

Depolarisation ratios were measured by examining the spectra with the plane of polarised light parallel and perpendicular to the axis of an analyser.

Mass Spectra

Mass spectra were obtained on an AEI MS 12 instrument using direct insertion probes or an all glass heated inlet system (AGHIS). Ionisation energies of 70 eV and ca. 12 eV were generally employed. For high molecular weight samples calibration with perfluorokerosene (PFK) was sometimes necessary.

Conductivity

Conductivity measurements were determined at 25°C using a Wayne-Kerr Autobalance bridge and a dip-type cell with platinum electrodes. A cell constant value of 1.56 cm^{-1} was determined by measuring the conductance of 0.1 M KCl (Λ_M = 128.96 $S\,cm^2\,mol^{-1}$).

Melting Points

Melting points were recorded on a Kofler hot stage apparatus and were uncorrected.

Analysis

Carbon, hydrogen and nitrogen analyses were determined by Dr.F.B. Strauss at the microanalytical laboratories, Oxford.

General

Standard Quickfit glassware was dried at 110°C for several hours prior to assembly and flushed with dry nitrogen gas. An inert atmosphere of dry nitrogen above reactions was routinely provided throughout.

APPENDIX 2

SOLVENTS, REAGENTS AND STARTING MATERIALS

Solvents

All Standard Laboratory Reagent grade solvents were dried over molecular sieves or sodium wire, as appropriate, and thoroughly purged with dry nitrogen gas prior to use. In addition several solvents required further treatment as outlined below.

Chloroform: $CHCl_3$ (100 cm^3), which had been routinely treated as above, was passed down an alumina column (Brockman 1, basic; 2 x 30 cm x 1.5 cm) to remove alcohol impurities. The freshly eluted solvent was stored in dark glass, nitrogen filled containers and used soon after purification.

Nitromethane: CH_3NO_2, for conductance measurements, was heated under reflux with P_2O_5 for several hours. The solvent was then distilled from fresh P_2O_5 and the fraction boiling between 99-100°C (P = 750 mmHg) was collected. Finally, to remove traces of P_2O_5, the nitromethane was distilled from 3A molecular sieves in a closed nitrogen flushed system. In this way the conductance of the solvent could be reduced to 1 x 10^{-7} S but strict exclusion of moisture was necessary to maintain this figure.

Tetrahydrofuran: THF was distilled twice from $LiAlH_4$, the first and last 20% being rejected in each case. The solvent was purged with nitrogen and stored in nitrogen filled vessels over solid calcium hydride.

Reagents

Unless otherwise stated Analar and Standard Laboratory Reagents were used as received without further purification. Some reagents

were conveniently prepared in the laboratory:

Tetraphenylphosphonium iodide: Ph_4PI was precipitated from aqueous Ph_4PCl by a stoichiometric quantity of aqueous KI. The solid product was filtered, washed with distilled water and dried *in vacuo*.

3-Bromocyclohexene: After initially inducing vigorous reaction by gentle warming, a suspension of N-bromosuccinimide (7.4 g) in cyclohexene (20 cm^3) and carbontetrachloride (30 cm^3) was heated under reflux for 0.5 h. On cooling the precipitate of succinimide was filtered off and the solvents removed (15 mm/25°). The product, 3-bromocyclohexene (70%), was carefully collected by vacuum distillation (10 mm/64-67°) and its purity checked by NMR spectroscopy. {(5.86 q, 2H), (4.86 dt, 1H), (2.3-1.7 m, 6H)}.

Sodium-Mercury Amalgam: In order to obtain 0.5% Na/Hg amalgam, sodium (1.0 g) was added to mercury (200 g/15 cm^3) as follows. Small pieces of sodium metal were impaled on a glass rod and held beneath the surface of a pool of mercury covered with a protective layer of paraffin oil. As the sodium dissolved a considerable evolution of heat occurred and it was sometimes necessary to cool the vessel in ice-water. When all the sodium had dissolved the amalgam was washed with several portions of petroleum ether and finally stored at 0°C under paraffin oil.

Starting Materials

Group VI transition metal tetracarbonyls[203,204]

$Mo(CO)_4L_2$, (L_2 = bipy, phen): $Mo(CO)_6$ (2.64 g/10 mmol) and the bidentate ligand L_2 (10 mmol) were heated under reflux in toluene (50 cm^3) for 2 h. The product which separated on cooling was filtered washed with toluene and dried *in vacuo*. Yields>90%.

$W(CO)_4L_2$, (L = bipy, phen): $W(CO)_6$ (1.76 g/5 mmol) and the bidentate ligand L_2 (5 mmol) were heated under reflux in xylene (50 cm^3) for 16 h. The products were obtained as above. Yields >80%.

Group VII halogenopentacarbonyls[205-209]

$Mn(CO)_5Cl$: $Mn_2(CO)_{10}$ (1.0 g/2.56 mmol) was suspended in CCl_4 (75 cm^3) and cooled to 0°C. A slow stream of chlorine was passed through the suspension until no further reaction could be detected (approximately 1 h). The solvent was removed (15 mm/25°) and the yellow product sublimed (0.1mm/40°) onto a water cooled finger. Yield >90%.

$Mn(CO)_5Br$: A solution of bromine (0.60 g/3.75 mmol) in CCl_4 (40 cm^3) was added dropwise to a stirred suspension of $Mn_2(CO)_{10}$ (1.0 g/ 2.56 mmol) in CCl_4 (40 cm^3). After 1 h the solvent was taken off (15 mm/25°) and the residue washed with distilled water to remove $MnBr_2$ impurities. The orange product was sublimed twice (0.1 mm/ 60°) onto a water cooled finger. Yield >80%.

$Mn(CO)_5I$: $Mn_2(CO)_{10}$ (0.50 g/1.28 mmol) and iodine (0.33 g/1.30 mmol) were heated at 130°C for 1 h in a sealed tube. The red-orange crystalline product was isolated by vacuum sublimation (0.1 mm/ 40°) from the residue. Yield 82%.

$Re(CO)_5Cl$: A slow stream of chlorine was passed through a suspension of $Re_2(CO)_{10}$ (1.0 g/1.53 mmol) in CCl_4 (40 cm^3) for 1 h. The product, which precipitated during the reaction, was collected on a sinter in essentially quantitative yield, washed with CCl_4 and dried *in vacuo*.

$Re(CO)_5Br$: To a stirred suspension of $Re_2(CO)_{10}$ (1.0 g/1.53 mmol) in CCl_4 (40 cm^3) a solution of bromine (0.28 g/1.75 mmol) in CCl_4 (40 cm^3) was added slowly. The colourless product was filtered,

washed with more solvent and dried in vacuo. Yield >90%.

$Re(CO)_5I$: An evacuated glass tube containing $Re_2(CO)_{10}$ (0.50 g/ 0.77 mmol) and iodine (0.20 g/0.79 mmol) was sealed and maintained at 130°C for 16 h. The colourless crystalline product was isolated by sublimation (0.1 mm/80°) onto a water cooled finger. Yield 74%.

Dihalogenotetracarbonylmanganate(1) anions[210,211]

$Et_4N[Mn(CO)_4Cl_2]$: $Mn(CO)_5Cl$ (0.23 g/1 mmol) and Et_4NCl (0.17 g/ 1 mmol) were heated under reflux in CH_2Cl_2 (10 cm^3) for 1 h. n-Heptane (50 cm^3) was added to the hot filtered solution and the product allowed to crystallise at 0°C for several hours. Yellow crystals were isolated by filtration, washed with heptane and dried in vacuo.

$Et_4N[Mn(CO)_4Br_2]$: $Mn(CO)_5Br$ (0.28 g/1 mmol) and Et_4NBr (0.21 g/ 1 mmol) in absolute ethanol (10 cm^3) were maintained at 40°C for 1 h. The solvent was removed (15 mm/40°), the residue dissolved in CH_2Cl_2 (20 cm^3) and filtered. Heptane (100 cm^3) was added to the solution which was allowed to stand at 0°C for several hours. The product was collected on a sinter, washed with heptane and dried in vacuo.

$Et_4N[Mn(CO)_4I_2]$: This material was prepared in a similar manner to the bromo-analogue except that the reaction temperature employed was 55°.

All of the above anions were also produced with Ph_4P^+ and Ph_4As^+ as counter-ions by similar methods, although the yields were generally lower.

The identity and purity of all starting materials were confirmed by reference to their infrared spectra in the $\nu(CO)$ region and by comparison with authentic samples.

η^3-Allyltetracarbonylmanganese(I)[93,118]

A solution of $Mn_2(CO)_{10}$ (3.9 g/10 mmol) in tetrahydrofuran (100 cm^3) was purged with dry nitrogen gas and transferred to a glove box. Cleavage of the Mn-Mn bond was accomplished by the slow addition of $Li[Et_3BH]$ (30 cm^3 of a 1 M solution in THF) with stirring. After thirty minutes the required $[Mn(CO)_5]^-$ had formed according to the equation.

$$Mn_2(CO)_{10} + 2Li[Et_3BH] \longrightarrow 2Li[Mn(CO)_5] + 2Et_3B + H_2$$

To this solution nitrogen saturated allyl chloride (12.2 g/160 mmol) was added and stirred for a further ten minutes in the glove box. The reaction vessel was then stoppered, removed from the box and magnetically stirred under a stream of nitrogen for four hours until all the $[Mn(CO)_5]^-$ had been consumed (IR) according to the equation:

$$Li[Mn(CO)_5] + C_3H_5Cl \longrightarrow [(\eta^1\text{-}C_3H_5)Mn(CO)_5] + LiCl$$

Removal of the solvent (15 mm/20°C) followed by vacuum distillation (0.1 mm/30°C) afforded a yellow liquid $[(\eta^1\text{-}C_3H_5)Mn(CO)_5]$ which was usually converted immediately to the η^3-allyl derivative either by heating in a sealed tube (80°C/4 h) or by photolysing in n-pentane solution (75 cm^3/100 W Hg vapour lamp) in a conventional, water cooled, quartz photochemical reactor for four hours. The product $[(\eta^3\text{-}C_3H_5)Mn(CO)_4]$ was purified by vacuum sublimation on to a CO_2 cooled finger. Yield: 3.10 g, 75%, m.p. 56°C.

Infrared spectrum ν(CO) (n-pentane): 2072 m, 1997 vs, 1980 vs, 1964 vs.

^{1}H NMR spectrum ($CDCl_3$):

Chemical shift (δ ppm)	Coupling constant (Hz)
H(a); 4.75 (tt)	J_{ax} = 12.5
2H(m); 2.76 (dt)	J_{am} = 7.5
2H(x); 1.78 (dt)	$J_{mx} = J_{mx'}$ = 1.2

The spectral data agree well with those reported previously[102,118].

$[Re_2(CO)_8(PPh_3)_2]$[313]

A solution of $Re_2(CO)_{10}$ (0.90 g/1.4 mmol) and PPh_3 (1.08 g/4.1 mmol) in xylene (40 cm^3) was heated under reflux for 20 h. On cooling (-20°C, overnight) pale yellow crystals were separated, washed with xylene and dried *in vacuo*. Yield: 1.27 g, 82%.

Infrared spectra ν(CO);(decalin): 1988 w, 1962 s

(Nujol): 2000 w, 1980 w, 1970 vs, br

Fac-$[Re(CO)_3(PPh_3)_2Br]$[314,315]

A solution of $Re(CO)_5Br$ (0.20 g/0.5 mmol) and PPh_3 (0.26 g/1 mmol) were heated in refluxing light petroleum (100-120°C) - benzene (1:1) mixture (25 cm^3) for 2.5 h. On cooling and reducing the volume of solvent to *ca.* 10 cm^3 the colourless crystalline product was filtered off, washed with light petroleum and dried *in vacuo*. Yield: quantitative.

Infrared spectra, ν(CO); ($CHCl_3$): 2036 s, 1961 s, 1905 s

(Nujol): 2018 s, 1950 s, 1893 s

APPENDIX 3

A GROUP THEORETICAL TREATMENT OF SELECTED MOLECULES

Group theory has been extensively applied to metal carbonyl complexes in order to predict the number of infrared and Raman active vibrations expected for a given stereochemistry. The procedure which assigns a molecule to its point group and then examines the effect of symmetry operations on selected parameters is well documented[226-228] and will not be discussed further. In this appendix the reducible representations and their subsequent reduction for selected molecules is given. The parameters chosen for study are usually the displacement vectors associated with the vibrations of interest.

1. Tricarbonyl Complexes; $[MX(CO)_3L_2]$: C_s Symmetry

Both fac- and mer- isomers (Figure 2.1) belong to the C_s point group and the reducible representation for the $\nu(CO)$ vibrations in both cases is:-

C_s	E	σ_h
$\Gamma_{\nu(CO)}$	3	1

which on application of the formula $a_i(\Gamma_i) = \frac{1}{h}\sum\chi(R)\chi_i(R)n$ reduces to:

$\Gamma_{\nu(CO)} = 2A' + A''$, all modes are infrared and Raman active.

2. The Anion; $[M_2(CO)_6(\mu\text{-}X)_3]^-$: D_{3h} Symmetry

A total representation for the molecular motions of an isolated $[M_2(CO)_6(\mu\text{-}X)_3]^-$ anion (Figure 3.2) may be obtained using a set of 51 vectors (3 Cartesian coordinate vectors x, y and z for each of the N atoms; N = 17) as follows:

Since those atoms which are displaced under the operation of a

certain symmetry element, R, contribute zero to its character, $\chi(R)$, the derivation of $\chi(R)$ for most classes is straightforward. However the C_3 operator involves rotation through 120° and the derivation of $\chi(C_3)$, which is not so clear, is now outlined:
The C_3 operation displaces all but the two metal atoms and so the submatrix for each metal atom is:-

$2C_3$	x	y	z
x'	$\cos\theta$	$\sin\theta$	0
y'	$-\sin\theta$	$\cos\theta$	0
z'	0	0	1

$\theta = 120^\circ$; $\cos\theta = -\frac{1}{2}$

The character of any matrix is the sum of the leading diagonal and so in this case $\chi(C_3) = 0$. Thus the total representation is given by:-

$D_{3}h$	E	$2C_3$	$3C_2$	σ_h	$2S_3$	$3\sigma_v$
Γ_{3N}	51	0	-1	3	0	7

Γ_{3N} includes translational (Γ_{trans}) and rotational (Γ_{rot}) descriptions which must be subtracted to give the vibrational representation:-

D_{3h}	E	$2C_3$	$3C_2$	σ_h	$2S_3$	$3\sigma_v$
Γ_{3N}	51	0	-1	3	0	7
Γ_{trans}	3	0	-1	1	-2	1
Γ_{rot}	3	0	-1	-1	2	-1
Γ_{vib}	45	0	1	3	0	7

This is clearly a reducible representation which gives the following irreducible representations:-

$$\Gamma_{vib} = 6A_1' + 2A_2' + 8E' + 2A_1'' + 5A_2'' + 7E''$$

Since A_2' and A_1'' vibrations are both infrared- and Raman- inactive they will not be considered further.

A description of the stretching vibrations may be derived by using the vectors generated by the linear distortion of the inter-atomic bonds (Figure A3.1) as follows:

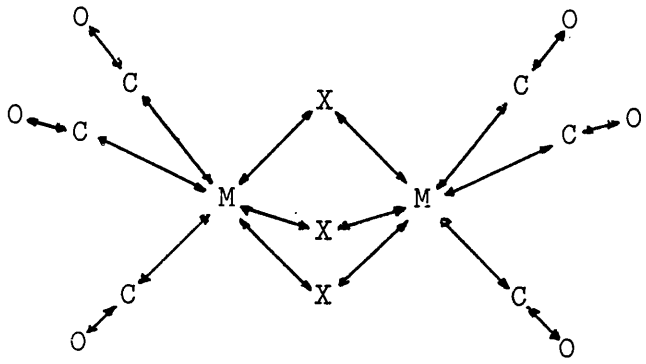

Figure A3.1: Linear distortion vectors for the D_{3h} anion

D_{3h}	E	$2C_3$	$3C_2$	σ_h	$2S_3$	$3\sigma_v$
$\Gamma_{\nu(CO)}$	6	0	0	0	0	2
$\Gamma_{\nu(MC)}$	6	0	0	0	0	2
$\Gamma_{\nu(MX)}$	6	0	0	0	0	2

These representations reduce to give:-

$$\Gamma_{\nu(CO)} = A_1' + E' + A_2'' + E'' \qquad (1)$$

$$\Gamma_{\nu(MC)} = A_1' + E' + A_2'' + E'' \qquad (2)$$

$$\Gamma_{\nu(MX)} = A_1' + E' + A_2'' + E'' \qquad (3)$$

For the δ(MCO) bending modes it is necessary to define two orthogonal angular distortion vectors for each MCO group (Figure A3.2).

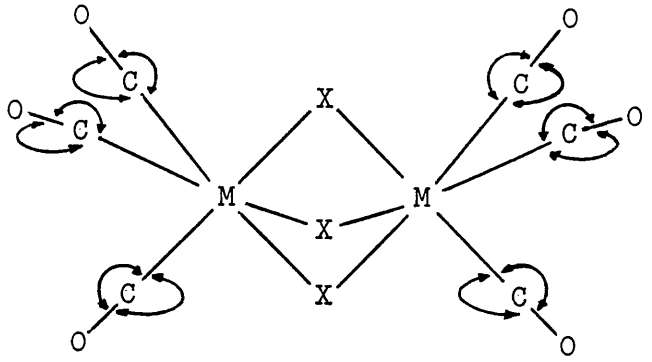

Figure A3.2: Angular distortion vectors for the D_{3h} anion

D_{3h}	E	$2C_3$	$3C_2$	σ_h	$2S_3$	$3\sigma_v$
$\Gamma_{\delta(MCO)}$	12	0	0	0	0	0

$\Gamma_{\delta(MCO)}$ reduces as follows:-

$$\Gamma_{\delta(MCO)} = A_1' + 2E' + A_2'' + 2E'' \qquad (4)$$

Independent descriptions for the skeletal deformations $\delta(XMX)$, $\delta(CMC)$ and $\delta(CMX)$ are difficult to ascertain, however an approximate representation of the $\delta(XMX)$ vibrations may be distinguished by considering the $[M_2(\mu\text{-}X)_3]$ unit in isolation (Figure A3.3):-

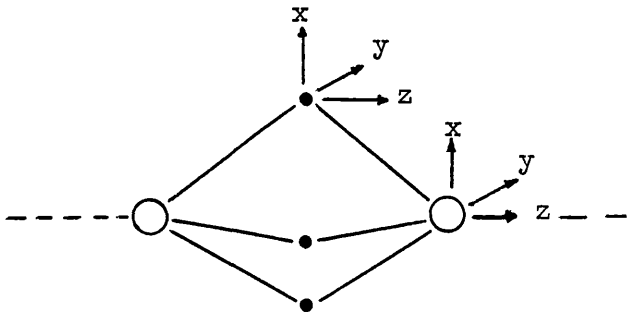

Figure A3.3: The $[M_2(\mu\text{-}X)_3]$ unit

The vibrational representation for this unit follows the same reasoning as for the complete molecule:-

D_{3h}	E	$2C_3$	$3C_2$	σ_h	$2S_3$	$3\sigma_v$
Γ_{3N}	15	0	-1	3	0	3
Γ_{trans}	3	0	-1	1	-2	1
Γ_{rot}	3	0	-1	-1	2	-1
Γ_{vib}	9	0	1	3	0	3

Thus $\Gamma_{vib} = 2A_1' + 2E' + A_2'' + E''$

This description includes the $\Gamma_{\nu(MX)}$ (3) representation already derived and so subtraction of these gives:-

$$\Gamma_{\delta(XMX)} = A_1' + E' \qquad (5)$$

If the vibrations accounted for in representations (1) - (5) are subtracted from the total Γ_{vib} then the remainder gives the skeletal vibrations δ(CMC) and δ(CMX):-

$$\left.\begin{matrix}\Gamma_{\delta(CMC)} \\ \Gamma_{\delta(CMX)}\end{matrix}\right\} = A_1' + 2E' + A_2'' + 2E''$$

3. The $[XM(CO)_5]$ Unit : C_{4v} Symmetry

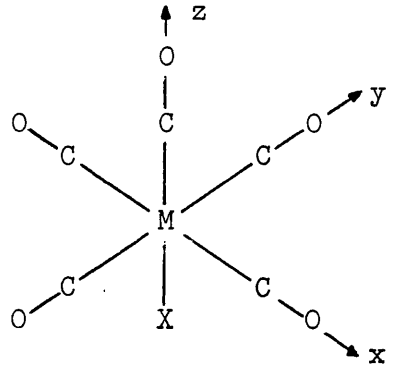

FigureA3.4: The $[XM(CO)_5]$ unit

An overall vibrational representation of the $[XM(CO)_5]$ unit may be derived as described in the preceding section by considering the effect of the C_{4v} symmetry operators on the 3 Cartesian coordinates

associated with each of the 12 atoms, thus:-

C_{4v}	E	$2C_4$	C_2	$2\sigma_v$	$2\sigma_d$
Γ_{3N}	36	4	-4	8	4
Γ_{trans}	3	1	-1	1	1
Γ_{rot}	3	1	-1	-1	-1
Γ_{vib}	30	2	-2	8	4

Reduction of Γ_{vib} gives the following result:-

$$\Gamma_{vib} = 7A_1 + A_2 + 4B_1 + 2B_2 + 8E$$

A_1 and E modes are both infrared and Raman active, B_1 and B_2 modes are Raman active only whilst the A_2 mode is formally inactive.

The vectors generated by the linear distortion of the CO and MC bonds give rise to the following descriptions for ν(CO), ν(MC) and ν(MX):-

C_{4v}	E	$2C_4$	C_2	$2\sigma_v$	$2\sigma_d$
$\Gamma_{\nu(tot)}$	11	3	3	7	3
$\Gamma_{\nu(CO)}$	5	1	1	3	1
$\Gamma_{\nu(MC)}$	5	1	1	3	1
$\Gamma_{\nu(MX)}$	1	1	1	1	1

These representations reduce to give:-

$$\Gamma_{\nu(CO)} = 2A_1 + B_1 + E$$
$$\Gamma_{\nu(MC)} = 2A_1 + B_1 + E$$
$$\Gamma_{\nu(MX)} = A_1$$

As pointed out previously the δ(MCO) vibrations are described by pairs of orthogonal angular distortion vectors (e.g. see Figure A3.2). Thus the reducible representation for the MCO deformations is

given by:-

C_{4v}	E	$2C_4$	C_2	$2\sigma_v$	$2\sigma_d$
$\Gamma_{\delta(MCO)}$	10	0	-2	0	0

Thus, $\Gamma_{\delta(MCO)} = A_1 + A_2 + B_1 + B_2 + 3E$

Figure A3.5 shows four of the eight vectors for the carbon-metal-carbon deformations, δ(CMC):-

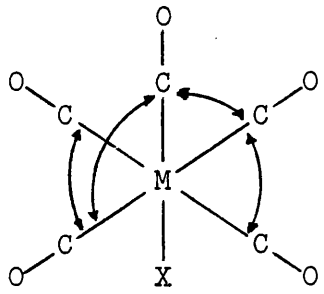

Figure A3.5: Vectors for the δ(CMC) vibrations

These vectors give rise to the reducible representation:-

C_{4v}	E	$2C_4$	C_2	$2\sigma_v$	$2\sigma_d$
$\Gamma_{\delta(CMC)}$	8	0	0	2	2

Thus, $\Gamma_{\delta(CMC)} = 2A_1 + B_1 + B_2 + 2E$

However in this reduction one of the A_1 modes corresponds to an impossible vibration (i.e. all angles increasing simultaneously) and is therefore redundant[228].

Finally the remaining E mode in Γ_{3N} must be due to the CMX deformation:-

$\Gamma_{\delta(CMX)} = E$

4. The η^1-Allyl Group: C_s Symmetry

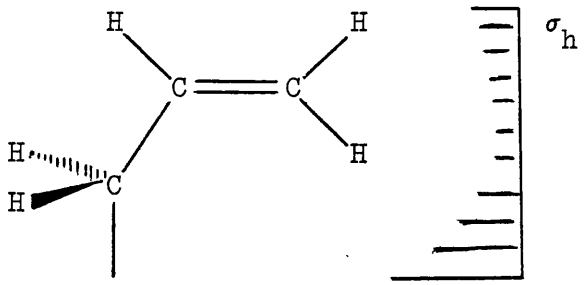

Figure A3.6: The η^1-allyl group with σ_h plane

The total representation for the η^1-allyl group is as follows:-

C_s	E	σ_h
Γ_{3N}	24	6
Γ_{trans}	3	1
Γ_{rot}	3	-1
Γ_{vib}	18	6

On reduction:- $\Gamma_{vib} = 12A' + 6A''$

The representation of the stretching vibrations, obtained in the usual way, reduces as follows:-

C_s	E	σ_h	
Γ_{str}	7	5	$= 6A' + A''$

Since A' modes are symmetric and A'' modes are asymmetric with respect to the σ_h plane the stretching descriptions follow by inspection:-

$\nu(=CH_2)$ 2A'

$\nu(-CH_2-)$ A' + A''

$\nu(=CH-)$ A'

$\nu(C=C)$ A'

$\nu(C-C)$ A'

The symmetric deformations are described by the vectors illustrated in FigureA3.7 (n.b. some redundancies are inevitable because all the angles cannot be deformed independently)

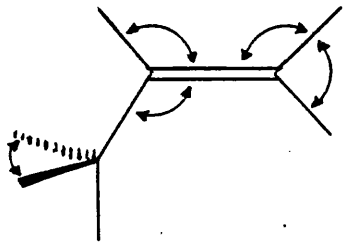

C_s	E	σ_h
Γ_{sym}	5	5

Figure A3.7: A representation for the symmetric deformations

Thus:- $\Gamma_{sym} = 5A'$

Approximate descriptions of these modes are:-

δ(scissors)(=CH_2)	A'
ρ(rock)(=CH_2)	A'
ρ(rock)(=CH-)	A'
δ(scissors)(-CH_2-)	A'
δ(in-plane)(C-C=C)	A'

The remaining vibrations are described by the vectors shown in Figure A3.8.

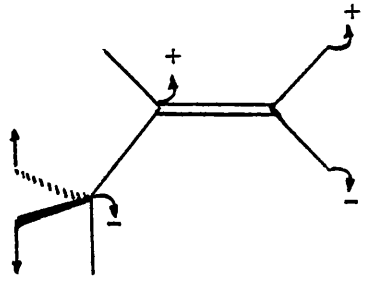

C_s	E	σ_h
Γ_{asym}	6	-4

Figure A3.8: A representation for the asymmetric deformations

Thus:- $\Gamma_{asym} = A' + 5A''$

Again only approximate descriptions of these vibrations can be suggested as follows:-

ρ(twist)(=CH_2)	A"
ρ(wag)(=CH_2)	A"
ρ(wag)(-CH_2-)	A'
ρ(twist)(-CH_2-)	A"
ρ(rock)(-CH_2)	A"
π(out-of-plane)(CCHC)	A"

5. The η^3-Allyl-Metal System: C_s Symmetry

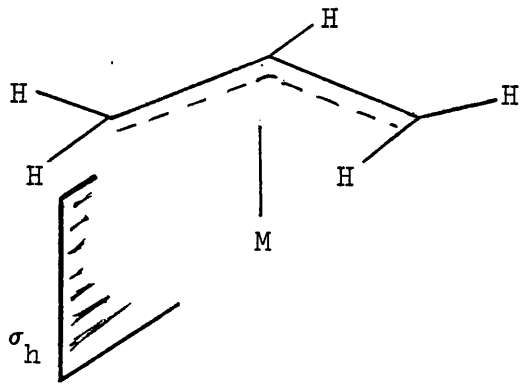

Figure A3.9: The η^3-allyl group with σ_h plane

The total representation for the planar allyl group alone is:-

C_s	E	σ_h
Γ_{3N}	24	2
Γ_{trans}	3	1
Γ_{rot}	3	-1
Γ_{vib}	18	2

On reduction:- Γ_{vib} = 10A' + 8A"

These modes may be represented by appropriate vectors in much the same manner as the preceding η^1-allyl system thus arriving at the approximate descriptions of the vibrations given in Table 1.4. If the metal atom is included in Γ_{3N} then the vibrational description becomes:- Γ_{vib} = 12A' + 9A" Clearly this description

now includes the three allyl-metal vibrations $\nu_s(A')$, $\nu_t(A')$ and $\nu_t(A'')$ (depicted on page 25).

6. The CH_3M Unit: C_{3v} Symmetry

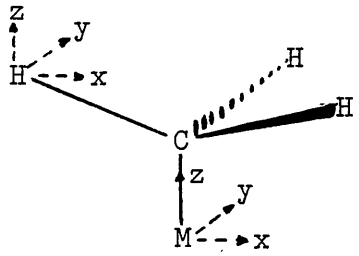

Figure A3.10: The CH_3M unit

A total representation of the unit shown in Figure A3.10 and its subsequent reduction according to the usual procedure is summarised in the table below:-

C_{3v}	E	$2C_3$	$3\sigma_v$
Γ_{3N}	15	0	3
Γ_{trans}	3	0	1
Γ_{rot}	3	0	-1
Γ_{vib}	9	0	3
$\Gamma_{\nu(CH_3)}$	3	0	1
$\Gamma_{\nu(MC)}$	1	1	1
Γ_{def}	5	-1	1

On reduction:- $\Gamma_{vib} = 3A_1 + 3E$

$\Gamma_{\nu(CH_3)} = A_1 + E$

$\Gamma_{\nu(MC)} = A_1$

$\Gamma_{def} = A_1 + 2E$

APPENDIX 4

THE SOLUTION OF SECULAR EQUATIONS

The procedure for the derivation of secular equations which describe the relationships between vibrational frequencies and sets of stretching and interaction parameters is treated in detail in several texts[232,233]. In this appendix the equations are stated and the mathematical manipulations necessary for their solution are presented.

n.b. throughout the following discussion:

$\lambda_i = 5.8915 \times 10^{-7}(\nu_i)^2$

$\mu = (M(C) + M(O))/(M(C) \times M(O)) = 0.1457583$

1. Fac-Tricarbonyls: C_s Symmetry

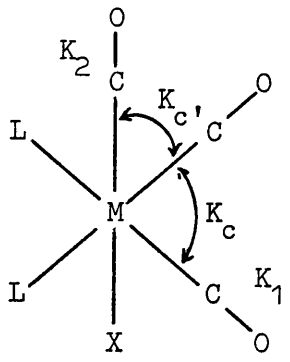

$$2A': \begin{vmatrix} K_2 - \lambda/\mu & \sqrt{2}K_{c'} \\ \sqrt{2}K_{c'} & K_1 - \lambda/\mu + K_c \end{vmatrix} = 0$$

$$A'': \quad K_1 = \lambda/\mu + K_c$$

Figure A4.1: Parameters and secular equations for fac-$[M(CO)_3L_2X]$

Let $\lambda(A'_1)/\mu = X$,

$\lambda(A'_2)/\mu = Y$,

$\lambda(A'')/\mu = Z$,

and $K_{c'} = K_c/\delta$.

Thus: $(K_2 - X)(K_1 - X + K_c) - 2K_{c'}^2 = 0$ (1)

$(K_2 - Y)(K_1 - Y + K_c) - 2K_{c'}^2 = 0$ (2)

$K_1 = Z + K_c$ (3)

Substitute in (1) and (2) for K_1 and K_c':

$$(K_2 - X)(Z + 2K_c - X) - 2K_c^2/\delta^2 = 0 \qquad (4)$$

$$(K_2 - Y)(Z + 2K_c - Y) - 2K_c^2/\delta^2 = 0 \qquad (5)$$

Subtract (5) from (4):

$$K_2(Y - X) + Y(Z + 2K_c - Y) - X(Z + 2K_c - X) = 0 \qquad (6)$$

Rearranging:

$$(Y - X)K_2 + (Y - X)(Z + 2K_c) - Y^2 + X^2 = 0$$

$$(Y - X)K_2 + (Y - X)(Z + 2K_c) - (Y - X)(Y + X) = 0$$

Thus: $K_2 = X + Y - Z - 2K_c \qquad (7)$

Combining (4) and (7):

$$(Y - Z - 2K_c)(Z + 2K_c - X) - 2K_c^2/\delta^2 = 0$$

Rearranging:

$$(4 + 2/\delta)K_c^2 - 2(X + Y - 2Z)K_c + (X - Z)(Y - Z) = 0 \qquad (8)$$

Equation (8) is a quadratic in K_c, the solution of which is given by:

$$K_c = \frac{2(X + Y - 2Z) \pm \sqrt{[2(X + Y - 2Z)]^2 - 4(4 + 2/\delta)(X - Z)(Y - Z)}}{2(4 + 2/\delta)}$$

The remaining constants follow:

$$K_c' = K_c/\delta$$

$$K_1 = K_c + Z$$

$$K_2 = X + Y - Z - 2K_c$$

In the method of Dalton et al.[220] the value of δ is estimated from maximum orbital overlap considerations and is calculated from the equation:

$$\delta = (X + Y - 2Z)/\ 2(X - Y)$$

Also a 'best fit' solution may be obtained by an iterative procedure where δ is varied between certain limits. Alternatively the problem may be reduced to that of the C-K approximation by putting $K_{c'} = K_c$, thus making $\delta = 1$.

2. Square Pyramidal Pentacarbonyls: C_{4v} Symmetry

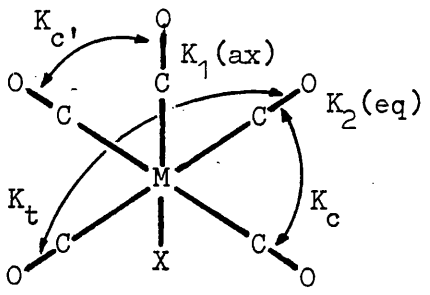

Figure A4.2: Force field for square pyramidal $[M(CO)_5]$

Using three infrared frequencies to fix five parameters (Figure A4.2) results in an undetermined force field with two degrees of freedom. These are removed by imposing the two constraints of the Cotton-Kraihanzel method, namely:-

$$K_c \cong K_{c'} = K_i$$

$$K_t = 2K_c$$

In this case the secular equations are:-

$$2A_1: \quad \begin{vmatrix} K_1 - \lambda/\mu & 2K_i \\ 2K_i & K_2 + 4K_i - \lambda/\mu \end{vmatrix} = 0$$

B_1: $K_2 = \lambda/\mu$ (redundant)

E : $K_2 - 2K_i = \lambda/\mu$

Let; $\lambda_{A_1(1)}/\mu = W$

$\lambda_E/\mu = Y$

$\lambda_{A_1(2)}/\mu = Z$

rearranging the secular determinants gives:

$$(K_1 - W)(K_2 + 4K_i - W) - 4K_i^2 = 0 \qquad (1)$$

$$(K_1 - Z)(K_2 + 4K_i - Z) - 4K_i^2 = 0 \qquad (2)$$

$$K_2 = Y + 2K_i \qquad (3)$$

Subtraction of (2) from (1) and substitution of (3) gives the result:-

$$K_1 = W + Z - Y - 6K_i \qquad (4)$$

K_1 may be eliminated from (1) and (2) by multiplying each by the other's coefficients of K_1 and subtracting thus:-

$$(K_2 + 4K_i - W)(Z)(K_2 + 4K_i - Z) + 4K_i^2(K_2 + 4K_i - W)$$
$$- (K_2 + 4K_i - Z)(W)(K_2 + 4K_i - W) - 4K_i^2(K_2 + 4K_i - Z) = 0$$

Substituting (3) for K_2 gives:-

$$(6K_i - W + Y)(Z)(6K_i - Z + Y) + 4K_i^2(6K_i - W + Y)$$
$$- (6K_i - Z + Y)(W)(6K_i - W + Y) - 4K_i^2(6K_i - Z + Y) = 0$$

Expanding:

$$(36K_i^2Z - 36K_i^2W + 4K_i^2Z - 4K_i^2W) + (-6K_iZ^2 + 6K_iYZ + 6K_iYZ + 6K_iW^2$$
$$-6K_iYW - 6K_iYW) + (WZ^2 - YZ^2 + Y^2Z - W^2Z + W^2Y - Y^2W) = 0$$

Rearranging and factorising (Z - W) gives:-

$$40K_i^2 - 6K_i(W + Z - 2Y) + (Y - W)(Y - Z) = 0 \qquad (5),$$

a quadratic equation in K_i which may be solved to give two roots, only one of which is likely to make 'chemical sense'.

If the B_1 mode is detected then a further check is obtained by calculating its position using K_1, K_2 and K_i thus:-

$$\nu_{B_1}(\text{calc}) = \sqrt{\frac{(Y + 2K_i)\mu}{5.8915 \times 10^{-7}}}$$

The three C-K force constants are summarised below:-

$$K_i = \frac{6(W + Z - 2Y) \pm \sqrt{[6(W + Z - 2Y)]^2 - 160(Y - W)(Y - Z)}}{80}$$

$$K_1 = W + Z - Y - 6K_i$$

$$K_2 = Y + 2K_i$$

APPENDIX 5

COMPUTER PROGRAMMES

1. Force Constant Calculation for Tricarbonyls of Fac-C_s Symmetry

```
      $JOB            BCC3DLP5W                                        .WHITE J W
      C      THIS PROGRAM CALCULATES  C-K FORCE CONSTANTS FOR  TRICARBONYLS OF
      C      CS SYMMETRY USING THE MAX ORBITAL OVERLAP APPROXIMATION
      C          THE A' MODE IS REPRESENTED BY V(1)
      C          THE A' MODE IS REPRESENTED BY V(2)
      C          THE A" MODE IS REPRESENTED BY V(3)
 1          REAL INTK(9),K(9),L(9),M,V(9)
 2          M=0.14583
 3          F=5.8915/(10.0**7)
 4          WRITE(6,600)
 5        600 FORMAT(1H1,T10,'SAMPLE',T22,'V(1)',T33,'V(2)',T44,'V(3)',T66,'K(1)
           2',T77,'K(2)',T86,'INTK(1)',T96,'INTK(2)',T107,'DELTA')
 6          WRITE(6,610)
 7        610 FORMAT(1H ,T22,'FREQUENCY IN WAVENUMBERS 1/CM',T71,'MILLIDYNES PER
           2 ANGSTROM UNIT',/)
 8          READ,N
 9          DO 80 I=1,N
10          READ,V(1),V(2),V(3)
11          L(1)=F*V(1)*V(1)
12          L(2)=F*V(2)*V(2)
13          L(3)=F*V(3)*V(3)
14          D=(L(1)+L(2)-2.0*L(3))/((L(1)-L(2))*SQRT(2.0))
15          A=4.0+2.0/(D*D)
16          B=2.0*(L(2)+L(1)-2.0*L(3))/M
17          C=(L(1)-L(3))*(L(2)-L(3))/(M*M)
18          E=B*B-4.0*A*C
19          IF(E)70,72,72
20         72 INTK(1)=(B+SQRT(E))/(2.0*A)
21          INTK(2)=(B-SQRT(E))/(2.0*A)
22          GOTO 75
23         70 WRITE(6,710)I
24        710 FORMAT(1HO,'FOR SAMPLE',I2,'INTK(2) IS NON REAL')
25          PRINT,E
26          INTK(1)=0.0
27          INTK(2)=0.0
28         75 CONTINUE
29          INTK(3)=INTK(1)/D
30          INTK(4)=INTK(2)/D
31          K(1)=L(3)/M+INTK(1)
32          K(2)=(L(2)+L(1)-L(3))/M-2.0*INTK(1)
33          K(3)=L(3)/M+INTK(2)
34          K(4)=(L(2)+L(1)-L(3))/M-2.0*INTK(2)
35          WRITE(6,700)I,V(1),V(2),V(3),K(1),K(2),INTK(1),INTK(3),D
36         80 WRITE(6,700)I,V(1),V(2),V(3),K(3),K(4),INTK(2),INTK(4),D
37        700 FORMAT(1HO,T12,I2,2X,3(4X,F7.1),T60,2(4X,F7.3),2(4X,F6.3),4X,F5.2)
38          STOP
39          END
```

2. Force Constant Calculation for Pentacarbonyls of C_{4v} Symmetry

```
      $JOB            BCCJDLP?W                                          WHITE J W
      C      PROGRAM FOR C4V PENTACARBONYLS RM(CO)5 BY THE C-K METHOD
      C      THE A1(1) MODE IS REPRESENTED BY V(1)
      C      THE B1(1) MODE IS REPRESENTED BY V(2)
      C      THE E     MODE IS REPRESENTED BY V(3)
      C      THE A1(2) MODE IS REPRESENTED BY V(4)
      C      THE B1 MODE IS REDUNDANT IN THIS CALCULATION BUT IS USED TO CHECK V(2)
    1         REAL INTK(2),K(9),L(9),M,V(9),CHK(9)
    2         M=0.1457583
    3         F=5.8915/(10.0**7)
    4         G=F/M
    5         WRITE(6,600)
    6       600 FORMAT(1H1,T10,'SAMPLE',T22,'V(1)',T33'V(2)',T44'V(3)',T55,'V(4)',
             1T62,'CHECK(V(2))',T81,'K(1)',T92,'K(2)',T100,'INTK')
    7         WRITE(6,610)
    8       610 FORMAT(1H0,T26,'FREQUENCY IN WAVENUMBERS 1/CM',T81,'MILLIDYNES PER
             1 ANGSTROM UNIT',/)
    9         READ,N
   10         DO 10 I=1,N
   11         READ,V(1),V(2),V(3),V(4)
   12         W=G*V(1)*V(1)
   13         Y=G*V(3)*V(3)
   14         Z=G*V(4)*V(4)
   15         A=40.0
   16         B=6.0*(W+Z-2.0*Y)
   17         C=(Y-W)*(Y-Z)
   18         D=B*B-4.0*A*C
   19         IF(D)20,30,30
   20        30 INTK(1)=(B+SQRT(D))/(2.0*A)
   21         INTK(2)=(B-SQRT(D))/(2.0*A)
   22         K(1)=W+Z-Y-6.0*INTK(1)
   23         K(2)=Y+2.0*INTK(1)
   24         K(3)=W+Z-Y-6.0*INTK(2)
   25         K(4)=Y+2.0*INTK(2)
   26         R=((Y+2.0*INTK(1)))/G
   27         S=((Y+2.0*INTK(2)))/G
   28         IF(R)50,60,60
   29        60 CHK(1)=SQRT(R)
   30         GO TO 80
   31        50 WRITE(6,640)I
   32       640 FORMAT(1H0,'FOR SAMPLE',I2,'CHK(1) IS NON REAL')
   33        80 CONTINUE
   34         IF(S)90,70,70
   35        70 CHK(2)=SQRT(S)
   36         GO TO 100
   37        90 WRITE(6,650)I
   38       650 FORMAT(1H0,'FOR SAMPLE',I2,'CHK(2) IS NON REAL')
   39       100 CONTINUE
   40         GO TO 40
   41        20 WRITE(6,620)I
   42       620 FORMAT(1H0,'FOR SAMPLE',I2,'INTK IS NON REAL')
   43        40 CONTINUE
   44         WRITE(6,630)I,V(1),V(2),V(3),V(4),CHK(1),K(1),K(2),INTK(1)
   45        10 WRITE(6,630)I,V(1),V(2),V(3),V(4),CHK(2),K(3),K(4),INTK(2)
   46       630 FORMAT(1H0,T12,I2,2X,5(4X,F7.1),T77,2(4X,F7.3),(4X,F6.3))
   47         STOP
   48         END
```

APPENDIX 6

CALCULATED AND OBSERVED STRUCTURE FACTORS AND THERMAL PARAMETERS

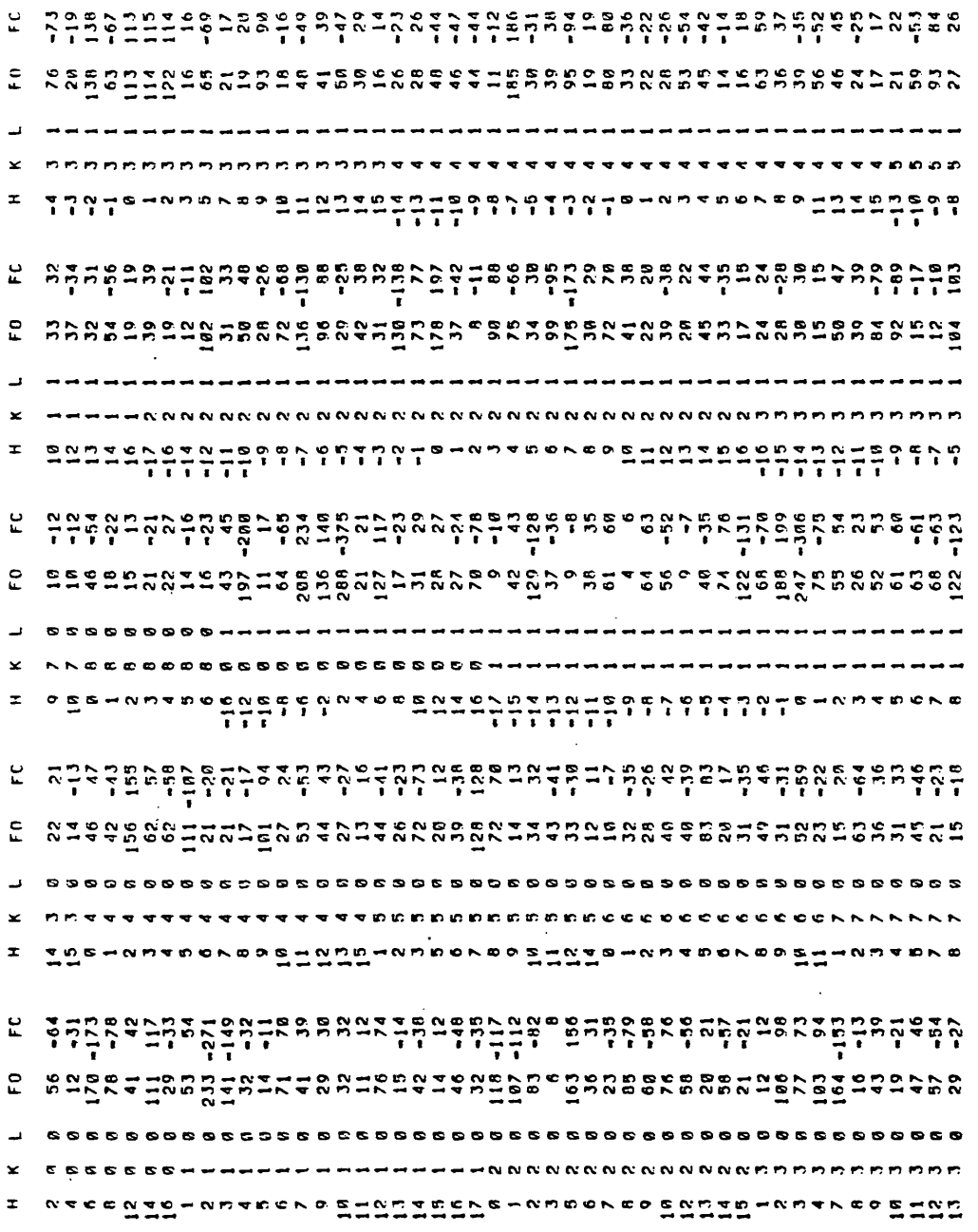

H	K	L	FO	FC	H	K	L	FO	FC	H	K	L	FO	FC	H	K	L	FO	FC	H	K	L	FO	FC	H	K	L	FO	FC
-7	5	1	40	-39	-9	7	1	12	-12	-9	1	2	63	-59	8	2	2	87	89	2	4	2	14	11	9	6	2	17	18
-6	5	1	63	61	-7	7	1	27	25	-8	1	2	75	-69	9	2	2	61	60	3	4	2	50	-48	10	6	2	40	38
-5	5	1	166	-163	-5	7	1	23	22	-7	1	2	12	14	10	2	2	56	-56	4	4	2	5	10	-10	7	2	14	-15
-4	5	1	79	-71	-4	7	1	36	36	-6	1	2	82	84	11	2	2	25	-24	5	4	2	66	61	-9	7	2	20	20
-3	5	1	17	14	-3	7	1	33	32	-5	1	2	72	80	12	2	2	35	35	6	4	2	24	-21	-8	7	2	28	-28
-2	5	1	16	-11	-2	7	1	20	16	-4	1	2	190	196	13	2	2	38	-38	7	4	2	51	-48	-6	7	2	13	11
-1	5	1	44	46	-1	7	1	37	-38	-3	1	2	27	-28	14	2	2	47	46	8	4	2	32	-34	-5	7	2	27	-26
0	5	1	14	-14	0	7	1	66	-62	-2	1	2	12	-9	-14	3	2	57	-55	9	4	2	68	-62	-2	7	2	45	-43
1	5	1	18	19	2	7	1	19	18	-1	1	2	102	95	-13	3	2	28	28	10	4	2	28	-29	-1	7	2	11	-12
2	5	1	28	-26	4	7	1	67	71	0	1	2	89	89	-12	3	2	32	-34	11	4	2	40	36	0	7	2	13	13
3	5	1	7	-5	5	7	1	17	-17	1	1	2	142	-140	-11	3	2	72	-70	12	4	2	9	-7	1	7	2	50	51
4	5	1	32	31	6	7	1	21	-23	2	1	2	55	54	-10	3	2	65	-61	13	4	2	61	61	2	7	2	64	67
5	5	1	51	50	7	7	1	36	38	3	1	2	87	85	-9	3	2	23	-20	-13	5	2	13	-12	3	7	2	8	-9
6	5	1	15	-13	10	7	1	13	17	4	1	2	71	-72	-8	3	2	73	74	-10	5	2	7	-5	4	7	2	30	-28
7	5	1	31	-30	-7	8	1	28	28	5	1	2	5	-1	-7	3	2	123	120	-8	5	2	46	44	5	7	2	16	18
8	5	1	25	24	-4	8	1	9	10	6	1	2	121	-121	-5	3	2	8	-9	-7	5	2	67	-66	6	7	2	55	-61
9	5	1	81	-75	-2	8	1	35	-38	7	1	2	55	-50	-4	3	2	49	-48	-5	5	2	25	26	8	7	2	12	12
10	5	1	83	-77	-1	8	1	30	-31	8	1	2	69	66	-3	3	2	96	-98	-4	5	2	15	-17	-7	8	2	17	-12
11	5	1	36	33	1	8	1	11	-14	9	1	2	77	71	-2	3	2	42	41	-3	5	2	116	116	-4	8	2	9	-11
12	5	1	11	-11	2	8	1	53	56	11	1	2	19	-21	-1	3	2	81	83	-2	5	2	121	122	0	8	2	34	35
13	5	1	33	31	3	8	1	11	13	12	1	2	19	-17	0	3	2	115	-111	-1	5	2	83	-81	1	8	2	11	10
-13	6	1	8	12	4	8	1	16	-17	13	1	2	25	26	1	3	2	106	106	0	5	2	17	-16	2	8	2	14	-13
-12	6	1	18	-15	5	8	1	16	17	14	1	2	25	23	2	3	2	38	-33	1	5	2	39	-36	3	8	2	15	16
-11	6	1	23	16	6	8	1	17	-20	15	1	2	39	-40	3	3	2	52	-49	3	5	2	22	20	4	8	2	44	-53
-10	6	1	21	21	-16	0	2	24	29	16	1	2	49	50	4	3	2	11	-9	5	5	2	11	-13	5	8	2	17	-18
-9	6	1	62	-59	-14	0	2	135	-134	-16	2	2	22	21	6	3	2	16	17	7	5	2	41	-43	6	8	2	18	18
-8	6	1	61	56	-12	0	2	85	83	-15	2	2	59	-57	7	3	2	52	51	8	5	2	20	-18	-16	0	3	29	33
-7	6	1	50	-43	-10	0	2	113	121	-14	2	2	27	28	8	3	2	17	-18	9	5	2	16	15	-14	0	3	16	-22
-6	6	1	58	-54	-8	0	2	81	-76	-13	2	2	25	25	9	3	2	66	-62	10	5	2	20	-19	-12	0	3	144	141
-5	6	1	24	-20	-4	0	2	66	-71	-11	2	2	23	-21	10	3	2	16	-16	11	5	2	75	71	-10	0	3	112	-108
-4	6	1	42	-43	-2	0	2	18	-16	-10	2	2	36	-38	11	3	2	47	-44	12	5	2	49	48	-8	0	3	119	-122
-3	6	1	72	72	0	0	2	111	-109	-9	2	2	45	-49	12	3	2	44	43	13	5	2	33	-32	-6	0	3	140	135
-2	6	1	75	74	2	0	2	70	74	-8	2	2	29	28	13	3	2	32	30	-12	6	2	13	-13	-4	0	3	17	8
-1	6	1	30	30	4	0	2	53	60	-7	2	2	50	49	14	3	2	23	-23	-10	6	2	15	16	-2	0	3	35	-34
0	6	1	23	-22	6	0	2	72	-68	-6	2	2	181	184	15	3	2	33	34	-9	6	2	32	-32	0	0	3	112	118
1	6	1	64	-65	8	0	2	87	-85	-5	2	2	164	167	-15	4	2	22	24	-7	6	2	87	86	2	0	3	245	258
2	6	1	9	8	10	0	2	21	22	-4	2	2	156	-153	-11	4	2	48	-45	-6	6	2	46	-43	4	0	3	42	-39
3	6	1	50	52	12	0	2	38	-39	-3	2	2	116	-117	-10	4	2	15	16	-4	6	2	72	71	6	0	3	101	-104
4	6	1	14	13	14	0	2	35	-33	-2	2	2	147	-158	-9	4	2	38	38	-3	6	2	11	-11	8	0	3	63	64
5	6	1	51	-49	16	0	2	8	-8	-1	2	2	47	-48	-7	4	2	43	44	-2	6	2	9	9	10	0	3	36	-36
6	6	1	40	39	-17	1	2	21	23	0	2	2	50	54	-6	4	2	20	-18	-1	6	2	93	-93	12	0	3	13	14
7	6	1	29	-29	-16	1	2	10	-10	1	2	2	86	-91	-5	4	2	143	-145	0	6	2	58	-57	14	0	3	23	24
8	6	1	32	-33	-15	1	2	20	19	2	2	2	55	-58	-4	4	2	34	-32	2	6	2	55	53	-17	1	3	8	9
9	6	1	14	12	-14	1	2	30	31	3	2	2	79	71	-3	4	2	86	82	3	6	2	51	49	-16	1	3	34	-37
10	6	1	18	-20	-13	1	2	70	-68	4	2	2	42	36	-2	4	2	49	-49	4	6	2	32	33	-15	1	3	40	-43
11	6	1	32	39	-12	1	2	134	131	5	2	2	27	-30	-1	4	2	92	90	5	6	2	18	-17	-14	1	3	22	23
12	6	1	31	29	-11	1	2	63	63	6	2	2	75	74	0	4	2	29	30	7	6	2	56	58	-13	1	3	12	-12
-10	7	1	32	34	-10	1	2	63	-61	7	2	2	72	71	1	4	2	84	-87	8	6	2	41	-44	-12	1	3	61	-56

H	K	L	FO	FC	H	K	L	FO	FC	H	K	L	FO	FC	H	K	L	FO	FC
-11	1	3	71	67	10	2	3	34	-32	2	4	3	11	-17	10	6	3	15	16
-10	1	3	45	-45	11	2	3	19	-18	3	4	3	60	59	-10	7	3	45	-42
-9	1	3	29	-29	12	2	3	49	49	4	4	3	16	15	-9	7	3	17	19
-8	1	3	103	97	13	2	3	19	18	7	4	3	30	-29	-7	7	3	35	-34
-7	1	3	120	113	14	2	3	12	-11	10	4	3	18	17	-6	7	3	20	18
-6	1	3	187	207	15	2	3	15	16	11	4	3	63	61	-5	7	3	7	10
-4	1	3	150	-158	-15	3	3	42	42	12	4	3	19	20	-4	7	3	20	-22
-3	1	3	167	-159	-13	3	3	28	-30	13	4	3	47	-45	-2	7	3	9	11
-1	1	3	32	-28	-12	3	3	51	54	-14	5	3	31	-31	-1	7	3	35	35
0	1	3	40	-37	-11	3	3	41	-40	-13	5	3	12	12	0	7	3	21	19
1	1	3	21	-22	-10	3	3	25	23	-11	5	3	16	17	2	7	3	20	-20
2	1	3	22	-30	-9	3	3	51	44	-8	5	3	55	55	4	7	3	70	-74
3	1	3	149	143	-8	3	3	8	-7	-7	5	3	42	42	6	7	3	38	37
4	1	3	104	-99	-7	3	3	19	19	-6	5	3	26	-27	7	7	3	15	-13
5	1	3	67	-67	-6	3	3	81	-78	-5	5	3	62	59	8	7	3	12	15
6	1	3	94	92	-5	3	3	113	-110	-4	5	3	56	57	-6	8	3	20	-20
7	1	3	18	20	-4	3	3	12	-13	-3	5	3	39	-37	-5	8	3	8	6
8	1	3	63	63	-3	3	3	57	58	-2	5	3	32	-29	-2	8	3	15	18
10	1	3	31	-30	-2	3	3	14	12	-1	5	3	135	-134	0	8	3	10	-14
11	1	3	37	-34	-1	3	3	96	92	0	5	3	86	-81	2	8	3	29	-31
12	1	3	21	20	0	3	3	46	-45	1	5	3	69	66	3	8	3	15	-12
13	1	3	21	22	1	3	3	38	-35	2	5	3	10	11	4	8	3	15	15
14	1	3	20	21	3	3	3	22	-17	3	5	3	8	-9	-16	0	4	18	-23
-17	2	3	37	-36	4	3	3	28	25	4	5	3	12	11	-14	0	4	41	-45
-16	2	3	27	25	5	3	3	62	62	6	5	3	20	21	-12	0	4	11	-13
-15	2	3	10	-11	6	3	3	18	-16	7	5	3	18	19	-10	0	4	153	-163
-14	2	3	69	-65	7	3	3	56	-53	8	5	3	7	9	-8	0	4	77	80
-13	2	3	81	79	9	3	3	64	-62	9	5	3	43	47	-6	0	4	157	153
-12	2	3	16	-23	11	3	3	31	28	10	5	3	17	20	-4	0	4	22	-24
-11	2	3	50	-50	12	3	3	21	16	11	5	3	13	-12	-2	0	4	58	56
-10	2	3	20	22	13	3	3	42	42	12	5	3	17	14	4	0	4	152	-162
-8	2	3	38	39	14	3	3	32	-33	-11	6	3	24	-23	6	0	4	107	102
-7	2	3	52	55	-15	4	3	47	-49	-9	6	3	9	-11	8	0	4	93	94
-6	2	3	57	-59	-14	4	3	31	33	-8	6	3	21	-22	10	0	4	85	-86
-5	2	3	115	-109	-13	4	3	17	-15	-7	6	3	10	11	12	0	4	19	20
-4	2	3	186	-191	-12	4	3	26	-26	-5	6	3	72	-70	14	0	4	14	-16
-3	2	3	91	-86	-11	4	3	21	22	-4	6	3	31	29	-16	1	4	16	17
-1	2	3	78	84	-9	4	3	42	39	-3	6	3	27	-26	-14	1	4	11	-11
0	2	3	52	-55	-8	4	3	21	-22	-2	6	3	78	-81	-13	1	4	63	63
1	2	3	130	128	-7	4	3	18	-19	-1	6	3	34	34	-12	1	4	52	-53
2	2	3	16	-12	-6	4	3	37	33	0	6	3	22	26	-11	1	4	18	-20
3	2	3	54	-56	-5	4	3	6	8	1	6	3	77	75	-10	1	4	33	35
4	2	3	6	6	-4	4	3	60	61	2	6	3	23	22	-9	1	4	58	-65
5	2	3	32	30	-3	4	3	100	102	3	6	3	7	-5	-8	1	4	80	82
6	2	3	21	22	-2	4	3	36	33	4	6	3	7	-26	-7	1	4	36	34
7	2	3	33	37	-1	4	3	54	-72	6	6	3	37	-40	-6	1	4	72	-75
8	2	3	42	-43	0	4	3	53	57	7	6	3	19	21	-5	1	4	101	-99
9	2	3	57	-54	1	4	3	64	-67	9	6	3	38	-42	-4	1	4	74	-72

H	K	L	FO	FC	H	K	L	FO	FC
-3	4	5	77	-77	-1	7	5	10	11
-1	4	5	60	57	0	7	5	29	-25
1	4	5	63	61	1	7	5	23	26
2	4	5	10	6	3	7	5	15	16
3	4	5	105	-107	4	7	5	25	26
4	4	5	24	23	-16	0	6	18	24
5	4	5	6	8	-12	0	6	13	-12
7	4	5	15	14	-10	0	6	67	69
8	4	5	31	-32	-8	0	6	69	-72
9	4	5	33	-33	-2	0	6	24	22
10	4	5	20	-25	0	0	6	65	-70
-13	5	5	39	-41	2	0	6	59	58
-12	5	5	20	-19	4	0	6	24	-22
-10	5	5	12	-11	8	0	6	33	-31
-8	5	5	23	22	10	0	6	51	53
-6	5	5	12	-9	-15	1	6	27	-29
-4	5	5	13	14	-13	1	6	14	16
-3	5	5	21	21	-12	1	6	12	13
-2	5	5	14	-11	-11	1	6	13	-16
-1	5	5	63	67	-10	1	6	18	-19
0	5	5	81	80	-9	1	6	46	53
1	5	5	112	-112	-7	1	6	30	-35
2	5	5	9	-12	-6	1	6	123	120
3	5	5	21	-19	-5	1	6	18	22
4	5	5	23	-25	-4	1	6	61	65
5	5	5	18	32	-3	1	6	12	12
6	5	5	17	16	-2	1	6	104	-97
7	5	5	12	16	-1	1	6	107	-98
8	5	5	28	-32	0	1	6	45	-42
-11	6	5	14	15	1	1	6	53	48
-10	6	5	21	21	3	1	6	13	14
-9	6	5	30	30	4	1	6	43	-39
-8	6	5	32	-33	5	1	6	47	48
-5	6	5	31	34	6	1	6	22	20
-4	6	5	10	-12	8	1	6	54	51
-2	6	5	52	50	9	1	6	37	-34
-1	6	5	68	-68	10	1	6	34	33
0	6	5	24	24	11	1	6	19	18
1	6	5	12	-14	-15	2	6	10	-15
3	6	5	20	18	-14	2	6	23	22
4	6	5	45	41	-13	2	6	21	20
5	6	5	61	65	-12	2	6	20	-23
-8	7	5	32	-32	-11	2	6	36	36
-7	7	5	21	-18	-10	2	6	48	-48
-6	7	5	25	-25	-9	2	6	67	-66
-5	7	5	9	7	-8	2	6	50	51
-4	7	5	55	54	-5	2	6	31	30
-3	7	5	27	-28	-4	2	6	27	-27

H	K	L	FO	FC	H	K	L	FO	FC	H	K	L	FO	FC	H	K	L	FO	FC	H	K	L	FO	FC	H	K	L	FO	FC
-3	1	4	20	19	-9	3	4	26	23	-8	5	4	8	-14	0	8	4	18	-21	-10	2	5	32	-33	-3	2	6	60	-56
-2	1	4	16	17	-8	3	4	52	-58	-6	5	4	42	-42	-16	0	5	23	26	-9	2	5	23	19	-2	2	6	125	-120
-1	1	4	43	41	-7	3	4	34	-39	-5	5	4	39	-42	-14	0	5	16	-18	-8	2	5	52	-50	-1	2	6	11	-7
0	1	4	65	-62	-6	3	4	19	16	-4	5	4	12	11	-12	0	5	26	-28	-7	2	5	43	-42	0	2	6	16	16
1	1	4	53	53	-5	3	4	22	24	-3	5	4	108	-107	-8	0	5	102	103	-6	2	5	62	58	1	2	6	78	76
2	1	4	117	-113	-3	3	4	79	88	-2	5	4	71	-71	-6	0	5	84	-87	-5	2	5	30	29	2	2	6	10	-9
3	1	4	34	-35	-2	3	4	11	14	-1	5	4	65	63	-4	0	5	17	-20	-4	2	5	75	71	3	2	6	23	17
4	1	4	75	69	-1	3	4	47	-47	1	5	4	56	56	-2	0	5	13	14	-3	2	5	52	50	4	2	6	22	-25
5	1	4	61	-56	0	3	4	56	51	2	5	4	50	46	0	0	5	35	-37	-2	2	5	33	-34	5	2	6	27	-26
6	1	4	39	39	1	3	4	52	-53	3	5	4	39	-37	2	0	5	14	16	-1	2	5	55	-50	6	2	6	59	60
7	1	4	39	37	2	3	4	70	63	4	5	4	30	-25	4	0	5	14	18	0	2	5	27	-23	8	2	6	9	-8
8	1	4	85	-83	3	3	4	74	75	6	5	4	29	29	6	0	5	32	33	1	2	5	30	-28	9	2	6	10	9
9	1	4	33	-30	4	3	4	19	13	8	5	4	26	-29	8	0	5	99	-99	3	2	5	34	35	10	2	6	46	-43
10	1	4	65	-62	5	3	4	32	-23	9	5	4	16	-16	10	0	5	97	-99	4	2	5	90	-85	11	2	6	11	-13
12	1	4	21	22	7	3	4	36	-33	11	5	4	18	-23	12	0	5	63	64	5	2	5	31	28	-15	3	6	29	33
13	1	4	39	41	8	3	4	30	29	-12	6	4	14	-11	-16	1	5	16	19	6	2	5	23	21	-14	3	6	15	16
14	1	4	9	-11	9	3	4	15	12	-11	6	4	43	-41	-15	1	5	18	-17	7	2	5	13	-10	-13	3	6	27	30
-17	2	4	20	20	10	3	4	10	9	-8	6	4	28	27	-13	1	5	21	19	8	2	5	69	71	-12	3	6	27	-28
-16	2	4	26	26	11	3	4	42	41	-7	6	4	24	-26	-12	1	5	31	31	10	2	5	13	25	-11	3	6	48	-48
-15	2	4	31	30	12	3	4	17	18	-6	6	4	21	22	-11	1	5	71	-72	11	2	5	38	41	-9	3	6	34	-34
-14	2	4	30	-28	13	3	4	37	-40	-4	6	4	31	-31	-10	1	5	95	95	-15	3	5	32	-35	-8	3	6	19	18
-12	2	4	71	67	-15	4	4	59	-59	-3	6	4	49	47	-9	1	5	41	37	-14	3	5	16	16	-7	3	6	59	57
-11	2	4	54	-64	-14	4	4	27	-29	-2	6	4	32	-31	-8	1	5	63	-63	-13	3	5	40	40	-6	3	6	36	-32
-10	2	4	46	49	-13	4	4	74	70	-1	6	4	50	50	-7	1	5	26	25	-12	3	5	52	-59	-4	3	6	13	-14
-9	2	4	31	29	-12	4	4	37	-37	0	6	4	61	58	-6	1	5	65	-64	-9	3	5	90	-83	-3	3	6	42	-43
-8	2	4	44	-43	-10	4	4	15	16	1	6	4	36	-39	-5	1	5	21	-23	-8	3	5	13	-14	-2	3	6	31	-26
-7	2	4	12	11	-9	4	4	33	-32	2	6	4	31	-32	-4	1	5	81	79	-6	3	5	26	28	-1	3	6	60	59
-6	2	4	57	-57	-7	4	4	9	11	3	6	4	45	-45	-3	1	5	75	69	-5	3	5	72	72	0	3	6	48	46
-4	2	4	34	32	-6	4	4	24	22	4	6	4	10	-11	-2	1	5	61	54	-4	3	5	21	23	1	3	6	37	35
-3	2	4	95	91	-5	4	4	88	86	5	6	4	11	10	-1	1	5	76	-74	-3	3	5	32	-24	2	3	6	39	-40
-2	2	4	17	18	-3	4	4	27	-24	6	6	4	15	18	0	1	5	12	10	-1	3	5	60	-60	3	3	6	53	-52
0	2	4	41	-43	-2	4	4	35	-33	7	6	4	8	10	1	1	5	12	-12	0	3	5	14	17	4	3	6	23	22
1	2	4	9	-10	-1	4	4	82	-79	9	6	4	19	-21	2	1	5	36	32	1	3	5	66	65	5	3	6	16	-16
2	2	4	76	91	1	4	4	68	67	-9	7	4	10	12	3	1	5	52	-50	2	3	5	49	-46	7	3	6	33	35
3	2	4	75	-69	2	4	4	28	-28	-8	7	4	49	51	4	1	5	30	28	3	3	5	30	30	8	3	6	44	-49
4	2	4	24	22	3	4	4	11	-11	-6	7	4	54	-52	5	1	5	42	38	4	3	5	32	-31	9	3	6	30	-35
5	2	4	91	90	4	4	4	14	17	-5	7	4	27	25	6	1	5	102	-104	6	3	5	63	64	10	3	6	9	13
6	2	4	59	-57	5	4	4	46	-47	-4	7	4	7	9	7	1	5	53	50	7	3	5	11	11	-13	4	6	53	-57
7	2	4	17	-17	6	4	4	16	18	-3	7	4	9	12	8	1	5	47	-45	8	3	5	7	-7	-11	4	6	23	-22
8	2	4	33	-29	7	4	4	26	27	-2	7	4	28	27	9	1	5	41	-37	9	3	5	9	10	-10	4	6	10	-11
9	2	4	52	-49	8	4	4	15	17	-1	7	4	22	-22	10	1	5	55	50	11	3	5	41	-40	-9	4	6	53	49
11	2	4	31	40	10	4	4	12	16	1	7	4	16	-16	11	1	5	40	37	12	3	5	23	-22	-7	4	6	23	22
12	2	4	39	38	12	4	4	23	-19	2	7	4	28	-26	12	1	5	34	32	-14	4	5	12	11	-6	4	6	11	10
14	2	4	14	-15	-14	5	4	21	19	4	7	4	16	17	-16	2	5	19	-23	-13	4	5	52	51	-4	4	6	36	32
-16	3	4	7	-9	-13	5	4	51	48	5	7	4	26	28	-15	2	5	33	-37	-11	4	5	46	-49	-3	4	6	8	9
-13	3	4	45	-44	-12	5	4	24	22	6	7	4	43	47	-13	2	5	15	-16	-9	4	5	17	-17	-2	4	6	20	24
-12	3	4	11	12	-11	5	4	22	-22	-4	8	4	23	27	-12	2	5	52	54	-7	4	5	42	38	-1	4	6	36	38
-10	3	4	7	-12	-10	5	4	10	-15	-1	8	4	14	-12	-11	2	5	13	15	-5	4	5	19	-17	0	4	6	24	22

ANISOTROPIC AND ISOTROPIC THERMAL PARAMETERS

ANISOTROPIC IN THE FORM EXP(-2*PI*PI*(U11*(ASTAR*H)**2 +....
...U23*BSTAR*CSTAR*K*L + ...))

ISOTROPIC EXP(-8*PI*PI*U*(SIN(THETA)/LAMBDA)**2)

ALL VALUES *1000

ATOM	U11(OR U)	U22	U33	U23	U13	U12
MN	33(1)	54(2)	37(1)	0(1)	5(1)	-1(1)
P(1)	40(2)	62(3)	49(3)	-8(2)	10(2)	-4(2)
P(2)	42(2)	75(3)	42(2)	-4(2)	7(2)	3(2)
O(1)	32(5)	89(6)	61(6)	-18(5)	8(4)	6(5)
O(2)	59(6)	96(7)	41(5)	0(5)	13(5)	-11(5)
O(3)	74(6)	60(6)	74(6)	-23(5)	11(5)	2(5)
O(4)	45(5)	109(7)	66(6)	-29(6)	16(5)	-6(5)
O(5)	90(6)	71(6)	74(6)	-4(6)	10(6)	24(6)
O(6)	68(6)	111(7)	38(5)	-13(5)	11(5)	-4(6)
C(1)	42(7)	129(9)	85(8)	-10(8)	19(7)	13(7)
C(2)	81(8)	134(9)	59(7)	15(8)	23(7)	-27(8)
C(3)	114(8)	63(8)	107(8)	7(8)	32(8)	14(8)
C(4)	79(8)	161(9)	82(8)	-36(8)	37(7)	11(8)
C(5)	105(8)	92(8)	108(9)	9(8)	-20(8)	31(8)
C(6)	71(8)	130(9)	70(8)	-13(8)	-7(7)	-14(8)
C(7)	36(6)	67(7)	45(7)	1(7)	9(6)	6(7)
O(7)	81(6)	67(6)	117(7)	5(6)	35(6)	-16(6)
C(8)	53(7)	58(7)	60(7)	6(7)	19(6)	0(6)
O(8)	78(6)	109(7)	53(6)	19(6)	-16(6)	25(6)
C(12)	60(7)	54(7)	76(8)	-11(7)	12(7)	-21(7)
C(13)	40(6)	71(8)	38(7)	-16(7)	0(6)	-26(6)
C(14)	37(7)	65(8)	46(7)	0(6)	-6(6)	-5(6)

REFERENCES

1. G.Wilke, B.Bogdanovic, P.Hardt, P.Heirnbach, W.Kiern, M.Kroner, W.Oberkirch, K.Tanaka, E.Steinruke, D.Walter and H.Zimmermann, Angew.Chem.Int.Ed.Engl., 1966, 5, 151-64.

2. R.Baker, Chem.Rev., 1973,73,487-530.

3. P.Heirnbach, P.W.Jolly and G.Wilke, Advan.Organometal. Chem., 1970,8,25-86.

4. C.E.H.Bawn, D.G.T,Cooper and A.M.North, Polymer, 1966, 7,113-24.

5. M.I.Lobach, B.D.Babitskii and V.A.Kormer, Russ.Chem.Rev., 1967,36,476-98.

6. J.J.Rooney and G.Webb, J.Catalysis, 1964,3,488-501.

7. T.A.Manuel, J.Org.Chem., 1962,27,3941-5.

8. R.Huttel and J.Krantzer, Chem.Ber., 1964,97,1438-52.

9. ICI Patent, Netherlands Application, 68-05418.

10. M.C.Rakowski, F.J.Hirsekorn, L.S.Stuhl and E.L. Muetterties, Inorg.Chem., 1976,15,2379-82.

11. L.S.Stuhl and E.L.Muetterties, Inorg.Chem., 1978,17, 2148-52.

12. M.Dubini, G.P.Chiusoli and F.Montino, Tetrahedron Letters, 1963,1591-5.

13. W.T.Dent, R.Long, and G.H.Whitfield, J.Chem.Soc., 1964, 1588-94.

14. G.N.Schrauzer,Ed. 'Transition Metals in Homogeneous Catalysis',Marcel Dekker, New York, 1971.

15. P.W.Jolly and G.Wilke, 'The Organic Chemistry of Nickel', Academic Press. New York, 1975, Vol II.

16. L.S.Stuhl, M.Rakowski, F.J.Hirsekorn, J.R.Bleeke, A.E.Stevens and E.L.Muetterties, J.Amer.Chem.Soc., 1978,100,2405-10.

17. C.M.Chen, Diss.Abstr.Int.B., 1977,37,6144-5.

18. R.Baker, R.C.Cookson and J.R.Vinson, JCS Chem.Comm., 1974,515-6.

19. Y.Ho, H.Aoyama, T.Hirao, A.Mochizuki and T.Saegusa, J.Amer.Chem.Soc., 1979,101,494-6.

20. B.A.Krentsel, E.A.Mushina and N.A.Borisova, Rev.Inst. Fr.Pet., 1977,32,59-71.

21. B.J.Brisdon, M.Cartwright and M.G.B.Drew, Inorg.Chim. Acta., in press.

22. H.Alper and Hang-Nan Paik, J.Organometal.Chem., 1976 122,C31-2.

23. A.F.Masters, K.Mertis, J.F.Gibson and G.Wilkinson, Nouveau J.Chim., 1977,1,389-95.

24. B.Bogdanovic , Z.Naturforsch, in press.

25. B.J.Brisdon and A.A.Woolf, J.Chem.Soc.Dalton Trans., 1978,291-5.

26. S.A.Kettle and R.Mason, J.Organometal.Chem., 1966,5, 573-7.

27. P.W.N.M.Van Leeuwen and A.P.Praat, J.Organometal.Chem., 1970,21,501-15.

28. M.L.H.Green and P.L.I.Nagy, Adv.an.Organometal.Chem.,1964, 2,325-63.

29. I.H.Hilliere and R.M.Canadine, Disc.Farad.Soc., 1969, 47,27-36.

30. D.A.Brown and A.Owens. Inorg.Chim.Acta, 1971,5,675-8.

31. N.Rosch and R.H.Hoffmann, Inorg.Chem., 1974,13,2656-66.

32. B.E.R.Schilling, R.Hoffmann and D.L.Lichtenberger, J.Amer.Chem.Soc., 1979,101,592-8.

33. B.J.Brisdon and M.Cartwright, J.Organometal.Chem., 1979, 164,83-96.

34. M.G.B.Drew, B.J.Brisdon, D.A.Edwards and K.E.Paddick, unpublished results.

35. J.W.Faller and D.A.Haitko, J.Organometal.Chem., 1978, 149.C19-23.

36. D.E.Axelson and C.E.Holloway, JCS.Chem.Comm., 1973,455-6.

37. J.C.Rousche and G.R.Dobson, J.Organometal.Chem., 1978, 150,239-45.

38. T.B.Chenskaya, L.A.Leites and V.T.Aleksanyou, J.Organometal.Chem., 1978,148,85-95.

39. A.Oudeman and T.S.Sorensen, J.Organometal.Chem., 1978, 156,259-64.

40. G.Davidson and D.C.Andrews, J.Chem.Soc.Dalton Trans., 1972,126-30.

41. I.R.Beattie, J.W.Emsley, J.C.Linden and R.M.Sabine, J.Chem.Soc.Dalton Trans., 1264-7.

42. J.W.Faller, D.A.Haikto, R.Adams and D.F.Chodosh, J.Amer.Chem.Soc., 1979,101,865-76.

43. M.Cooke, Chem.Soc., Specialist Periodical Reports, Organometallic Chemistry, 1976,5,333-51.

44. IUPAC Nomenclature of Inorganic Chemistry, Definitive Rules 1970, Pure Appl.Chem., 1971,28,1-110.

45. F.A.Cotton, J.Amer.Chem.Soc., 1968,90,6230-2.

46. E.L.Muetterties, Inorg.Chem., 1979,18,902-3.

47. G.Raper and W.S.McDonald, J.Chem.Soc.Dalton Trans., 1972,265-9.

48. T.Aoki, A.Furusaki, Y.Tomie, K.Ono and K.Tanaka, Bull.Chem.Soc.Japn., 1969,42,545-7.

49. E.J.Lanpher, J.Amer.Chem.Soc., 1957,79,5578.

50. B.E.Mann, B.L.Shaw and G.Shaw, J.Chem.Soc.A, 1971,22, 3536-44.

51. B.Bogdanovic, Angew.Chem., in press.

52. M.G.B.Drew, B.J.Brisdon, D.A.Edwards and K.E.Paddick, Inorg.Chim.Acta., in press.

53. R.H.Fenn and A.J.Graham, J.Organometal.Chem., 1972, 37,137-50.

54. C.F.Putnik, J.J.Welter, G.D.Stucky, M.J.D'Aniello, B.A.Sosinsky, J.F.Kirner and E.L.Muetterties, J.Amer. Chem.Soc., 1978,100,4107-16.

55. A.E.Smith, Inorg.Chem., 1972,11,2306-10.

56. H.L.Clarke, J.Organometal.Chem., 1974,80,155-73.

57. J.A.Kaduk,A.T.Poulos and J.A.Ibers, J.Organometal.Chem., 1977,127,245-60.

58. M.R.Churchill and T.A.O'Brien, Inorg.Chem., 1967,6, 1386-90.

59. M.R.Churchill and R.Mason, Nature, 1964,204,777.

60. A.E.Smith, Acta.Cryst., 1965,18,331-40.

61. W.E.Oberhausli and L.F.Dahl, J.Organometal.Chem., 1965,3,43-54.

62. K.Vrieze and P.W.M.N.Van Leeuwen, Prog.Inorg.Chem., 1971,14,1-63.

63. A.Streitwieser Jr., 'M.O. Theory for Organic Chemists', Wiley, New York, 1961.

64. J.M.Rowe, Proc.Chem.Soc., 1962,66.

65. G.deBrouckere, Theoret.Chim.Acta., 1970,19,310-25.

66. M-M.Rohmer,J.Demuynik and A.Veillard, Theoret.Chim.Acta., 1977,36,93.

67. M.R.Churchill and R.Mason, Advan.Organometal.Chem., 1967,5,125-8.

68. G.E.Coates, M.L.H.Green, P.Powell and K.Wade, 'Principles of Organometallic Chemistry', Methuen, London, 1971.

69. J.A.Kaduk and J.A.Ibers, J.Organometal.Chem., 1977, 139, 199-207.

70. M.G.B.Drew and L.S.Pu, Acta.Cryst., 1977, B33, 1207-11.

71. K.W.Egger, J.Organometal.Chem., 1970, 24, 501-6.

72. V.I.Tel'noi, I.B.Rabinovich, V.D.Tikhonov, V.N.Latyaeva, L.I.Vyshinskaya and G.A.Razuvaev, Dokl.Akad.Nauk.SSSR., 1967, 174, 1374-6.

73. J.L.Roustan, J.Organometal.Chem., 1972, 38, C37-40.

74. P.M.Maitlis, A.Sonoda and B.E.Mann, JCS.Chem.Comm., 1975, 108-9.

75. M.Green, B.Lewis, J.J.Daly and F.Sanz, J.Chem.Soc. Dalton Trans., 1975, 1118-27.

76. R.M.Tuggle and D.L.Weaver, Inorg.Chem., 1971, 10, 1504-10.

77. W.K.Olander and T.L.Brown, J.Amer.Chem.Soc., 1972, 94, 2139-40.

78. R.G.Hayter, J.Organometal.Chem., 1968, 13, P1-3.

79. C.E.Chidsey, W.A.Donaldson, R.P.Hughes and P.F.Sherwin, J.Amer.Chem.Soc., 1979, 101, 233-5.

80. P.T.Cheng, T.R,Jack, C.J.May, S.C.Nyburg and J.Powell, JCS.Chem.Comm., 1975, 369-70.

81. R.Aumann, J.Organometal.Chem., 1974, 77, C33-6.

82. G.Hutter, H.H.Brintzinger, L.G.Bell, P.Friedrich, V.Bejenke and D.Neugebauer, J.Organometal.Chem., 1978, 145, 329-33.

83. D.A.T.Young, J.R.Holmes and H.D.Kaesz, J.Amer.Chem.Soc., 1969, 91, 6968-77.

84. D.A.Clement. J.F.Nixon and B.Wilkins. J.Organometal.Chem., 1972, 37, C43-6.

85. B.A.Sosinsky, S.A.R.Knox and F.G.A.Stone, J.Chem.Soc. Dalton Trans., 1975, 1633-43.

86. J.Evans, B.F.G.Johnson, J.Lewis and D.J.Yarrow, J.Chem. Soc.Dalton Trans., 1974,2375-80.

87. A.Westerhof and H.J.De LiefdeMeijer, J.Organometal.Chem., 1978,149,321-5.

88. T.Inglis, M.Kilner and T.Reynoldson, JCS.Chem.Comm., 1972,774-5.

89. N.Yshimura, S.I.Murakashi and I.Moritani, J.Organometal. Chem., 1973,52,C58-9.

90. H.Sakurai, Y.Kamiyama and Y.Nakadaira, J.Amer.Chem.Soc., 1976,98,7453-4.

91. A.R.Kane and E.L.Muetterties, J.Amer.Chem.Soc., 1971, 93,1041-2.

92. F.A.Bovey, 'NMR Data Tables for Organic Compounds', Vol. II, Interscience, New York, 1967.

93. W.R.McClelland, H.H.Hoehn, H.N.Cripps, E.L.Muetterties and B.W.Howk, J.Amer.Chem.Soc., 1961,83,1601-7.

94. G.W.A.Fowles, L.S.Pu and D.A.Rice, J.Organometal.Chem., 1973,54,C17-8.

95. H.J.Neese and H.Burger, J.Organometal.Chem., 1971,32, 213-22.

96. J.Powell and A.W.L.Chan, J.Organometal.Chem., 1972,35, 203-15.

97. R.F.Heck and D.S.Breslow, J.Amer.Chem.Soc., 1960,82, 750-1.

98. E.L.Muetterties and W.D.Phillips, Advan.Inorg.Chem. Radiochem., 1962,4,253-5.

99. S.F.Dyke, A.J.Floyd, M.Sainsbury and R.S.Theobald, 'Organic Spectroscopy' Penguin London, 1971.

100. H.S.Gutowsky, M.Karplus and D.M.Grant, J.Chem.Phys., 1959,31,1278-89.

101. M.Karplus, J.Amer.Chem.Soc., 1960,82,4431-2.

102. F.A.Cotton, J.W.Faller and A.Musco, Inorg.Chem., 1967,6,179-82.

103. B.E.Mann, Advan.Organometal.Chem. 1974,12,135-213.

104. B.E.Mann, R.Pietropaolo and B.L.Shaw, J.Chem.Soc. Dalton Trans., 1973,2390-3.

105. J.K.Becconsall and S.O'Brien, JCS.Chem.Comm., 1966,302-3.

106. J.K.Becconsall, B.E.Job and S.O'Brien, J.Chem.Soc.A, 1967,423-30.

107. C.A.Reilly and H.Thyret, J.Amer.Chem.Soc., 1967,89, 5144-9.

108. J.W.Faller and M.J.Incorvia, Inorg.Chem., 1968,7,840-2.

109. K.Vrieze and H.C.Volger, J.Organometal.Chem., 1967,9, 537-48.

110. F.A.Cotton and L.M.Jackman,(Eds.), 'Dynamic NMR Spectroscopy', Academic Press,New York, 1975.

111. L.F.Farnell, E.W.Randall and E.Rosenberg, JCS.Chem. Comm., 1971,1078.

112. L.A.Chulyaeva, M.A.Lobach, G.P.Kondratenkov and V.A.Kormer, J.Organometal.Chem., 1972,39,C23-4.

113. B.J.Brisdon, D.A.Edwards and K.E.Paddick, J.Organometal.Chem., in press.

114. G.Davidson, Organometal.Chem.Rev.Sec.A, 1972,8,303-50.

115. H.A.Martin, P.J.Lemaire and F.Jellinek, J.Organometal. Chem., 1968,14,149-56.

116. F.W.Siegart and H.J.De LiefdeMeijer, J.Organometal. Chem., 1970,23,177-83.

117. M.L.H.Green and A.W.Stear, J.Organometal.Chem., 1964, 1,230-4.

118. H.D.Kaesz and R.B.King, Z.Naturforsch, 1960,15b,682-3.

119. G.Sbrana, G.Braca,F.Piacenti and P.Pino, J.Organometal. Chem., 1968,13,240-2.

120. G.Davidson and D.C.Andrews, J.Chem.Soc.Dalton Trans., 1972,1381-4.

121. G.Davidson and D.C.Andrews, J.Organometal.Chem., 1973, 55,383-93.

122. G.Paliani, A.Poletti, G.Cardaci, S.M.Murgia and R.Catallotti, J.Organometal.Chem., 1973,60,157-64.

123. G.Paliani, S.M.Murgia, G.Cardaci and R.Catallotti, J.Organometal.Chem., 1973,63,407-13.

124. K.Shobatake and K.Nakamoto, J.Amer.Chem.Soc., 1970,92, 3339-42.

125. D.M.Adams and A.Squire, J.Chem.Soc.A, 1970,1808-13.

126. H.P.Fritz, Chem.Ber., 1961,94,1217-24.

127. K.Nakamoto. 'Infrared Spectra of Inorganic and Coordination Compounds', Wiley, New York, 1977.

128. H.L.Clarke and N.J.Fitzpatrick, J.Organometal.Chem., 1972,40,379-86.

129. E.Maslowsky, 'Vibrational Spectra of Organometallic Compounds', Wiley, New York, 1977.

130. J.K.Becconsall and S.O'Brien, JCS.Chem.Comm., 1966, 720-2.

131. M.S.Lupin and M.Cais, J.Chem.Soc.A, 1968,3095-100.

132. R.B.King and M.Ishaq, Inorg.Chim.Acta., 1970,4,258-60.

133. S.Otsuka, A.Nakamura and K.Tani, J.Chem.Soc.A, 1968, 2248-53.

134. R.B.King, J.Amer.Chem.Soc., 1968,90,1417-29.

135. S.O'Brien, JCS.Chem.Comm., 1968,757-9.

136. R.B.King, Org.Mass Spectrom., 1969,2,401-12.

137. J.Kwiatek and J.K.Seyler, J.Organometal.Chem., 1965,3, 421.

138. M.L.H.Green and P.L.I.Nagy, J.Chem.Soc., 1963,189-97.

139. H.C.Volger and K.Vrieze, J.Organometal.Chem.,1968,13, 479-93.

140. R.B.King, Acc.Chem.Res., 1970,3,417-27.

141. W.Hieber, W.Beck and G.Braun, Angew.Chem., 1960,72,795.

142. R.B.King, Advan.Organometal.Chem., 1964,2,157-256.

143. J.Ellis, J.Organometal.Chem., 1975,86,1-56.

144. J.Y.Merour, C.Charrier, J.Benaim, J.L.Rouston and D.Commereuc, J.Organometal.Chem., 1972,39,321-8.

145. B.J.Brisdon and G.F.Griffin, J.Organometal.Chem.,1974, 76,C47-9.

146. B.J.Brisdon and G.F.Griffin, J.Chem.Soc.Dalton Trans., 1975,1999-2002.

147. G.Doyle, J.Organometal.Chem., 1977,132,243-54.

148. K.Stanley and D.W.McBride, Canad.J.Chem., 1975,53, 2537-41.

149. U.Franke and E.Weiss, J.Organometal.Chem., 1978,153, 39-51.

150. P.K.Wong, K.S.Y.Lau and J.K.Stille, J.Amer.Chem.Soc., 1974,96,5956-7.

151. R.G.Pearson, Fortschu.Chem.Forsch., 1973,41,76.

152. J.A.Labinger, A.V.Kramer and J.A.Osborn, J.Amer.Chem. Soc., 1973,95,7908-9.

153. J.A.Osborn, Y.Ishii and M.Tsutsui,(Eds.), 'Organo-Transition Metal Chemistry', Plenum Publishing Corp., New York,1975.

154. C.G.Hull and M.H.B.Stiddard. J.Organometal.Chem., 1967. 9,519-25.

155. B.Bogdanovic, P.Borner, H.Breil, P.Hardt, P.Heinbach, G.Herrmann, H.J.Kaminsky, W.Keim, M.Kroner, H.Muller, W.Orberkirch, J.Schneider, J.Stedefeder, K.Tanaka, K.Weyer and G.Wilke. Angew.Chem.Int.Ed.Engl., 1963, 2,105-15.

156. M.L.H.Green, J.Knight, L.C.Mitchard, G.G.Roberts and W.E.Silverthorn, JCS.Chem.Comm., 1971,1619-21.

157. M.L.H.Green, L.C.Mitchard and W.E.Silverthorn, J.Chem. Soc.Dalton Trans., 1973,1952-4.

158. E.W.Abel and S.Moorhouse, Angew.Chem.Int.Ed.Engl., 1971,10,339-41.

159. E.W.Abel and S.Moorhouse, J.Chem.Soc.Dalton Trans., 1973,1706-11.

160. M.Green and R.I.Hancock, JCS.Chem.Comm., 1966,572-3.

161. M.Green and R.I.Hancock, J.Chem.Soc., 1968,109-11.

162. C.A.Tolman, J.Amer.Chem.Soc., 1970,92,6785-90.

163. R.Huttel,J.Kratzer and M.Bechter, Chem.Ber., 1961, 94,766-80.

164. P.Powell, J.Organometal.Chem., 1977,129,175-9.

165. H.D.Murdoch, J.Organometal.Chem., 1965,4,119-26.

166. R.D.Rieke, A.V.Kavaliunas, L.D.Rhyme and D.J.J.Fraser, J.Amer.Chem.Soc., 1979,101,246-8.

167. E.O.Fischer and G.Burger, Z.Naturforsch,B, 1961,16,702.

168. M.J.Piper and P.L.Timms, JCS.Chem.Comm., 1972,50.

169. M.Ephritikhine, B.R.Francis, M.L.H.Green, R.E.Mackenzie and M.J.Smith, J.Chem.Soc.Dalton Trans., 1977,1131-5.

170. K.Ehrlich and G.F.Emerson. J.Amer.Chem.Soc., 1972, 94, 2464-70.

171. M.I.Bruce, M.Z.Iqbal and F.G.A.Stone, J.Organometal. Chem., 1969,20,161-8.

172. A.N.Nesmeyanov, S.P.Gubin and A.Z.Rubezhov, J.Organometal.Chem., 1969,16,163-75.

173. B.Kanellokopulos, D.Nothe, K.Weidenhammer, H.Wienand and M.L.Ziegler. Angew.Chem.Int.Ed.Engl., 1977,16,261-2.

174. G.Vittulli, P.Pertici, C.Agami and L.Porri, J.Organometal.Chem., 1975,84,399-405.

175. D.W.Lichtenberg and A.Wojcicki, J.Organometal.Chem., 1975,94,311-26.

176. H.Kurosawa and R.Okawara, J.Organometal.Chem., 1974, 81,C31-2.

177. D.A.Clement, J.F.Nixon and B.Wilkins, J.Organometal. Chem., 1972,37,C43-6.

178. W.S.Trahanowsky and R.A.Hall, J.Amer.Chem.Soc., 1977, 99,4850-1.

179. R.B.King and M.S.Saran, Inorg.Chem., 1974,13,2453-7.

180. A.T.T.Hsieh and B.O.West, J.Organometal.Chem., 1976, 112,285-96.

181. A.J.Graham and R.H.Fenn, J.Organometal.Chem., 1970, 25,173-91.

182. A.J.Graham and R.H.Fenn, J.Organometal.Chem., 1969, 17,405-22.

183. E.M.Holt, S.L.Holt and K.J.Watson, J.Chem.Soc.Dalton Trans., 1973,2444-7.

184. P.Meakin, S.Trofimenko and J.P.Jesson, J.Amer.Chem.Soc., 1972,94,5677-8.

185. S.Trofimenko, J.Amer.Chem.Soc., 1969,91,3183-9.

186. F.A.Cotton, B.A.Frenz and A.G.Stanislowski, Inorg.Chim. Acta., 1973,7,503-8.

187. F.A.Cotton, B.A.Frenz and C.A.Murillo, J.Amer.Chem.Soc., 1975,97,2118-22.

188. B.J.Brisdon, J.Organometal.Chem., 1977,125,225-30.

189. B.J.Brisdon and K.E.Paddick, J.Organometal.Chem., 1978, 149,113-22.

190. J.W.Faller, D.A.Haitko, R.D.Adams and D.F.Chodosh, J.Amer.Chem.Soc., 1977,99,1654-5.

191. M.L.H.Green and W.E.Silverthorn,J.Chem.Soc.Dalton Trans., 1973,301-6.

192. G.Doyle, J.Organometal.Chem., 1978,150,67-73.

193. F.Dawans, J.Dewailly, J.Meunier-Piret and P.Piret, J.Organometal.Chem., 1974,76,53-63.

194. J.W.Faller and A.M.Rosan, J.Amer.Chem.Soc., 1976,98, 3388-9.

195. M.Cousins and M.L.H.Green, J.Chem.Soc., 1963,889-94.

196. C.E.Holloway,J.D.Kelly and M.H.B.Stiddard, J.Chem. Soc.A, 1969,931-5.

197. H.tom Dieck and H.Friedel, J.Organometal.Chem., 1968, 14,375-85.

198. F.A.Cotton and J.R.Pipal, J.Amer.Chem.Soc., 1971,93, 5441-5.

199. N.A.Bailey, W.G.Kita, J.A.McCleverty, A.J.Murray, B.E.Mann and N.W.J.Walker, JCS.Chem.Comm., 1974, 592-3.

200. 1958, Brit.Patent 874618.

201. (a) W.R.McClelland, 1961, US Patent, 2990418.
(b) O.E.H.Klopfer, 1962, US Patent,3050562.
(c) J.E.Brown, 1964, US Patent, 3160592.
(d) R.D.Closson and T.H.Coffield, 1966, US Patent,3256306.

202. IUPAC Commission on Molecular Structure and Spectroscopy, Pure Appl.Chem., 1961,1,540.

203. M.H.B.Stiddard, J.Chem.Soc., 1962,4712-5.

204. G.C. Kulasingham and W.R.McWhinnie, J.Less Common Met., 1966,10,72-4.

205. E.W.Abel and G.Wilkinson, J.Chem.Soc., 1959,1501-5.

206. R.B.King,'Organometallic Synthesis', Vol.1,p.174, Academic Press, New York, 1965.

207. E.O.Brimm, M.A.Lynch and W.J.Sesney, J.Amer.Chem.Soc., 1954,76,3831-5.

208. R.Colton and J.E.Knapp, Aust.J.Chem., 1972,25,9-16.

209. K.Moedritzer, Synth.Inorg.Metal-org.Chem., 1971,1,63-8.

210. R.J.Angelici, Inorg.Chem., 1964,3,1099-1103.

211. E.W.Abel and I.S.Butler, J.Chem.Soc., 1964,434-7.

212. S.P.Gubin, A.Z.Rubezhov and L.I.Voronchinkhina, J. Organometal.Chem., 1978,149,123-39.

213. N.N.Druz, V.I.Klepikora, M.I.Lobach and V.A.Kormer, J.Organometal.Chem., 1978,162,343-5.

214. M.L.H.Green, A.G.Massey, J.T.Moelwyn-Hughes and P.L.I. Nagy, J.Organometal.Chem., 1967,8,511-5.

215. F.A.Hartman and A.Wojcicki, Inorg.Chim.Acta., 1968,2, 289-95.

216. F.A.Cotton and M.W.Extine, J.Amer.Chem.Soc., 1978,100, 3788-92.

217. M.Dubek and R.A.Schell, Inorg.Chem., 1964,3,1757-60.

218. M.G.B.Drew and G.F.Griffin, personal communication.

219. D.H.Gibson, W-L.Hsu and D-S.Lin, J.Organometal.Chem., 1979,172,C7-12.

220. J.Dalton, I.Paul, G.Smith and F.G.A.Stone., J.Chem. Soc.A., 1968,1208-11.

221. J.Ellis and R.A.Faltynek, J.Organometal.Chem., 1975, 93,205-17.

222. M.Schneider and E.Weiss, J.Organometal.Chem., 1974,73, C7-9.

223. F.Hohmann, J.Organometal.Chem., 1977,137,315-28.

224. H.Behrens, E.Lindner and G.Lehnert, J.Organometal.Chem., 1970,22,665-76.

225. L.W.Houk and G.R.Dobson, Inorg.Chem., 1966,5,2119-23.

226. F.A.Cotton, 'Chemical Applications of Group Theory', Interscience, New York, 1963.

227. D.S.Urch, 'Orbitals and Symmetry', Penguin, London, 1970.

228. G.Davidson, 'Group Theory for Chemists', Elsevier, London, 1971.

229. L.E.Orgel, Inorg.Chem., 1962,1,25-9.

230. R.H.Reimann and E.Singleton, J.Chem.Soc.Dalton Trans., 1973,841-6.

231. G.J.Kruger, R.O.Heckroodt, R.H.Reimann and E.Singleton, J.Organometal.Chem., 1975,87,323-32.

232. E.B.Wilson, J.C.Decius and P.C.Cross, 'Molecular Vibrations', McGraw-Hill, New York, 1955.

233. P.S.Bratermann, 'Metal Carbonyl Spectra', Academic Press, London, 1975.

234. L.F.Wuyts and G.P.VanderKelen, Inorg.Chim.Acta., 1977, 23,19-22.

235. R.J.Angelici, F.Basolo and A.J.Poe, J.Amer.Chem.Soc., 1963,85,2215-9.

236. L.H.Staal, A.Oskam and K.Vrieze, J.Organometal.Chem., 1979,170,235-45.

237. R.F.Fenske and R.L.Decock, Inorg.Chem., 1970,9,1053-60.

238. L.W.Houk and G.R.Dobson, J.Chem.Soc.A., 1966,317-9.

239. R.J.H.Clark and B.C.Crosse. J.Chem.Soc.A., 1969,224-8.

240. W.M.Carmichael and D.A.Edwards, J.Inorg.Nucl.Chem., 1968, 30,2641-6.

241. R.Colton and I.B.Tomkins, Aust.J.Chem., 1969,20,13-4.

242. B.Hutchinson and K.Nakamoto, Inorg.Chim.Acta., 1969 3,591-5.

243. J.C.Rousche and G.R.Dobson, J.Organometal.Chem., 1978 150,239-45.

244. E.W.Abel, I.S.Butler, M.C.Ganorkar, C.R.Jenkins and M.H.B.Stiddard, Inorg.Chem., 1966,5,25-7.

245. K.Moedritzer, Syn Inorg.Metal-org.Chem., 1972,2,209-15.

246. M.J.Hawkes and A.P.Ginsberg, Inorg.Chem., 1969,8, 2189-95.

247. J.L.Cihonski, M.L.Walker and R.A.Levenson, J.Organometal. Chem., 1975,102,335-7.

248. R.L.Davies and N.C.Baenziger, Inorg.Nucl.Chem.Letters, 1977,13,475-7.

249. C.P.Hrung, M.Tsutsui, D.L.Cullen and E.F.Meyer, J.Amer. Chem.Soc., 1976,98,7878-80.

250. C.P.Hrung, M.Tsutsui, D.L.Cullen, E.F.Meyer and C.N.Morimoto, J.Amer.Chem.Soc., 1978,100,6068-76.

251. W.J.Geary, Coord.Chem.Rev., 1971,7,81-

252. J.G.Dunn and D.A.Edwards, J.Organometal.Chem., 1971, 27,73-7.

253. R.H.Reimann and E.Singleton, J.Organometal.Chem., 1973,59,C24-6.

254. M.F.Farona and K.F.Kraus, Inorg Chem., 1970,9,1700-4.

255. D.M.Adams and A.Squire, J.Chem.Soc.A, 1970,814-21.

256. S.F.A.Kettle and I.Paul, J.Chem.Soc.Dalton Trans., 1974,2293-7.

257. D.M.Adams amd A.Squire, J.Organometal.Chem., 1973,63, 381-8.

258. E.W.Abel, R.A.N.McLean, P.S.Braterman, A.P.Walker, P.J.Hendra, J.Mol.Spectroscopy, 1969,30,29-50.

259. R.A.N.McLean, Canad.J.Chem., 1974,52,213-5.

260. I.J.Hyams and E.R.Lippincott, Spectrochim.Acta, 1969, 25A,1845-54.

261. W.A.McAllister and A.L.Marston, Spectrochim.Acta , 1971, 27A,523-5.

262. D.N.Kariuki and S.F.A.Kettle, Inorg.Chem., 1978,17, 1018-22.

263. D.A.Edwards and J.Marshalsea, J.Organometal.Chem., 1977, 131,73-91.

264. U.Sartorelli, V.Valenti and F.Zingales, Chim.Ind.(Milan), 1967,49,754-6.

265. G.L.Bottger and A.L.Geddes, Spectrochim.Acta, 1967,23A, 1551-9.

266. R.Mason, G.A.Rusholme, W.Beck, H.Englemann, K.Joos, B.Lindenberg and H.S.Smedal, J.C.S.Chem.Comm., 1971, 496-7.

267. A.P.Ginsberg and M.J.Hawkes, J.Amer.Chem.Soc., 1968,90, 5930-2.

268. A.A.Ioganson, B.V.Lokshin, E.E.Kolobova and K.N.Anisimov, Zh.Obshc.Khim., 1974,44,23-7.

269. M.Freni and P.Romiti, Atti Acad.Naz.Lincei Cl.Sci.Fis. Mat.Nat.Rend., 1974,55,515-7.

270. J.F.White and M.F.Farona, J.Organometal.Chem., 1972,37, 119-25.

271. F.Hohmann and H.tom Dieck, J.Organometal.Chem., 1976, 118,C35-6.

272. B.J.Wilford and F.G.A.Stone, Inorg.Chem., 1965,4,389-93.

273. W.Hieber, G.Braun and W.Beck, Chem.Ber., 1960,93,901-8.

274. J.A.Gladysz, G.M.Williams, W.Tam and D.L.Johnson, J. Organometal.Chem., 1977,140,C1-6.

275. J.A.Gladysz, G.M.Williams, W.Tam, D.L.Johnson, D.W.Parker and J.C.Selover, Inorg.Chem., 1979,18,553-8.

276. K.Inkrett, R.Goetze and S.G.Shore, J.Organometal.Chem., 1978,154,337-42.

277. J.E.Ellis and E.A.Folm, J.Organometal.Chem., 1975,99, 263-8.

278. W.Beck, W.Hieber and G.Braun, Z.Anorg.Allegem.Chem., 1961,308,23-32.

279. W.Hieber and G.Braun, Z.Naturforsch, 1956,146,132-3.

280. Supplementary Publication, SUP 20729,Table 4, associated with reference 159.

281. A.Davidson, J.A.McCleverty and G.Wilkinson, J.Chem.Soc., 1963,1133-8.

282. M.J.Mays and R.N.F.Simpson, J.Chem.Soc.A, 1967,1936-9.

283. D.J.Patmore and W.A.G.Graham, Inorg.Chem., 1966,5,2222-6.

284. K.Edgar, B.F.G.Johnson, J.Lewis, I.G.Williams and J.M.Wilson, J.Chem.Soc.A, 1967,379-82.

285. R.B.King, Inorg.Chem., 1966,5,2227-30.

286. G.Davidson, P.G.Harrison and E.M.Riley, Spectrochim. Acta, 1968,29A,1265-72.

287. C.Sourisseau and B.Pasquier, J.Organometal.Chem., 1972, 39,51-74.

288. R.D.McLachlan and R.A.Nyquist, Spectrochim.Acta, 1968, 24A,103-14.

289. H.D.Kaesz, R.Bau, D.Hendrikson and M.J.Smith, J.Amer. Chem.Soc., 1967,89,2844-51.

290. D.K.Ottenstan, H.B.Gray, L.H.Jones and M.Goldblatt, Inorg.Chem., 1973,12,1051-61.

291. L.H.Jones, R.S.MacDowell and M.Goldblatt, J.Chem.Phys., 1968,48,2663-70.

292. D.M.Adams, J.Chem.Soc., 1964,1771-6.

293. R.W.Cattrall and R.J.H.Clark, J.Organometal.Chem., 1966, 6,167-72.

294. A.R.Manning, J.Chem.Soc.A, 1971,106-10.

295. C.Jeanne, R.Prince and R.Poilblanc, Spectrochim.Acta, 1975,31A,818-38.

296. J.C.Decius and R.M.Hexter, 'Molecular Vibrations in Crystals' McGraw-Hill, London, 1977.

297. J.M.Smith and L.H.Jones, J.Mol.Spectroscopy, 1966,30, 248-57.

298. L.H.Jones, R.S.MacDowell and M.Goldblatt, Inorg.Chem., 1963,8,2349-63.

299. R.L.Amster, R.B.Hannan and M.C.Tobin, Spectrochim.Acta, 1963,19,1489-94.

300. D.C.Andrews and G.Davidson, J.Chem.Soc.Dalton Trans., 1972,1381-4.

301. J.Howard and T.C.Waddington, J.Chem.Soc.Faraday II, 1978, 74,879-88.

302. J.Hiraishi, Spectrochim.Acta, 1969,25A,749-60.

303. N.Sheppard, Unpublished obs., presented at 2nd Int. Raman Conf., Oxford, Sept 1970.

304. W.L.Smith and I.M.Mills, J.Chem.Phys., 1964,40,2095-2109.

305. K.M.Mackay and S.R.Stobart, J.Chem.Soc.Dalton Trans., 1973,214-7.

306. G.Davidson and E.M.Riley, J.Organometal.Chem., 1973,51, 297-306.

307. G.Davidson and D.A.Duce, J.Organometal.Chem., 1976,120, 229-37.

308. H.M.Seip and R.Seip, Acta Chem.Scand., 1970,24,3431-3.

309. D.W.Rankin and A.Robertson, J.Organometal.Chem., 1975, 85,225-35.

310. D.W.Rankin and A.Robertson, J.Organometal.Chem., 1976, 105,331-40.

311. A.B.Dempster, D.B.Powell and N.Sheppard, J.Chem.Soc.A, 1970,1129-33.

312. D.C.McKean, Spectrochim.Acta, 1973,294,1559-74.

313. P.W.Jolly and F.G.A.Stone, J.Chem.Soc., 1965,5259-60.

314. M.Freni, V.Valenti and D.Guisto, J.Inorg.Nucl.Chem., 1965,27,2635-9.

315. R.H.Reimann and E.Singleton, J.Organometal.Chem., 1973, 59,309-15.

316. E.L.Muetterties and F.J.Hirsekorn, J.Amer.Chem.Soc., 1974,96,4093-4.

317. E.L.Muetterties, M.C.Rakowski, F.J.Hirsekorn, W.D.Larson V.J.Basus and F.A.L.Anet, J.Amer.Chem.Soc., 1975,97,1266-7.

318. Shelx 76, G.M.Sheldrick, private communication.

319. International Tables for X-Ray Crystallography, Vol IV, Kynoch Press, Birmingham,1974.

320. W.Hiebar, G.Faullaber and F.Theubert, Z.Naturforsch, 1960, 15B,326-7.

321. D.Drew, D.J.Darensbourg and M.Y.Darensbourg, Inorg.Chem., 1975,14,1579-84.

322. P.W.Jolly, M.I.Bruce and F.G.A.Stone, J.Chem.Soc., 1965, 5830-7.

323. S.Onaka, Y.Yoshikawa and H.Yamatera, J.Organometal.Chem., 1978,157,187-98.

324. J.E.Ellis and R.A.Faltynek, J.C.S.Chem.Comm., 1975,966-7.

325. J.E.Ellis and R.A.Faltynek, J.Amer.Chem.Soc., 1977,99, 1801-8.

326. W.Beck, A.Melinkoff and R.Stahl, Chem.Ber., 1966,327[1]-7.

327. A.R.Manning, J.Chem.Soc.A, 1967, 984-7.

328. D.Steele, Quart.Rev., 1964,18,21-44.

329. R.K.Harris, Canad.J.Chem., 1964,42,2275-81.

330. R.D.Bertrand, P.Ogilivie and J.G.Verkade, J.Amer.Chem.Soc., 1970,92,1908-15.

331. F.B.Ogilivie, J.M.Jenkins and J.F.Verkade, J.Amer.Chem.Soc., 1970,92,1916-23.

332. D.A.Duddel, J.G.Evans, P.L.Goggin, R.T.Goodfellow, A.J.Best and J.G.Smith, J.Chem.Soc., 1969,2134-8.

333. P.J.Parker and A.Wojcicki, Inorg.Chim.Acta, 1974,11,9-16.

334. F.J.Hirsekorn, M.C.Rakowski and E.L.Muetterties, J.Amer. Chem.Soc., 1975,97,237-8.

335. W.K.Dean, G.L.Simon, P.M.Treichel and L.F.Dahl, J.Organometal.Chem., 1973,50,193-207.

336. J.H.Enemark and J.A.Ibers, Inorg.Chem., 1967,6,1575-81.

337. J.H.Enemark and J.A.Ibers, Inorg.Chem., 1968,7,2339-44.

338. R.F.Bryan, J.Chem.Soc.A, 1967,172-81.

339. H.Vahrenkamp, Chem.Ber., 1971,104,449-55.

340. C.Barbeau, K.SorrentoDichmann and L.Ricard, Canad.J.Chem., 1973,51,3027-31.

341. G.J.Kruger, R.O.Heckroodt, R.H.Reimann and E.Singleton, J.Organometal.Chem., 1976,111,225-33.

342. P.V.Rinze and U.Muller, Chem.Ber., 1979 112,1973-80.

343. F.W.B.Einstein and J.S.Field, J.Chem.Soc.Dalton Trans., 1975,172-5.